POLY(VINYL ALCOHOL)/α-CHITIN/NANOCELLULOSE COMPOSITES DEVELOPED FROM OIL PALM EMPTY FRUIT BUNCH (OPEFB) FOR REMOVAL OF CATIONIC DYES

MOK CHUN FAH

FACULTY OF ENGINEERING
UNIVERSITY OF MALAYA
KUALA LUMPUR

2020

POLY(VINYL ALCOHOL)/ α-CHITIN/NANOCELLULOSE COMPOSITES DEVELOPED FROM OIL PALM EMPTY FRUIT BUNCH (OPEFB) FOR REMOVAL OF CATIONIC DYES

MOK CHUN FAH

THESIS SUBMITTED IN FULFILMENT OF THE REQUIREMENTS FOR THE DEGREE OF DOCTOR OF PHILOSOPHY

FACULTY OF ENGINEERING
UNIVERSITY OF MALAYA
KUALA LUMPUR

2020

UNIVERSITY OF MALAYA
ORIGINAL LITERARY WORK DECLARATION

Name of Candidate: MOK CHUN FAH

Matric No: KHA140040

Name of Degree: DOCTOR OF PHILOSOPHY

Title of Project ~~Paper~~/~~Research Report~~/~~Dissertation~~/Thesis (“this Work”):

POLY(VINYL ALCOHOL)/α-CHITIN/NANOCELLULOSE COMPOSITES DEVELOPED FROM OIL PALM EMPTY FRUIT BUNCH (OPEFB) FOR REMOVAL OF CATIONIC DYES

Field of Study:

ADVANCE MATERIALS/NANOMATERIALS (ENGINEERING AND ENGINEERING TRADES)

I do solemnly and sincerely declare that:

I am the sole author/writer of this Work;
This Work is original;
Any use of any work in which copyright exists was done by way of fair dealing and for permitted purposes and any excerpt or extract from, or reference to or reproduction of any copyright work has been disclosed expressly and sufficiently and the title of the Work and its authorship have been acknowledged in this Work;
I do not have any actual knowledge nor do I ought reasonably to know that the making of this work constitutes an infringement of any copyright work;
I hereby assign all and every rights in the copyright to this Work to the University of Malaya (“UM”), who henceforth shall be owner of the copyright in this Work and that any reproduction or use in any form or by any means whatsoever is prohibited without the written consent of UM having been first had and obtained;
I am fully aware that if in the course of making this Work I have infringed any copyright whether intentionally or otherwise, I may be subject to legal action or any other action as may be determined by UM.

Candidate’s Signature Date:

Subscribed and solemnly declared before,

Witness’s Signature Date:

Name:

Designation:

POLY(VINYL ALCOHOL)/α-CHITIN/NANOCELLULOSE COMPOSITES DEVELOPED FROM OIL PALM EMPTY FRUIT BUNCH (OPEFB) FOR REMOVAL OF CATIONIC DYES

ABSTRACT

In search of an eco-friendly polymeric adsorbent for dye effluent treatment application, poly(vinyl alcohol) (PVA)/chitin/nanocellulose composites were synthesized. The composites were reinforced by oil palm empty fruit bunch fibers (OPEFB)-derived nanocrystalline cellulose (NCC). With addition of 1 wt.% NCC, a maximum improvement of 57.64% and 50.66% in tensile strength and Young's Modulus were achieved, respectively. However, the PVA-based composites exhibited low resistance in aqueous medium. Hence, maleic acid (MA) was incorporated, in view of modifying PVA-based composites through cross-linking reactions. The effect of varying chitin content (10 wt.%-30 wt.%) and MA content (10%-50% based on total solid content of composite) towards the swelling, gel content and contact angle of the PVA/Chitin/NCC composites were evaluated. The effect of PVA-based composite composition, solution pH, adsorbent dosage and initial dyes concentration on removal of methylene blue (MB) as model cationic dye from aqueous solution were investigated by batch adsorption studies. The best adsorption performance was determined for PVA/Chitin-10/NCC/MA-30 sample after experimental parameters were optimized, with the calculated maximum adsorption capacity amounted to 467.5 mg/g. The adsorption kinetics were determined to be of pseudo-second order. From thermodynamic studies, it was found that the adsorption processes were spontaneous, exothermic and less-ordered reactions. Lastly, the PVA/Chitin-10/NCC/MA-30 adsorbent showed high adsorption reusability since the adsorption percentage was retained at 83.67 ± 1.08% even at the fifth adsorption-desorption cycle.

Keywords: Poly(vinyl alcohol), chitin, cellulose, dye, adsorption

KOMPOSIT POLI(VINIL ALKOHOL)/CHITIN/SELULOSA DIPEROLEHI DARIPADA TANDAN KOSONG BUAH KELAPA SAWIT (OPEFB) DALAM PENGALIHAN PEWARNA KATIONIK

ABSTRAK

Demi memperokai komposit yang mesra alam untuk applikasi dalam perawatan effluen pewarna, komposit Poli(vinil alkohol) (PVA)/chitin/selulosa telah disediakan. Komposit tersebut adalah diperkukuhkan oleh selulosa bersaiz nano yang diperolehi daripada tandan kosong buah kelapa sawit (OPEFB). Dengan penambahan 1% selulosa bersaiz nano, peningkatan sebanyak 57.64% serta 50.66% dari segi kekuatan tegangan dan modulus Young telah tercapai. Walaupun sedemikian, komposit tersebut mempunyai rintangan rendah dalam larutan akueus. Oleh itu, asid maleic (MA) telah diperkenalkan untuk mengubai suai komposit berasaskan PVA melalui tindak balas perangkaian silang. Kesan-kesan yang disebabkan oleh kandungan chitin (10% -30% berat) dan kandungan MA (10%-50% berat berdasarkan jumlah kandungan pepejal komposit) kepada pembengkakan, kandungan gel dan sudut sentuhan PVA/Chitin/NCC komposit telah dinilaikan. Kesan-kesan daripada komposisi komposit berasaskan PVA, pH larutan, dos penjerap dan kepekatan asal pewarna kepada pengalihan pewarna contoh kation metilena biru (MB) dari larutan akueus adalah diterokai melalui cara penjerapan kelompok. Prestasi penjerapan yang terbaik adalah dikecapi oleh PVA/Chitin-10/NCC/MA-30 setelah parameter eksperimen telah dioptimumkan adalah sebanyak 467.5 mg/g. Kinetik penjerapan telah ditentukan sebagai kinetik pseudo-kedua. Daripada kajian termodinamik, ia adalah didapati bahawa proses penjerapan adalah reaksi spontan, eksotermik dan kurang peraturan. Akhirnya, penjerap menunjukkan kegunaan penjerapan semula yang tinggi kerana peratusan penjerapan adalah dikekalkan pada 83.67 ± 1.08% walaupun pada kitaran penjerapan-desorpsi kelima.

Kata kunci: Poli (vinil alkohol), chitin, selulosa, pewarna, penjerapan

ACKNOWLEDGEMENTS

First and foremost, I would like to dedicate my appreciation to University of Malaya for providing the financial grants and research ammenities for this research study.

Secondly, I would like to express my greatest gratitude to my research project supervisors, which are Associate Professor Ir. Dr. Ching Yern Chee, Dr. Farina Binti Muhamad and Professor Ir. Dr. Noor Azuan Bin Abu Osman. I am really grateful for their patience, inspirations, encouragements, financial supports, technical advices and knowledges shared. Their unconditional guidances and advices had help me to successful completion of this research work.

Besides, I am sincerely grateful to my friends who support and help me througout the study. They are Ms. Elaine Choo Hui Wen, Ms. Yee Yin Yin, Ms. Lim Kar Min, Mr. Tee Yee Siang and Mr. Choh Jing Lang. Appreciation is also dedicated to Ms. Goh Kar Yin, Mr. Mhd. Ahd. Cader Mhd. Haniffa and Mr. Sampath Gunathilake for discussions shared.

My sincere thanks also go to the staffs of University of Malaya for their assistance towards the success of this research. I have gained fruitful experiences and guidances from them for various lab conducts.

Last but not least, I would like to express my gratitude to my siblings for their kind considerations. Special thanks to my parents, Mr. Mok Choi and Mdm. Ng Kiew Mooi for their endless support and love.

TABLE OF CONTENTS

CHAPTER 4: RESULTS AND DISCUSSION 112

LIST OF FIGURES

LIST OF TABLES

LIST OF SYMBOLS AND ABBREVIATIONS

α : Alpha

β : Beta

γ : Gamma

a : Reaction order for example chemical species X

A : Adsorbate in solution

A_{ads} : Surface area per unit gram of adsorbent

A_o : Number of active sites available on the adsorbent

A_t : Number of occupied active sites of the adsorbent at time t

a.u. : Arbitrary units

b : Reaction order for example chemical species Y

°C : Degree Celsius

C_o : Initial concentration of adsorbate

C_A : Concentration of adsorbate in solution at equilibrium

C_{ad} : Concentration of adsorbate onto the adsorbent at equilibrium

cal. : Calculated

cm : Centimetre

Da : Dalton

D90 : 90% of the particles

Endo. : Endothermic

exp. : Experimental

F_0 : Fisher's ratio

g : Gram

ΔG^o : Standard Gibbs free energy change of adsorption

ΔH^o : Standard enthalpy change of adsorption

ΔH_f	:	Enthalpy change of fusion
ΔH_M	:	Mean site energy of adsorption
h	:	Hour
J	:	Joule
k	:	Rate constant
k_1	:	Rate constant of pseudo-first order kinetic model
k_2	:	Rate constant of pseudo-second order kinetic model
K_{ads}	:	Adsorption equilibrium constant
K_F	:	Freundlich isotherm constant related to adsorption capacity
K_L	:	Langmuir constant
K_c	:	Thermodynamic equilibrium constant
kV	:	Kilo-volts
kDa	:	Kilodalton
M	:	Molar
MW	:	Molecular weight
mg	:	Milligram
min	:	Minute
mm	:	Millimetre
mL	:	Millilitre
N	:	Newton
1/n	:	Freundlich adsorption intensity parameter
nm	:	Nanometre
p	:	Para
P	:	P value
pH	:	Potential hydrogen
pH_{pzc}	:	Point of zero charge

pKa : Acid dissociation constant

q_A : Amount of adsorbate adsorbed per gram of adsorbent at equilibrium

$q_{A\ (cal.)}$: Calculated equilibrium uptake by the adsorbent

$q_{A\ (exp.)}$: Experimental equilibrium uptake by the adsorbent

q_t : Amount of adsorbate adsorbed per gram of adsorbent at time t

q_M : Maximum adsorption capacity of adsorbate per gram of adsorbent

R : Universal gas constant

R^2 : Correlation coefficient

R_L : Dimensionless equilibrium parameter for Langmuir’s isotherm

RH : Relative humidity

rpm : Rounds per minute

ΔS^o : Standard entropy change of adsorption

s : Seconds

SA : Adsorbate-bounded surface sites

S_T : Total number of adsorption site

S_v : Vacant surface sites

T : Absolute temperature

T_g : Glass transition temperature

T_m : Melting temperature

TSC% : Percentage of total solid content

µL : Microlitre

µm : Micrometre

V : Volume

vol. % : Percentage by volume

w : Weight fraction

W_d : Dry weights of sample

W_f : Final dry weights of sample

W_i : Initial dry weights of sample

W_s : Initial weight of OPEFB raw fibers used

W_w : Swollen weights of sample for swelling test

wt. % : Weight percentage

[X] : Concentration of chemical species X

X_c : Degree of crystallinity

[Y] : Concentration of chemical species Y

APS : Ammonium persulfate

ASTM : American society for testing and materials

ATP : Attapulgite

ATR : Attenuated total reflection

BC : Before Christ

Co. : Company

DSC : Differential scanning calorimetry

DMA : Dynamic mechanical analysis

DMTA : Dynamic mechanical thermal analysis

FTIR : Fourier transform infrared spectroscopy

GA : Glutaraldehyde

Ltd. : Limited

MA : Maleic acid

MB : Methylene blue

MW : Molecular weight

NCC : Nanocrystalline cellulose

OPEFB : Oil palm empty fruit bunch

PVA : Poly(vinyl alcohol)

PEO	:	Poly(ethylene oxide)
SA	:	Adsorbate-bounded surface sites
SEM	:	Scanning electron microscopy
TGA	:	Thermogravimetry analysis
U.S.A.	:	United States of America
UV-Vis	:	Ultraviolet-visible

LIST OF APPENDICES

CHAPTER 1: INTRODUCTION

1.1 Introduction

Water pollution is becoming a major threat around the world due to industrialization. Remarkable amount of dyes is discharged regularly from various industries which include textile, paper-making, pharmaceuticals, tannery and dyes. Without proper treatment, dyes expelled to the water channel and resource system would pose severe threat to both environment and humans. This is because most dyes will remain unchanged in the environment for a long time, if left untreated (Carmen & Daniela, 2012). The presence of even trace amount of dyes is aesthetically unacceptable, and its presence is easily recognized in wastewater due to its color. Moreover, the water turbidity resulted from dyes would lead to reduction of reoxygenation capacity of the receiving water since sunlight is cutoff from plants or algae. As a result, oxygenic photosynthesis of aquatic plants or algae is hindered which disrupts the balance of ecosystem (Carmen & Daniela, 2012; Zaharia et al., 2009). In addition, it is alarming to note that most dyes are toxic, mutagenic and carcinogenic towards living organisms (Golka et al., 2004; Yahagi et al., 1975).

Treatment of dyes effluent is challenging due to the reason that some dyes do not decompose in the effects of heat and light, oxidizing agents or aerobic digestion. Conventional wastewater treatments consist of physical, chemical and biological treatment measures such as chemical coagulation, activated sludge, trickling filter, carbon adsorption and photo-degradation are applied for the removal of dyes (Dhananasekaran et al., 2016; Yagub et al., 2014). However, adsorption process is a favorable and attractive proposition for the treatment of dyes effluent (Yagub et al., 2014). It is a cost effective, simple and effective method to remove dyes from the effluents. Dyes adsorption is a process of transfer of dye molecules from bulk solution phase to the surface of the adsorbent. In recent years, polymeric adsorbent is gaining more interest over classical adsorbents such as clays and activated carbon due to its tunable physicochemical properties, structural diversity, reusability and selectivity. The application of polymers or polymer-based composites as the adsorbents in the removal of cationic or anionic dyes can be found in literature (Rashidzadeh & Olad, 2013; S. Umoren et al., 2013; X. Yang et al., 2016). Therefore, an attempt will be made to study the adsorption of dye by a poly(vinyl alcohol) (PVA)-based composite which acts as the adsorbent.

PVA, chitin and cellulose respectively had been recognized as an adsorbent by previous researchers. In view of this, this study serves to investigate the unique combinations comprised of the materials in the form of PVA/chitin/nanocrystalline cellulose (PVA/Chitin/NCC) composite for the dye adsorption process. PVA is a raw material of vinylon and can be mass produced inexpensively. PVA also offers various advantages such as high durability, biocompatibility, good tensile strength and degradability (Ghemati & Aliouche, 2014; Rashidzadeh & Olad, 2013; X. Yang et al., 2016). Besides, PVA has been proven to be serving as an adsorbent for heavy metal ions, anionic and cationic dyes due to the abundance of free hydroxyl (-OH) and acetate ($-O-CO-CH_3$) groups residing on the PVA polymeric chains (Agarwal et al., 2016; Rashidzadeh & Olad, 2013; Wiśniewska, 2012). In addition, PVA has been reported to be modified by cross-linkers and blended with other polymers for the adsorption of dye molecules. PVA had been incorporated with materials such as zeolites (Baheri et al., 2016; Rashidzadeh & Olad, 2013), polyaniline (Rashidzadeh & Olad, 2013), clays (Kamal, 2014; L. Yang et al., 2011), graphene oxide (X. Yang et al., 2016) and others (Casey & Wilson, 2015; Ghemati & Aliouche, 2014; Pour & Ghaemy, 2015; Safa & Bhatti, 2011) in search of advanced adsorbent. Furthermore, PVA is also reported to increase the adsorption property of chitosan, which is a derivative of chitin. This is attributed to the higher content of hydroxyl (-OH) and amine ($-NH_2$) groups of chitosan/PVA blend as compared to neat PVA (Muhd Julkapli et al., 2011).

In view of this, blending of synthetic PVA and natural polymers served as a viable approach in an effort to obtain PVA-based composites with improved functionalities and physicochemical properties. This is because polymer blending has been regarded as an effective way of altering and improving the physicochemical properties of a polymer material (J. S. Park et al., 2001; Zhu et al., 2013). Among the natural polymers, chitin or poly(N-acetyl-D-glucosamine) is the second most abundant high molecular weight polysaccharide after cellulose which is less being studied (J. Li et al., 1997). Chitin exhibits naturally in three distinct crystal structures, which are the α-chitin, β-chitin, and γ-chitin, respectively (Y. M. Lee et al., 1996; Peesan et al., 2003). Extraction of economically available α-chitin from crustacean exoskeleton shells and its utilization in wastewater treatment could be a sustainable solution for reducing the seafood shells waste (Filipkowska & Rodziewicz, 2009).

Several merits of this material is that it is naturally available, cheap, biodegradable and non-toxic material (Lesbani et al., 2015). Moreover, chitin possesses antioxidant and antibacterial properties. It also displays traits as a good chelating agent. Chitin is more hydrophobic in nature with the presence of acetyl amine ($-NHCOCH_3$) along with amine ($-NH_2$) and hydroxyl (-OH) functional groups (Zargar et al., 2015). These functional groups would serve as the active binding sites for adsorption. Mechanical properties of chitin can be improved through blending with PVA which is high in tensile strength and durability. Hence, it is envisioned that blending of chitin with PVA served as to capitalize selected advantages characteristics of both types of polymers.

In addition, polymeric materials can acquire significantly improved mechanical properties if they exhibit multi-component phase separated morphology at the nanoscale (Dasari et al., 2005; Kietzke et al., 2003). The extent of improvement is governed by the microstructure represented by the size and homogeneity of the reinforcement in the polymeric matrix (Dasari et al., 2005; Kojima et al., 1993). Thus, cellulose extracted from oil palm empty fruit bunch (OPEFB) fiber is suitable to be incorporated into the polymeric blend for reinforcement due to its low cost but high specific strength and good thermal properties (Lani et al., 2014). Previous studies have shown that the tensile strength of PVA films could be efficiently reinforced by nano-sized cellulose even at 1 wt.% loading (S.-Y. Lee et al., 2009; Nigrawal et al., 2012). However, nanocellulose prepared from different resources, such as Kenaf fibers (Shi et al., 2011), microcrystalline cellulose (S.-Y. Lee et al., 2009) and cotton linter (Roohani et al., 2008) contributed to different reinforcements in the PVA matrix. Furthermore, cellulose which acts as the filler is biodegradable. Its density is low which implies that the polymer composites would exhibit higher mechanical performance while remaining lightweight.

However, some of the PVA-based composites can be used only after cross-linking since partially hydrolyzed PVA has high water solubility. Cross-linking of PVA-based composite could be performed based on the chemical reaction of dialdehydes (Abdeen, 2011), dicarboxylic acids (Riyajan et al., 2009; Viyapuri Rubentheren et al., 2015; Z. Xie et al., 2011) or sodium tetraborate (J. Han et al., 2013) with the free hydroxyl groups in composite. Our interest is towards a simple functionalization method. Hence, reaction involved dicarboxylic acid is intended for this current work. In this work, cis-butenedioic acid or better known as maleic acid (MA) will serve as the cross-linker of the composites through esterification reaction. Adsorption property of the composite can be further improved with the electron-rich olefinic functional groups presence in MA introduced which contribute to more active binding sites for dyes. In brief, composite materials offer advantages in this application due to improvements in stability, chemical properties and mechanical strength relative to the properties of the single component (Casey & Wilson, 2015; Rashidzadeh & Olad, 2013). Moreover, it is essential to utilize a facile technique to effectively immobilize the adsorbent in an optimized manner that could eliminate the costly and time-consuming phase separation process (F. Li et al., 2009). Therefore, flat films of adsorbent is advantageous over bead-sized adsorbent in preparation due to its simplicity, lower production cost and ease of handling during recycling (Lin et al., 2012; Xin Luo et al., 2016).

In the present research, PVA/Chitin/NCC composites were first prepared and characterized in terms of physicochemical, thermal as well as mechanical properties. Methylene blue (MB) is considered as a standard cationic dye and the adsorption performance of the composites towards MB were analyzed. The utility of PVA/Chitin/NCC composite for environmental remediation or monitoring applications is proposed due to the associated versatile mechanical properties and ability to cast into various shapes. The adsorption process is dependent on the composition of PVA/Chitin/NCC composite, solution pH, initial dye concentration and adsorbent dosage loaded with the dye. The isotherm models are used to confirm that PVA/Chitin/NCC composite could be used as a suitable adsorbent material for the removal of dyes from effluents. The results reported herein will contribute to a greater understanding of the adsorptive properties of such composite materials and extend the utility of such materials for adsorptive-based applications, especially in dye effluent treatment.

1.2 Problem Statement

Conventional wastewater treatment methodologies used for the removal of dyes contaminants comprised of physical, chemical and biological approaches. These include chemical coagulation, activated sludge, membrane filtration, adsorption and photo-degradation. Despite this, each process is associated to some drawbacks. Biological treatment which involves the use of microorganisms such as algae, fungi and yeast could be restricted due to technical constraints. The constraints of the biodegradation system are that it requires large tracts of land space for optimal effects, sensitivity toward temperature and time consuming. Other processes which involve chemical treatments such as coagulation, flocculation, oxidation and precipitation would lead to secondary pollution. In addition, oxidizing agents used for oxidation are often expensive. Nonetheless, physical method such as membrane filtration shows disadvantages during application as well. This is because membrane fouling could occur, and periodic replacement of membrane is costly. Hence, the adsorption process remains as a favorable and attractive manner for the treatment of dyes contaminated water.

Dyes adsorption is a process whereby dye molecules are transferred from bulk solution phase and attached on the adsorbent. This is mainly associated to the ease of operation, insensitivity to toxic pollutants, low cost, flexibility and simplicity of operation designs. Furthermore, the utilization of adsorbents for adsorption process does not result in the formation of harmful substances. Examples of conventional adsorbents are commercial activated carbon and synthetic ion-exchange resins. However, activated carbon adsorbent presents some limitations such as hydrophobicity, non-selectivity, high initial cost and poor reusability. Activated carbon displays poor reusability because high thermal cost is incurred to reactivate the saturated activated carbon’s adsorption sites. When activated carbon is treated by thermal volatilization, 5%-10% of the active sites could be lost by burn-off and attrition during each cycle of thermal treatment (Chowdhury, 2013; Lim & Okada, 2005). As for synthetic ion-exchange resins, the adsorption application are often limited due to its poor contact with aqueous pollutants and modification is required to improve its wettability. Another drawback of the synthetic resins is that it is sourced from fossil fuel-based raw materials only.

Polymeric adsorbent served as an attractive alternative over classical adsorbent such as activated carbon due to its tunable physicochemical properties, structural diversity and reusability (Kamal, 2014; Mohy Eldin et al., 2016; S. Umoren et al., 2013). Therefore, an attempt will be made by using unique combinations of PVA/Chitin/NCC composites which acts as the polymeric adsorbent (Dhananasekaran et al., 2016). Utilization of PVA/Chitin/NCC polymeric adsorbent offers advantages due to enhancement in stability, physicochemical and mechanical properties relative to the properties of a single component (Casey & Wilson, 2015). This would be beneficial to be used as adsorbent for the removal of dyes from wastewater.

Furthermore, utilization of synthetic PVA and natural polymer such as chitin and nanocellulose is an interesting approach in an effort to obtain a compatible composite with advantages of environmental sustainability and durability. PVA is a degradable and biocompatible polymer despite of its synthetic origin. However, PVA has been reported to have high water solubility in water based on its degree of hydrolysis, molecular weight and tendency of PVA in forming hydrogen bond in aqueous mediums (Hassan et al., 2002). Therefore, insolubilization of PVA-based composite is imperative to be achieved through modification reactions such as heat treatment (Gohil et al., 2006; J.-C. Park et al., 2010; Sriupayo et al., 2005), radiation (Mishra et al., 2007), hybridization with inorganic components (Z. Xie et al., 2011), and cross-linking (Abdeen, 2011; Gohil et al., 2006; R. A. Lusiana et al., 2013; Peresin et al., 2014; Riyajan et al., 2009) to obtain a more stabilized component. Among the modification techniques, cross-linking is the more direct and common approach which provides inherent advantage of further enhancing the functionality and selectivity of composites. Hence, maleic acid (MA) is to be introduced as the cross-linker in this work. In addition, the extraction of chitin and nanocellulose will help in reducing waste disposal problem associated to the respective origin raw materials. In this study, the origin of raw materials being used are chitin derived from the crustacean exoskeleton shells waste and the nanocellulose which is extracted from oil palm empty fruit bunch (OPEFB) fibers.

1.3 Research Objectives

The main aim of this research is to develop a novel PVA-based composite for potential application in removal of model cationic dyes through adsorption. In order to achieve this, the following objectives are pursued:

i. To evaluate the effects of NCC loaded on the mechanical and physicochemical properties of the PVA/Chitin/NCC composite, corresponding to the role of NCC loaded as the reinforcing fillers.

ii. To study the effects of chitin loading with maleic acid content on the mechanical, physicochemical properties and adsorption capacity of the PVA/Chitin/NCC composite.

iii. To evaluate the effects of dyes solution's pH, initial dyes concentration and adsorbent dosage on the adsorption capacity of the selected PVA/Chitin/NCC composites through batch adsorption studies. The isotherm, kinetics and thermodynamics parameters of the selected composite adsorbents under investigation were evaluated.

1.4 Scope of Studies

The overall aim of this research is to develop a novel PVA-based composite for potential application in removal of model cationic dyes through adsorption. For this reason, PVA/Chitin/NCC composites which were reinforced by oil palm empty fruit bunch (OPEFB) fibers-derived nanocrystalline cellulose (NCC) were first prepared. NCC was extracted from the OPEFB fibers with the aid of ammonium persulphate which acted as the oxidant. The effects of NCC loaded on the mechanical properties of the PVA/Chitin/NCC composite, corresponding to the role of NCC loaded as the reinforcing fillers were evaluated using the universal tensile machine. PVA/Chitin/NCC composites were also characterized by using several analytical techniques which include Fourier transform infrared (FTIR) spectroscopy analysis, differential scanning calorimetry (DSC) analyses and field emission scanning electron microscopy (FESEM) to confirm on the interaction of the NCC with the PVA/Chitin matrices. Selected physicochemical properties (swelling, water solubility, gel content and contact angle) of the selected PVA/Chitin/NCC composites were also being evaluated. It was to investigate the effect of PVA/Chitin/NCC composites in aqueous medium, when chemical cross-linker were not incorporated.

Based on the findings, it was determined that PVA-based composite came with a drawback which was being not resistant in water. Hence, insolubilization of PVA-based composites were proposed through modification reaction which involve chemical cross-linking using maleic acid (MA). In this research, cis-butenedioic acid or better known as MA was intended to serve as the cross-linker of the composite through esterification reaction. FTIR study was utilized to investigate the interactions of the cross-linker to the polymeric networks. Besides, thermal transitions of the cross-linked composites were assessed by DSC. The effect of varying chitin content (10 wt.%-30 wt.%) and MA content (10%-50% based on total mass of composite) towards the mechanical properties and selected physicochemical properties (swelling, water solubility, gel content and contact angle) of the MA cross-linked PVA/Chitin/NCC composites were also examined.

Furthermore, the adsorption performances of MA cross-linked PVA/Chitin/NCC composites were analyzed using a model cationic dye which was the MB dye. FTIR analysis was used to identify the chemical changes incurred on the PVA/Chitin/NCC composite when MB dye was attached on the adsorbent. By utilizing the pH drift method, the basic or acidic nature of the selected composite adsorbents could be indicated by the point of zero charge (pH_{pzc}). The effects of composite composition, solution pH, initial dye's concentration and adsorbent dosage on dyes removal capabilities of the selected PVA/Chitin/NCC composites were investigated. In addition, isotherm, kinetic, thermodynamic and reusability studies of the selected PVA/Chitin/NCC composite samples were also tabulated. This work contributes to a greater understanding of the adsorptive properties of PVA/Chitin/NCC composites and promotes the utility of this alternative adsorbent for the application of dyes removal from aqueous solution.

1.5 Thesis Outline

This report comprised of five chapters, as follows:

Chapter 1 provides an overview of the importance of dye effluent treatment through adsorption process. The application of PVA-based composite in dyes removal was discussed. The problem statement and philosophy of the research work were stated, followed by the objectives of the research and finally the composition of this thesis.

Chapter 2 discusses the literature review of polymers, colorants and dyes removal technique utilized in the present study. The inherent characteristics of PVA, chitin and cellulose were discussed. In addition, the polymer cross-link options of PVA-based composites were disclosed. Previous works on PVA-based composites for the application of dyes removal from other researchers were also reviewed. Furthermore, adsorption studies based on the individual polymer were reported. Overview of colorants and classification of dyes were remarked. In addition, the characteristics of MB and its effects towards human and environment were reported. Lastly, the theories of dyes removal through adsorption were discussed.

Chapter 3 discloses the detailed research methodologies in preparing the nanocellulose sourced from oil palm empty fruit bunch (OPEFB) and chitin. Preparation of PVA/chitin/nanocellulose and PVA/chitin/nanocellulose treated with maleic acid (MA) were disclosed in detail. Detailed experimental procedures in characterizing the PVA-based composites in terms of physicochemical, mechanical and morphological were reported. Last but not least, the methodologies used to evaluate the adsorption performance of the composite towards MB using the batch adsorption studies were discussed.

Chapter 4 is mainly focused in presenting the results obtained after the characterizations of the composites. The chemical changes of the composites before and after introduction of MA were investigated and discussed. Swelling and water solubility properties of PVA-based composites were investigated to examine the behavior of the composites under aqueous condition. Mechanical properties of the composites were monitored to determine the effects of chitin, NCC and MA towards the composites. Morphological analyses were reported to discuss the surface morphology of the composites. Finally, the composites were subjected to adsorption studies to evaluate the performance in dyes removal. The effect of composite's composition, dyes solution's pH, initial dyes concentration and adsorbent dosage on the adsorption capacity of PVA/Chitin/NCC composite were evaluated. Studies to evaluate the adsorption isotherms, kinetics and thermodynamic behaviors of the adsorbate-adsorbent systems were included. All the detailed analysis of each result was discussed.

Chapter 5 concludes research findings of this work. In addition, recommendations of future works were discussed to further improve the composite for potential application in removal of dyes from wastewater.

CHAPTER 2: LITERATURE REVIEW

2.1 Poly(vinyl alcohol) and Its Chemical Structure

Poly(vinyl alcohol) (PVA) is a semi-crystalline synthetic polymer with chemical formula as $[CH_2CH(OH)]_n$. PVA is white and odorless. PVA is commonly found in powder form, but sometimes it is also distributed in the beads or solutions forms. The molecular weight (MW) of PVA products is in the range of 20,000 Da to 400,000 Da. The variance of MW is due to the synthesis parameters such as the initial chain length of vinyl acetate polymer, the extent of hydrolysis to reduce the acetate groups and whether the hydrolysis is allowed under alkaline or acidic conditions (DeMerlis & Schoneker, 2003; Gaaz et al., 2015).

PVA can be synthesized by hydrolysis from varieties of poly(vinyl esters) and poly(vinyl ethers). However, most commercially available PVA is synthesized through partial or complete hydrolysis of poly(vinyl acetate) (see Figure 2.1). This is because monomer of vinyl alcohol is not stable at standard ambient temperature and pressure. The vinyl alcohol monomers exhibit great tendency to form into acetaldehyde due to keto-enol tautomerism. Keto-enol tautomerism is defined as a chemical equilibrium established between a keto form (a ketone or an aldehyde) and an enol (an alcohol). Enol is characterized as an alcohol which contains a pair of doubly bonded carbon atoms adjacent to a hydroxyl (-OH) group, -C=C-OH. A compound containing a carbonyl group (C=O) such as ketone or aldehyde is generally in rapid equilibrium with an enol tautomer due to the movement of an alpha hydrogen atom (electrons donor) and the reorganisation of bonding electrons (Alavudeen et al., 2006). Hence, PVA is synthesized by first polymerizing vinyl acetate to poly(vinyl acetate) through radical polymerization, followed by hydrolysis of poly(vinyl acetate) to PVA (Hallensleben et al., 2000; Marin et al., 2014).

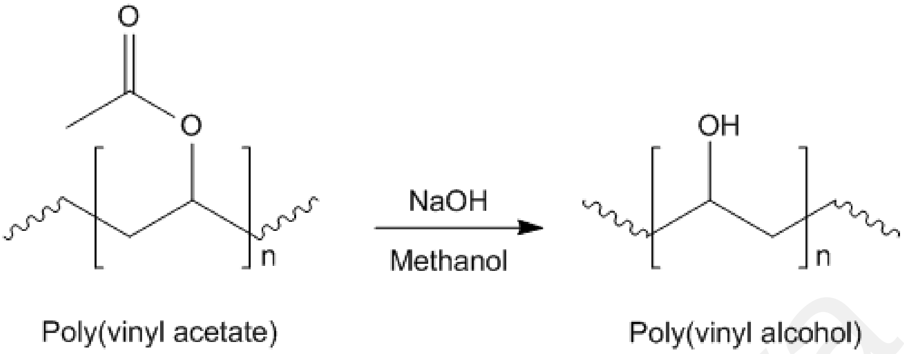

Figure 2.1: Hydrolysis of polyvinyl acetate to obtain polyvinyl alcohol.

The higher the degree of hydrolysis and polymerization of the PVA, the lower it is in terms of crystallinity as well as solubility in water. PVA is commercially graded according to its degree of hydrolysis and viscosity. PVA are generally grouped into partially hydrolyzed grades range (84.2%-89.0%), moderately hydrolyzed grade (92.5%-96.5%) and the completely hydrolyzed grade (98.0%-99.0%) (Marin et al., 2014). Figure 2.2 illustrates the structural formula for PVA which is partially or moderately hydrolyzed and completely hydrolyzed, respectively.

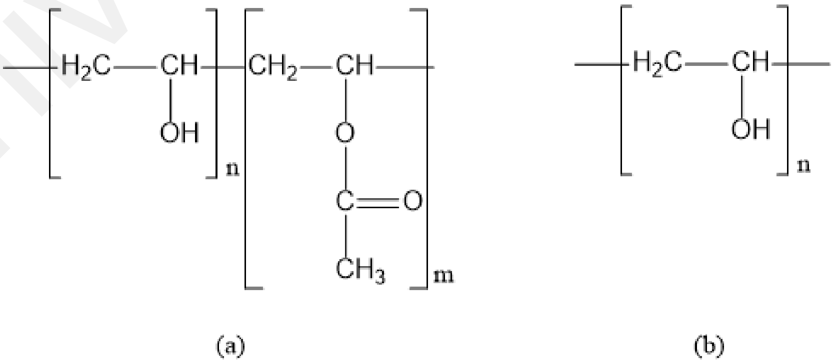

Figure 2.2: Structural formula for PVA which is (a) partially or moderately hydrolyzed and (b) completely hydrolyzed.

In fact, the degree of hydrolysis is the determining factors on the physical, chemical and mechanical properties of the resulting PVA. This is because the properties of the polymer are corresponding to the content of residual ester groups in PVA (DeMerlis & Schoneker, 2003; Gaaz et al., 2015). PVA is an atactic polymer which consists of high crystallinity. From the viewpoint on microstructure, PVA is primarily constituent of 1,3-diol units [-CH_2-CH(OH)-CH_2-CH(OH)-]. However, the content of 1,2-diol units [-CH_2-CH(OH)-CH(OH)-CH_2-] could vary between 1%-2%, depending on the polymerization condition of the vinyl ester precursor (Hallensleben et al., 2000).

2.1.1 Properties of PVA

Being a good formability material, PVA has been fabricated into various forms and sizes. These include films and coatings that have high tensile strength, flexibility, as well as high oxygen and aroma barrier properties. However, properties such as tensile strength, elongation at break and barrier properties are dependent on humidity. This is due to the hygroscopic nature of PVA, which results in higher water moisture absorbed by PVA when the humidity is high. The water retained in PVA, which acts as a plasticizer will eventually reduce PVA film's tensile strength and Young's modulus but increases its elongation at break.

PVA is a semi-crystalline polymer with high degree of swelling, biodegradability, nontoxicity, adhesiveness, bio-inertness, non-carcinogenicity thus making it as a promising biomaterial. Despite of its water solubility, PVA appears resistant to most organic solvents, oil and grease (DeMerlis & Schoneker, 2003; Lani et al., 2014; Marin et al., 2014; Pavaloiu et al., 2014).

It is important to determine the thermal properties of PVA polymer as it provides indication on the processing conditions for the desired end application. On elevated temperature, PVA undergoes glass, structural and melting transitions before decomposing at high temperature.

In terms of glass transition temperature (T_g), it is generally determined to be at the 80°C-85°C region. However, T_g of PVA is dependent on the structures of PVA which varies in terms of degree of hydrolysis and molecular weight. Moreover, T_g decreases as the exposure to relative humidity (RH) increases owing to the plasticizing effect of water molecules for PVA chains (Rault et al., 1995; Roohani et al., 2008). Previous works showed that T_g values corresponding to the two different completely hydrolyzed PVA films which were conditioned at 0% RH and 35% RH, were determined to be at 40°C-48°C and 46°C-51°C, respectively. For films made from partially hydrolyzed PVA grade, T_g were determined to be at 71°C-59°C and 45°C-50°C regions when the films were conditioned at 0% RH and 35% RH, respectively (Roohani et al., 2008).

Furthermore, melting point (T_m) of PVA is dependent on degree of hydrolysis of PVA. For completely hydrolyzed PVA grade (98.0%-99.0%), Cho et al. (2001) determined that the T_m was at around 230°C. Contrarily, T_m of PVA was found at the range of 180°C-190°C for partially hydrolyzed PVA grade (84.2%-89.0%). On the other hand, PVA was found to be susceptible to decomposition when exposed to heating temperature of above 270°C as it underwent pyrolysis at high temperature (Peesan et al., 2003; Tubbs, 1965).

2.1.2 Application of PVA for Adsorption of Dyes

PVA exhibits adsorption properties owing to the presence of abundant hydroxyl groups. It was proven that the free hydroxyl groups of PVA could serve as the adsorption sites for heavy metal ions, anionic dyes and cationic dyes (Rashidzadeh & Olad, 2013; X. Yang et al., 2016). Previous works had elucidated the effectiveness of neat PVA in the removal of bromothymol blue and methylene blue from wastewater (Agarwal et al., 2016; S. Umoren et al., 2013). Table 2.1 summarizes the adsorption studies of abundant types of dyes onto PVA.

Table 2.1: Adsorption studies of abundant types of dyes onto PVA.

Adsorbent Name	Name of dyes	Adsorbent Dosage (g/L)	Initial Dyes Concentration (mg/L)	Solution pH	Maximum adsorption capacity (mg/g)	References
Poly(vinyl alcohol)	Methylene blue	4	25	4	13.80	(S. Umoren et al., 2013)
Poly(vinyl alcohol)	Bromothymol blue	-	30	6	276.20	(Agarwal et al., 2016)
Poly(vinyl alcohol)	Methylene blue	-	30	6	23.30	(Agarwal et al., 2016)
Poly(vinyl alcohol) hydrogel	Crystal violet	140	4	-	-	(Papancea & Patachia, 2015)
Poly(vinyl alcohol)	Methylene blue	140	26	-	-	(Papancea & Patachia, 2015)
Poly(vinyl alcohol)	Congo red	140	14	-	-	(Papancea & Patachia, 2015)

The study on the unmodified PVA as an adsorbent for methylene blue dye from wastewater has been carried out at 303 K-333 K by S. Umoren et al. (2013). The results revealed that the maximum adsorption capacity of PVA was 13.80 mg/g at 303 K. The experimental settings were varied. Moreover, the adsorption data were found statistically well correlated to Langmuir, Freundlich and Temkin adsorption isotherm models. As for the research attempted by Agarwal et al. (2016), the authors discovered that the maximum adsorption capacities of PVA obtained from Langmuir model were 276.2 mg/g and 123.3 mg/g for bromothymol blue and methylene blue, respectively. Based on the optimization studies conducted, highest removal efficiency was achieved at pH 6. In terms of removal efficiency for bromothymol blue and methylene blue, it was determined to be 98.65% and 61.32%, respectively.

Furthermore, PVA hydrogel membranes were subjected to diffusion using different type of dyes such as Crystal Violet, Methylene Blue, Congo Red (Papancea & Patachia, 2015). This study was different from the conventional approach which utilized UV-Vis spectrophotometer to identify the dye concentration in the supernatant through a calibration curve prepared from a series of MB standard solution. In this study, the color differences of the dyes loaded hydrogels were monitored through CIEL*a*b* system. Through this system, it allows researchers to make difference between two very close colors by considering parameters such as hue, saturation and luminosity. However, the authors only derived simple kinetic study from this colorimetric analysis approach and there was no discussion on external parameters which could affect the adsorption studies.

Besides, PVA had been blended with other polymers and cross-linked to be applied as the adsorbents of dyes. Through this effort, it was determined that the composite adsorbents exhibited good chemical and mechanical properties (M Abd El-Latif et al., 2010; Rashidzadeh & Olad, 2013; Zendehdel et al., 2010).

2.2 Chitin and Its Chemical Structure

Chitin, a linear polysaccharide composed of (1-4)-linked 2-acetamido-2-deoxy-β-D-glucopyranose units is the second most abundant high molecular weight polysaccharide after cellulose (J. Li et al., 1997). Figure 2.3 illustrates the molecular structure for chitin. In addition, chitin is a rigid and inelastic nitrogenous polysaccharide which is white color in appearance.

Being a predominantly fibrillar crystalline material, chitin has three polymorphic crystal structures, known as α-chitin, β-chitin and γ-chitin, respectively (Y. M. Lee et al., 1996; Peesan et al., 2003). α-chitin is the most crystalline orthorhombic with the chains arranged in an anti-parallel and compact manner. Generally, α-chitin is extracted from the exoskeleton shells of crabs, lobsters and shrimps. Meanwhile, β-chitin sourced mainly from the squid pen has the monoclinic form arranged in parallel while γ-chitin is a mixture of α-chitin and β-chitin. In general, chitin is a biorenewable material with estimated annual production of 10 billion from abundance of natural resources such as algae, crustaceans, fungus, insects and other organisms (Zargar et al., 2015).

The immediate derivative for chitin is chitosan. Chitosan has a lower degree of acetylation (in the range of 5%-50%), in comparison to chitin. Chitosan is actually the deacetylated form of chitin, with amino group ($-NH_2$) in substitution to the acetamide group ($-NHCOCH_3$) at the C2 position of the glucopyranose structure. In chitin, the degree of acetylation is typically 50%-95%, indicating the presence of amino groups. Generally, chitosan is synthesized by deacetylation of α-chitin using 40%–50% of concentrated alkali solution under heat treatment at 100°C-160°C for a few hours (Khor, 2014; Zargar et al., 2015).

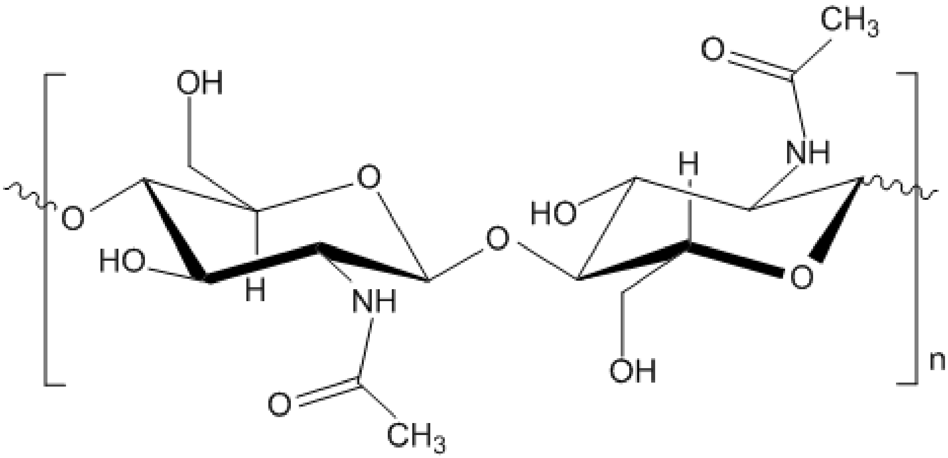

Figure 2.3: Molecular structure of chitin.

2.2.1 Properties of Chitin

Due to the extensive hydrogen bonding in the semi-crystalline structure of chitin, it is highly hydrophobic when untreated. Hence, neat chitin is insoluble in aqueous solution and common organic solvents. However, dissolution of chitin is reported to be possible in dimethylacetamide-5% lithium chloride solvents blend, hexafluoro-isopropanol, hexafluoroacetone and chloroalcohols-mineral acids solvents blend (M. N. R. Kumar, 2000). Although dissolution of chitin could be prompted with the strong solvating systems, but the used solvents also cause extensive de-polymerization of chitin. This limitation has been resolved with the introduction of dissolution of chitin in the mild conditions of calcium solvent system by other researchers (Tamura et al., 2006; Tokura et al., 1996).

Chitin is an example of basic polysaccharide with natural origins. The basicity of the chitin is ascribed to the amino group ($-NH_2$). The existence of the amino groups shows that solution pH considerably changes the charged state and properties of chitin. From literature, it is determined that free amino group which has pKa value of 5.5-6.3 acts as strong nucleophile when it is deprotonated (Casey & Wilson, 2015; Zargar et al., 2015). Generally, the free amines in chitin gain protons and become positively charged at solution pH lower than the pKa of chitin. This results in chitin becoming cationic. Contrarily, the free amines in chitin become deprotonated as the solution pH increased to above pKa of chitin. Then, chitin loses its charge and remains as a neutral polymer (M. N. R. Kumar, 2000; Zargar et al., 2015). Moreover, the presence of abundance reactive groups (-NH_2, -$NHCOCH_3$) in chitin render a greater functionality on chemical activation and cross-linking reactions. Besides, other properties of chitin include film forming capability, adsorption and chelating property. Being non-toxic, biodegradable and biocompatible, chitin also has proven records of boosting some biological activities such as antibacterial, immunological, healing and drug delivery (Jayakumar et al., 2011; M. N. R. Kumar, 2000; Younes & Rinaudo, 2015; Zargar et al., 2015).

Chitin is a semi-crystalline polymer. Therefore, T_g which is characteristic of an amorphous material could be expected. Despite this, it is controversial whether polysaccharides consist of T_g since T_g of many natural polymers are above the thermal decomposition temperature. From previous studies, many authors have not observed the T_g of chitin (González‐campos et al., 2009).

Nonetheless, it was reported that glass transition temperature (T_g) for α-chitin was assigned at 235°C with degradation temperature reported at 250°C-280°C (Kim et al., 1994). However, T_g value for neat chitin film could not be easily observed by differential scanning calorimetry (DSC) technique, as shown by some previous works (Cho et al., 2001; Kim et al., 1994; Peesan et al., 2003). Moreover, dynamic mechanical thermal analysis (DMTA) technique which is a more sensitive technique employed by Kim et al. (1996) had been successful in measuring the T_g of β-chitin, which was determined to be approximately 170°C. Other researchers also reported a surprisingly high value of T_g of 350°C-412°C for β-chitin, which showed a degradation temperature of 450°C (Chandumpai et al., 2004).

Natural polymer with a rigid-rod polymer backbone such as chitin consisted of crystallinity. However, it is worthy to note that melting temperature (T_m) of neat chitin is not easily determined under DSC analysis. Similar to characteristic of typical polysaccharide, chitin is susceptible to degradation before melting, which is due to the extensive hydrogen bonding (Kim et al., 1994; Younes & Rinaudo, 2015). In the work carried out by Peesan et al. (2003), it was found that β-chitin film portrayed two degradation peaks at 262°C and 349°C, respectively. In a separate work by Kim et al. (1994), the author reported that the thermal decomposition of α-chitin was expected at 250°C-280°C.

2.2.2 Application of Chitin for Adsorption of Dyes

The potential of chitin and its derivatives for the adsorption of metal ions, dyes and various other aquatic pollutants have been extensively reviewed by researchers previously (Bhatnagar & Sillanpää, 2009; Ngah et al., 2011). Chitin has attracted commercial interest for adsorption application due to its biorenewability and chelating properties. This is due to the high percentage of nitrogen atoms in chitin which makes it a useful chelating agent (M. N. R. Kumar, 2000). Table 2.2 shows the various studies conducted in recent years on evaluating the affinity of chitin and chitosan towards the many classes of dyes.

Table 2.2: Adsorption studies of abundant types of dyes onto chitin.

Adsorbent Name	Name of dyes	Adsorbent Dosage (g/L)	Initial Dyes Concentration (mg/L)	Solution pH	Maximum adsorption capacity (mg/g)	References
α-chitin	Methylene blue	1	10	6	6.90	(Dhananasekaran et al., 2016)
α-chitin	Bromophenol blue	1	15	6	22.72	(Dhananasekaran et al., 2016)
α-chitin	Coomassie brilliant blue	1	25	10	8.55	(Dhananasekaran et al., 2016)
Chitin	Reactive yellow 2	4	450	6	38	(Akkaya et al., 2007)
Chitin	Reactive black 5	4	450	8	65	(Akkaya et al., 2007)
Chitin	Indigo carmine dye	0.5	11	-	3.26	(Prado et al., 2004)
Untreated chitin	Reactive red 141	3	400	11	167	(Dolphen et al., 2007)
Sodium hypochlorite-treated chitin	Reactive red 141	3	400	11	124	(Dolphen et al., 2007)

Among the studies, the adsorption capability of α-chitin had been explored by utilizing the three major industrial dyes, namely bromophenol blue, coomassie brilliant blue and methylene blue (Dhananasekaran et al., 2016). Based on the work done on various experimental settings, the α-chitin sourced from shrimp waste portrayed as a simple, fast and low-cost alternative for efficient removal of the dyes being investigated. Upon analyzing the experimental data utilizing Langmuir isotherm and Freundlich isotherms, it was proven to be best fitted to the Langmuir isotherm. In the work, α-chitin showed adsorption capacities towards bromophenol blue, coomassie brilliant blue and methylene blue to the extent of 22.72 mg/g, 8.55 mg/g and 6.90 mg/g, respectively. Based on the kinetic studies, it was proven that the adsorption processes were of pseudo-second order.

Akkaya et al. (2007) examined the removal of reactive dyes by chitin through adsorption. In the work, the adsorption limiting factors such as initial dyes concentration, temperature, pH and orbital shaking frequency towards the adsorption of reactive yellow 2 as well as reactive black 5 using chitin were being evaluated. The result showed that the adsorption capacities for reactive yellow 2 was 38 mg/g at 293 K while for reactive black 5, it was 65 mg/g at 333 K.

In another study, adsorption studies were carried out utilizing both untreated chitin and sodium hypochlorite-treated chitin for the treatment of synthetic reactive dye wastewater. The untreated chitin was determined to be better adsorbent over the treated chitin at temperature from 30°C to 60°C. The untreated chitin showed improvement of adsorption capacity of Reactive Red 141 from 133 mg/g to 167 mg/g when the temperature varies from 30°C to 60°C. Contrarily, sodium hypochlorite-treated chitin showed reduction of adsorption capacity of Reactive Red 141 from 124 mg/g to 59 mg/g due to the temperature arisen (Dolphen et al., 2007).

Moreover, adsorption studies in batch mode of indigo carmine dye onto chitin and chitosan were investigated by Prado et al. (2004). According to the research, the affinities of the dyes towards the studied adsorbents were tested to be fitted with adsorption isotherms. It was determined that the adsorption capacities expressed in mole per gram for chitin and chitosan were $0.24 \pm 0.16\times10^{-5}$ mol/g and $1.54 \pm 0.03\times10^{-4}$ mol/g, respectively.

2.3 Cellulose and Its Chemical Structure

Cellulose is a natural polymer, a long chain made by the linking of sugar, β-D-glucose. In the cellulose chain, the glucose units are in 6-membered rings, called pyranoses. The glucose units are joined by single oxygen atoms (acetal linkages) in between C-1 of one pyranose ring and C-4 of the next ring (Kalia et al., 2011). Figure 2.4 shows the typical molecular structure of cellulose. Similar to chitin, the natural function of cellulose is that of a structural polysaccharide, but its properties are varied from chitin. Despite of the similarity in chemical structures, cellulose and chitin play pivotal roles in structural support to plants and animals, respectively (Zargar et al., 2015).

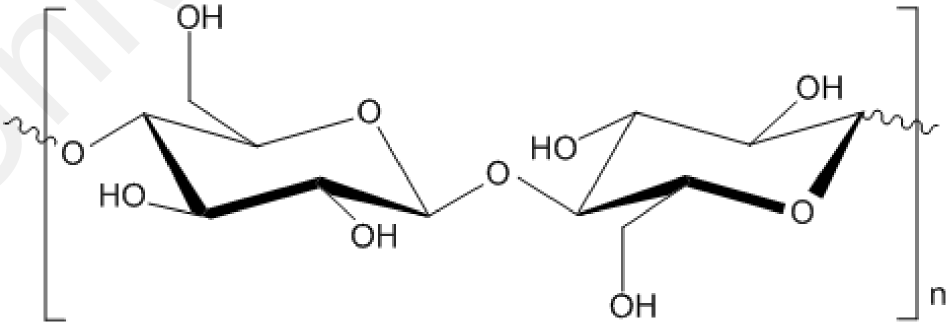

Figure 2.4: Molecular structure of cellulose.

Nanocellulosic material are characterized as cellulose in nano-sized with width of <100 nm or celluloses in micron-sized with at least one dimension of the structures are in nano-sized. On the other hand, nanocellulose is a common name of nano-sized cellulose which comprises cellulose nanofibers, nanocrystals cellulose extracted from the lignocellulosic biomasses and bacterial nanocellulose sourced from specific bacteria strains (Aitomäki & Oksman, 2014). Generally, NCC sourced from lignocellulosic biomass can be synthesized in two major stages. The first stage is the pretreatment of raw cellulosic biomass to remove non-cellulosic components such as hemicellulose and lignin. Second stage is the disintegration of cellulose nanocrystals from the individual cellulose fiber matrix through various techniques. Examples of techniques utilized are chemical, mechanical, combination of mechanical and chemical as well as enzymatic process (Mondal, 2017; Ng et al., 2017).

2.3.1 Properties of Cellulose

Cellulose is being used as potential reinforcing material because of its many advantages such as abundantly available, low weight, biodegradable, cheap and renewable. In addition, it has low abrasive nature and exhibits good mechanical properties (Bledzki et al., 1996; Kalia et al., 2011). On the other hand, cellulose also portrays some other disadvantages such as moisture absorption, quality variations, low thermal stability and poor compatibility with the hydrophobic polymer matrix (Saheb & Jog, 1999). Cellulose is hygroscopic in nature due to the abundance of hydroxyl groups render on the structure. This leads to significant amount of water to be absorbed by the non-hydrogen bonded hydroxyl groups on the cellulose's surface (Mondal, 2017).

Generally, T_g and T_m could not be easily detected due to the rigid-rod backbone structure of polysaccharides. It is very difficult to detect the behavior of molecular motion of neat cellulose by the DSC technique. Difficulty in the thermal characteristic of cellulose is due to the reason that the material is susceptible to thermal degradation before T_g and T_m are detectable (Kim et al., 1994). In terms of T_g of cellulose, several papers reported that the T_g values were found in the range of 200°C-260°C through various techniques (Kim et al., 1994; Nakamura et al., 1970; Nishio & Manley, 1988). In the attempt by Nishio and Manley (1988), T_g of cellulose from solution-coagulated cellulose/PVA films were predicted to be at least 230°C using the dynamic mechanical analysis (DMA) technique. In a separate approach using mechanical relaxation studies of regenerated cellulose, T_g of the regenerated cellulose was determined to be approaching 250°C via the torsional braid analysis (Nakamura et al., 1970).

Since cellulose is categorized as the semi-crystalline polymer, the crystalline melting peak is expected. However, for the determination of T_m for cellulose, the challenge in its determination is apparent because the thermal decomposition of the polymer occurs even before the second-order transition temperature (Kim et al., 1994).

2.3.2 Application of Cellulose for Reinforcement in Polymer Composites

Application of nanocellulsoe (cellulose nanofibrils or cellulose nanocrystal) in polymer reinforcement has been researched progressively in recent years. The reason of this extensive utilization of nanocellulose as the strengthening constituent in composites is due to its proven effectiveness in stress transfer. As shown in Figure 2.5, this is contributed by the strong bonding ability between nanocellulose and polymer matrix which enables the effective transfer of applied straining stress from matrix to filler (Mittal, 2015; Mohammad Mahdi Dadfar et al., 2014; Mondal, 2017). Cellulose nanocrystal (NCC) incorporated could serve as the load bearing entities for relieving the loads applied on the polymer matrix during tensile straining. Hence, the increment in tensile strength of polymer composite is strongly dependent on the efficiency of stress transfer. This is also because effective stress transfer could induce more axial stress applied on deformed matrix, resulting to the delay of the straining damage to higher stress (Sehaqui et al., 2011).

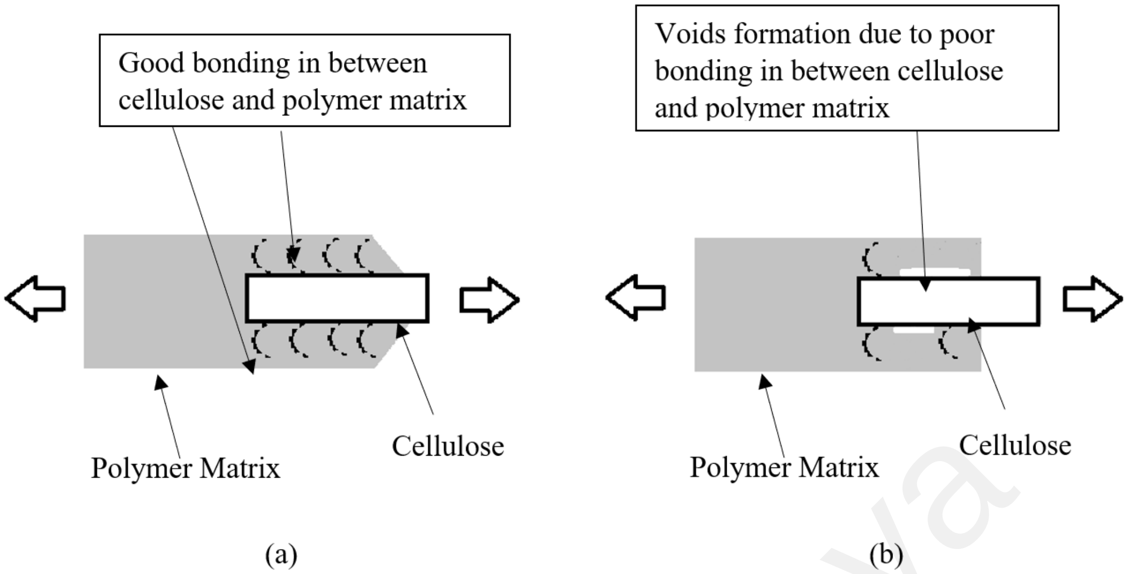

Figure 2.5: Schematic representation of load transfer between cellulose which acts as the reinforcement phase and the polymer matrix:(a) good bonding and excellent load transfer; (b) poor bonding and voids formation (Mondal, 2017).

Theoretically, the tensile strength of polymer composite can be enhanced with increasing content of NCC loaded, in conjunction with the increased contact sites between NCC and polymer matrix for improved intermolecular interactions. Due to this, it allows better stress transfer from matrix to NCC fillers. However, improvement of tensile strength proportional to NCC loading is only achieved under the conditions of high quality fillers dispersion. When the NCC being loaded has exceeded the optimum filler content for the polymer matrix, aggregations or agglomerations of NCC would be inevitable. The aggregated and agglomerated NCC would lead to local stress concentrations at the fillers’ surface or tend to act as defective points which weaken the stress transfer from the fillers to matrix (Azizi et al., 2014; Ng et al., 2017). Moreover, the inhomogeneous dispersion of NCC in polymer matrix also results in uneven stress distribution throughout the polymer during tensile straining which also contribute to reduction in tensile strength (Ng et al., 2017).

In terms of Young's modulus improvement for polymer composite, one can exploit the high rigidity of highly crystalline NCC to impose significant reinforcement effect in the elastic region of composite material (Sehaqui et al., 2011). From literature, it was reported that the high modulus value of NCC over polymer matrix rendering NCC the capability to exert stiffening action in composite materials. This is followed by the formation of stiffer composite systems (S.-Y. Lee et al., 2009; Mondal, 2017). In addition, the improved rigidity of polymer composites could be ascribed to reduced amount of nanoholes inside the polymer matrix by the increased loading content of NCC. This is in accordance with the findings from previous publications that concluded the improvement in tensile modulus was due to the increased content of rigid cellulosic filler in the polymer composites (Ng et al., 2017).

As for the elongation at break of polymer composite with NCC as filler, it is mainly depends on the interaction between NCC-polymer matrix, the dispersion of the NCC in the matrix and the volume fraction of the NCC incorporated (Ng et al., 2017). Generally, improved stiffness or strength of polymer composites can be achieved at the expense of the percentage of elongation at break. Besides, the nucleating effects of NCC also lead to improvement of composites' crystallinity. However, this improved crystallinity may cause decreased numbers of polymer inter-chains available for slippage. Therefore, the percentage of elongation at break tends to reduce accordingly with increased loading of NCC as filler (Brinchi et al., 2013; Ng et al., 2017).

2.3.3 Application of Cellulose for Adsorption of Dyes

Cellulose is a biopolymer that has been previously explored by researchers for its potential adsorption applications. It was reviewed that adsorption studies based on cellulosic materials could be categorized into two major perspectives. The first perspective focuses on studying the experimental condition and adsorption limiting parameters towards the maximum removal capacity for a given dye. While, the second perspective focuses on the theoretical studies to elucidate the adsorption process by explaining experimental data based on existing or proposed theoretical models in general (Silva et al., 2015). Table 2.3 summarizes the adsorption studies of unmodified cellulose and selected modified cellulose which showed adsorption towards methylene blue.

It was determined that the adsorptions of one or more dyes on the surface of cellulosic materials were elucidated by many researchers. Most of the works involved the modification of cellulose which aimed on obtaining the maximum adsorption capacity for one or more dyes. Among the studies, Ali Ashjarana and Hajilarib (2013) investigated the adsorption of direct blue 71 dye onto bacterial cellulose and cotton cellulose, respectively. Direct dyes are water soluble and contain one or more ionic groups which are mainly sulfonic acid or amino groups. In the work, the adsorption thermodynamic and kinetic parameters were also discussed.

A comparative study of cellulose agricultural wastes for adsorption of violet B dye from aqueous solutions was conducted by Hashemian (2014). The cellulose agricultural wastes studied were almond shell, pistachio shell, walnut shell, tea waste and orange peel. Among the agricultural wastes tested, it was found that adsorption efficiency of violet B by almond shell was the highest, amounted to 96 mg/g. Furthermore, the adsorption of violet B by the almond shell was best fitted to pseudo-second order kinetic model and Langmuir isotherm model.

Table 2.3: Adsorption studies of abundant types of dyes onto cellulose and modified cellulose.

Adsorbent Name	Name of dyes	Adsorbent Dosage (g/L)	Initial Dyes Concentration (mg/L)	Solution pH	Maximum adsorption capacity (mg/g)	References
Cotton Cellulose	Direct blue 71 dye	2	100	3	22.00	(Ali Ashjarana & Hajilarib, 2013)
Bacterial Cellulose	Direct blue 71 dye	2	100	3	25.15	(Ali Ashjarana & Hajilarib, 2013)
Cellulose Almond Shell	Violet B	20	30	11	96	(Hashemian, 2014)
Cellulose	Reactive blue BFRN	0.002	2000	7	9	(K. Xie et al., 2008)
Magnetic cellulose beads with activated carbon	Methylene blue	250	320	-	1.40	(Xiaogang Luo & Zhang, 2009)
Partially hydrolyzed polyacrylamide/cellulose nanocrystal	Methylene blue	0.1	5	5	326.08	(Zhou et al., 2014)

In many cases, cellulose was modified in view of the potential of further improving the functionalities of cellulose for adsorption. An example was that K. Xie et al. (2008) modified cellulose by incorporating cationic and anionic groups from the reaction with compounds of the triazine derivatives. With the proposed modifications, the authors were able to increase the adsorption capacity for the reactive blue dye BFRN, which was from a value of 9.00 mg/g for the unmodified cellulose, to 20 mg/g for the modified cellulose. From this finding, it further helped to justify the proposed modifications on cellulose.

Moreover, fabrication of millimeter-scale magnetic cellulose beads via an optimal dropping technology was carried out by Xiaogang Luo and Zhang (2009). The cellulose beads with maghemite (Fe_2O_3) nanoparticles incorporated portrayed sensitive magnetic response. Therefore, the modified cellulose could be recovered from water stream upon usage, with the facilitation of applying magnetic field. Adsorption performance of the modified cellulose was examined using methylene blue, with maximum adsorption capacity evaluated to be 4.39×10^{-3} mmol/g which was also equivalent to 1.40 mg/g. Data collected from adsorption experiments revealed that the adsorption process was best fitted to Langmuir isotherm and pseudo-second order kinetic equation.

A series of partially hydrolyzed polyacrylamide/cellulose nanocrystal nanocomposite hydrogels were prepared and applied for the removal of MB dye from the aqueous solution (Zhou et al., 2014). From the systematic studies, the results proved that improved MB adsorption capacities were acquired by increasing anionic nature of hydrolyzed polyacrylamide, cellulose nanocrystal content up to 20 wt.% and decreasing solution pH value. The optimized nanocomposite hydrogels achieved more than 90% in removal percentage of MB from aqueous solution. Besides, it was determined that the adsorption isotherms of nanocomposite hydrogels were well correlated to the Langmuir equation. In terms of kinetic studies, the adsorptions were described by pseudo-second order and Elovich models. However, Elovich model is generally useful for applications to determine the kinetics of chemisorption of gases onto solids with heterogeneous adsorbing surfaces. Moreover, the kinetic rate decreases with time due to an increase in surface coverage (Y.-S. Ho, 2006; Plazinski et al., 2009).

2.4 PVA/Chitin

Chitin is non-toxic, biodegradable and biocompatible. Besides, chitin has proven records of boosting some biological activities such as antibacterial and antioxidant (Jayakumar et al., 2011). Despite the many benefits of chitin, it possesses poor mechanical properties such as brittleness and rigidity which causes its film-making a challenge. Due to this, attempts have been made to blend chitin with other polymers having flexible molecular chains, such as PVA and polyethylene oxide (PEO) (Cho et al., 2001). Moreover, chitin is a typical carbohydrate polymer which lacks properties of synthetic polymer such as flexibility and melting processability (Grande & Carvalho, 2011). Therefore, blending chitin with synthetic polymer serves as a viable solution for obtaining new material that capitalizes selected advantages of both types of polymers.

Yet, there are limited studies of PVA/chitin systems with most PVA/chitin studies are based on β-chitin in which polymeric chains are arranged in parallel (Abd El-Kader et al., 2014; Y. M. Lee et al., 1996; Peesan et al., 2003). The authors have highlighted proof of miscibility between β-chitin/PVA systems because β-chitin has much weaker intermolecular hydrogen bonding than α-chitin which ascribable to the parallel chain arrangement of β-chitin. Through FTIR, it was proven that the intermolecular interactions between the β-chitin and PVA were based on hydrogen bonding. Upon blending of β-chitin and PVA, shifting of both hydroxyl and carbonyl stretching bands were observed from the FTIR spectra (Y. M. Lee et al., 1996).

Thermal properties of the PVA/chitin blends were examined by DSC. The variations of thermal transitions in relation to PVA/chitin blend composition also indicated the degree of intermolecular interaction between chitin and PVA in the blends. In the work of Cho et al. (2001), PVA/β-chitin blends were prepared by using aqueous acetic acid solution as a co-solvent. In the work, chitin homopolymer portrayed no significant transition in the DSC scan. Meanwhile, T_g and T_m determined for the PVA were 72°C and 229°C, respectively. With increasing chitin component, the PVA/β-chitin blends resulted in elevation of T_g but decrease in T_m and heat of fusion (ΔH_m) of PVA in blends. Similar findings on shifting of both T_g and T_m were also determined in a separate work of Peesan et al. (2003) which indicated miscibility of PVA/β-chitin blends. Decrease of T_m indicated that the development of PVA crystallite decreased in the presence of chitin due to improved interaction between the two polymers. The author also emphasized that similar decrease trend in T_m had been determined in several polymeric blends exhibiting good miscibility (Cho et al., 2001).

As for mechanical properties, the ultimate tensile strength has been recorded to be below 6 MPa regardless of PVA/β-chitin composition, with great reduction of elongation at break especially when PVA content is below 40 wt.% (Y. M. Lee et al., 1996; Peesan et al., 2003). As in the work of Cho et al. (2001), the author suggested that blending of chitin with PVA was a viable method to enhance the flexibility of the chitin film without a severe loss of its tensile strength and modulus.

In contrast, α-chitin with main chains arranged in anti-parallel order has not been extensively studied. α-chitin is characterized by low solubility and reactivity and its physical properties being very rigid and brittle. α-chitin has only been incorporated as reinforcing fillers in the form of insoluble nanofibers or nanowhiskers when blended with PVA (Deng et al., 2014; Junkasem et al., 2006; Sriupayo et al., 2005). With the incorporation of α-chitin into PVA matrix, tensile strength and Young's modulus have been improved while retaining its transparency (Deng et al., 2014; Junkasem et al., 2006). The observed increase in the tensile strength of the PVA/α-chitin films was associated to the interaction between PVA and chitin whiskers via hydrogen bonding. However, the interaction had resulted to stiffness of the composite along with decrease in the elongation at break (Junkasem et al., 2006; Sriupayo et al., 2005). In addition, Sriupayo et al. (2005) figured out that both the addition of α-chitin whiskers and heat treatment helped in improving water resistance of the PVA/α-chitin. This also led to decreased percentage degree of swelling of the PVA/α-chitin nanocomposite.

2.5 PVA/Nanocellulose

Application of nanocellulose in polymer reinforcement has been researched progressively in recent years. The reason of this extensive utilization of NCC in composites is driven by the fact that one can exploit the high stiffness of the cellulose crystal for reinforcement. Some of the advantages associate with composites constituent of the abundance NCC are improvement in mechanical properties, lightweight and biodegradability. There are three types of NCC which are cellulose nanocrystals, cellulose nanofibrils and bacterial cellulose. These three types of NCC are varied in terms of production methods and properties. Destruction methods are usually employed to gain cellulose nanocrystals or cellulose nanofibrils whereas bacterial cellulose is synthesized in the presence of bacteria.

PVA/NCC composite films were prepared by S.-Y. Lee et al. (2009), with the reinforcement of NCC into a PVA matrix at different filler loading levels (1 wt.%, 3 wt.%, 5 wt.%). NCC was prepared through acid hydrolysis of microcrystalline cellulose by using hydrobromic acid. With increasing loading of NCC, the tensile and thermal properties of PVA/NCC films were significantly enhanced. It was determined that tensile strength of the composite films was the highest at the loading of 1 wt.% NCC. The tensile strength value obtained for PVA with 1% NCC loaded was 49.0 % higher than neat PVA film. The author suggested that the intermolecular interactions enabled the inherent tensile strength of the NCC remained intact and resulted to overall improvement of the mechanical strength of the PVA/NCC films (S.-Y. Lee et al., 2009).

In another study, polymer composites from the combination of PVA and NCC fibers which were extracted from sisal fibers were prepared by solution casting method. The amount of NCC fibers incorporated into PVA was varied from 0 wt.% to 4 wt.%. It was determined that increase in NCC content obtained from sisal increased the tensile strength of the PVA composites. Accordingly, the elongation at break decreased from 126.5% to 8.82% when NCC was varied from 1 wt.% to 4 wt.%. Among the NCC fiber reinforced PVA composites studied, the highest elongation at break was retained at 1 wt.%. Morphology studies of the PVA/NCC composites were conducted by scanning electron microscopy which revealed the uniform dispersion of NCC in the PVA. A modified thermal behavior of PVA on addition of NCC fibers were determined through differential scanning calorimetry (Nigrawal et al., 2012). It was noted that the T_g of the nanocomposite with 2 wt.% NCC incorporated was shifted to the higher temperature side in comparison to neat PVA. The improved T_g value of the sample was attributed to the increased interactions between functional groups of NCC and PVA, which hindered the free rotation of the polymeric chains in the composite. Moreover, the increase in sisal fiber NCC increased the enthalpy of fusion (ΔH_f) of the PVA-based composites which indicated the increase in crystallinity of the composites by increased nucleation.

In the approach by Pereira et al. (2014), cellulose nanocrystals was extracted from the banana pseudostems fibers of the Pacovan variety which was then used as the fillers for the PVA-based nanocomposites. 1 wt.% to 5 wt.% of NCC were applied for the preparations of the respective PVA/NCC composites. With higher content of NCC, the water vapor barrier of the films increased, while the optical properties remained relatively constant. Interactions between NCC and water molecules resulted in the rearrangements of water molecules in the PVA matrix which lowered the plasticizing effect and increased the barrier properties of the material. Increasing the content of the NCC up to 3 wt.% significantly increased the mechanical properties of the nanocomposite. As a result, the tensile strength of PVA with 3 wt.% NCC content presented an increment of 19.5% over the neat PVA film. DSC analysis showed that the addition of NCC reduced the T_g and T_m of the PVA-based composites. This was attributed to the hydrophilicity of the NCC, which increased the amount of adsorbed water of the film. The water adsorbed acted as a plasticizer and thus led to the decreased thermal transitions observed. As a result, this improved the processability of the PVA-based composites as the melting temperature decreased slightly.

Peresin et al. (2014) had synthesized cellulose nanocrystals from ramie fibers and incorporated the NCC into the PVA to produce composite mats via electrospinning method. With the incorporation of the NCC, the electrospun PVA fibers had achieved three-fold increments in storage modulus. Strong interactions were demonstrated between the hydrophilic NCC reinforcement nanoparticles and the PVA continuous polymer matrix which were mainly due to hydrogen bonding or bond network. In this work, smooth nonwoven mats with homogeneous nanofibers were obtained.

Through freezing and thawing technique, Gonzalez et al. (2014) had successfully prepared PVA/NCC composite hydrogels with improved mechanical properties and barrier properties. Improvement on mechanical and barrier properties were attributed to the homogenously distributed NCC in PVA which gave the superior reinforcement effect. In addition, the water vapor transmission rate of the PVA/NCC composite hydrogels were in the range of wound dressing applications. Further evaluation of the hydrogels against microbial penetration showed that the hydrogels acted as good barrier against different microorganisms, thereby helping in accelerating the wound healing process. All these positive results suggested that PVA/NCC hydrogels were promising material as wound dressing.

Besides, W. Li et al. (2014) had extracted long filamentous nanocellulose fibrils from pine wood pulps via chemical-thermomechanical techniques. The nanocellulose fibrils obtained were used to cast PVA/NCC by the solvent casting method. It was determined that the nanocellulose fibrils increased the tensile strength and Young's modulus by a factor of 2.8 and 2.4 times higher over the neat PVA. With the introduction of 2 wt.%-14 wt.% nanocellulose fibrils in PVA, there were higher maximum decomposition temperatures in the first process, which was 0.4°C-9.1°C higher over the neat PVA. In short, the composites portrayed higher thermal stability and excellent transparency. It was found that the highest transmittance at the visible light region for the prepared PVA/NCC was 73.7%.

On the other hand, in situ production of PVA/bacterial cellulose nanocomposites was reported by Castro et al. (2014). In situ method was utilized to achieve better homogenization and effectiveness in the intermixing of components. The authors modified the culture medium of bacteria by adding PVA and glyoxal cross-linker together to become the matrix of composites. Chemical cross-linking with glyoxal improved the functional properties of composite and structural integrity of PVA matrix during purification steps. Reinforcement with bacterial cellulose contributed to improvement in terms of mechanical, dimensional properties and moisture resistance. At loading of 16% bacterial cellulose, Young’s modulus and tensile strength were determined to be increased by 680% and 40% respectively, in comparison to the control sample with no bacterial cellulose incorporated. The main reason of the improved properties of composite was due to the good hydrogen bonding and chemical cross-linking between the reinforcing phase and polymer matrix (Castro et al., 2014).

2.6 Polymer cross-link of PVA-based Composites

Generally, cross-linking process of PVA could be achieved through physical or chemical reactions. Physical cross-linking is based on crystallization of the polymeric chains, annealing, hydrogen bonding between chains, freeze-thawing, protein interaction or irradiation (Hennink & van Nostrum, 2002). On the other hand, modification on the chemical and physical properties of polymer composites could be achieved through chemical cross-linking process.

Chemical cross-linking is a chemical modification method on polymers which enables multidirectional chain extension of polymers. In the presence of cross-linker, cross-linking process could be induced by introducing heat, pressure, change in pH and radiation on the polymer matrices. When polymer chains are linked together by these new links, the polymer chains lose some of the ability to move about as an individual polymer chain. This results to the compaction of polymers structure. Hence, the structural integrity and properties of the polymer composites are altered (Hennink & van Nostrum, 2002; Marin et al., 2014). Figure 2.6 depicts the illustration of chemical cross-linking process.

PVA is a polymer with abundance of free hydroxyl groups, which allows the chemical modification of polymers through cross-linking. Theoretically, all chemical compounds that are reactive to the hydroxyl groups of PVA could be potential cross-linking agent of the PVA-based composites. As reviewed by Marin et al. (2014), chemical modifications of PVA by cross-linking could be achieved through reactions with dialdehydes, sodium tetraborate and polycarboxylic acids. Moreover, free radical formation, complexation reaction and acid-catalyzed dehydration are also the suitable means for cross-linking PVA-based composites.

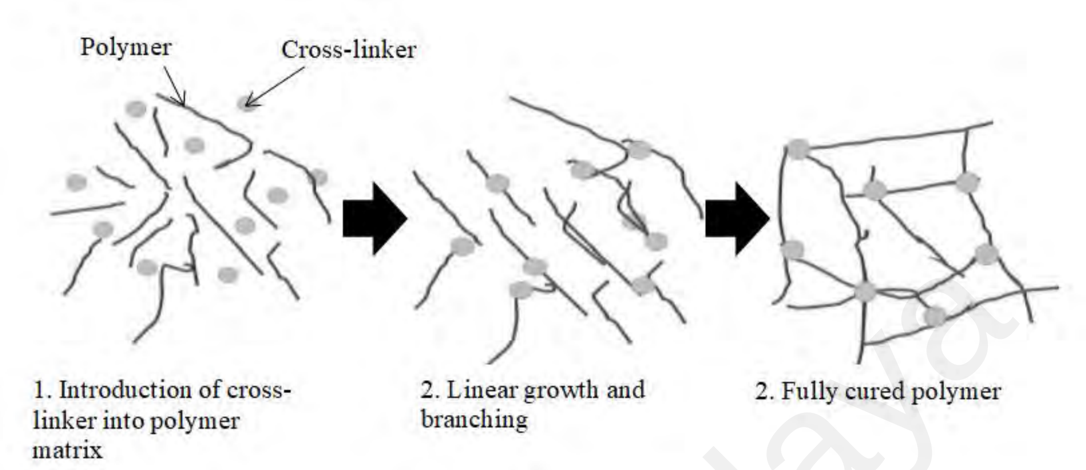

Figure 2.6: Schematic diagram illustrating the steps involved in chemical cross-linking.

Previous works showed that 1.5 wt.% of either glutaraldehyde or hexamethylenetetramine served as the cross-linker for PVA/tropical fruit waste composites (Ooi et al., 2012). In the attempt, glutaraldehyde or hexamethylenetetramine cross-linked PVA-based composites films portrayed slight improvements on tensile strength, Young's modulus, water vapor barrier and water resistance. However, it was deduced that hexamethylenetetramine displayed better cross-linking effect over the glutaraldehyde. Furthermore, both types of the cross-linked PVA/tropical fruit waste composites displayed comparable weight losses which were lower than the non-cross-linked control sample. Despite the potential of hexamethylenetetramine as the cross-linker for PVA, hexamethylenetetramine is a tertiary amine which could lead to the formation of carcinogenic nitroso compounds when ingested by human (E. Bachmann & C. Deno, 1951; Loeppky et al., 1983).

The utilization of glutaraldehyde is a typical reaction of hydroxyl groups of PVA with the dialdehyde via acetal bond formations. In another study, it was reported that cross-linking of PVA with glutaraldehyde in acidic condition resulted in water insoluble end products with excellent disintegrating properties in aqueous media (Patel & Vavia, 2010). Considering the toxicity of glutaraldehyde, glyoxal had been applied as the alternative cross-linker in the preparation of PVA/micro fibrillated cellulose composites. Similar to the case of glutaraldehyde, the cross-linking was initiated at low pH medium. By applying the short chain glyoxal as the cross-linker, the composites established restricted segmental motion of PVA chains. This was proven by the fact that the glass transition temperature of the PVA-based composites increased (Zhang et al., 2010).

Another example of cross-linker is the sodium tetraborate ($Na_2B_4O_7 \cdot 10H_2O$). It was recognized as a non-toxic food additive that was proven effective in the cross-linking of PVA/NCC composites. Due to the formation of complexes between borate ions and hydroxyl functional groups of PVA, the resultant composite hydrogels exhibited remarkable increase in viscoelasticity and compressive strength. The reinforcing effect of the nanocellulose further enhanced the stiffness and strength of the composite hydrogels (J. Han et al., 2013). Nevertheless, the reactions were reported to be very sensitive to the solution pH and content of sodium tetraborate introduced (Marin et al., 2014).

For the cross-linking mechanism involving radical formation, the chemical reaction involves a free radical initiator to the polymerization reaction. The free radicals attack the bonding of PVA and result in internal polymerization. Consequently, this increases the molecular weight and hydrophobicity of the PVA-based composites. Furthermore, this reaction is undesirable due to its complex nature and the unreacted free radicals in the final product could be toxic (Marin et al., 2014). On the other hand, the chemical cross-linking associated to acid-catalyzed dehydration was more useful for the preparation of polymer membranes. This is because the membrane obtained was useful to retain a high salt concentration at low flow rate (Marin et al., 2014). Similarly, cross-linking reaction which involved complexation reaction between PVA and poly(methyl vinyl ether-co-maleic acid) was found to be a suitable coating material. The resulting film exhibited reduced volume and possessed better oxygen barrier than the neat PVA or neat poly(methyl vinyl ether-co-maleic acid) (Labuschagne et al., 2008).

Last but not least, PVA could react with polycarboxylic acids through the reaction known as esterification. Esterification is catalyzed in acidic medium and the by-product of the reaction is the water. Excess water could be easily removed by mild heating and subsequently the composites are cured. Examples of polycarboxylic acid that has been used for cross-liking are lactic acid, maleic acid, sulfosuccinic acid, acrylic acid and methacrylic acid. Among the polycarboxylic acid listed, only maleic acid consists of unreacted double bonds. In view of this, it is believed that the additional functional group would further improve the efficacy of the cross-linked PVA-based composites for adsorption application. In brief, the PVA-based materials that are cross-linked by the polycarboxylic acid are useful for many applications which include manufacture of resins, fibers, hot-melt, adhesives and membranes (Marin et al., 2014).

2.6.1 Cross-linking of PVA by Maleic Acid

Maleic acid or cis-butenedioic acid is an organic compound that has a double bond at the center and two carboxylic functional groups at the terminals of the chemical structure. Figure 2.7 shows the chemical structure of maleic acid (MA).

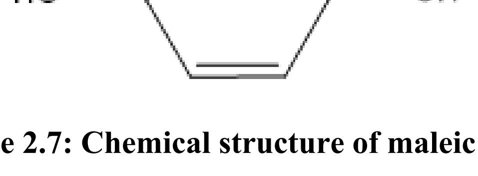

Figure 2.7: Chemical structure of maleic acid.

Several researchers have studied the effects of MA as the cross-linker for PVA. Gohil et al. (2006) had proven the effectiveness of MA to serve as the cross-linker of the completely hydrolyzed PVA (degree of hydrolysis = 98%-99%). MA concentration of 30 wt.%-40 wt.% with curing at 140°C for 90 min was determined to be optimum conditions for cross-linking PVA. The stability of MA cross-linked PVA in hot water was greatly enhanced, with the average gel content recorded at 96%-97%. As deduced by DSC thermograms, a shift in glass transition temperature was observed for MA cross-linked PVA, which was ascribed to the formation of ester linkages between the PVA chains.

In the work of Huang and Rhim (1993), cross-linking of PVA using MA was carried out in the presence of triethanolamine/water catalysts. It was reported that the tensile modulus and tensile strength increased, whereas the elongation at break decreased as the cross-linking density increased. The resulting optimized PVA membranes can be used at low temperatures rather than at high temperatures for the pervaporation separation of acetic acid-water mixture, with recorded highest separation factor of 7.80. Moreover, films constituent of PVA and natural rubber polymer blends, in the presence of MA as the cross-linking agent were studied by Riyajan et al. (2012). Under the investigation by attenuated total reflection mode-Fourier transform infrared spectroscopy, the presence of peak at 1152 cm^{-1} indicated the successful cross-linking between PVA and MA through ester linkage. The swelling capability of the polymer blend decreased proportionally with the increased MA content. As for the tensile strength of the polymer blend, it increased with the increase of both the content of MA and curing time.

2.7 Advantages and Limitations of Polymeric Adsorbent

In comparison with conventional adsorbents such as commercial activated carbons and synthetic ion-exchange resins, contaminants adsorption using PVA/Chitin/NCC polymeric adsorbents offers several advantages and limitations as described in Table 2.4.

Table 2.4: Advantages and limitations of conventional adsorbents and PVA/Chitin/NCC polymeric adsorbents (Alaba et al., 2018).

Adsorbent	Advantages	Limitations
Activated Carbon	1. Effective adsorbent 2. High surface area 3. Porous adsorbent 4. High adsorption kinetics and capacity 5. Commercially utilized for removal of dyes and organic pollutants 6. High capacity for adsorption of a wide range of contaminants	1. Requires high thermal energy for synthesis of activated carbon 2. Range of costing depending on quality 3. Adsorption performance depending on type of carbon used 4. Requires complexing agents for enhanced removal efficiency 5. Poor selectivity 6. Not suitable for adsorbing hydrophilic substances 7. Not suitable for adsorbing vat and disperse dyes 8. High cost for reactivation of carbon 9. Poor reusability due to loss of carbon 10. Inability to reduce contaminant concentrations beyond ppm range

'Table 2.4, continued'

Adsorbent	Advantages	Limitations
Ion-exchange resin	1. Variation in physicochemical properties 2. Sufficiently high surface area 3. Effective adsorbent with hierarchical of pore structure 4. Remarkable selectivity toward aromatic pollutants 5. Excellent reusability	1. Expensive 2. Sourced from fossil fuel-based raw materials 3. Sensitive to particles 4. Adsorption performance depends on the type of resin 5. Not suitable for all dyes 6. Performance is pH dependent 7. Poor contact with aqueous pollutants 8. Modification is required for improved wettability
PVA/Chitin/ NCC polymeric adsorbent	1. Blend of flexible PVA polymer and natural polymers 2. Biodegradable 3. Environmentally benign 4. Recycle shrimp waste for chitin 5. Utilize abundantly available cellulose 6. Amphiphilic in nature 7. Dyes binding capabilities 8. High selectivity in treating both very dilute or concentrated solutions 9. Can be processed into different shapes and sizes 10. Good reusability	1. Nonporous sorbent and low specific area 2. The sorption capacity depends on the polymer compositions 3. Adsorption is dependent on pH and temperature 4. Requires chemical modification by maleic acid for structural integrity in aqueous medium

2.8 PVA-based Composites for Dyes Removal

Composite material is a material constituent of two or more chemically or physically different phases (matrix phase and dispersed phase) and exhibiting bulk properties significantly different from that constituent when presented alone. The primary phase of composite is the matrix phase which presents a continuous character, being more ductile and less hard phase. It holds and shares the loads with the dispersed phase. The secondary phase is the dispersed phase, or sometimes known as reinforcing phase. Usually, the secondary phase is on better strength than the matrix phase as it embedded in the matrix in a discontinuous manner. On the basis of composites classification, they are classified based on the matrix types. Composites can be categorized into metal matrix composites, ceramic matrix composites and polymer matrix composites. In brief, polymer matrix composite or commonly called as polymer composite is a composite with polymer as its matrix (Malhotra et al., 2012).

In recent years, PVA-based composite adsorbents have been extensively explored to be utilized in removal and recover of pollutants from wastewater (Refer Table 2.5). Attention was given to polymer composites due to the characteristic properties on adsorption, reusability, economic feasibility and processability. In addition, polymer composites contain variance of ionic and non-ionic functional groups that can adsorb and remove dyes from wastewater (Kamal, 2014). For comparisons between adsorption capacities of the materials studied in this work, Table 2.5 summarizes the adsorption capacities and conditions of the PVA, chitin, cellulose and PVA-based composites for removal of dyes.

Table 2.5: Adsorption capacities of different adsorbents for removal of dyes.

Adsorbent Name	Name of dyes	Adsorbent Dosage (g/L)	Initial Dyes Concentration (mg/L)	Solution pH	Maximum adsorption capacity (mg/g)	References
Poly(vinyl alcohol)	Methylene blue	4	25	4	13.80	(S. Umoren et al., 2013)
Poly(vinyl alcohol)	Bromothymol blue	-	30	6	276.20	(Agarwal et al., 2016)
Poly(vinyl alcohol)	Methylene blue	-	30	6	23.30	(Agarwal et al., 2016)
α-chitin	Methylene blue	1	10	6	6.90	(Dhananasekaran et al., 2016)
α-chitin	Bromophenol blue	1	15	6	22.72	(Dhananasekaran et al., 2016)
α-chitin	Coomassie brilliant blue	1	25	10	8.55	(Dhananasekaran et al., 2016)
Chitin	Reactive yellow 2	4	450	6	38	(Akkaya et al., 2007)

'Table 2.5, continued'

Adsorbent Name	Name of dyes	Adsorbent Dosage (g/L)	Initial Dyes Concentration (mg/L)	Solution pH	Maximum adsorption capacity (mg/g)	References
Chitin	Reactive black 5	4	450	8	65	(Akkaya et al., 2007)
Chitin	Indigo carmine dye	0.5	11	-	3.26	(Prado et al., 2004)
Untreated chitin	Reactive red 141	3	400	11	167	(Dolphen et al., 2007)
Sodium hypochlorite-treated chitin	Reactive red 141	3	400	11	124	(Dolphen et al., 2007)
Cotton Cellulose	Direct blue 71 dye	2	100	3	22.00	(Ali Ashjarana & Hajilarib, 2013)
Bacterial Cellulose	Direct blue 71 dye	2	100	3	25.15	(Ali Ashjarana & Hajilarib, 2013)
Cellulose Almond Shell	Violet B	20	30	11	96	(Hashemian, 2014)
Cellulose	Reactive blue BFRN	0.002	2000	7	9	(K. Xie et al., 2008)

‘Table 2.5, continued’

Adsorbent Name	Name of dyes	Adsorbent Dosage (g/L)	Initial Dyes Concentration (mg/L)	Solution pH	Maximum adsorption capacity (mg/g)	References
Magnetic cellulose beads with activated carbon	Methylene blue	250	320	-	1.40	(Xiaogang Luo & Zhang, 2009)
Partially hydrolyzed polyacrylamide/cellulose nanocrystal	Methylene blue	0.1	5	5	326.08	(Zhou et al., 2014)
Poly(vinyl alcohol)/chitosan	Methylene blue	20	20	9	~30.00	(Casey & Wilson, 2015)
PVA/GA/β-cyclodexrin	Methylene blue	-	25	11	27.25	(Ghemati & Aliouche, 2014)
PVA/GA/β-cyclodexrin	Reactive dye	-	25	3	44.55	(Ghemati & Aliouche, 2014)
Poly(vinyl alcohol)/attapulgite	Methylene blue	5	40	5	169.5	(L. Yang et al., 2011)
Poly(vinyl alcohol)/alginate/rice husk biomass	Direct blue-67	2	50	3	3.02	(Safa & Bhatti, 2011)
Poly(vinyl alcohol)/poly(acrylic acid	Methylene blue	2.5	50	6	34.20	(Kamal, 2014)

‘Table 2.5, continued’

Adsorbent Name	Name of dyes	Adsorbent Dosage (g/L)	Initial Dyes Concentration (mg/L)	Solution pH	Maximum adsorption capacity (mg/g)	References
Poly(vinyl alcohol)/poly(acrylic acid /clay	Methylene blue	2.5	50	6	28.80	(Kamal, 2014)
Poly(vinyl alcohol)/4A-zeolite	Methylene blue	1	10	8.5	41.08	(Baheri et al., 2016)
Poly(vinyl alcohol)/polyaniline/clinoptilolite	Methylene blue	1	10	-	44.44	(Rashidzadeh & Olad, 2013)
Poly(vinyl alcohol)/attapulgite	Methylene blue	5	40	5	169.5	(L. Yang et al., 2011)
Poly(vinyl alcohol)/graphene oxide	Methylene blue	0.5	50	6	476.20	(X. Yang et al., 2016)
Poly(vinyl alcohol)/carboxymethyl starch-g-polyvinyl imidazole	Crystal violet	1	20	8	96.15	(Pour & Ghaemy, 2015)
Poly(vinyl alcohol)/carboxymethyl starch-g-polyvinyl imidazole	Congo red	1	20	5	89.25	(Pour & Ghaemy, 2015)

2.8.1 Poly(vinyl alcohol)/Chitosan

Polymer composites of poly(vinyl alcohol)/chitosan were prepared by blending and drop-casting to form films for physicochemical, thermal and adsorption tests (Casey & Wilson, 2015). PVA/chitosan composites displayed greater thermal stability, distinctive morphology and improved stability in acidic medium. Thus, this extended the pH range applicable for the chitosan-containing adsorbent material. When the composites were exposed to methylene blue (MB) and *p*-nitrophenol dyes for adsorption tests, better dyes uptake were observed for MB, especially at high pH. Negligible binding of *p*-nitrophenol were determined by all polymer composites regardless of solution pH. At low pH, adsorption tendencies of the composites towards the cationic MB were reduced. This is due to the protonation of chitosan which contributed to electrostatic repulsion with the MB, as evidenced by the adsorption results at pH 5. Experimentally, it was determined that the maximum adsorption capacity of the optimized PVA/chitosan composite for MB was about 30 mg/g when tested at pH 9 and 298 K with initial dyes concentration of 20 μM. This favorable result was extended by the improved mechanical, thermal properties and improved water resistance of the composite film determined, thereby making the composite as a promising tunable adsorbent material for cationic pollutants. On the other hand, PVA/chitosan composites had been studied for the removal of Cu (II) and Cd (II) were proven to be effective adsorbents (M. Kumar et al., 2009; Ngah et al., 2004).

2.8.2 Glutaraldehyde Cross-linked Poly(vinyl alcohol) (PVA/GA) and Glutaraldehyde Cross-linked PVA Incorporated with β-Cyclodextrin (PVA/GA/β-Cyclodextrin)

Glutaraldehyde cross-linked poly(vinyl alcohol) (PVA/GA) and glutaraldehyde-cross-linked PVA incorporated with β-cyclodextrin (PVA/GA/β-cyclodextrin) membranes were researched by Ghemati and Aliouche (2014). β-cyclodextrin is a cyclic oligosaccharide which tends to form inclusion complexes with organic host molecules. Adsorption of reactive, methyl orange and MB dyes on PVA/GA/β-cyclodextrin membranes were independently experimented at wavelengths of 547 nm, 463 nm and 660 nm, respectively using UV-Vis spectrophotometer. For all these studies, equilibriums were reached in 24 h. Characterization results proved that the β-cyclodextrin was impregnated into the PVA-based matrix without covalent bond formation. However, in all cases, β-cyclodextrin enhanced the adsorption capacity of the membranes due to adsorption mechanism by inclusion complex formation. In particular, the size, shape and polarity of the dyes molecules are detrimental factors in this adsorption mechanism. Moreover, solution medium pH plays a significant role in the adsorption of different types of dyes from the solution. For instance, MB which is cationic (positively charged) is preferentially adsorped in basic solution medium but reactive dyes and orange methyl dyes, being as anionic structures are favorable in acidic medium. This is because the adsorptions are based on electrostatic forces. The PVA-based composites gained net negatively charged in basic medium while net positively charged in acidic medium. When fitted to Langmuir isotherm, the maximum adsorption capacity for PVA/GA/β-cyclodextrin was reported to be 44.55 mg/g for reactive dye at pH 3 meanwhile 27.25 mg/g for MB at pH 11. It was remarked that the adsorption by PVA/GA/β-cyclodextrin was a favorable process since it was spontaneous in nature.

2.8.3 Poly(vinyl alcohol)/Attapulgite

A novel spherical composite of poly(vinyl alcohol) and attapulgite (PVA/ATP) with macro-reticular structure was introduced as a potential adsorbent for both dyes and metal ions (L. Yang et al., 2011). The composite designed hold advantages of both PVA and ATP characteristics. PVA is a linear chain polymer with great processability. Besides, PVA consists of large number of side hydroxyl functional groups which making it a highly reactive and hydrophilic polymer. Due to this, PVA is beneficial for functional modification such as cross-linking. Similar to PVA, attapulgite which is a type of fuller’s earth is abundant in nature, cheap and easily obtainable. ATP offers better hydrothermal stability, complementing PVA which is more thermal sensitive. In this context, nano-sized ATP was used. In this work, PVA/ATP composite was fabricated into a unique spherical macro-reticular structure. This unique structure allowed excellent mass transfer property and increased adsorption capacity. The adsorption performance was proven with adsorption studies of both MB and lead in aqueous solution. For solely MB adsorption, PVA/ATP founded to have a calculated maximum monolayer adsorption capacity of 169.5 mg/g and fitted to Langmuir isotherm. However, when it was processed into macro-reticular structure, Langmuir isotherm could not be complied at all, but it was fitted to Freundlich isotherm. In terms of kinetic, all of the adsorption processes were of second order.

2.8.4 Poly(vinyl alcohol)/Alginate/Kaolin

Feasibility on utilizing poly(vinyl alcohol)/alginate/kaolin composite in the removal of MB from aqueous solution was investigated by M Abd El-Latif et al. (2010). In this research, boric acid-calcium chloride solution was introduced for cross-linking of polymers. Batch adsorption technique was implemented to evaluate the effects of process variables on the adsorption. Process variables studied were on mass of organic-kaolin composite, contact time, bead size, swelling of beads, initial dye concentration, pH, stirring speed and temperature on the adsorption process. However, it was mentioned that the effects on bead size and the swelling of beads were not significant (M Abd El-Latif et al., 2010). Kaolin, which is a type of clay have been investigated to be an economical adsorbent for removing heavy metals from wastewater due to its abundance and easy availability. However, it comes with the drawback of difficulty to be separated from the wastewater. The composite formed from the mixed polymers which refer to the PVA and alginate showed rubber-like elastic properties. Based on these works, alginate incorporated led to alteration of surface properties, rendering the composite to be less agglomerated. This trait was important especially when the adsorbents were being are applied in bead size. As for PVA, it improved the composite's strength and durability (Dave & Madamwar, 2006; M Abd El-Latif et al., 2010). Both PVA and alginate served as the organic binding polymers for the granulation of kaolin. This preparation of adsorbent was advantageous in terms of the simplicity of preparation method and excellent physicochemical properties. Batch studies' results indicated that poly(vinyl alcohol)/alginate/kaolin composite showed MB adsorption efficiency of 61.6% to 100% when initial dyes concentration range from 500 mg/L to 10 mg/L at 22°C. Under these optimized conditions, the maximum adsorption capacity of MB was 30.8 mg/g. The adsorption equilibrium was reached in 6 h. Moreover, the kinetic studies were presented which proved that the adsorption process was of first order (M Abd El-Latif et al., 2010).

2.8.5 Poly(vinyl alcohol)/Alginate/Rice Husk

Safa and Bhatti (2011) examined poly(vinyl alcohol)/alginate/rice husk biomass composite to be used for the adsorption of Everdirect Orange-3GL and Direct Blue-67 dyes. PVA/alginate matrix served mainly for immobilizing the rice husk which acted as the biosorbent. It is known that such immobilization of biosorbent gave advantages such as allowing reusability of biosorbent, controlling of biosorbent's dispersion size, improving mechanical strength and reduced flocculation in the continuous system (Bayramoğlu et al., 2003). At low pH, maximum adsorption capacity was established for both dyes. Comparative study of adsorption was done for both dyes, fitting Langmuir isotherm type II using the poly(vinyl alcohol)/alginate/rice husk biomass. The results showed that the calculated maximums of adsorption capacity for Everdirect Orange-3GL and Direct Blue-67 were at 8.77 mg/g and 3.02 mg/g, respectively. For both cases, the adsorption equilibriums were reached in 360 min. Moreover, the adsorption processes were determined to be temperature-dependent. Lastly, it was concluded that the reactions were spontaneous at high temperature based on the values of Gibbs free energy being calculated.

2.8.6 Poly(vinyl alcohol)/Poly(acrylic acid)/Clay

Composites of poly(vinyl alcohol)/poly(acrylic acid) with inorganic clay in the form of hydrogel were investigated by Kamal (2014). The composites were prepared by gamma irradiation technique, in the presence of organic cross-linker known as methylene bisacrylamide or inorganic cross-linker known as Bentonite (clay). It was determined that the adsorption capacity of MB dyes by the poly(vinyl alcohol)/poly(acrylic acid) composite filled with Bentonite was enhanced by two times over neat poly(vinyl alcohol)/poly(acrylic acid) composite. The adsorption results obtained were fitted with Freundlich and Langmuir isotherm models. It was determined that the maximum adsorption capacity was obtained when poly(vinyl alcohol)/poly(acrylic acid) was at 3:7 composition ratio. Moreover, adsorption capacity was found to be optimum at 2 wt.% of clay when tested over the 0 wt.%-5 wt.% range. Besides, the kinetic studies on the adsorption process were in agreement to the pseudo-second order kinetic model. The results obtained implied that poly(vinyl alcohol)/poly(acrylic acid)/clay composites were efficient adsorbent for MB dyes removal from wastewater.

2.8.7 Poly(vinyl alcohol)/Polyaniline/Clinoptilolite

Poly(vinyl alcohol)/polyaniline/clinoptilolite composite was synthesized by Rashidzadeh and Olad (2013). It the attempt, the composite was fabricated based on the oxidative polymerization of anilinium cations inside and outside of the clinoptilolite zeolite’s channels. PVA was incorporated as a solution to comprehend the poor processing characteristics of polyaniline as well as serving as the adsorption site.

Moreover, the hydroxyl groups on PVA can also serve to adsorb cationic MB dye molecules. In this work, the adsorption is mainly governed by chelation, which is through coordinate bonds. Coordinate bonds are formed between the unpaired electrons on nitrogen atoms in polyaniline or oxygen atoms in PVA with the MB cationic dyes.

The prepared polymer composite consisted of nano dimension and hence it was also known as nanocomposite. It was reported that the removal efficiency was about 98% when it was applied as the adsorbent for MB dye in the powdered form. In this case, it was calculated from the linearized Langmuir isotherm that the maximum adsorption capacity was 44.44 mg/g. Under this experimental condition, Langmuir isotherm model was best fitted to experimental data over those of Freundlich isotherm. This indicated that there was higher tendency of monolayer adsorption over multilayer adsorption when poly(vinyl alcohol)/polyaniline/clinoptilolite composite served as the adsorbent. The batch sorption kinetics was carried out and proven that the rate determining step was pseudo-first order.

2.8.8 Poly(vinyl alcohol)/4A-zeolite

In a pursuit of improving MB adsorption, novel poly(vinyl alcohol)/4A-zeolite membranes were investigated by Baheri et al. (2016). This poly(vinyl alcohol)/4A-zeolite membranes were a mixed matrix membrane adsorbents with varied zeolite content (5 wt.%-20 wt.%) incorporated. Membrane adsorbent could be utilized merely as an adsorbent (batch method) or enhancing membrane property for adsorbing specific target materials during membrane processes (flow-through method). In this attempt, zeolite was introduced to improve adsorption performance since zeolite was renowned for its high void volume structure, high surface area and electrostatic attraction towards dyes molecules. Batch adsorption studies were carried out and optimized in terms of zeolite’s content, contact time, solution temperature, pH and initial dyes concentration.

Both maximum adsorption capacity and removal efficiency were achieved at pH 10.5, 25°C and 20 wt.% of zeolite loading. However, maximum adsorption capacity of 41.08 mg/g was achieved when MB concentration was at 100 mg/L while removal efficiency of 87.41% was achieved when MB concentration was at 5 mg/L, respectively. When the adsorption processes were analyzed by fitting them to Freundlich, Langmuir and Tempkin adsorption isotherm models, best correlation was met from Freundlich isotherm. Furthermore, the MB adsorption rate onto the composite was conformed to pseudo-second order.

2.8.9 Poly(vinyl alcohol)/Graphene Oxide

Poly(vinyl alcohol)/graphene oxide composite as the effective adsorbents for MB were first discovered by X. Yang et al. (2016). Using the experimental settings proposed, the calculated maximum adsorption capacity for the neat PVA used was 196.5 mg/g. In this context, PVA was proposed to be used mainly serving as the carrier in immobilizing the graphene oxide. This immobilization practice would avoid the problem of second pollution that may be caused by the tiny sized graphene oxide. It was reported that the adsorptions were significantly affected by the content of graphene oxide being introduced, pH, temperature and concentration of adsorbate. At 50% of graphene oxide content, maximum adsorption capacity could reach up to 476.2 mg/g. The removal efficiencies of 77% to 90% were achieved in the 2.1-9.2 pH range. These studies indicated that the adsorption processes were best fitted to the Freundlich isotherm model in comparison to the Langmuir and Dubinin–Radushkevich models. Kinetic studies gave evidences that the adsorptions were resembled those of pseudo second-order kinetic model. Moreover, the adsorption processes were investigated thermodynamically. It was proven to be favorable processes since the reactions were spontaneous and endothermic in nature.

2.8.10 Poly(vinyl alcohol)/Carboxymethyl starch-g-polyvinyl imidazole

Novel magnetic nanocomposites of poly(vinyl alcohol)/carboxymethyl starch-g-polyvinyl imidazole were prepared through instantaneous gelation, followed by cross-linking using glutaraldehyde (GA) (Pour & Ghaemy, 2015). The composites were shaped into highly porous and magnetic sensitive adsorbents, desired for removal of crystal violet dye, congo red dye and metal ions from water. In this work, batch adsorption results indeed proved the composite's efficacy in treating the water from dyes and metal ions. Focusing on crystal violet and congo red dyes adsorption studies, both agreed well with the Langmuir adsorption model. The experimental adsorption capacities for crystal violet and congo red dyes were 91.58 mg/g and 83.66 mg/g, while the calculated values fitted to Langmuir were 96.15 mg/g and 89.25 mg/g, respectively. The adsorptions were due to fact that the reactions were of pseudo-second order in nature. Besides, the Gibbs free energies were of negative values, implying the spontaneities of the dyes adsorptions. In brief, all the studied results indicated that the composites were efficient alternative adsorbents for the treatment of dye and heavy metal ions from water.

2.9 Colorants and Dyes

Since prehistoric time, humans had started utilizing natural colorants. However, the boom of modern synthetic dye industry was due to William Perkin's discovery of mauve dye in 1856. Since then, various synthetic dyes were introduced, and mass produced due the great economic gain from synthetic dyes production. Colorants define as substances which exhibit the ability to absorb or emit light in the visible light region (380 nm-760 nm) (Marzec, 2014). Due to this, they appeared to be colored when observed under naked eyes. Colorants are categorized into two major groups which are the organic and inorganic colorants. Each of the major group is than subdivided into colorant compounds constituents of natural or synthetic origin. Colorants are inclusive of both dyes and pigments.

Dyes are organic compounds that are soluble in, or at least partially soluble due to its affinity towards the substrate being colored. On the other hand, pigments remain as insoluble counterparts towards the substrate being colored (Hasan, 2008). Dyes are ionic, aromatic organic compounds with chromophore groups. Chromophore group is the chemical structure responsible for the light absorption and light reflection in dye molecules since it is the delocalized electron system with conjugated double bonds. Examples of chromophores are -C=C-, -C=N-, -C=O, -N=N-, -N=O and quinoid rings (Marzec, 2014). With the presence of auxochromes (-NH_3, -COOH, -SO_3H and -OH) in dyes molecules, intensification of the color attributed by chromophore is achieved by altering the overall energy of the electron system. There have been more than a hundred thousand of dyes variance reported since the early of 21st century. The variances are namely acid, basic, direct, disperse, metal complex, mordant, reactive, sulfur and vat dyes (Hunger, 2007).

2.9.1 Classification of Dyes

Dyes have been classified commonly in two different approaches, either accordance to their chemical structure or according to the application method. The former classification method is preferred among the practicing dyes chemists while the latter is dominantly used among dyes technologists (Hunger, 2007). Classification of dyes based on chemical structures is a classification in accordance to the chromophore group present in the dye molecules. Examples under this classification are azo, nitro, indigoid, anthraquinone, phthalein, triphenyl methyl and nitroso dyes types (Marzec, 2014).

On the other hand, classification according to the application method gives information on the principal substrates, application methods and the representative chemical types for each application dyes class. The classification of dyes based on application method is summarized in Table 2.6. However, there is hardly a chemical class of dye which occurs solely in one coloristic group and vice versa. Hence, both classifications based on chemical structures and application methods are applied by Color Index, in complimentary to each other (Hunger, 2007; Marzec, 2014).

Table 2.6: Classification of dyes based on application methods (Hunger, 2007).

Type of Dye	Characteristics	Substrate
Acid	Anionic (negatively charged) compounds in solutions which bind to cationic groups on substrate	Cosmetics, inks, leather, polyamide, paper, silk, wool
Azoid components and compositions	Colorants of a reaction between a coupling component impregnated into fibers and a stabilized diazonium salt solution	Cotton, cellulose acetate, polyester, rayon
Basic	Cationic (positively charged) compounds in solutions which bind to anionic groups on substrate	Ink, modified nylon, polyacrylonitrile, synthetic fibers, paper
Direct	Apply from neutral and slightly basic solution baths doped with electrolytes	Cellulose fibers, cotton, viscose, leather, nylon, paper, polyamide, rayon
Disperse	Dispersed fine aqueous dyes solution that is applied under high pressure, high pressure or carrier-assisted under lower temperature; dyes may be baked on, thermo-fixed or lay on top of substrates	Acetate, acrylic, plastic, polyester, polyamide
Fluorescence brighteners	Apply through mass produced solution, suspension or dispersion which is purposed for masking the yellowish tint on the materials	All fibers, detergents and soaps, oils, paints, plastic
Metal complex	Strong complexes of a metal ion (often chromium, copper, cobalt or nickel) and one or two dye molecules (acid dyes or reactive dyes)	Silk, polyamide, wool

‘Table 2.6, continued’

Type of Dye	Characteristics	Substrate
Mordant	Introduce in conjunction with chemicals such as chromium salts which bind the dyes with substrate	Anodized aluminum, wool, leather, silk
Reactive	Reactive sites on dyes would form covalent bonds with -NH, -OH or -SH groups of substrates under influence of heat and high pH	Cotton, nylon, wool, silk and polyamide
Solvent	Non-ionic dyes that cause dissolution in the substrates	Fats, gasoline, inks, lacquers plastic, varnish, stains, oils, waxes
Sulfur	Results in insoluble polymeric aromatics complex with heterocyclic sulfur-containing rings	Cellulose fibers, cotton, viscose, rayon
Vat	Initially water insoluble dyes is dissoluted by reducing them with sodium hydrogensulfite but re-oxidized upon fixing on fibers	Cotton, wool, rayon

2.9.2 Methylene Blue

Methylene blue (MB) is a positively charged dye (or better known as cationic dye) applied for biological staining purpose, medicine and various dyeing industries. MB is one of the cationic dyes that is applied in textile industry (S. A. Umoren et al., 2013). According to Mia et al. (2019), the textile industry is utilizing 1.3 million tons of dyes and pigments per year, wherein most of the dyes applied are toxic and synthetic in nature. Among the dyes used, 10-25% textile dyes are wasted during the dyeing process which also led to 2-20% of dyes remained discharged as industrial effluent (Mia et al., 2019). Molecular formula of MB is $C_{16}H_{18}NSCl$ and its chemical structure is consisting of a heterocyclic aromatic component, as shown in Figure 2.8 (S. Umoren et al., 2013). Although MB is used in some medical treatments, it can cause eye burn which could be a permanent damage for both human beings and animals. On acute exposure through inhalation, it may results in difficult breathing or even methemoglobinemia (MM Abd El-Latif et al., 2010; X. Yang et al., 2016). Methemoglobinemia occurs when red blood cells contain methemoglobin exceeding 1%. This results in oxygen deficiency to the body tissues. External contacts by the skins may cause irritation. Moreover, ingestion would lead to complications such as burning sensation, nausea, vomiting, perspiration, diarrhea, gastritis and shock (S. Umoren et al., 2013; X. Yang et al., 2016). In addition, MB is determined to be mutagenic to *Escherichia coli*, *Micrococcus aureus*, and *Salmonella typhimurium* which are microorganisms in natural water bodies (Program, 1990). Hence, it is imperative that MB should be removed from wastewater before it is being discharged to the environment, despite MB is not the most concerned dyes pollution by volume caused in textile dyeing industries (Yaseen & Scholz, 2019). Thus, the removal of MB from wastewater is one of the major environmental concerns to be tackled.

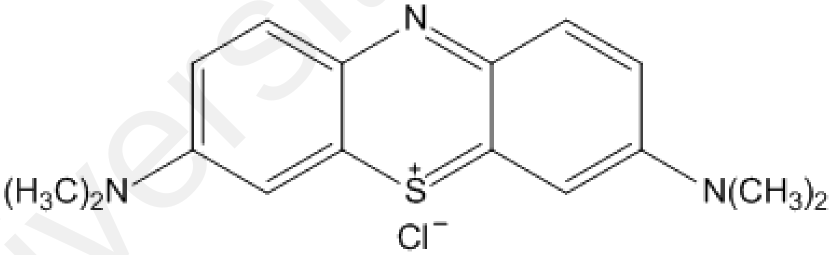

Figure 2.8: Structure of methylene blue.

2.10 Adsorption

Adsorption is a phenomenon whereby substances are accumulated on a surface interface through a mass transfer process. This theory was first discovered by Lowitz in 1785, in which subsequently he applied it for colorants removal in the sugar refineries. However, its application has been recorded since ancient time. Date back to 4000 BC in Sanskrit texts, a similar method had been reported to enhance the taste and odor of drinking water. The mass transfer process happens when a substance which is abundance in the bulk phase (adsorbate) diffuse and adhered onto a solid phase (adsorbent) (Liang et al., 2014).

i. The efficacy of adsorption is dependent on several factors, such as:
ii. The nature of surface functional groups on the adsorbent.
iii. The initial concentration of the adsorbate.
iv. The nature of adsorbent or adsorbate.
v. The effective surface area of adsorbent.
vi. The solubility of the adsorbate in aqueous phase.
vii. The surroundings temperature of the adsorbent-adsorbate system.
viii. Solution pH in the case of liquid phase applications.

2.10.1 Types of Adsorption

Adsorption can be categorized into two distinctions which are the chemical adsorption or physical adsorption. Chemical adsorption or chemisorption is an adsorption which occurs when the adsorbate interacts with the adsorbent's interface to form chemical or ionic bonds. The chemical interactions between the adsorbent and adsorbate are attractive forces akin to covalent bonds formed between atoms and comply with Coulomb's law.

For physical adsorption, adsorbates undergo physical interactions through columbic attractions that exclude covalent bonding with the adsorbent's interface. Sometimes, it is difficult to differentiate in between physical adsorption and chemisorption. In comparison with chemisorption, physical adsorption is built up from weaker forces and thus the energy of bonding is relatively lower. However, this attraction by physical means works over a longer distance as compared with chemisorption. In addition, there are no preferential adsorption sites for the adsorbate to be accumulated on adsorbent's interface through physical adsorption. For instance, the adsorption of organic molecules from water to a non-polar adsorbent is dictated by the Van der Waals forces that exist between the organic molecules and the adsorbent. Moreover, non-polar compounds which are larger tend to be adsorbed more intensely to the non-polar adsorbents through hydrophobic bonding. In terms of attraction by means of Van der Waals forces, the interactions increase proportionally with the adsorbate's polarizability and size (Liang et al., 2014). Table 2.7 shows the comparison of chemical and physical adsorption.

Table 2.7: Comparison of chemical and physical adsorption (Chowdhury, 2013).

Parameters	Chemical Adsorption	Physical Adsorption
Adsorption layer	Monolayer only	Multilayers
Enthalpy Change (kJ/mol)	40-400	20-40
Effect of Temperature	Favored at high temperature	Favored at low temperature
Sorption/mass ratio	Small	Large
Specificity	High	Low
Surface coverage	Incomplete	Complete
Nature of interaction	Irreversible	Reversible

2.10.2 Adsorption Mechanism

Adsorption mechanisms are often divided into two groups which involved chemisorption and physisorption, respectively. Adsorption is realized due to the interactions between adsorbent and adsorbate, which includes one or combinations of the interactions as summarized in Table 2.8 (Dobias et al., 1999).

Table 2.8: Adsorption mechanisms involved chemisorption and physisorption (Dobias et al., 1999).

Types of Adsorption	Types of Interactions	Remarks
Chemisorption	Covalent bonding	Formation of covalent bonds between adsorbate and adsorbent based on chemical bond that involves the sharing of electron pairs between atoms.
	Ionic Bonding	Relates to the electrostatic attraction between oppositely charged ions, which are the cations and anions.
	Surface complexing	Involves chelation which is a type of bonding of ions and molecules to metal ions through coordinate bonds. For a coordinate bond, two electrons are derived from the same atom.
	Surface precipitate	Adsorbates together with ions from the electric double layer or its bordering solution form insoluble products on the surface of adsorbent.
Physisorption	Hydrogen bridges	Formation of hydrogen bonding between adsorbent and adsorbate. Hydrogen bonding is resulted from the partially electrostatic attraction between hydrogen atom and a more electronegative atom, such as nitrogen, oxygen, or fluorine.
	Van der Waals forces (dipole-dipole forces)	Dipole-dipole interaction is the attraction occurs when both adsorbate and adsorbent are polar molecules.
	Van der Waals forces (dipole-induced dipole forces)	Dipole-induced dipole interaction happens when a polar molecule induces a dipole in an atom or in a nonpolar molecule by disturbing the arrangement of electrons in the nonpolar species.
	Van der Waals forces (London dispersion)	Dispersive interactions are always attractive and occur between any pair of molecules, polar or non-polar, that are nearby to each other due to fluctuating dipoles.

2.10.3 Types of Adsorption Studies

Generally, there are two types of adsorption studies which are the batch mode and continuous flow mode. In batch mode adsorption studies, the same adsorbate remains in contact with a certain quantity of the adsorbent, until equilibrium is achieved between the solute present in liquid phase and the solute adsorbed per unit mass of the adsorbent. The equilibrium achieved is static in nature as it does not vary profoundly with time. Batch mode of adsorption studies are easy to operate and control on the laboratory scale. In addition, preference for adsorption studies have been carried out through batch mode as practiced by many researchers because it is a less time-consuming technique and less adsorbent material is required. Most importantly, batch equilibrium experiment indicates the adsorption capacity of the adsorbent. Through this study mode, the fundamental information about the effectiveness of adsorbate-adsorbent system could be evaluated (Chowdhury, 2013).

Contrarily, influent enters and elutes from a column packed with adsorbent in a continuous flow mode of adsorption study. As a result, complete equilibrium is never achieved in between the solutes present in the solution and the amount adsorbed during the short contact time. Equilibrium has to be continuously re-established when fresh influent enters. Therefore, equilibrium system in column mode is also known as the dynamic equilibrium of sorption. Furthermore, adsorption system in continuous flow mode is effective on large scale wastewater treatment and cyclic adsorption-desorption. From experiments, breakthrough curve is attainable from continuous flow mode of adsorption study which further assists in evaluating operation life span and reusability of column bed (Chowdhury, 2013; Russo et al., 2017). From critical review of Russo et al. (2017), the authors conclude that the ideal way to design an adsorption column is starting from a detailed laboratory-scale batch adsorption studies and interpret the data with a rigorous model. Upon investigating the crucial aspects of the adsorption system, the behavior of an adsorption column could be more predictable, and this is beneficial for the scale-up of the adsorption system.

2.10.4 Adsorption Isotherm

Adsorption isotherms are used to express the relationship between the mass of adsorbate adsorbed per unit mass of the adsorbent and the liquid phase adsorbate's concentration at equilibrium states. This adsorption equilibrium relationship is known as the isotherm and it allows the adsorption capacity of the adsorbent to be calculated at any given aqueous-phase adsorbate's concentration. The adsorption capacity at equilibrium states is determined using a mass balance equation, as follows:

$$q_A = \frac{V}{m}(C_o - C_A) \tag{2.1}$$

where q_A is amount of adsorbate adsorbed per gram of adsorbent at equilibrium (mg/g), C_o is initial concentration of adsorbate (mg/L), C_A is concentration of adsorbate at equilibrium (mg/L), V is the total volume of experimental solution (L), and m is the mass of adsorbent (g). The experimental data obtained from the effect of varied initial adsorbate concentrations in adsorption process is used to calculate the adsorption isotherms.

Table 2.9 lists some of the previous works determined for PVA, chitin, cellulose and PVA-based composites for dyes removal which follows different isotherm models. Based on the review, it was determined that two isotherm models, namely Langmuir and Freundlich isotherms were adopted commonly in investigation of adsorbent system with dyes adsorbate. Hence, Langmuir and Freundlich isotherms were applied in the present investigation and thus reviewed in detail in this section.

Table 2.9: Summary of adsorption isotherms determined for PVA, chitin, cellulose and PVA-based composites.

Adsorbent Name	Name of dyes	Adsorption Isotherm	References
Poly(vinyl alcohol)	Methylene blue	Freundlich isotherm	(S. Umoren et al., 2013)
Poly(vinyl alcohol)	Bromothymol blue	Langmuir isotherm	(Agarwal et al., 2016)
Poly(vinyl alcohol)	Methylene blue	Langmuir isotherm	(Agarwal et al., 2016)
α-chitin	Methylene blue	Langmuir isotherm	(Dhananasekaran et al., 2016)
α-chitin	Bromophenol blue	Langmuir isotherm	(Dhananasekaran et al., 2016)
α-chitin	Coomassie brilliant blue	Langmuir isotherm	(Dhananasekaran et al., 2016)
Chitin	Reactive yellow 2	H-type isotherms	(Akkaya et al., 2007)
Chitin	Reactive black 5	H-type isotherms	(Akkaya et al., 2007)
Untreated chitin	Reactive Red 141	Langmuir isotherm	(Dolphen et al., 2007)
Chitin	Indigo carmine dye	Langmuir isotherm	(Prado et al., 2004)
Cellulose Almond Shell	Violet B azo dye	Langmuir isotherm	(Hashemian, 2014)
Magnetic cellulose beads with activated carbon	Methylene blue	Langmuir isotherm	(Xiaogang Luo & Zhang, 2009)
Partially hydrolyzed polyacrylamide/cellulose nanocrystal	Methylene blue	Langmuir isotherm	(Zhou et al., 2014)

'Table 2.9, continued'

Adsorbent Name	**Name of dyes**	**Adsorption Isotherm**	**Reference**
Poly(vinyl alcohol)/chitosan	Methylene blue	-	(Casey & Wilson, 2015)
PVA/GA/β-cyclodextrin	Methylene blue	Freundlich isotherm	(Ghemati & Aliouche, 2014)
PVA/GA/β-cyclodextrin	Reactive dye	Langmuir isotherm	(Ghemati & Aliouche, 2014)
Poly(vinyl alcohol)/attapulgite	Methylene blue	Langmuir isotherm	(L. Yang et al., 2011)
Poly(vinyl alcohol)/alginate/rice husk biomass	Direct Blue-67	Langmuir isotherm	(Safa & Bhatti, 2011)
Poly(vinyl alcohol)/poly(acrylic acid	Methylene blue	Freundlich isotherm	(Kamal, 2014)
Poly(vinyl alcohol)/poly(acrylic acid/clay	Methylene blue	Freundlich isotherm	(Kamal, 2014)
Poly(vinyl alcohol)/4A-zeolite	Methylene blue	Freundlich isotherm	(Baheri et al., 2016)
Poly(vinyl alcohol)/attapulgite	Methylene blue	Langmuir isotherm	(L. Yang et al., 2011)
Poly(vinyl alcohol)/graphene oxide	Methylene blue	Freundlich isotherm	(X. Yang et al., 2016)
Poly(vinyl alcohol)/carboxymethyl starch-g-polyvinyl imidazole	Crystal violet	Langmuir isotherm	(Pour & Ghaemy, 2015)
Poly(vinyl alcohol)/carboxymethyl starch-g-polyvinyl imidazole	Congo red	Freundlich model	(Pour & Ghaemy, 2015)

2.10.4.1 Langmuir Adsorption Isotherm

Langmuir isotherm model is the best representing adsorption isotherm model for monolayer adsorption. This isotherm describes the reversible chemical equilibrium between the adsorbate and adsorbent at the surface-solution interface (Langmuir, 1918). The chemical reaction of the adsorption process defines that the adsorbate (A) will diffuse to the surface's vacant sites (S_v) to form adsorbate-bounded surface sites (SA). The equation could be represented as follows:

$$S_V + A \leftrightarrow SA \tag{2.2}$$

where S_V is the vacant surface sites (mmol/m^2), A is adsorbate in solution (mmol) and SA is adsorbate-bounded surface sites (mmol/m^2).

Assumption is made that the reaction as expressed in Equation 2.2 is consisted of a constant value to standard Gibbs free energy change (ΔG°) for all surface sites. Furthermore, it is predefined that each vacant site is capable of binding only one molecule. The model approves for accumulation of adsorbate is only up to a single layer onto the adsorbent. The equilibrium equation is represented as:

$$K_{ads} = \frac{SA}{S_V C_A} = e^{\left(-\Delta G^o /_{RT}\right)} \tag{2.3}$$

where K_{ads} is the adsorption equilibrium constant (L/mg), C_A is the concentration of adsorbate A in solution (mg/L), ΔG° is the standard Gibbs free energy change for adsorption (J/mol), R is the universal gas constant of 8.314 J/K·mol and T is the absolute temperature (K).

Equation 2.3 can be simplified and expressed by eliminating the S_v constant upon fixing the total number of adsorption site (S_T), as follows:

$$S_T = SA + S_V = SA + \frac{SA}{K_{ads}C_A} \tag{2.4}$$

where S_T is the total number of sites available for a single layer coverage. Upon expressing Equation 2.4 in terms of SA, it gives:

$$SA = \frac{S_T}{1+(\frac{1}{K_{ads}C_A})} = \frac{K_{ads}C_AS_T}{1+K_{ads}C_A} \tag{2.5}$$

It is known that mass loading, q_A:

$$q_A = (SA)(A_{ads})(MW) \tag{2.6}$$

where q_A is amount of adsorbate A adsorbed per gram of adsorbent at equilibrium (mg/g), A_{ads} is the surface area per unit gram of adsorbent (m^2/g), MW is the molecular weight of adsorbate A (g/mol). When redefining Equation 2.5 in terms of mass loading, q_A:

$$q_A = \frac{K_{ads}C_AS_TA_{ads}MW}{1+K_{ads}C_A} = \frac{q_MK_{ads}C_A}{1+K_{ads}C_A} = \frac{q_MK_LC_A}{1+K_LC_A} \tag{2.7}$$

where C_A is the concentration of adsorbate A in solution at equilibrium (mg/L), q_M is the maximum adsorption capacity of adsorbate per unit mass of adsorbent (mg/g), K_L is the Langmuir adsorption constant of adsorbate A (L/mg). K_{ads} is the adsorption equilibrium constant, whereby it is termed as Langmuir adsorption constant (K_L) when assumptions for Langmuir isotherm model are obeyed (Langmuir, 1918; Liang et al., 2014).

Lastly, the Equation 2.7 could be represented to a linear form, as follows:

$$\frac{C_A}{q_A} = \frac{1}{K_Lq_M} + \frac{C_A}{q_M} \tag{2.8}$$

The plot using experimental data expressing the relationship of C_A/q_A against C_A will give a straight line with $1/q_M$ expressed as the slope while $1/(K_L \cdot q_M)$ is the intercept

(Dhananasekaran et al., 2016). Correlation coefficient (R^2) has to be calculated to show the fitting of adsorption process to Langmuir isotherm model.

Further analysis of Langmuir equation could be carried out and a dimensionless equilibrium parameter (R_L) is termed. R_L is used as an indicator of adsorption's feasibility of an experiment.

$$R_L = \frac{1}{1 + K_L C_o} \tag{2.9}$$

where K_L is the Langmuir constant and C_o is the initial concentration of adsorbate.

The value of R_L indicates the adsorption nature of the dye with the adsorbent. If the R_L value is more than 1, the adsorption process is unfavorable. If R_L value is equal to 1 or the value lies in between 0 and 1 indicates that the adsorption is linear and favorable. R_L equals to 0 indicates irreversible adsorption process (Dhananasekaran et al., 2016; M. Kumar et al., 2009).

2.10.4.2 Freundlich Adsorption Isotherm

For heterogeneous adsorbents, it is best modeled to the Freundlich adsorption isotherm equation (Dhananasekaran et al., 2016; Liang et al., 2014). This is because Freundlich isotherm predicts the reversible adsorption of a heterogeneous system whereby it is not of monolayer formation. Freundlich adsorption isotherm equation is:

$$q_A = K_F C_A^{(\frac{1}{n})} \tag{2.10}$$

In linearized form, it is expressed as:

$$log(q_A) = log(K_F) + \frac{1}{n} log(C_A) \tag{2.11}$$

where q_A is the amount of adsorbate adsorbed per gram of adsorbent at equilibrium (mg/g), C_A is the concentration of adsorbate in solution at equilibrium (mg/L), K_F is the

Freundlich isotherm constant related to adsorption capacity [(mg/g)·(L/mg)$^{1/n}$] and 1/n is the unit less Freundlich adsorption intensity parameter.

When the 1/n value is between 0.1 and less than equal to 0.5 the adsorption process is most favorable. If the value is between 0.5 and 1, the process is easy to adsorb and if the value is greater than 1 it is highly unfavorable and difficult to adsorb (Dhananasekaran et al., 2016). Moreover, the value of 1/n gives indication on adsorbent's surface heterogeneity whereby value closer to zero signifies greater heterogeneity (Nassar et al., 2017).

Freundlich equation (Equation 2.10) is derived from the Langmuir equation (Equation 2.5), with additional two assumptions made to model the adsorption of a given free energy:

i. The adsorption's surface site energies is with Boltzmann distribution with mean site energy (ΔH_M^o).
ii. the change of surface sites' entropy is a linear function of change of site enthalpy ($-\Delta H^o$).

Given these assumptions, the Freundlich adsorption intensity parameter is 1/n and n is:

$$n = \frac{\Delta H_M^o}{RT} - \frac{r\Delta H^o}{R} \qquad (2.12)$$

where ΔH_M^o is the mean site energy (J/mol), ΔH^o is the change of site enthalpy (J/mol), R is the universal gas constant at 8.314 J/(K·mol), T is absolute temperature (K) and r is a proportionality constant (Liang et al., 2014).

According to Halsey (1952), Freundlich maximum adsorption capacity can be estimated by the equation:

$$K_F = \frac{q_M}{C_o^{1/n}}, \tag{2.13}$$

where C_o is the initial adsorbate concentration (mg/L) and q_M is the Freundlich maximum adsorption capacity (mg/g). This estimation of maximum adsorption capacity by Freundlich constant had been reported by other researchers (Hamdaoui & Naffrechoux, 2007; Nassar & Abdallah, 2016).

2.10.5 Adsorption Kinetics

Kinetic study involves the investigation on the rates of chemical processes in order to understand the factors which affect the rates. Adsorption kinetics study requires meticulous monitoring on the experimental conditions which could affect the speed of completion of the adsorption reaction. This allows the adsorption equilibrium to be attained in a reasonable duration of time. Upon determining the reaction rates and the dependent factors of adsorption involved, the data obtained could be beneficial in developing the adsorbent materials for industrial application. In addition, it would help in understanding the complex dynamics of the adsorption process (S. S. Gupta & Bhattacharyya, 2011).

Rate of adsorption is depending on the concentrations of the chemical species involved in the adsorption process. Conventionally, rate law could be expressed in the form of Equation 2.14.

$$\text{Rate} = k[X]^a[Y]^b \ldots\ldots \tag{2.14}$$

where k is the rate constant, a and b define the reaction order of chemical species. X and Y represent concentrations of chemical species involved in the adsorption study.

With the derivation of the rate law, it yields information on the possible adsorption mechanism involved. It is essential to establish the rate law of adsorbate-adsorbent interactions in the effort of understanding the mechanism by which the adsorbate accumulates and adsorbed onto the surface of the solid adsorbent. Adsorption models are theoretical equations which express the adsorption kinetics. With the best fitting of experimental data to the adsorption kinetic model being studied, it is interpreted as the adsorption process indeed follows the adsorption kinetic proposed in the kinetic model chosen (S. S. Gupta & Bhattacharyya, 2011; McKay et al., 1999).

Table 2.10 summarizes some of the works reported in the literature on adsorption kinetics of dyes onto PVA, chitin, cellulose and PVA-based adsorbents. From literature, it was observed that most of the equilibrium data were investigated against the pseudo-first order or pseudo-second order kinetic models. Therefore, it was determined that the maleic acid cross-linked PVA/Chitin/NCC investigated in the present study is to be fitted with the pseudo-first order and pseudo-second order kinetic models.

Table 2.10: Summary of adsorption kinetics determined for PVA, chitin, cellulose and PVA-based composites.

Adsorbent Name	Name of dyes	Kinetic Model	References
Poly(vinyl alcohol)	Methylene blue	Pseudo-second order	(S. Umoren et al., 2013)
Poly(vinyl alcohol)	Bromothymol blue	Pseudo-second order	(Agarwal et al., 2016)
Poly(vinyl alcohol)	Methylene blue	Pseudo-second order	(Agarwal et al., 2016)
α-chitin	Methylene blue	Pseudo-second order	(Dhananasekaran et al., 2016)
α-chitin	Bromophenol blue	Pseudo-second order	(Dhananasekaran et al., 2016)

'Table 2.10, continued'

Adsorbent Name	Name of dyes	Kinetic Model	References
α-chitin	Coomassie brilliant blue	Pseudo-second order	(Dhananasekaran et al., 2016)
Chitin	Reactive yellow 2	Intraparticle diffusion	(Akkaya et al., 2007)
Chitin	Reactive black 5	Intraparticle diffusion	(Akkaya et al., 2007)
Untreated chitin	Reactive Red 141	-	(Dolphen et al., 2007)
Sodium hypochlorite-treated chitin	Reactive Red 141	-	(Dolphen et al., 2007)
Chitin	Indigo carmine dye	-	(Prado et al., 2004)
Cotton Cellulose	Direct blue 71	Pseudo-second order	(Ali Ashjarana & Hajilarib, 2013)
Bacterial Cellulose	Direct blue 71	Pseudo-second order	(Ali Ashjarana & Hajilarib, 2013)
Cellulose Almond Shell	Violet B azo dye	Pseudo-second order	(Hashemian, 2014)
Magnetic cellulose beads with activated carbon	Methylene blue	Pseudo-second order	(Xiaogang Luo & Zhang, 2009)
Partially hydrolyzed polyacrylamide/cellulose nanocrystal	Methylene blue	Pseudo-second order and Elovich	(Zhou et al., 2014)
Poly(vinyl alcohol)/chitosan	Methylene blue	-	(Casey & Wilson, 2015)
PVA/GA/β-cyclodextrin	Methylene blue	-	(Ghemati & Aliouche, 2014)
PVA/GA/β-cyclodextrin	Reactive dye	-	(Ghemati & Aliouche, 2014)
Poly(vinyl alcohol)/attapulgite	Methylene blue	Pseudo-second order	(L. Yang et al., 2011)

‘Table 2.10, continued’

Adsorbent Name	**Name of dyes**	**Kinetic Model**	**References**
Poly(vinyl alcohol)/alginate/rice husk biomass	Direct Blue-67	Pseudo-second order	(Safa & Bhatti, 2011)
Poly(vinyl alcohol)/poly(acrylic acid	Methylene blue	Pseudo-second order	(Kamal, 2014)
Poly(vinyl alcohol)/4A-zeolite	Methylene blue	Pseudo-second order	(Baheri et al., 2016)
Poly(vinyl alcohol)/polyaniline/clinoptilolite	Methylene blue	Intraparticle diffusion	(Rashidzadeh & Olad, 2013)
Poly(vinyl alcohol)/graphene oxide	Methylene blue	Pseudo-second order	(X. Yang et al., 2016)
Poly(vinyl alcohol)/carboxymethyl starch-g-polyvinyl imidazole	Crystal violet	Pseudo-second order	(Pour & Ghaemy, 2015)
Poly(vinyl alcohol)/carboxymethyl starch-g-polyvinyl imidazole	Congo red	Pseudo-second order	(Pour & Ghaemy, 2015)

2.10.5.1 Pseudo-first Order Kinetic

The Lagergren pseudo-first order equation is believed to be the earliest known kinetic model pertaining to the rate of adsorption in the liquid-solid phase systems based on the adsorption capacity (Lagergren, 1898; H. Qiu et al., 2009). Besides, the Lagergren rate equation has been one of the most widely used equations for adsorption of solutes from the liquid solution. It can be presented as in Equation 2.15.

$$\frac{dq_t}{dt} = k_1(q_A - q_t) \tag{2.15}$$

where q_A and q_t (mg/g) are the adsorption capacities at equilibrium time and time t (min), respectively. k_1 (1/min) is the pseudo-first order kinetic rate constant. With boundary conditions of t = 0, $q_t = 0$ and t = t, $q_t = q_t$, the integrated form of Equation 2.15 could be rearranged for linearized data plotting as shown by Equation 2.16:

$$log(q_A - q_t) = log(q_A) - \frac{k_1}{2.303}t \tag{2.16}$$

From this linearized equation, the value of k_1 can be determined from the slope of the linear plot log (q_A-q_t) versus t. However, when experimental data is used to apply on Equation 2.16 and the parameter q_A evaluated will generally deviated from the true first-order equation in two ways. Firstly, q_A is not the exact number of available sites for adsorption. Secondly, log q_A is an adjustable parameter whereby it is often not equal to the intercept of the log (q_A-q_t) against t plot. This finding is contradicted to the ideal first-order reaction system whereby log q_A should be equal to the intercept of the linear plot (Y. Ho et al., 2000).

In fact, Equation 2.16 is only an approximate solution to the ideal first-order mechanism (H. Qiu et al., 2009). Equilibrium sorption capacity, q_A must be pre-determined when fitting Equation 2.16 to experimental data. In practical case, accurate determination of q_A is a difficult task. This is due to the fact that chemisorption tends to become immeasurably slow after the initial fast response in most cases of adsorbate-adsorbent interactions. It is very difficult to ascertain that equilibrium for a reaction has been achieved.

Hence, a best approximation has to be made about q_A which introduces the element of uncertainty in the calculations. From literature, it is reported that there is possibility that equilibrium sorption capacity, q_A obtained even after a long interaction time is still significantly smaller than the actual equilibrium value (S. S. Gupta & Bhattacharyya, 2011; Y. Ho et al., 2000). In many adsorption cases, it is remarked that Lagergren pseudo-first order model is found fitting only to the initial portions of adsorption reaction and not meant for the whole range of contact time (McKay et al., 1999). On the other hand, the adsorption rate constant, k_1 varies from system to system, depending on the initial concentration of the adsorbate in an adsorption process. Generally, k_1 value decreases with the increase of initial adsorbate concentration in the adsorption process (S. S. Gupta & Bhattacharyya, 2011).

Practically, the validation of Equation 2.16 arises from the comparison of the data derived from the q_A value determined experimentally and those data derived from the ideal plot of log (q_A-q_t) against t. In the event whereby fitting test is not validated, then higher order of kinetic models are to be validated with respect to the experimental results. This implies that the adsorption process is of a much more complex nature over the basis of simple first-order kinetics (S. S. Gupta & Bhattacharyya, 2011).

2.10.5.2 Pseudo-second Order Kinetic

As discussed by McKay et al. (1999), for a reaction which follows pseudo-second order kinetic model, the rate equation is expressed as:

$$\frac{dA_t}{dt} = k\ (A_t - A_o)^2 \tag{2.17}$$

where A_t and A_o are the number of occupied active sites of the adsorbent at time t and the active sites available on the adsorbent, respectively. k is the rate constant.

Hypothesis was made that the adsorption capacity increases proportionally to the number of occupied active sites. Hence, rate equation is deduced as:

$$\frac{dq_t}{dt} = k_2(q_A - q_t)^2 \tag{2.18}$$

where q_A and q_t (mg/g) are the adsorption capacity at equilibrium time and time t (min), respectively. k_2 [g/(mg·min)] is the rate constant of pseudo-second order kinetic model. This shows that adsorption reaction is governed by a second-order rate equation

(Largitte & Pasquier, 2016). Similarly, the second-order rate equation as disclosed by McKay et al. (1999) are known as pseudo-second order rate equation to distinguish kinetic equations based on adsorption capacity from concentration of solution (H. Qiu et al., 2009).

By integration of Equation 2.18 in boundary conditions ($q_t = 0$ at $t = 0$ and $q_t = q_t$ at $t = t$) and rearrangement of variables yields in a linear expression in the form as follows:

$$\frac{t}{q_t} = \frac{1}{k_2 q_A^2} + \frac{1}{q_A} t \qquad (2.19)$$

With the correlation of data to pseudo-second order kinetic model, the plot of t/q_t against t gives a straight line. Thus, k_2 and q_A can be determined from the intercept and slope of the t/q_t against t graph directly.

Previous theoretical and experimental investigations imply that k_2 is significantly depend on the initial adsorbate's concentration in the bulk phase. In addition, k_2 decreases in conjunction with increasing initial adsorbate's concentration, with condition that k_2 is the time-scaling factor. Thus, a longer time is needed to achieve adsorption equilibrium when a higher initial concentration of adsorbate is applied. As a result, k_2 decrease in value accordingly. Besides, it is also reported that there is high possibility of this pseudo-second order kinetic model to be applicable on wider range of adsorption studies (S. S. Gupta & Bhattacharyya, 2011). With the correlation of experimental adsorption data to the this pseudo-second order kinetic model, it indicates that chemisorption is the rate determining step (McKay et al., 1999; H. Qiu et al., 2009).

2.10.6 Adsorption Thermodynamic

From the standard Gibbs free energy change (ΔG°), the degree of spontaneity of an adsorption process could be determined. A higher negative value of ΔG° indicates a more energetically favorable adsorption. According to thermodynamic law, ΔG° of adsorption is calculated as follows:

$$\Delta G^o = -2.303RT\log K_c \tag{2.20}$$

in which R is the universal gas constant (8.314 J/ mol·K), T is the absolute temperature in kelvins and K_c is the dimensionless thermodynamic equilibrium constant. In the adsorption study, Equation 2.20 is applied in the determination of ΔG° (kJ/mol). Moreover, ΔG° is related to standard enthalpy change of adsorption (ΔH°) and standard entropy change of adsorption (ΔS°) in an expression, as follows:

$$\Delta G^o = \Delta H^o - T\Delta S^o \tag{2.21}$$

By substituting Equation 2.20 into Equation 2.21, it is determined:

$$\log K_c = -\frac{\Delta H^o}{2.303RT} + \frac{\Delta S^o}{2.303R} \tag{2.22}$$

Theoretically, log K_c against 1/T plot gives yield to a straight line which allows ΔH° (kJ/mol) and ΔS° (J/mol·K) to be estimated from the respective slope and interception of Equation 2.22. This estimation on the thermodynamic parameters served as insight for the types and mechanism of an adsorption process. From ΔH°, the adsorption process could be determined either to be of exothermic or endothermic reaction. Positive value of ΔH° signifies that the adsorption is an endothermic process whereas negative value of ΔH° implies the exothermic nature of adsorption reaction. According to literature, if the enthalpy change ΔH° value of adsorbent is in the 40-400 kJ/mol range, the process is chemisorption whereas the enthalpy change value of less than 40 kJ/mol reveals that the adsorption is physisorption (Ma et al., 2012; Öztürk & Malkoc, 2014; Raj, 2002; Taleb et al., 2009).

On the other hand, negative ΔS° corresponds to decrease in degree of freedom of the adsorbed species at the solid-solution interface during the adsorption process (Baheri et al., 2016; Baraka, 2012; Taleb et al., 2009; S. Umoren et al., 2013). Moreover, it indicates the ease of regeneration of the adsorbent (Baraka, 2012). Contrarily, positive value of ΔS° indicates the increased randomness at the solid-solution interface during adsorption process. In addition, it should be noted that the determination of ΔG°, ΔH° and ΔS° are depending on the estimation of thermodynamic equilibrium constant (K_c), as stated in Equation 2.20.

In many studies of adsorption thermodynamics with low adsorbate concentration, the thermodynamic equilibrium constant (K_c) is expressed as Equation 2.23 (M. Kumar et al., 2009; Paşka et al., 2014; Safa & Bhatti, 2011; Shu et al., 2017).

$$K_c = \frac{C_{ad}}{C_A} \tag{2.23}$$

where C_{ad} is the equilibrium concentration of adsorbate onto the adsorbent (mg/L) and C_A is the equilibrium concentration of adsorbate in solution (mg/L). C_{ad} resembles the amount of adsorbate on the adsorbent per liter of the solution at equilibrium of adsorption process. Table 2.11 summarizes the adsorption thermodynamics determined for PVA, chitin, cellulose and PVA-based composites.

Table 2.11: Summary of adsorption thermodynamics determined for PVA, chitin, cellulose and PVA-based composites.

Name of Adsorbent	Name of Adsorbate	Temperature (K)	ΔG° (kJ/mol)	ΔH° (kJ/mol)	ΔS° (J/mol·K)	References
Poly(vinyl alcohol)	Methylene blue	303	7.08	-2.30	-30.9	(S. Umoren et al., 2013)
Poly(vinyl alcohol)	Bromothymol blue	298	-	-	-	(Agarwal et al., 2016)
Poly(vinyl alcohol)	Methylene blue	298	-	-	-	(Agarwal et al., 2016)
α-chitin	Methylene blue	298	-	-	-	(Dhananasekaran et al., 2016)
α-chitin	Bromophenol blue	298	-	-	-	(Dhananasekaran et al., 2016)
Chitin	Reactive yellow 2	293	-	-	-	(Akkaya et al., 2007)
Chitin	Reactive black 5	293	-	-	-	(Akkaya et al., 2007)
Untreated chitin	Reactive Red 141	303	-	-	-	(Dolphen et al., 2007)
Sodium hypochlorite-treated chitin	Reactive Red 141	303	-	-	-	(Dolphen et al., 2007)
Chitin	Indigo carmine dye	298.1	2.99 ± 0.39	−40.12 ± 3.52	−145 ± 13	(Prado et al., 2004)

‘Table 2.11, continued’

Name of Adsorbent	**Name of Adsorbate**	**Temperature (K)**	**ΔG° (kJ/mol)**	**ΔH° (kJ/mol)**	**ΔS°m (J/mol·K)**	**References**
Cotton Cellulose	Direct blue 71	303	-14.30	-18.07	-198	(Ali Ashjarana & Hajilarib, 2013)
Bacterial Cellulose	Direct blue 71	303	-16.20	-26	-228	(Ali Ashjarana & Hajilarib, 2013)
Cellulose Almond Shell	Violet B azo dye	298	-	-	-	(Hashemian, 2014)
Partially hydrolyzed polyacrylamide/cellulose nanocrystal	Methylene blue	298	-	-	-	(Zhou et al., 2014)
Poly(vinyl alcohol)/chitosan	Methylene blue	-	-	-	-	(Casey & Wilson, 2015)
PVA/GA/β-cyclodexrin	Methylene blue	296	-2.17	-	-	(Ghemati & Aliouche, 2014)
Poly(vinyl alcohol)/attapulgite	Methylene blue	303	-	-	-	(L. Yang et al., 2011)
Poly(vinyl alcohol)/alginate/rice husk b	Direct Blue-67	303	6.09	23.03	54.99	(Safa & Bhatti, 2011)
Poly(vinyl alcohol)/poly(acrylic acid	Methylene blue	303, 318	-	-193.2	-	(Kamal, 2014)

‘Table 2.11, continued’

Name of Adsorbent	**Name of Adsorbate**	**Temperature (K)**	**ΔG° (kJ/mol)**	**ΔH° (kJ/mol)**	**ΔS° (J/mol·K)**	**References**
Poly(vinyl alcohol)/poly(acrylic acid /clay	Methylene blue	303, 318	-	-178.9	-	(Kamal, 2014)
Poly(vinyl alcohol)/4A-zeolite	Methylene blue	298	-3.47	-75.65	-242.1	(Baheri et al., 2016)
Poly(vinyl alcohol)/polyaniline/ clinoptilolite	Methylene blue	298	-	-	-	(Rashidzadeh & Olad, 2013)
Poly(vinyl alcohol)/graphene oxide	Methylene blue	303	-1697.4	13.2	-	(X. Yang et al., 2016)
Poly(vinyl alcohol)/carboxymethyl starch-g-polyvinyl imidazole	Crystal violet	298	-6.283	36.476	142.718	(Pour & Ghaemy, 2015)
Poly(vinyl alcohol)/carboxymethyl starch-g-polyvinyl imidazole	Congo red	298	-4.870	35.540	134.753	(Pour & Ghaemy, 2015)

2.10.7 Reusability of Adsorbent

The feasibility of prepared adsorbent for commercial application depends on several factors which include consideration of its reusability and disposal upon usage. Therefore, it is important that polymeric adsorbent prepared which is PVA/Chitin/NCC has high reusability. For reusability of adsorbent, treatments include thermal volatilization, bio-regeneration and chemical extraction by washing solvents have been employed to re-activate the sites of adsorption.

Re-activation of adsorbents by thermal volatilization requires high energy consumption despite it seems to be a convenient treatment for reusability of adsorbents. Nonetheless, when activated carbon is treated by thermal volatilization, 5%-10% of the active sites could be lost by burn-off and attrition during each cycle of thermal treatment (Chowdhury, 2013; Lim & Okada, 2005).

On the other hand, bio-regeneration technique could be considered as the most economical process. However, this technique is limited by the non-biodegradability and toxicity of the adsorbents towards microorganisms. Furthermore, the biological process is time-consuming since the rates of biological activities are slow (Chowdhury, 2013).

Therefore, reusability treatment through washing solvent can be considered as the preferred option in which loss of active sites for adsorption is minimized. It is viable to reactivate adsorbents by using washing solvent because the interaction between the adsorbent and the pollutant which could be driven by hydrophobic, electrostatic or ion-exchange interactions could be distorted (Alaba et al., 2018).

2.11 Summary

Properties of PVA, chitin and cellulose had been investigated and summarized. Utilization of the more flexible synthetic PVA with natural polymers such as the chitin and cellulose could serve as a viable approach to obtain PVA-based composite with improved functionalities, processability and physicochemical properties. It was determined that the adsorptions of one or more dyes on the surface of PVA, chitin and cellulosic materials were elucidated by many researchers. Moreover, there had been extensive utilization of NCC as the reinforcing constituent in composites due to its proven effectiveness in stress transfer. Despite of the fact that PVA, chitin or cellulose could act as an adsorbent, it was reviewed that there had been no report on the preparation of PVA/Chitin/NCC composites for the removal of dyes.

In comparison with conventional adsorbents such as commercial activated carbon and synthetic ion-exchange resins, adsorption of contaminants using polymeric adsorbents offer several additional advantages. There is an emerging trend in the development of alternative polymeric adsorbents due to the improved processability, reusability, selectivity to pollutants, stability, tunable properties and cost effectiveness of the adsorbents. However, there are limited studies carried out on the utilization of PVA-based composites in the application of dyes removal. Several recent studies focused on improvement strategies to enhance the adsorption capacities of the PVA-based composites. Strategies involved the stoichiometric mixtures of compatible materials which include natural polymers, synthetic polymers, inorganics and fillers. In addition, the adsorption studies on PVA-based composites carried out mainly focused on two major perspectives. The first perspective focuses on studying the experimental condition and adsorption limiting parameters towards the maximum removal capacity for a given dye. While, the second perspective focuses on the theoretical studies to elucidate the adsorption process by explaining experimental data based on existing or proposed theoretical models in general.

The potential application of the PVA/Chitin/NCC composite adsorbent could be evaluated through batch adsorption studies to determine the adsorption capacity of the adsorbent towards a model dye studied. Classification of dyes are based on chemical structures or according to the application method. The effective application of an adsorbent onto a model dye also indicate the suitability of the adsorbent for the similar class of dyes characterized based on the chemical structures. Nonetheless, factors which govern the extent of adsorption include nature of adsorbents and external adsorption parameters such as solution pH, adsorbent dosage and initial dyes concentration.

Furthermore, adsorption isotherm, kinetics, thermodynamics and reusability studies that were associated to the PVA-based adsorbent in relation to dyes adsorbate had been reviewed and summarized. It was determined that two isotherm models, namely Langmuir and Freundlich isotherms were adopted commonly in the investigation of PVA-based adsorbent with dyes adsorbate. Furthermore, it was observed that most of the adsorption equilibrium data were investigated against the pseudo-first order or pseudo-second order kinetic models. Thermodynamic studies on the various PVA-based adsorbents were limited. However, estimation on the thermodynamic parameters ($\Delta G°$, $\Delta H°$, $\Delta S°$) served as an insight for the types and mechanism of an adsorption process. In addition, reusability of adsorbent opts to be explored as it is an important consideration for commercial application. In brief, the fundamental information about the effectiveness of adsorbate-adsorbent system could be evaluated through all these adsorption studies.

CHAPTER 3: MATERIALS AND METHODOLOGY

3.1 Introduction

This chapter describes the methodologies to prepare nanocellulose from OPEFB fibers, chitin, PVA/Chitin/NCC composites and PVA/Chitin/NCC composites with maleic acid (MA) incorporated, respectively. This is followed by characterization techniques used to analyze PVA/Chitin/NCC composites and MA-treated PVA/Chitin/NCC composites. At the final stage, the feasibility of using MA-treated PVA/Chitin/NCC composites for adsorption applications were evaluated by monitoring the adsorption equilibriums of MB dye.

3.2 Materials

Poly(vinyl alcohol) utilized was under trade name Kuraray PVA-220S (degree of hydrolysis = 87%-89%, molecular weight (MW) = ~78 kDa) and manufactured by Kuraray Co. Ltd. (Singapore). Commercial chitin flakes (acetylation degree ≥ 95%, MW = ~100kDa) originated from shrimp shells was purchased from Sigma-Aldrich (M) Ltd. (Malaysia). Chitin flakes was purified before usage. OPEFB fiber was obtained from Sabutek Ltd. (Malaysia). Ammonium persulfate which was the oxidant for the OPEFB fiber treatment was supplied by R&M Chemicals Ltd. (Malaysia). Maleic acid, methylene blue (MB), calcium chloride dihydrate ($CaCl_2 \cdot 2H_2O$), 37% hydrochloric acid (HCl), methanol, sodium hydroxide (NaOH) and potassium hydroxide (KOH) pellets were sourced from Friendemann Schmidt Chemicals Ltd. (Germany). 95% ethanol was purchased from Fisher Scientific (M) Ltd. (Malaysia). Methylene blue which was the model cationic dye used was obtained from Systerm Ltd. (Malaysia). All of these chemicals were of analytical grade and used as received.

3.3 Methodology

3.3.1 Preparation of Nanocellulose from OPEFB Fiber

OPEFB fibers were first further grounded into finer powder using a Philips 600W HR-2115 Waring blender (Netherlands). Then, OPEFB fibers were passed through a 45 μm sieve. NCC was synthesized according to the methodology as described by Castro-Guerrero and Gray (2014) but with minor modification. 10 g of powdered OPEFB fiber was suspended with a liter of 1 M ammonium persulfate solution. The suspension was kept at 60°C for 24 h under constant vigorous stirring at 500 rpm using a Fisher Scientific 11-102-49SH hot plate magnetic stirrer mixer (U.S.A.) to give yield to NCC. NCC suspension was neutralized by drop-wise addition of 0.1 M NaOH to pH 7. The pH of the suspension was monitored by the Ohaus Starter 3000 bench pH meter (U.S.A.).

Subsequently, NCC was washed with distilled water by centrifugation at 10,000 rpm. The washing process was repeated for three times using the Gyrozen 1248b centrifuge (Korea). At each interval, the supernatant was being decanted and fresh distilled water was refilled into the 50 mL centrifugal tubes. After the three times washing, the NCC was re-suspended into a 200 mL NCC suspension. The 200 mL of NCC suspension was further dialyzed against 2 L of distilled water using cellulose membrane tubing to remove any potential salt impurities. The Sigma-Aldrich D9402-100FT (U.S.A.) cellulose membrane tubing used was with a molecular mass cut off at 12,000. The distilled water which served as the wash water was changed every hour for the first 3 h and twice a day on the days after. After dialysis for 48 h, the suspension was sonicated using the SASTEC ST-UB3300LDT digital ultrasonic cleaner (Malaysia) for 30 min to disperse the NCC formed. 1 mL of the suspension was drawn out from the total suspension using a micropipette. The weight of the sample withdrawn was determined using the KERN ABS 220-4N analytical balance (Germany). The weight of the suspension drawn out from the total suspension and the total volume of suspension were recorded as W_i and V, respectively. 1 mL of the suspension was oven dried at 60ºC until constant weight was achieved. The dry weight of NCC obtained after drying was recorded as W_f. The percentage of total solid content (TSC%) was calculated using the Equation 3.1. TSC% of a sample lot was determined three times to calculate the production yield using the Equation 3.2. The initial weight of OPEFB raw fibers used for the synthesis of NCC was recorded as W_S in Equation 3.2. In brief, the yield was calculated as the percentage of the ratio of the dry mass of NCC to the initial dry mass of the starting raw material used for synthesizing NCC (Filson et al., 2009; Jia et al., 2014). The production yield of three different sample lots were determined to be 17%-20%. NCC was kept in the suspension form and stored in a refrigerator.

$$TSC\% = \frac{W_f}{W_i} \times 100\% \tag{3.1}$$

$$Yield = \frac{(TSC\% \times V)}{W_S} \times 100\% \tag{3.2}$$

3.3.2 Preparation of Chitin

Purification of chitin was carried out since commercial chitin flakes consisted of residual proteins, mineral salts and pigments. For purification, chitin flakes was first soaked in the 7% HCl for 24 h to remove mineral salts. Then, it was transferred into a 5 wt.% KOH solution for 12 h to remove residual proteins. This was followed by depigmentation process whereby chitin was dispersed in the 50 wt.% ethanol for 12 h. At the interval of each mentioned steps above, chitin was neutralized with distilled water before proceeding to the consecutive step.

Upon purification, chitin was grounded into fine powder using a Philips 600W HR-2115 Waring blender (Netherlands) and dried at 60°C using the convection oven. The grounded chitin was passed through a 63 µm sieve to obtain chitin powder with narrow size distribution. Chitin flakes were processed into powder form to increase the surface contact area for efficient solvation by calcium chloride dihydrate ($CaCl_2•2H_2O$)/methanol solvent (Fan et al., 2007; Tamura et al., 2006). Upon drying, purified chitin was processed according to the literature as described by Tamura et al. (2006) but with minor modification. Briefly, saturated calcium chloride dihydrate ($CaCl_2•2H_2O$)/methanol solvent was first prepared by dissolving 680 g $CaCl_2•2H_2O$ in 800 mL methanol under reflux heating at 110°C for 45 min. The reflux heating was carried out at 110°C since boiling point of methanol and water were below of 110°C. Next, 12 g of powdered α-chitin was added into the prepared $CaCl_2•2H_2O$ /methanol solvent and heated reflux at 110°C for 24 h under vigorous stirring. Subsequently, 100 mL of distilled water was added into the viscous solution of α-chitin to dilute the α-chitin. α-chitin was agitated via a mechanical stirrer for 1 h to cool down the chitin to 40ºC before it was transferred to dialysis tubing cellulose membrane. This was to prevent heat damage onto the dialysis tubing cellulose membrane. Sigma-Aldrich D9402-100FT (U.S.A.) cellulose membrane tubing with the molecular mass cut off at 12,000 was used to dialyze the chitin against 2 L distilled water for five days to remove the calcium ions and methanol (Tamura et al., 2006). The distilled water which served as the wash water was changed every hour for the first 3 h. Subsequently, the wash water was changed twice daily for the consecutive five days. The resultant pure α-chitin obtained was then homogenized using the Waring blender to obtain a 2.00 ± 0.10 wt.% homogenized chitin. The percentage of total solid content of chitin was calculated using the Equation 3.1. Chitin was kept in the homogenized form before blending with PVA for the preparation of PVA/Chitin/NCC composites.

3.3.3 Preparation of PVA/Chitin/NCC Composite

10 wt.% of PVA solution was prepared by dissolving 80 g PVA in 720 g of distilled water at 85°C and stirred under constant stirring at 500 rpm for 4 h to ensure the complete dissolution of PVA. After stirring, α-chitin and NCC were added based on the composition ratio to obtain film with 5 g total solid content, as tabulated in Table 3.1. Prior usage, the NCC suspension was sonicated using a SASTEC ST-UB3300LDT digital ultrasonic cleaner (Malaysia) in the distilled water bath for 30 min. Then, the mixture was stirred for 3 h using an IKA RW20 digital overhead stirrer (Germany) to ensure that the composite blends were homogenized. The mixture was placed in an SASTEC ST-UB3300LDT ultrasonic bath for 45 min to remove air bubbles and then allowed to cool until room temperature. Lastly, the PVA-based composite was transferred onto the 18 cm × 18cm non-stick mold and afterward oven-dried for 24 h at 60°C to obtain a thin sheet. The neat PVA and neat chitin thin film were prepared for use as the control in this study. All samples were prepared to an average thickness of 0.15 ± 0.02 mm, as verified using a Mitutoyo absolute digital thickness gauge series 547-301 (Japan). The dried composite films were then removed from the non-stick molds. Then, the composites were stored in a drying cabinet at 23 ± 2°C under 50 ±5 % relative humidity (RH) for future usage.

Table 3.1: Compositional ratio for the PVA/Chitin blends reinforced with varied amount of NCC.

Sample Name	Mass Ratio of PVA/Chitin	Nanocellulose, NCC (wt.%)
PVA	100/0	
PVA/Chitin-10	90/10	
PVA/Chitin-20	80/20	
PVA/Chitin-30	70/30	
PVA/NCC-0.5	100/0	0.5
PVA/Chitin-10/NCC-0.5	90/10	0.5
PVA/Chitin-20/NCC-0.5	80/20	0.5
PVA/Chitin-30/NCC-0.5	70/30	0.5
PVA/NCC-1	100/0	1.0
PVA/Chitin-10/NCC-1	90/10	1.0
PVA/Chitin-20/NCC-1	80/20	1.0
PVA/Chitin-30/NCC-1	70/30	1.0
PVA/NCC-1.5	100/0	1.5
PVA/Chitin-10/NCC-1.5	90/10	1.5
PVA/Chitin-20/NCC-1.5	80/20	1.5
PVA/Chitin-30/NCC-1.5	70/30	1.5

3.3.4 Preparation of PVA/Chitin/NCC Composite with Maleic Acid

PVA solution of 10 wt.% was prepared by immersing 80g of PVA powder in 720g distilled water and heated at 85°C while being continuously stirred at 500 rpm using a Fisher Scientific 11-102-49SH hot plate magnetic stirrer mixer (U.S.A.). Meanwhile, the NCC suspension was sonicated using a SASTEC ST-UB3300LDT digital ultrasonic cleaner (Malaysia) in the distilled water bath for 30 min before it was blended into PVA solution. After dissolution of PVA, α-chitin, NCC and MA were added into PVA solution based on the composition ratio as shown in Table 3.2 to obtain PVA/Chitin/NCC composite in total solid content of 5 g. The PVA/Chitin/NCC mixture was agitated continuously for 3 h at 500 rpm with the help of mechanical stirrer IKA

RW20 digital overhead stirrer (Germany) for a thorough blending of materials. Samples of PVA/Chitin and PVA/Chitin/NCC without MA incorporated were prepared and served as the reference samples.

For MA-treated samples, the desired MA content (content varied from 10% to 50% based on the total mass of PVA/Chitin/NCC) was dispersed into the polymer blend. The pre-determined amount of MA was first dissolved in a separate beaker with 10 mL distilled water before its addition into the polymer blend. In addition, 3 drops of 37% HCl were added into the MA-treated samples as a catalyst for esterification. Then, the mixture was stirred for additional 1 h using the mechanical stirrer. Subsequently, the mixture was ultrasonicated for 45 min in a water bath to remove the trapped air and then poured onto the 18 cm × 18 cm non-stick mold to form thin sheet. The PVA-based composite was oven-dried for 24 h at 60°C to obtain a thin sheet. For adsorption testing, specimens were cut into 1 cm × 1 cm dimension before being further cured. Lastly, the cut specimens were further cured at 140°C for 90 min to ensure that the esterification reaction was completed. With reference to the work of Gohil et al. (2006), the curing conditions (140°C, 90 min) were determined for optimized curing of PVA. All samples were prepared to an average thickness of 0.15 ± 0.02 mm, as measured using a Mitutoyo absolute digital thickness gauge series 547-301 (Japan). The MA-treated PVA/Chitin/NCC composites were stored in a drying cabinet at 23 ± 2°C under 50 ± 5% RH for future usage.

Table 3.2: Compositional contents for the PVA/Chitin/NCC composites with varied MA content.

Sample Name	Mass Ratio of PVA/Chitin	Nanocellulose, NCC (wt.%)	Maleic acid, MA (% to total mass)
PVA/NCC/MA-0	100/0	1	0
PVA/NCC/MA-10			10
PVA/NCC/MA-30			30
PVA/NCC/MA-50			50
PVA/Chitin-10/MA-0	90/10	0	0
PVA/Chitin-10/MA-10			10
PVA/Chitin-10/MA-30			30
PVA/Chitin-10/MA-50			50
PVA/Chitin-10/NCC/MA-0	90/10	1	0
PVA/Chitin-10/NCC/MA-10			10
PVA/Chitin-10/NCC/MA-30			30
PVA/Chitin-10/NCC/MA-50			50
PVA/Chitin-20/NCC/MA-0	80/20	1	0
PVA/Chitin-20/NCC/MA-10			10
PVA/Chitin-20/NCC/MA-30			30
PVA/Chitin-20/NCC/MA-50			50
PVA/Chitin-30/NCC/MA-0	70/30	1	0
PVA/Chitin-30/NCC/MA-10			10
PVA/Chitin-30/NCC/MA-30			30
PVA/Chitin-30/NCC/MA-50			50

3.4 Characterizations of NCC-reinforced PVA/Chitin Composites

3.4.1 Particle Size Distribution by Laser Diffraction Particle Size Analyzer

Horiba LA-960 laser particle size analyzer (Japan) was employed in determining particle size distribution of NCC. NCC suspension was introduced drop-wise into the instrument's sample space. Sample dispersion was circulated at level selection 6 and agitation was set to level selection 4. The sample (cellulose) refractive index was set as 1.470 and dispersant (water) refractive index was set as 1.330 (Leng, 2016; Sultanova et al., 2009). For reproducibility of results, three samples measurements were taken. The mean particle size and D90 values (90% of the particles are smaller than the stated dimension) were determined.

3.4.2 FTIR Spectroscopic Analysis

In order to verify the purification of raw OPEFB fiber into NCC was obtained from chemical treatment using ammonium persulfate, FTIR spectroscopic analysis was carried out. In addition, FTIR spectra were recorded on a Perkin Elmer Spectrum 400 FTIR spectrometer (U.S.A.) in the attenuated total reflection (ATR) mode to determine the chemical properties of the NCC-reinforced PVA/Chitin composites (PVA/Chitin/NCC) and MA cross-linked PVA/Chitin/NCC. Scanning was performed at a resolution of 4 cm^{-1} after 32 continuous scans, in the 450 cm^{-1}-4000 cm^{-1} region. All of the samples were dried in the drying cabinet before measurements.

3.4.3 Mechanical Properties

Mechanical properties (tensile strength, elongation at the break and Young's modulus) of the composites were determined using the Shimadzu AGS-X series tensile machine (Japan) with a 500 N load cell. Stress-strain measurements were carried out at a crosshead speed of 25 mm/min and gauge length distance of 50 mm. Five samples were measured for each sample and the results recorded were the mean values. In brief, sample preparations and methodology were in accordance with the ASTM D882-02.

3.4.4 Morphological Studies

The morphologies of neat PVA and a series of NCC-reinforced PVA/Chitin composites were investigated using a JEOL JSM-7600F field emission scanning electron microscopy (FESEM) from Japan at an accelerating voltage of 5 kV. The morphologies of the selected samples of MA cross-liked PVA/Chitin/NCC were investigated using a Phenom ProX desktop scanning electron microscopy (SEM) manufactured from Netherlands at an accelerating voltage of 15 kV. In order to prevent charging effect, all of the samples were coated with a thin layer of platinum via a JEOL JFC-1600 ion sputter coater (U.S.A.) prior analyses.

3.4.5 Differential Scanning Calorimetry (DSC) Analysis

DSC analyses were performed using the TA Instruments DSC Q20 (U.S.A). Thermograms of the samples were obtained from 25°C to 250°C at the heating rate of 10°C/min. The glass transition temperature (T_g) was taken at the inflection point of the heat capacity change while the peak top of the endothermic melting peak in the thermogram was recorded as the melting temperature (T_m). Degree of crystallinity (X_c) of the PVA component in composite was determined using the Equation 3.3.

$$X_c = \frac{\Delta H_f}{w \Delta H_f^o} \times 100\% \tag{3.3}$$

where ΔH_f^o=161 J/g from the work of Dorigato and Pegoretti (2012) is the enthalpy of fusion for the fully crystallized PVA, ΔH_f is the enthalpy of fusion of sample and w is the mass fraction of the PVA in the composite.

3.4.6 Swelling Test

Samples were cut into 2 cm × 2 cm dimension and oven-dried at 60°C to remove the residual moisture and solvent. Before immersion into water, each sample was weighed. The sample was removed from the submersion periodically and excess surface water was removed by a filtered paper before weighing. The sample was soaked in the water until the equilibrium degrees of swelling was achieved. The degree of swelling was determined through gravimetric approach using the Equation 3.4.

$$\text{Swelling} = \frac{W_w - W_d}{W_d} \times 100\% \tag{3.4}$$

where W_w and W_d were the swollen and dry weights of the sample (g), respectively. The reported value was the average value of triplicates while the deviation from the mean was deduced by the error bars.

3.4.7 Water Solubility Test

For water solubility test, test samples (2 cm × 2 cm) were oven-dried thoroughly at 60°C and weighed. Each sample was immersed in water for 1 h before removal for drying. The samples were dried in a convection oven at 60°C until it reached a constant dry weight. This difference in dry weight before and after immersion was to find the solubility, as expressed in Equation 3.5.

$$\text{Solubility} = \frac{W_i - W_f}{W_i} \times 100\% \tag{3.5}$$

where W_i and W_f were the initial and final dry weights of the samples (g), respectively.

3.4.8 Gel Content

Prior testing, sample (2 cm × 2 cm) was oven-dried thoroughly at 60°C and weighed. Each sample was immersed in either cold or hot water for 24 h before removal for drying. For cold water test, the distilled water used was of 25°C whereas for hot water test it was set at 80°C. The sample was dried in a convection oven at 60°C until it reached a constant dry weight. The sample was weighed to the nearest 0.0001 g. The difference in dry weight before and after immersion was to find the gel content, as expressed in Equation 3.6.

$$\text{Gel Content} = \left(1 - \frac{W_i - W_f}{W_f}\right) \times 100\% \tag{3.6}$$

where W_i and W_f were the initial and final dry weights of the sample (g), respectively.

3.4.9 Contact Angle Measurement

The hydrophilicity of the PVA/Chitin/NCC samples' surfaces were assessed by a Dataphysics OCA 15EC (Germany) equipped with image capturing SCA-20 software. The static contact angle, which is the angle of a liquid formed on a solid surface at the solid–liquid-vapor contact line was determined using the sessile drop method. 3 µL of water drop was formed on the leveled surface of a sample and the contact angle was recorded after 10 s. Measurements were taken at 3 points for mean and standard deviation calculation.

3.5 Adsorption Studies

3.5.1 FTIR Spectroscopic Analysis

FTIR spectra of the selected MA cross-linked PVA/Chitin/NCC adsorbent, before and after the adsorption were determined with a Perkin Elmer Spectrum 400 FTIR spectrometer (U.S.A.) in the attenuated total reflection (ATR) mode. Measurements were performed at a resolution of 4 cm^{-1} for 32 scans, in the 450 cm^{-1}-4000 cm^{-1} region.

3.5.2 Determination for Point of Zero Charge by pH Drift Method

pH drift method was applied in order to measure the point zero charge (pH_{pzc}) of PVA, chitin, the selected PVA/Chitin/NCC and MA cross-linked PVA/Chitin/NCC composites. With reference to previous works (Gatabi et al., 2016; Y. Yang et al., 2004), 20 mL 0.01 M of NaCl solutions were prepared and the pH values were to be adjusted in the range of 2 to 11 ($pH_{initial}$) respectively using 0.1 M NaOH and 0.1 M HCl. Then, 60 mg of testing material was added into the respective capped container and equilibrated for 48 h under constant shaking of 100 rpm. Then, the final pH (pH_{final}) of samples was determined using a calibrated Ohaus Starter 3000 bench pH meter (U.S.A.) and plotted against initial pH. The pH_{pzc} is the intersection point of the pH_{final} against

$pH_{initial}$ graph with a line ($pH_{initial} = pH_{final}$) passing through the origin which acted as the reference line.

3.5.3 Batch Adsorption Studies

Adsorption experiments were carried out in batch modes. Stock solution of the dyes was prepared and diluted with distilled water to obtain the desired solutions of 50 mg/L MB concentration. The pH of the dye solutions were adjusted using 0.1 M NaOH or 0.1 M HCl and obtained the desired pH. For each experiment, 50 mL of known dye solution was taken and 25 mg of PVA/Chitin/NCC composite was added. The mixture was adjusted to pH 9 and kept at 25 ± 1°C under constant agitation (100 rpm). Contact time for all adsorption studies were fixed at 30 h since it was pre-determined that adsorption equilibriums will reach after 6 to 24 h, depending samples. The calibration curve as shown in Figure 3.1 was obtained by using the Shimadzu UV-2600 UV-Vis spectrophotometer (Japan). It was prepared by analyzing a series of known concentrations of MB solutions as standard solutions at the wavelength of 665 nm. The standard solutions used were 1, 2, 3, 4, 5 and 6 mg/L MB solutions, respectively. At each sampling, the dye concentration in the supernatant was analyzed against the calibration curve prepared by the MB standard solutions using the UV-Vis spectrophotometer. The absorbance at 665 nm was used to obtain the adsorbed MB concentration dyes.

The percentage removal of dye was calculated using the following Equation 3.7:

$$\text{Percentage Removal} = \frac{C_o - C_A}{C_o} \times 100\% \qquad (3.7)$$

where C_o and C_A are the initial and final concentrations of dye before and after the adsorption in aqueous solution (mg/L).

Quantity of adsorbed dyes at equilibrium (q_A) was calculated using the following Equation 3.8:

$$q_A = \frac{V}{m}(C_o - C_A) \tag{3.8}$$

where C_o is the initial concentration of dyes adsorbate (mg/L), C_A is the dye concentration at equilibrium (mg/L), V is the volume of experimental solution (L) and m is the mass of adsorbent (g). Each experiment was performed in triplicate at identical conditions and the mean values were calculated. The effect of composite composition, solution pH, adsorbent dosage and initial MB dye concentration were investigated.

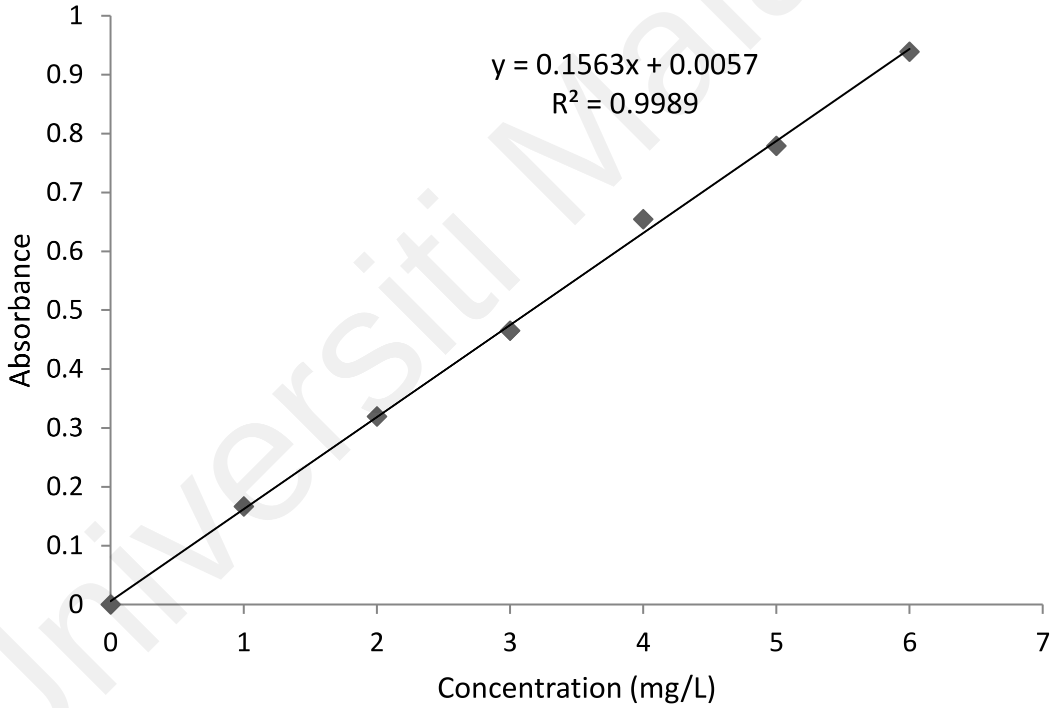

Figure 3.1: Calibration curve for sorption of MB dyes.

3.5.3.1 Effect of MA Cross-linked Composite Composition

In this study, composite samples as shown in Table 3.3 were studied.

Table 3.3: Compositional contents for the PVA/Chitin/NCC composites with varied MA content tested as adsorbent.

Sample Name	Mass Ratio of PVA/Chitin	Nanocellulose, NCC (wt.%)	Maleic acid, MA (% to total mass)
PVA/MA-0	100/0	0	0
PVA/MA-10			10
PVA/MA-30			30
PVA/MA-50			50
PVA/NCC/MA-0	100/0	1	0
PVA/NCC/MA-10			10
PVA/NCC/MA-30			30
PVA/NCC/MA-50			50
PVA/Chitin-10/MA-0	90/10	0	0
PVA/Chitin-10/MA-10			10
PVA/Chitin-10/MA-30			30
PVA/Chitin-10/MA-50			50
PVA/Chitin-10/NCC/MA-0	90/10	1	0
PVA/Chitin-10/NCC/MA-10			10
PVA/Chitin-10/NCC/MA-30			30
PVA/Chitin-10/NCC/MA-50			50
PVA/Chitin-20/NCC/MA-0	80/20	1	0
PVA/Chitin-20/NCC/MA-10			10
PVA/Chitin-20/NCC/MA-30			30
PVA/Chitin-20/NCC/MA-50			50
PVA/Chitin-30/NCC/MA-0	70/30	1	0
PVA/Chitin-30/NCC/MA-10			10
PVA/Chitin-30/NCC/MA-30			30
PVA/Chitin-30/NCC/MA-50			50

In order to study the effect of MA cross-linked composite composition on the MB adsorption uptake and percentage removal, 50 mL of MB solutions with known 50 mg/L initial concentrations and pH value of 9 were prepared in a series of capped containers. In each container, 25 mg of the respective composite sample as shown in

Table 3.3 was added. Then, the containers were placed into the orbital shaker incubator and conditioned at 25 ± 1°C under constant agitation of 100 rpm for 30 h. At equilibrium time, the dye concentration in the supernatant for each container was determined based on the calibration curve prepared from the MB standard solutions using the UV-Vis spectrophotometer. Quantity of adsorbed dyes at equilibrium (q_A) of the composite adsorbents tested were determined based on Equation 3.8.

3.5.3.2 Effect of Solution pH

The effect of solution pH was investigated by varying the initial pH of the solutions from 2 to 11 for adsorption of MB onto the selected composite adsorbents as shown in Table 3.4. The pH of the MB dye solutions were adjusted using 0.1 M NaOH or 0.1 M HCl to obtain the desired pH at 2 to11. pH values were measured using the Ohaus Starter 3000 bench pH meter (U.S.A.). For each container, the initial MB concentration was fixed at 50 mg/L with adsorbent dosage loaded at 0.5 g/L.

During the adsorption studies, the 50 mL MB solution temperature was retained at 25 ± 1°C under constant agitation at 100 rpm for 30 h using the orbital shaker incubator. At equilibrium time, the dye concentration in the aqueous solution was determined based on the calibration curve (Figure 3.1) plotted. The amount of MB adsorbed by the composite adsorbent at equilibrium was calculated using Equation 3.8.

Table 3.4: Compositional contents for the PVA/Chitin/NCC composite adsorbents selected to study the effect of external parameters on the MB adsorption.

Sample Name	Mass Ratio of PVA/Chitin	Nanocellulose, NCC (wt.%)	Maleic acid, MA (% to total mass)
PVA/Chitin-10/MA-10	90/10	0	10
PVA/Chitin-10/NCC/MA-10	90/10	1	
PVA/Chitin-20/NCC/MA-10	80/20	1	
PVA/Chitin-10/MA-30	90/10	0	30
PVA/Chitin-10/NCC/MA-30	90/10	1	
PVA/Chitin-20/NCC/MA-30	80/20	1	
PVA/Chitin-10/MA-50	90/10	0	50
PVA/Chitin-10/NCC/MA-50	90/10	1	

3.5.3.3 Effect of Adsorbent Dosage

The effect of adsorbent dosage on the adsorption process was studied by varying the adsorbent dosage at 0.25, 0.50, 0.75, 1.00 and 1.25 g/L while other process parameters such as initial dye concentration, agitation speed, temperature, volume and pH of the solution were remained constant. The selected composite adsorbents as shown in Table 3.4 were used in this adsorption study. Briefly, varied adsorbent dosage of a type of PVA/Chitin/NCC composite adsorbent were preloaded in separate 50 mL containers. Then, each container was filled with 50 mL of 50 mg/L dye solution which was pH 9. The composite adsorbents were in contact with the MB solution for 30 h while the containers were kept at 25 ± 1°C under constant agitation at 100 rpm. After dye concentration equilibrium was reached at 30 h, the dye concentration remained in the supernatant was obtained using the calibration curve shown in Figure 3.1. By using Equation 3.8, quantity of adsorbed MB dyes onto the composite adsorbents (q_A) tested were determined.

3.5.3.4 Effect of Initial MB Dye Concentration

In order to study the effect of adsorbate concentration on the adsorption process, series solutions with varied MB dye concentrations (40, 50, 60, 70, 80, 90 mg/L) were prepared. For each experiment, 25 mg of the selected composite adsorbent was added into the 50 mL of known MB dye concentration solution. For this study, the selected composite adsorbents as tabulated in Table 3.4 were used. The solution pH was fixed at pH 9 and conditioned at 25 ± 1°C under constant agitation of 100 rpm. Contact time for all adsorption studies were fixed at 30 h. The MB concentrations were monitored using the Shimadzu UV-2600 UV-Vis spectrophotometer (Japan). Quantity of adsorbed dyes at equilibrium (q_A) of the composite adsorbents tested were determined based on Equation 3.8.

3.5.3.5 Adsorption Isotherms

Isotherms were used to express the relationship between the mass of dye adsorbed per unit mass of the adsorbent and the liquid phase dye concentration. In the present investigation, two isotherm models, namely Langmuir and Freundlich isotherms were adopted. The experimental data obtained from the effect of six varied initial adsorbate concentrations in adsorption process were used to calculate the adsorption isotherms. In this study, six different MB adsorbate concentrations (40, 50, 60, 70, 80 and 90 mg/L) were used. Experimental conditions were fixed at 25 ± 1°C temperature and pH solution of 9 and constant agitation of 100 rpm. Langmuir and Freundlich parameters were calculated based on the linearized Langmuir isotherm equation (Equation 3.9) and Freundlich isotherm equation (Equation 3.10). Details on the isotherm equations were also discussed in Section 2.10.4. Correlation coefficients (R^2) were also calculated from the Langmuir and Freundlich isotherm plots, respectively. Lastly, R^2 values of Langmuir isotherm and Freundlich isotherm were compared. Those of higher R^2

indicated better fit and deduced that the adsorption process of the adsorbent fitted with the isotherm's theory.

$$\frac{C_A}{q_A} = \frac{1}{K_L q_M} + \frac{C_A}{q_M} \tag{3.9}$$

$$log(q_A) = log(K_F) + \frac{1}{n} log(C_A) \tag{3.10}$$

where q_A is the amount of adsorbate adsorbed per gram of adsorbent at equilibrium (mg/g), C_A is the concentration of adsorbate in solution at equilibrium (mg/L), q_M is the maximum adsorption capacity of adsorbate per unit mass of adsorbent (mg/g) and K_L is the Langmuir adsorption constant (L/mg). Moreover, K_F is the Freundlich isotherm constant related to adsorption capacity $[(mg/g)\cdot(L/mg)^{1/n}]$ and 1/n is the unit less Freundlich adsorption intensity parameter. Raw data on C_A and the calculated q_A of these experiments were shown in Appendix A. The values determined based on Langmuir and Freundlich isotherm plots were tabulated in Table 4.5 of Section 4.2.7, respectively.

3.5.3.6 Adsorption Kinetics

The methodology for kinetic study was identical to that of batch adsorption study disclosed in Section 3.4.3. Samples were taken at predetermined time points (0, 15, 30, 45, 60, 90, 120, 180, 240, 300, 360, 1440, 1560, 1680, 1800 minutes). The residual adsorbate concentrations of the samples were similarly determined using UV-Vis spectrophotometer. For the present investigation, two kinetic models were applied in order to understand the adsorption process. The models were the pseudo-first order and pseudo-second order models, discussed in Section 2.10.5. Kinetic values were calculated based on the pseudo-first order model equation (Equation 3.11) and pseudo-second order model equation (Equation 3.12). The experimental data obtained from the adsorption process were used to determine the kinetics parameters. R^2 values of the two kinetic models were compared. Those of higher R^2 indicated better fit of the adsorption process with the kinetic model proposed.

$$log(q_A - q_t) = log(q_A) - \frac{k_1}{2.303}t \tag{3.11}$$

$$\frac{t}{q_t} = \frac{1}{k_2 q_A^2} + \frac{1}{q_A}t \tag{3.12}$$

where q_A and q_t (mg/g) are the adsorption capacity at equilibrium time and time t (min), respectively. k_1 (1/min) is the pseudo-first order kinetic rate constant. k_2 [g/(mg·min)] is the rate constant of pseudo-second order kinetic model. The experimental data and kinetic parameters determined based on pseudo-first order kinetic model and pseudo-second order kinetic model equation plots were tabulated in Table 4.6 of Section 4.2.8. Data for the plotting of pseudo-first order kinetic and pseudo-second order kinetic graphs were also shown in Appendix B.

3.5.3.7 Adsorption Thermodynamics

In order to evaluate the thermodynamic characteristics of the MB adsorption onto the selected adsorbents in this study, the experimental data obtained from the batch adsorption experiment conducted earlier were analyzed using the thermodynamic equations expressed by Equations 3.13-3.16. Details on the thermodynamic equations were also discussed in Section 2.10.6. The values of ΔH° and ΔS° were determined respectively from the slope and intercept of the plot of log K_c versus l/T. K_c is the equilibrium constant, as expressed by Equation 3.13 and T is absolute temperature in Kelvin.

$$K_c = \frac{C_{ad}}{C_A} \tag{3.13}$$

$$\Delta G^o = -2.303RT \log K_c \tag{3.14}$$

$$\Delta G^o = \Delta H^o - T\Delta S^o \tag{3.15}$$

$$\log K_c = -\frac{\Delta H^o}{2.303RT} + \frac{\Delta S^o}{2.303R} \tag{3.16}$$

in which K_c is the dimensionless thermodynamic equilibrium constant, R is the universal gas constant (8.314 J/ mol·K) and T is the absolute temperature in Kelvin. As expressed in Equation 3.15, standard Gibbs free energy change, ΔG° (kJ/mol) is related to standard enthalpy change of adsorption, ΔH° (kJ/mol) and standard entropy change of adsorption, ΔS° (J/mol·K). The parameters determined based on the thermodynamic equations were shown in Table 4.7 of Section 4.2.9. Data for the plotting of the log K_c against 1/T graph was tabulated in Appendix C.

3.5.3.8 Reusability of the Adsorbent

Desorption study was performed by contacting used adsorbent with 1M HCl solution and agitated for 30 h. Then, the desorbed amount of MB was obtained spectrophotometrically. Desorption percentage was calculated using Equation 3.17:

$$\text{Desorption} = \frac{C}{C_o} \times 100\% \tag{3.17}$$

where C is the amount of MB dye desorbed to the HCl elution medium (mg/L) , C_o is the amount of MB dye adsorbed on the adsorbent (mg/L). To determine the reusability of the composite, same sample was repetitively tested for five times via consecutive adsorption-desorption cycle. Data on the adsorption percentage and desorption percentages of the selected composite adsorbents were shown in Appendix D.

3.6 Summary

In this chapter, the chemicals and materials to be prepared for four methodologies of preparation works were first summarized. Then, four detailed research methodologies in preparing the nanocellulose sourced from oil palm empty fruit bunch (OPEFB), chitin, PVA/chitin/NCC and PVA/chitin/NCC treated with maleic acid (MA) were disclosed, respectively. Detailed experimental procedures in characterizing the PVA-based composites, with and without the presence of MA, in terms of physicochemical, mechanical and morphological were also reported. Last but not least, the methodologies used to evaluate the adsorption performance of the PVA/Chitin/NCC composite towards MB using the batch adsorption studies were discussed. Batch adsorption studies designated to evaluate the other external adsorption parameters such as solution pH, adsorbent dosage and initial dyes concentration towards the adsorption capacities of PVA/Chitin/NCC composites for MB were also reported. Besides, studies to determine the isotherm, kinetics and thermodynamics parameters of the selected composite adsorbents under investigation were reported in detailed. Last but not least, a methodology to evaluate reusability of the adsorbent through a five consecutive adsorption-desorption cycles have been summarized.

CHAPTER 4: RESULTS AND DISCUSSION

4.1 Introduction

This chapters consists of results and discussions over two major parts which are characterizations of NCC-reinforced PVA/Chitin composites, and adsorption studies to evaluate the adsorption performance of PVA/chitin/NCC composites towards MB cationic dye.

4.2 Characterizations of NCC-reinforced PVA/Chitin Composites

NCC-reinforced PVA/Chitin composites, or also known as PVA/Chitin/NCC composites were characterized using FTIR, DSC and morphological studies to investigate the miscibility among PVA, chitin and NCC polymers, upon polymers blending. The PVA/Chitin/NCC composites were further evaluated in terms of mechanical properties using universal testing machine. The effects of incorporating PVA, chitin and NCC towards mechanical properties, swelling and solubility of PVA/Chitin/NCC composites were discussed. All these studies help to provide insight over the processability and workability of the PVA/Chitin/NCC composites in aqueous medium.

Incorporation of maleic acid (MA) contributed to changes in properties of PVA/Chitin/NCC composites. FTIR and DSC techniques were utilized to investigate the chemical interaction and physical alteration resulted from the MA introduced. The effects of MA on the mechanical properties of PVA/Chitin/NCC composites were also evaluated. Morphological changes of PVA/Chitin/NCC composites with varied MA content were monitored. The extent of cross-linking for PVA/Chitin/NCC composites using varied content of MA were evaluated using FTIR, tensile, swelling and gel content test. It was anticipated that the water resistance of the PVA/Chitin/NCC composites were improved with MA introduced while the surface hydrophilicity of polymer composites were retained to be hydrophilic. As a result, surface hydrophilicity of polymer composites were measured using contact angle measurement.

4.2.1 Determination of Particle Size Distribution of NCC by Laser Diffraction Particle Size Analyzer

Laser diffraction particle size analyzer was used to confirm the size distribution of cellulose synthesized from the processing of raw OPEFB fibers which could be of micron-scale or nano-scale sized. Figure 4.1 illustrates the differential distribution curves of particle size by volume in the range of 10 nm to 5000 microns for NCC obtained from chemical treatment of OPEFB fibers with ammonium persulfate. The unimodal particle size distribution obtained indicated that that mean particle size of NCC was 64.80 ± 14.20 nm and 90% of the particles (D90) were smaller than 83.00 nm.

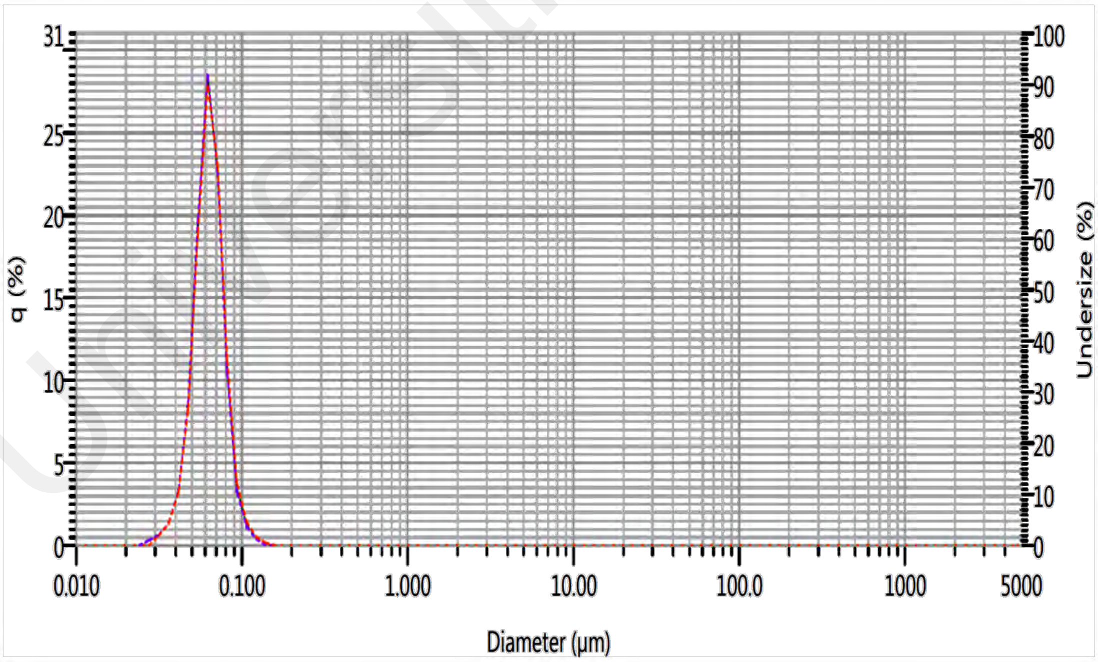

Figure 4.1: Differential distribution curves of particle size by volume in the range of 10 nm to 5000 microns for nanocellulose obtained from chemical treatment of OPEFB fibers with ammonium persulfate.

NCC has been widely reported to be of elongated rod-like particles or in long fibrous structures (Kargarzadeh et al., 2017; Leng, 2016; Tang & Weder, 2010). Therefore, the result obtained from the laser light scattering instrument shows predominantly the longitudinal size of NCC. This is because the intensity of the scattered light in the longitudinal direction is much higher over the scattered light determined for the particles' lateral direction (Kargarzadeh et al., 2017). Interesting to note that the nano-scale particle size distribution determined in this study was corresponded to another isolation attempt of cellulose from Oil Palm Empty Fruit Bunch via steam explosion and hydrolysis with HCl (Gea et al., 2018).

4.2.2 FTIR Spectroscopic Analysis

Generally, NCC sourced from lignocellulosic biomass such as OPEFB fibers can be synthesized in two major stages. The first stage is the pretreatment of raw cellulosic biomass to remove non-cellulosic components such as hemicellulose and lignin. Second stage is the disintegration of cellulose nanocrystals from the individual cellulose fiber matrix. In order to determine that the non-cellulosic components were removed, FTIR spectroscopic analysis was employed to determine the chemical changes on raw OPEFB fibers after the ammonium persulfate treatment.

Moreover, FTIR spectroscopic analysis is utilized to confirm on the successful preparation of the PVA/Chitin/NCC composites, as deduced by the presence of characteristic bands of PVA, chitin and NCC. Furthermore, it is essential to determine the chemical interactions among the polymers in PVA/Chitin/NCC composites by investigating the vibrational shifting of functional groups of the peaks in the FTIR spectra.

Lastly, it is known that incorporation of MA contributed to changes in properties of PVA/Chitin/NCC composites. FTIR technique was used to investigate the differences of chemical structures between PVA/Chitin/NCC composites and MA cross-linked PVA/Chitin/NCC composites.

4.2.2.1 Raw OPEFB Fibers and the NCC Obtained from Chemical Treatment of OPEFB Fibers

Figure 4.2 illustrates the FTIR spectra of the raw OPEFB fibers and the NCC obtained from chemical treatment of OPEFB fibers with ammonium persulfate (APS), respectively. From the FTIR (Figure 4.2), it was observed that the APS chemical treatment had successfully removed the lignin and hemicellulose from the raw OPEFB fibers. This was depicted due to the absence of lignin's characteristic bands at 1464 cm^{-1} that was attributed by methoxyl ($-O-CH_3$) and the band at 1510 cm^{-1} correlated to the C=C stretching vibration in the aromatic ring of lignin (Lani et al., 2014; Sain & Panthapulakkal, 2006; H. Yang et al., 2007). In addition, the absorption band at 1734 cm^{-1} which could be associated with the C=O stretching in the acetyl and uronic ester groups of hemicelluloses or the ester carbonyl groups in the para-coumaric units of the lignin was diminished after the APS chemical treatment (Lani et al., 2014; Sain & Panthapulakkal, 2006). Moreover, the intensified band at 1603 cm^{-1} assigned to shifted C=O was proof of oxidation of cellulose to comprise sodium carboxylates ($-COO^{-}Na^{+}$) functional group, as reported by Castro-Guerrero and Gray (2014). It was suggested that persulfate oxidation led to formation of surface carboxyl on cellulose nanocrystal instead of surface sulfate half-esters as in the common sulfuric acid hydrolysis (Castro-Guerrero & Gray, 2014; Leung et al., 2011).

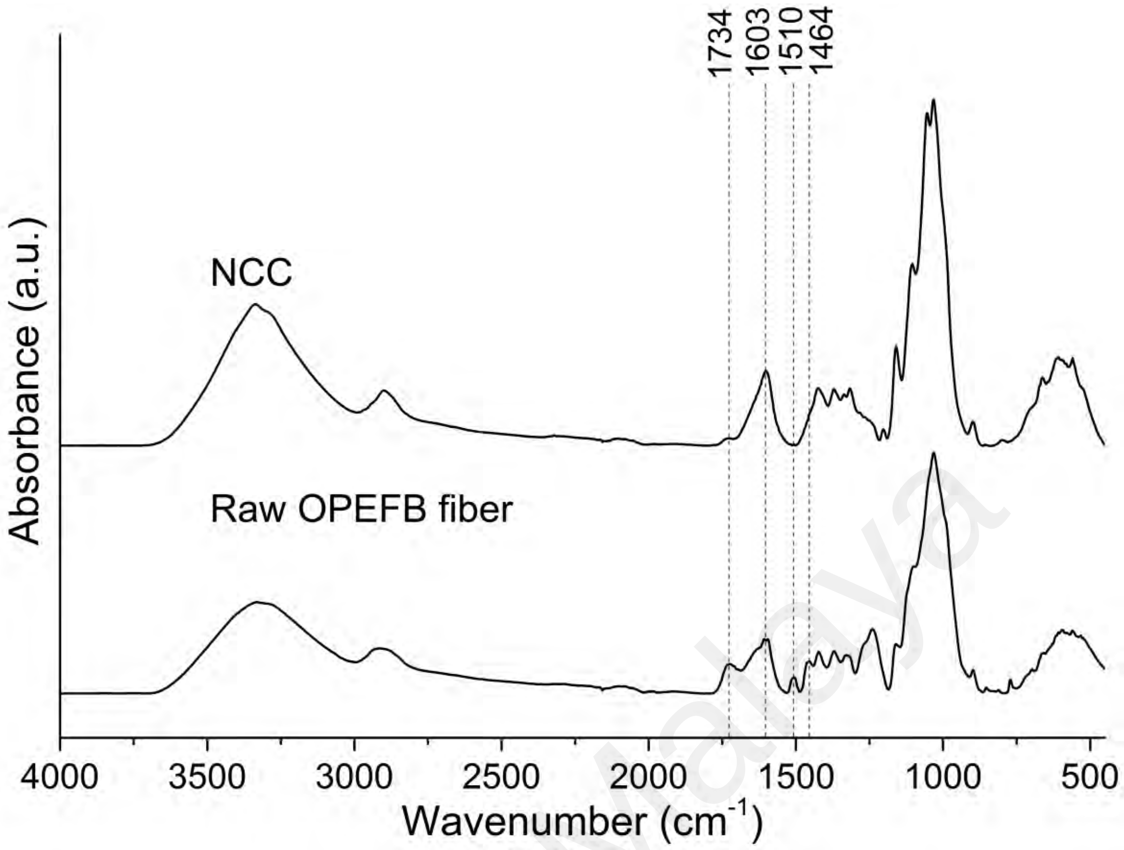

Figure 4.2: FTIR spectra of the (a) raw OPEFB fiber and the (b) NCC obtained from chemical treatment of OPEFB fibers with ammonium persulfate.

4.2.2.2 PVA/Chitin/NCC Composites

Figure 4.3 shows that the absorption bands characteristic to PVA were observed for PVA and PVA-based composite which could be assigned to the vibrations of C=O, C-O and CH_2 bonds. The bands at 1733 cm^{-1} (antisymmetric C=O stretching) and 1713 cm^{-1} (symmetric C=O stretching) were attributed to the residual acetate in PVA, resulting from incomplete alcoholysis of poly(vinyl acetate) during the manufacturing of PVA (Jiang et al., 2015; Rogojanu et al., 2011). At 1428 cm^{-1}, the band was assigned to C-H stretching of PVA. In addition, the bands at 1088 cm^{-1} and 1022 cm^{-1} were observed due to the C-O stretching vibrations (Deng et al., 2014; Sriupayo et al., 2005; Yu & Li, 2008). In addition, the presence of two CH_2 rocking peaks at 916 cm^{-1} and 844 cm^{-1} indicated the atactic form of PVA. This is because the band at 916 cm^{-1} is characteristic to syndiotacticity of PVA polymer and the band at 844 cm^{-1} is ascribed to isotacticity of the polymer (Nkhwa et al., 2014; Rogojanu et al., 2011).

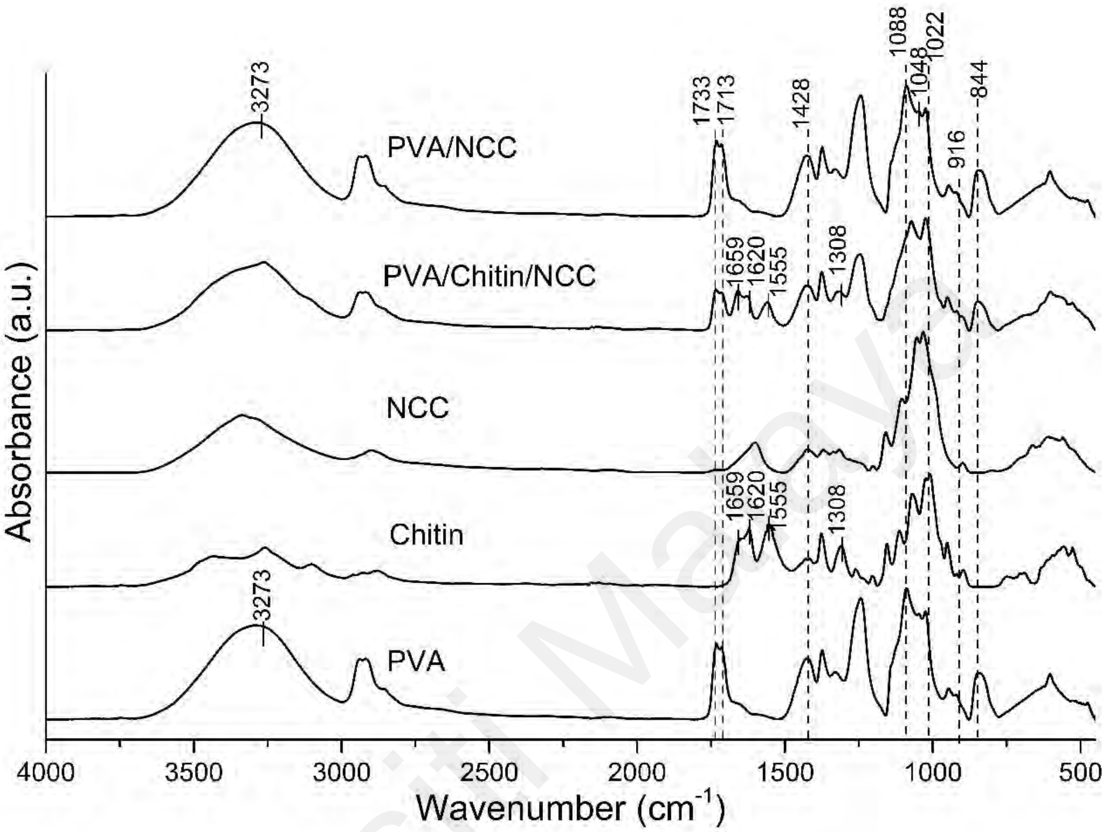

Figure 4.3: FTIR spectra of the neat PVA, chitin, NCC, PVA/Chitin/NCC composite and PVA/NCC composite.

Chitin was successfully purified in conformance with the work done by Deng et al. (2014). Four significant peaks at 1659 cm^{-1} and 1620 cm^{-1} (amide I), 1555 cm^{-1} (amide II) and 1308 cm^{-1} (amide III) were observed at Figure 4.3 which allowed the identification of chitin as α, β or γ crystal forms (Deng et al., 2014; Kaya et al., 2014). It is known that two peaks at 1659 cm^{-1} and 1620 cm^{-1} are characteristics for α-chitin (amide I) while only a single peak at 1659 cm^{-1} could be observed for β-chitin (amide I) (Kaya et al., 2014). Thus, this gives evidence that the chitin structures used is in α crystal form.

As shown in Figure 4.3, O-H stretching band which centred at 3273 cm^{-1} for the neat PVA became more intense upon addition of NCC (E Fortunati et al., 2013). The intensification of O-H band was mostly attributed to the interaction between OH group on the surface of NCC and the OH group of the PVA matrix. As reported by E. Fortunati et al. (2013), the addition of NCC had resulted in the appearance of additional peak in the spectra at 1048 cm^{-1}. The band corresponded to the C-OH bending vibrations of alcohol groups present in cellulose. Furthermore, it was confirmed that the PVA/Chitin/NCC composites were successfully prepared, as indicated by the comparisons of the FTIR spectra in Figure 4.3. The spectra of the PVA/Chitin/NCC composite showed the respective characteristics bands of PVA, α-chitin and NCC.

Figure 4.4 shows that the absorption bands characteristics to partially hydrolyzed PVA at 1733 cm^{-1} (asymmetric C=O stretch), 1713 cm^{-1} (symmetric C=O stretch) and 1428 cm^{-1} (C-H stretching) were observed in all of the PVA-based composites. With increasing chitin content from 10 wt.% to 30 wt.%, both of the C=O stretch bands of PVA decreased in intensities. Moreover, the characteristic peaks of α-chitin at 1659 cm^{-1} (amide I), 1620 cm^{-1} (amide I) and 1555 cm^{-1} (amide II) were apparent in all of the spectra and their intensities improved as chitin content increased from 10 wt.% to 30 wt.% (Junkasem et al., 2006; Sriupayo et al., 2005). The indication of possible interaction between the polymer pair in the blending form through specific polar groups was examined using FTIR analysis as well (Figure 4.4). It was observed that absorption band at 1330 cm^{-1} (O-H bending and C-H wagging) gradually shifted to lower frequencies at 1319 cm^{-1} with increasing α-chitin content, which could be an indication of intermolecular interactions between PVA matrix and α-chitin through hydroxyl functional group (Sriupayo et al., 2005). The shift of C-O stretching vibration band from 1088 cm^{-1} to 1072 cm^{-1} also indicated that the polymeric interaction through hydrogen bonding (Tolstov et al., 2012; Xu et al., 2009).

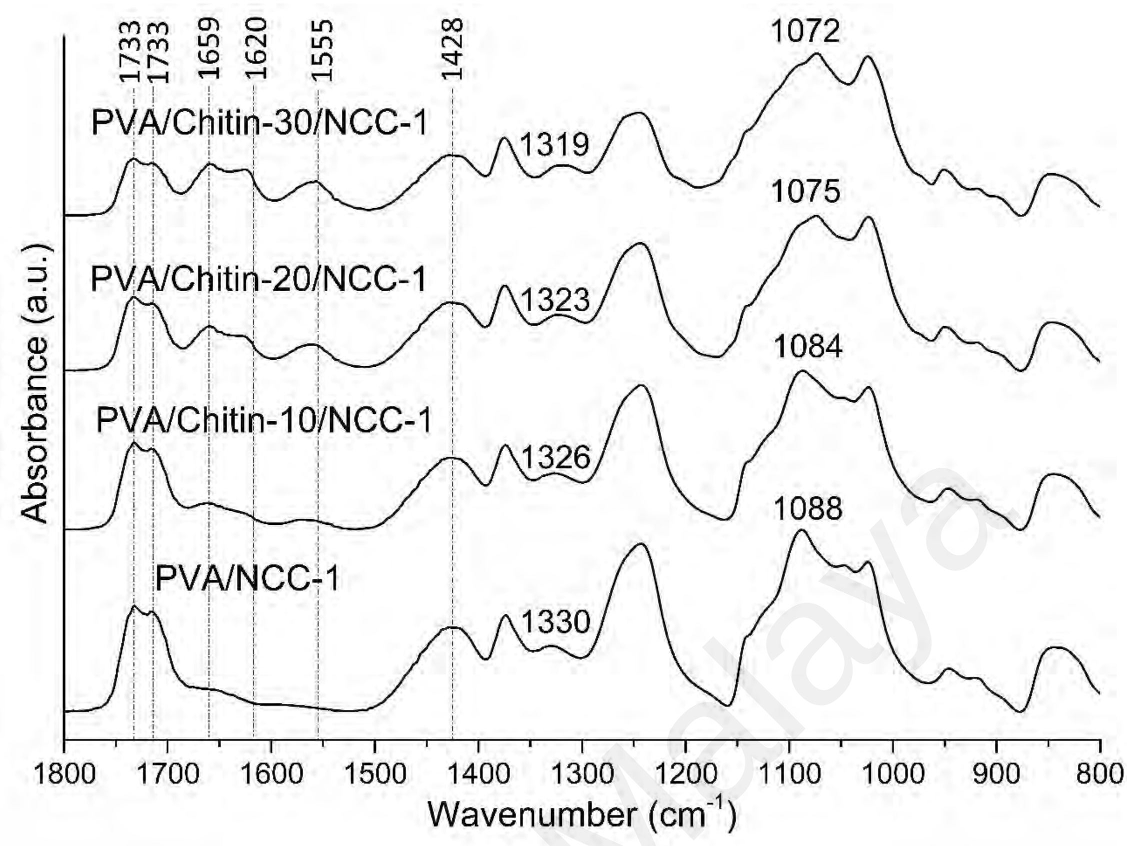

Figure 4.4: FTIR spectra of the PVA/NCC-1, PVA/Chitin-10/NCC-1, PVA/Chitin-20/NCC-1 and PVA/Chitin-30/NCC-1 composites under selected magnified range: 1800 cm^{-1}-800 cm^{-1}.

4.2.2.3 MA Cross-linked PVA Chitin/NCC Composites

FTIR technique was used to investigate the difference of chemical structures between PVA/Chitin/NCC composites and MA cross-linked PVA/Chitin/NCC composites. Figure 4.5 (a) shows the absorption bands characteristic to the partially hydrolyzed PVA at 1733 cm^{-1} (asymmetric C=O stretch), 1713 cm^{-1} (symmetric C=O stretch) and 1419 cm^{-1} (C-H stretching) were identified in the respective FTIR spectrum of PVA-based composite (Deng et al., 2014; Sriupayo et al., 2005). The peaks observed at 3263 cm^{-1} and 2924 cm^{-1} were associated to the stretching of O-H hydroxyl groups and aliphatic C-H, respectively (Peresin et al., 2014; Z. Xie et al., 2011). Moreover, the peak at 1048 cm^{-1} corresponded to the C-OH bending vibrations of alcohol groups present in cellulose, which confirmed the presence of NCC in the PVA/NCC and composites with NCC incorporated. This characteristic peak attributed to NCC has been reported by Ku et al. (2011) and E Fortunati et al. (2013). Previous work had concluded that oxidation of OPEFB fibers by ammonium persulfate led to formation of surface carboxyl on NCC. The spectrum of NCC obtained from chemical treatment of OPEFB fibers with ammonium persulfate was shown and discussed in detail in Section 4.1.2.1.

By comparing the spectrum of PVA/Chitin-10/NCC/MA-10 and PVA/Chitin-30/NCC/MA-10, it was observed that three prominent peaks at 1733 cm^{-1}, 1713 cm^{-1} and 1252 cm^{-1} became less intense. This was due to decreased PVA content in conjunction with higher chitin content introduced. The three peaks were attributed by the residual acetate groups which remained in the partially hydrolyzed PVA (Gohil et al., 2006; Hyder, 2008; Peresin et al., 2014). The 1733 cm^{-1} and 1713 cm^{-1} peaks were associated to asymmetric and symmetric C=O stretch of acetate group, respectively. Moreover, the presence of 1252 cm^{-1} peak was due to the combination effect of C–H wagging vibration and C–O stretching of acetyl groups. Besides, it was clearly illustrated the intensification of peaks characteristic to α-chitin at 1659 cm^{-1} (amide I), 1630 cm^{-1} (amide I) and 1555 cm^{-1} (amide II) as the chitin content increased from 10 wt.% to 30 wt.%, respectively (Deng et al., 2014; Junkasem et al., 2006; V. Rubentheren et al., 2016). The presence of two peaks at 1659 cm^{-1} and 1630 cm^{-1} (amide I) clearly denoted that the α-chitin was incorporated instead of β-chitin which only portrayed single peak for amide I at 1659 cm^{-1} (Deng et al., 2014; Kaya et al., 2014).

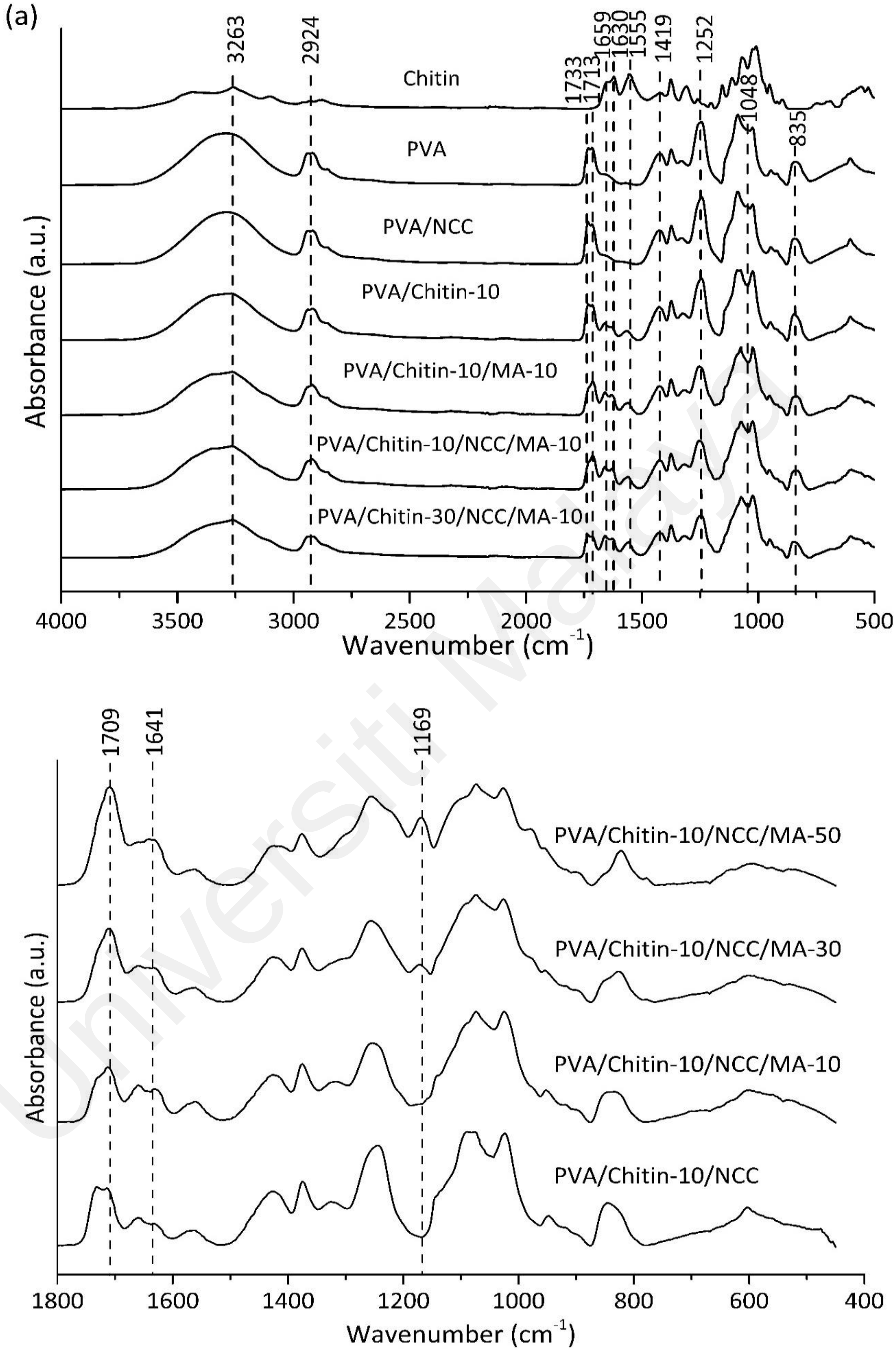

Figure 4.5: (a) FTIR spectra of the PVA, PVA/NCC, PVA/Chitin, PVA/Chitin/MA and PVA/Chitin/NCC/MA sample composites; (b) FTIR spectra of the selected PVA/Chitin-10/NCC composite with 0% to 50% of MA incorporated under selected magnified region: 1800 cm^{-1}-400 cm^{-1}.

Figure 4.5 (b) illustrates the FTIR spectra of the selected PVA/Chitin-10/NCC with varying dosage of MA, ranging from 0% to 50%. MA with carboxylic di-functional groups could react with -OH groups of PVA or chitin which resulted in grafting or cross-linking of the polymers. The possible esterification reactions due to MA are illustrated in Figure 4.6. It was shown that the PVA-based composite had been successfully cross-linked by MA, as indicated by the sharp characteristic C=O stretching band of conjugated ester at 1709 cm^{-1}. Besides, C-O stretching band attributed to ester linkage was remarked at 1169 cm^{-1} (Meng et al., 2000; Peresin et al., 2014). The presence of 1641 cm^{-1} peak was a clear indication of the olefinic -CO-CH=CH- stretching, which contributed to the conjugation of ester (Gohil et al., 2006). Moreover, this olefinic stretching had submerged the characteristic peaks of chitin amide at the 1650 cm^{-1}-1630 cm^{-1} region. As expected, these three peaks increased in intensity with increasing content of MA.

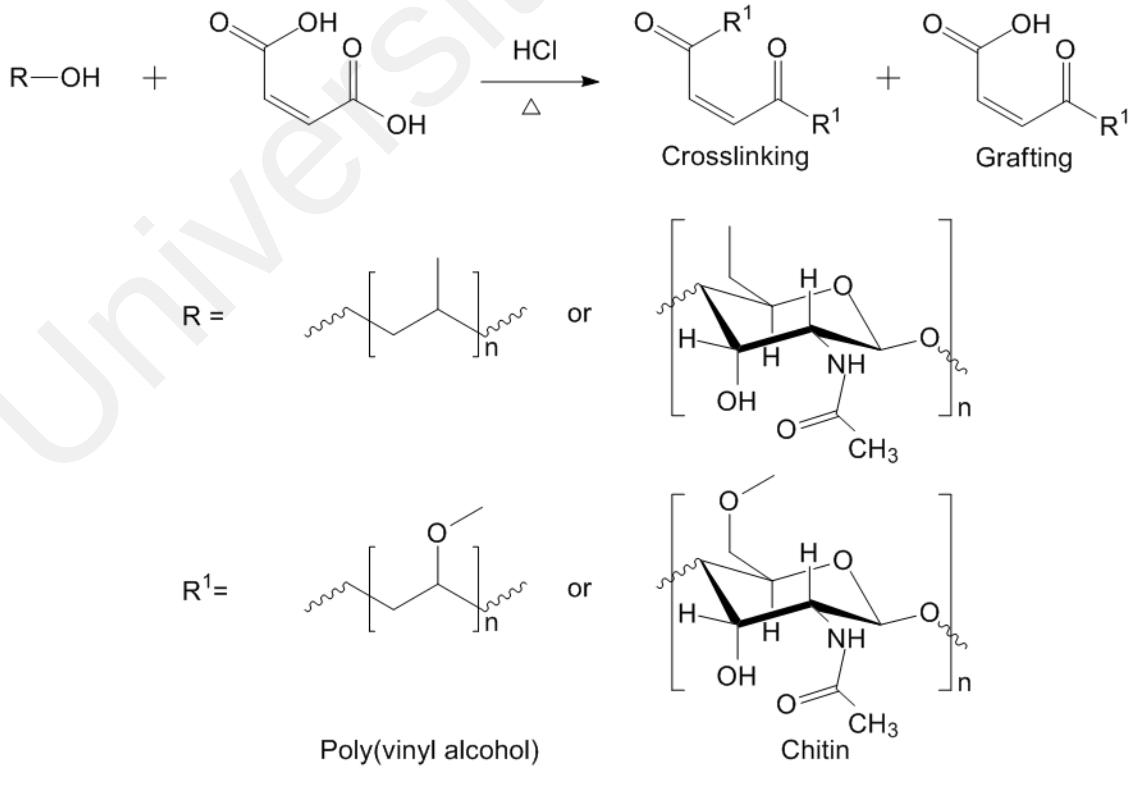

Figure 4.6: Possible esterification reactions: formation of bis-esters, resulting to cross-linking or formation of mono-ester which results in grafting.

4.2.3 Mechanical Properties

The mechanical properties, in terms of tensile strength, percentage of elongation at break and Young's Modulus for PVA/Chitin/NCC, with varying NCC content of 0 wt.% to 1.5 wt.% were determined. It was desired to determine the amount of NCC content to be incorporated into PVA/Chitin/NCC so that NCC would serve as effective reinforcing fillers. In addition, the mechanical properties of PVA/NCC, PVA/Chitin and PVA/Chitin/NCC samples as a function of MA content were evaluated.

4.2.3.1 PVA/Chitin/NCC Composites

The mechanical properties, in terms of tensile strength, percentage of elongation at break and Young's Modulus for neat PVA and a series of PVA-based composites, with varying NCC content of 0 wt.% to 1.5 wt.% were determined.

(a) Tensile Strength

The control PVA exhibited a tensile strength of 44.02 ± 1.03 MPa (Figure 4.7). Observed tensile strength value of 44.02 ± 1.03 MPa for the neat PVA showed little discrepancy from the reported value of about 40 MPa for the PVA prepared by Cho et al. (2001). Tensile strength of the studied blends were lower than the PVA homopolymer, in accordance with the findings by Y. M. Lee et al. (1996). The authors showed evidence of better tensile strength of β-chitin/PVA blend over neat PVA however only when chitin content was at least 40 wt.%. This is because incorporation of small amount of chitin has caused misalignment of PVA molecular chains, causing a lack of interfacial adhesion among the two components.

However, there was a significant increase of tensile strength with increasing α-chitin content from 10 wt.% to 30 wt.%, which was from 29.06 ± 2.49 MPa to 39.27 ± 1.57 MPa. This is due to the polar natures of both PVA and chitin having hydroxyl groups (-OH) in their chemical structures. Intermolecular hydrogen bonding between PVA and chitin became more pronounced which improved the integrity of the blend as the chitin content was increased, as suggested by Sriupayo et al. (2005). Based on FTIR analysis in Figure 4.4, it is known that interaction between PVA and α-chitin is mostly through hydrogen bonding. Consequently, it seems reasonable to suggest that the enhancement of mechanical properties of the composites is due to the intermolecular interaction by hydrogen bonding.

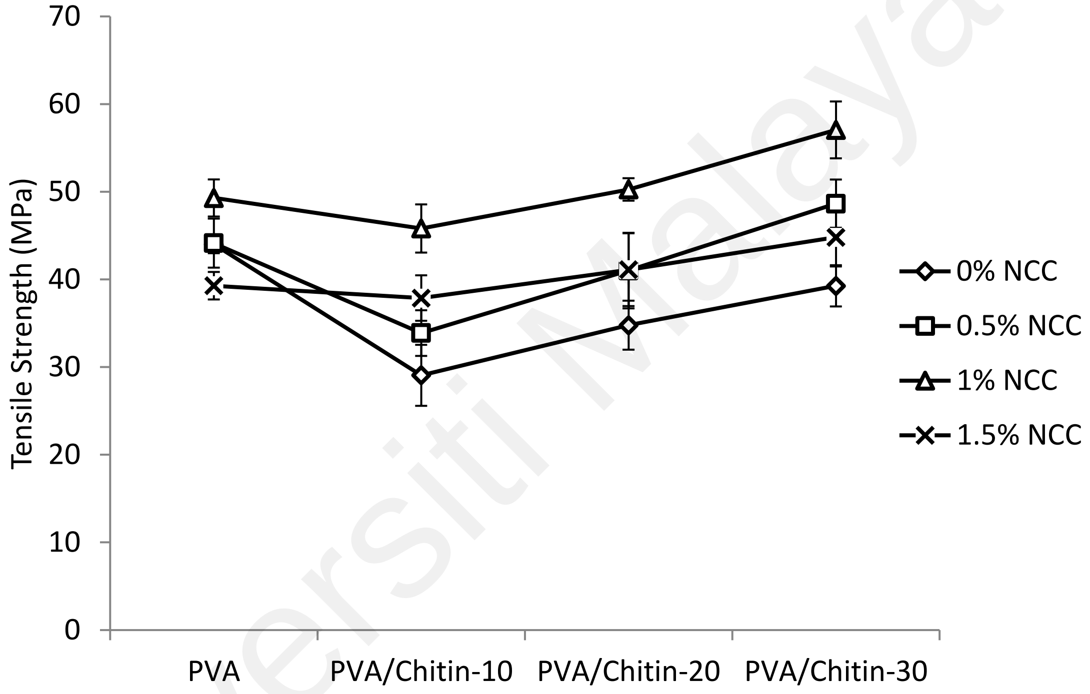

Figure 4.7: Tensile strength of the PVA/Chitin/NCC composites.

Figure 4.7 shows that the incorporated NCC filler further improved the tensile strength of PVA/α-chitin composite. Specifically, the tensile strength of PVA/Chitin-10 was increased for 57.64% upon addition of 1 wt.% NCC, which was from 29.06 ± 2.49 MPa to 45.81± 4.31 MPa. This increase in tensile strength is attributed to the improved interfacial adhesion between the hydrophilic NCC filler and the hydrophilic PVA matrix (Silvério et al., 2013). Compatible filler-matrices interface allows efficient stress transfer from the matrix to the filler which leads to improved tensile strength of the composites (Mittal, 2015; Mohammad Mahdi Dadfar et al., 2014; Mondal, 2017).

However, tensile strength decreased upon reaching maximum at 1 wt.% NCC loading. This decrease is due to the more intense agglomeration of fillers that results in creation of weak points in the composite's matrix when 1.5 wt.% NCC is loaded (Azizi et al., 2014). The agglomerated NCC could lead to local stress concentrations at the fillers' surface or tend to act as defective points which weaken the stress transfer from the matrix to fillers (Azizi et al., 2014; Ng et al., 2017).

(b) ***Elongation at Break***

PVA/Chitin blend exhibited improved tensile strength with increasing α-chitin content, at the expense of the percentage of elongation at break. As shown in Figure 4.8, it was reported that the elongation at break of PVA decreased from 181.31 ± 14.53% to 32.66 ± 3.63% when the α-chitin content varied from 0 wt.% to 30 wt.%. Intermolecular interaction causes the composite to become more rigid with increasing α-chitin content, resulting in decrease of the elongation at break monotonically (Sriupayo et al., 2005).

The drawback of the reinforcement effect by the cellulose is the reduction of flexibility of the composite, as proven by past work (Nigrawal et al., 2012). It was shown that the elongation at break of PVA/Chitin-10 composite experienced decline by 44.10% upon incorporation of 1 wt.% NCC (Figure 4.8). In other words, the elongation at break decreased from 149.00 ± 12.27% to 83.29 ± 5.12% when the NCC content of PVA/Chitin-10 varied from 0 wt.% to 1 wt.%. It is interesting to note that reinforcement by 1 wt.% and 1.5 wt.% NCC resulted in similar elongation at break. However, severe losses of mechanical properties (tensile strength, Young's modulus) were observed for 1.5 wt.% NCC could be due to inefficient stress transfer led by the poorer dispersion of NCC (Ng et al., 2017).

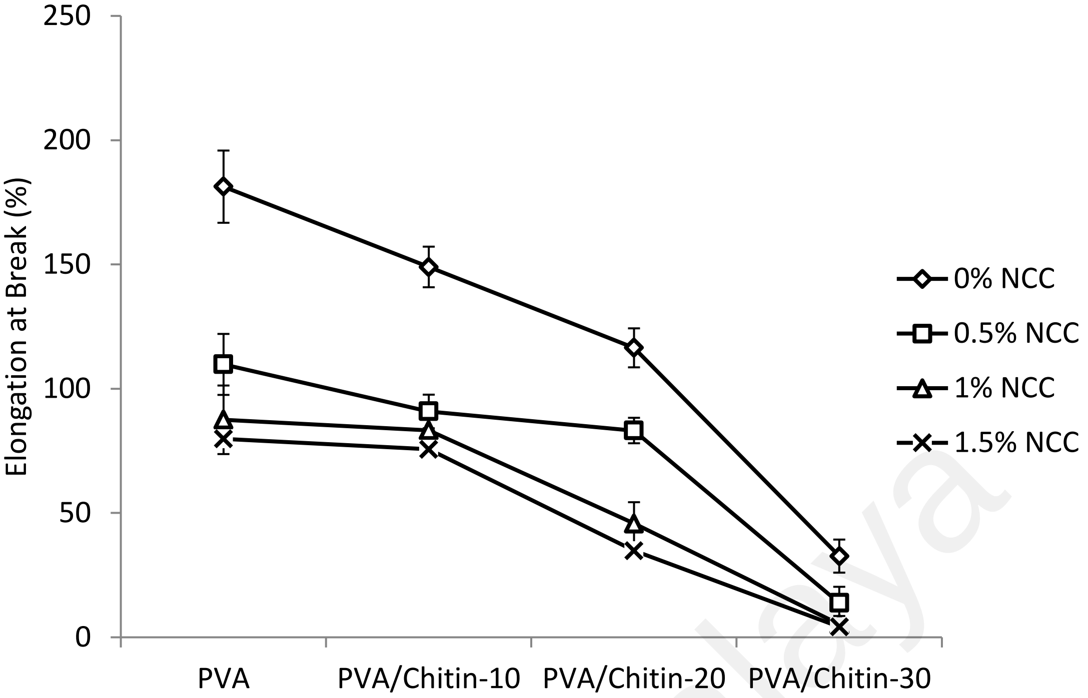

Figure 4.8: Elongation at break of the PVA/Chitin/NCC composites.

(c) Young's Modulus

Initial decrease of Young's Modulus upon addition of 10 wt.% of α-chitin as shown in Figure 4.9 is due the distortion of regularity of PVA molecular chains by chitin (C. Wang et al., 2015). However, incorporation of α-chitin from 10 wt.% to 30 wt.% into the composite increased the Young's Modulus (stiffness) of the PVA-based matrix from 976.44 ± 81.32 MPa to 1267.19 ± 39.71 MPa, as shown in Figure 4.9. This observed increment of stiffness is mostly due to the formation of the high strength network between chitin as chitin content is increased. Moreover, there are interactions between PVA and chitin via hydrogen bonding as suggested by previous research works (Junkasem et al., 2006; Sriupayo et al., 2005).

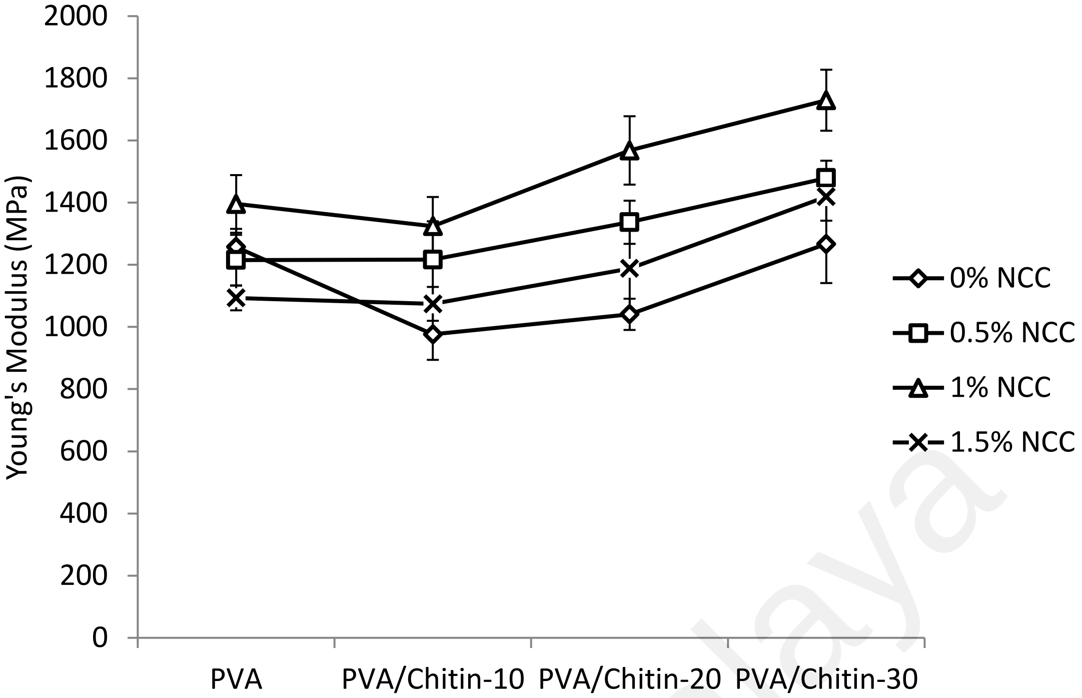

Figure 4.9: Young’s Modulus of the PVA/Chitin/NCC composites.

Effect of reinforcement by NCC on Young’s Modulus of PVA/Chitin/NCC composites could be depicted from Figure 4.9. Further enhancement of modulus was shown with loading of 1 wt.% NCC, which reached its maximum at 1729.47 ± 147.14 MPa when chitin content was 30 wt.%. With addition of 1 wt.% NCC in PVA/Chitin-20, an improvement of 50.66% in terms of Young’s Modulus was achieved. According to S.-Y. Lee et al. (2009), the increased Young’s modulus is because of the increased stiffness and brittleness of hybrid composites upon incorporation of the rigid NCC filler.

4.2.3.2 MA Cross-linked PVA Chitin/NCC Composites

The tensile strength, elongation at break and Young’s Modulus of PVA/NCC, the selected PVA/Chitin-10 and PVA/Chitin/NCC samples as a function of MA content are shown in Figure 4.10-4.12.

(a) Tensile Strength

Figure 4.10 shows that the maximum tensile strength of the respective PVA/Chitin/NCC composites achieved at different content of MA, dependent on the PVA/Chitin mass ratio. For PVA/Chitin-10/NCC, the highest tensile strength of 51.48 ± 3.30 MPa was reached at 50% of MA. As for PVA/Chitin-30/NCC, the maximum could be achieved at 10% of MA. This is due to the reason that as the PVA content is higher, more MA has to be incorporated to bond between PVA chains with increased abundance of -OH functional groups to form more aligned polymer network with improved interchain bonding (Reddy & Yang, 2010). This explanation was in agreement with the increasing trend of tensile strength observed with increased MA content obtained for PVA/NCC and PVA/Chitin-10, respectively. Upon reaching the respective maximum tensile strength, tensile strength reduced due to the excessive cross-linking which results in restrained intermolecular mobility among the macromolecules in PVA/Chitin/NCC composites (Gao et al., 2014).

In the presence of MA, it was noted that the cross-linked PVA/NCC composites without chitin incorporated generally exhibited better tensile properties over those of cross-linked PVA/Chitin/NCC composites. This is due to the reason that alignment of PVA chains are distorted when chitin polysaccharides with acetyl amine groups are incorporated, reducing tensile strength of the cross-linked PVA/Chitin/NCC. Similar result had been determined from the previous work on PVA/Xylan polysaccharide blend films with tetracarboxylic acid (Gao et al., 2014). However, despite of this reduced mechanical performance of the cross-linked PVA/Chitin/NCC, this compounding formulation exhibited improved functionality due to chitin while gained dimensional stability in water.

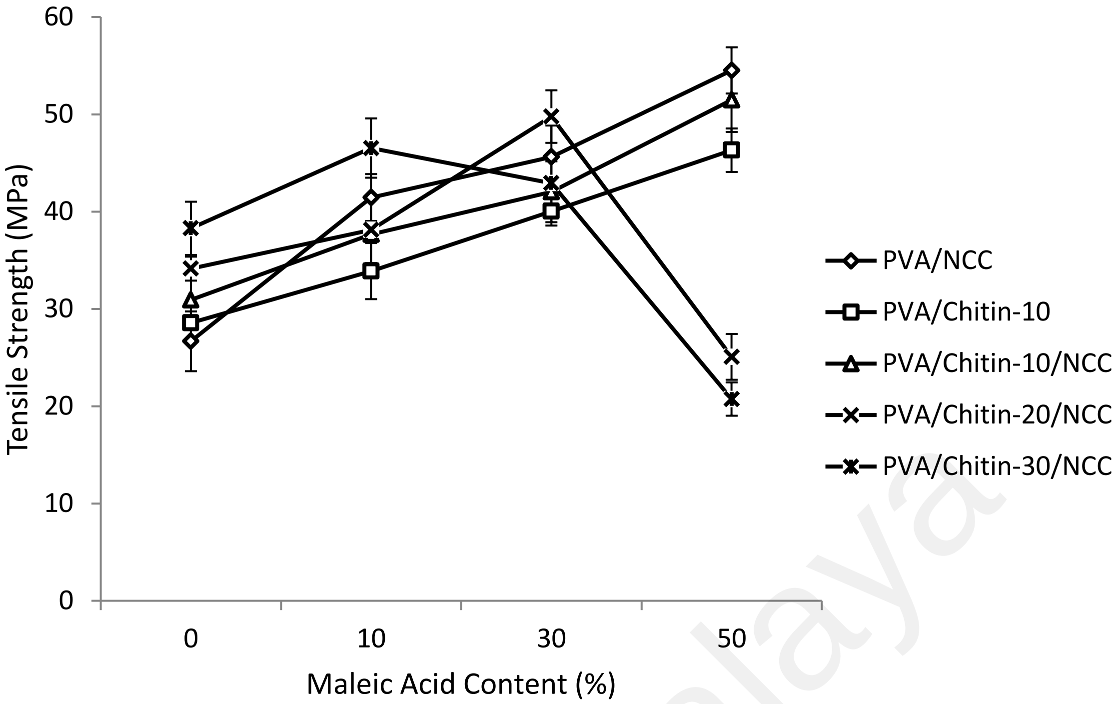

Figure 4.10: Tensile strength of PVA/NCC, PVA/Chitin and PVA/Chitin/NCC samples as a function of maleic acid content.

By comparing the tensile strength of PVA/Chitin-10 and PVA/Chitin-10/NCC under varied MA, it was deduced that the presence of MA did not undermine the good filler-matrix interactions between the NCC filler and PVA/Chitin matrix (Figure 4.10). Compatible filler-matrix interface allows efficient stress transfer from the matrix to the filler which leads to improved tensile strength of the PVA/Chitin/NCC composites (Mittal, 2015; Mohammad Mahdi Dadfar et al., 2014).

It was interesting to note that incorporation of MA led to tensile strength increment of the PVA/Chitin/NCC composites initially, followed by a decrease upon reaching the respective maximum tensile strength which varied according to MA composition (Figure 4.10). The enhancement of tensile strength is attributed to the increased chemical cross-linking of free -OH groups from PVA and chitin with the -COOH groups of MA through ester linkages at the amorphous phase (Abd El-Mohdy & Mostafa, 2013). The cross-linking causes composites network formed with strengthened intermolecular forces between polymers chains (Gao et al., 2014; R. Lusiana & Isdadiyanto, 2016). In addition, the increased degree of crystallinity of the semi-crystalline PVA-based composites in response to MA contributed to the enhanced tensile strength (Thomas et al., 2013). This is because there is improved secondary interchain bonding caused by the adjacent aligned chain segments as degree of crystallinity increases.

(b) ***Elongation at Break***

As shown in Figure 4.11, it was shown that the elongation at break of PVA/Chitin/NCC decreased from 9.37 ± 0.41% to 2.89 ± 0.23% when the α-chitin content varied from 0 wt.% to 30 wt.% while the MA content was constant at 30%. Intermolecular interaction causes the composite to become more rigid with increasing α-chitin content, resulting in decrease of the elongation at break monotonically (Sriupayo et al., 2005). In addition, composite containing higher fraction of PVA over chitin is more flexible as it is clear that the stiff chitin reduces overall flexibility of composite (Sriupayo et al., 2005).

In the presence of MA, good filler-matrix interactions between the NCC filler and PVA/Chitin matrix were achieved. This is supported by the fact that the inclusion of NCC resulted to increased strength of PVA/Chitin/NCC composites. Generally, improved stiffness or strength of polymer composites are achieved at the expense of the percentage of elongation at break. As a result, it was reasonable to observe that PVA/Chitin/NCC exhibited lower elongation at break in comparison to PVA/Chitin when MA content was constant at 30% (Figure 4.11). Due to the 1 wt.% NCC introduced, the slight decrease of elongation at break was amounting to a change of 13.2%, which was from 8.24 ± 0.31% to 7.15 ± 0.57%. Besides, the nucleating effects of NCC also lead to improvement of composites' crystallinity, as proven by the DSC results shown in Table 4.1. However, this improved crystallinity causes decreased numbers of polymer inter-chains available for slippage. Therefore, the percentage of elongation at break reduced with the loading of NCC which acted as the reinforcing filler (Brinchi et al., 2013; Ng et al., 2017).

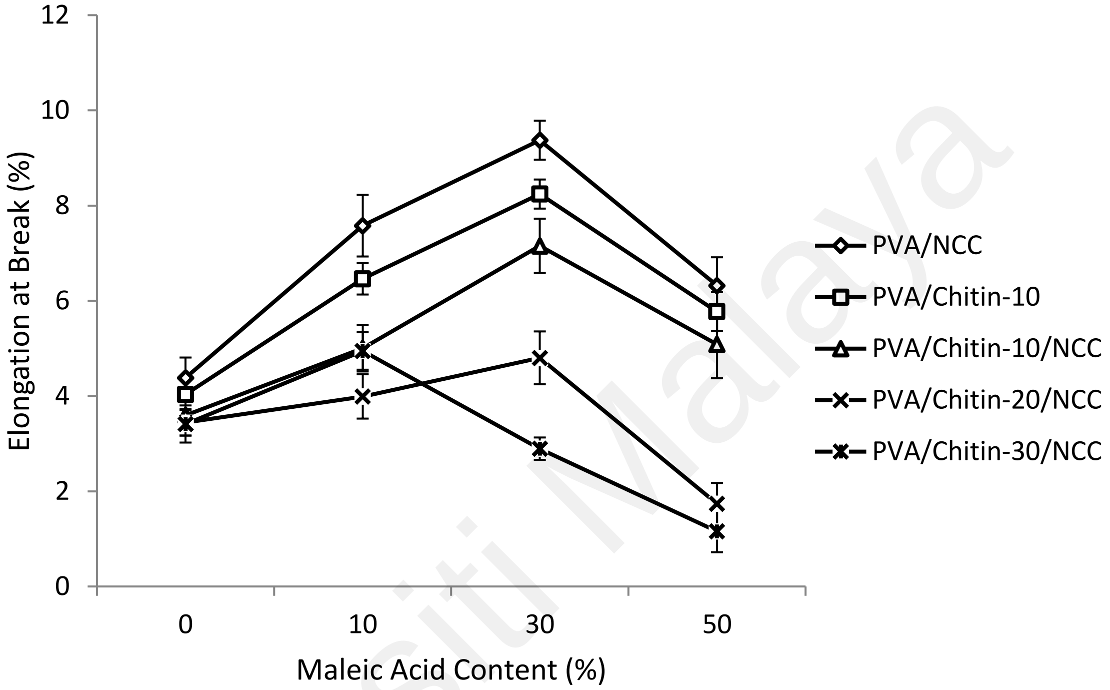

Figure 4.11: Elongation at break of PVA/NCC, PVA/Chitin and PVA/Chitin/NCC samples as a function of maleic acid content.

From Figure 4.11, it was determined that increasing MA content would enhance elongation at break of the PVA/NCC, PVA/Chitin and PVA/Chitin/NCC composites, respectively. Upon reaching the maximum flexibility, the elongation at break decreased for the respective composite. Similar trend was reported by Abd El-Mohdy and Mostafa (2013). For the PVA/Chitin/NCC composite, the highest elongation at break shown was 7.15 ± 0.57%, when the PVA/Chitin mass ratio was 9:1 and 30% of MA was introduced (Figure 4.11). Besides, the incorporation of MA provides carboxyl functional groups to be reacted with the hydroxyl-rich PVA/Chitin/NCC. Previous works have suggested that the films with both carboxyl and hydroxyl functional groups are stronger and able to elongate more over those films which only constituent of hydroxyl functionality (Abd El-Mohdy & Mostafa, 2013; Yoon et al., 2006). Moreover, elongation at break is dependent on network structures whereby materials with higher chemical and physical cross-linking could be more flexible (Oya et al., 2012). However, the decreased elongations at break observed after reaching the maximum for the respective composite samples were associated to the restrained interchain mobility due to the increased cross-linking (Gao et al., 2014; K. Qiu & Netravali, 2013) and crystallization (A. P. Gupta & Arora, 2011).

(c) ***Young's Modulus***

Figure 4.12 depicts that incorporation of α-chitin from 10 wt.% to 30 wt.% into the 30% MA cross-linked PVA/Chitin/NCC composites increased the Young's Modulus of the composites from 1386.89 ± 69.24 MPa to 2413.81 ± 167.36 MPa. This observed increment of stiffness is mostly due to the formation of the high strength network between chitin as chitin content is increased. Moreover, there are interactions between PVA and chitin via hydrogen bonding as suggested by previous research works (Junkasem et al., 2006; Sriupayo et al., 2005). Unlike synthetic polymer like PVA, chitin is a typical carbohydrate polymer with stiffer chains. Thus, composites exhibited increased Young's Modulus with higher chitin content.

By comparing the Young's modulus results of PVA/Chitin and PVA/Chitin/NCC as a function of varied MA content, it was remarked that the inclusion of NCC further contributed to enhancement in Young's Modulus of the composites (Figure 4.12). Specifically, the Young's modulus of PVA/Chitin-10 increased by 15.41% upon addition of the 1 wt.% NCC, which was from 1201.74 ± 67.22 MPa to 1386.89 ± 69.24 MPa. The greater Young's Modulus imposed by the presence of NCC is related to the increased stiffness and brittleness of the composites upon incorporation of the rigid nanocellulose filler (S.-Y. Lee et al., 2009).

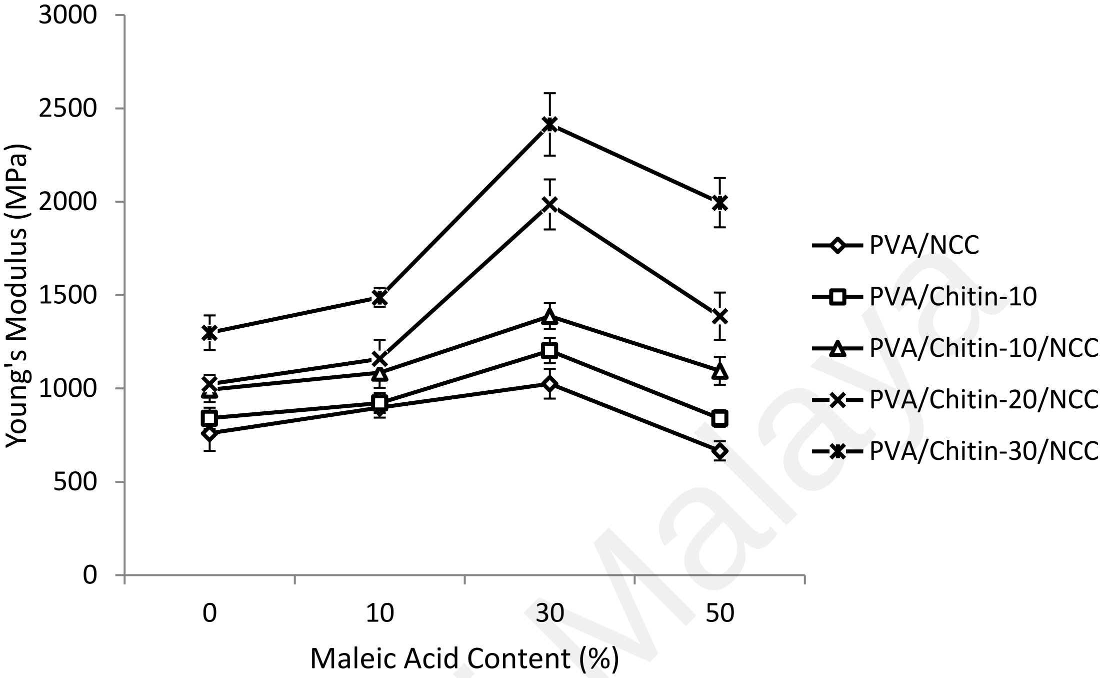

Figure 4.12: Young’s Modulus of PVA/NCC, PVA/Chitin and PVA/Chitin/NCC samples as a function of maleic acid content.

There is a significant improvement of Young’s Modulus of PVA/NCC, PVA/Chitin-10 and PVA/Chitin/NCC with increased content of MA, as shown in Figure 4.12. It can be observed that increment of stiffness is due to the formation of the high strength network between polymers by esterification (K. Qiu & Netravali, 2013). Nonetheless, excess MA acting as curing agent may lead to creation of weak points or dilution of the network, thus reducing Young’s Modulus (Wilder et al., 2006). The Young’s Modulus of PVA/Chitin-30/NCC was the highest among all compositions, with its maximum achieved at 30% MA dosage, amounting to 2413.81 ± 167.36 MPa.

4.2.4 Morphological Studies

This study provides information on the distribution condition of the NCC filler over the PVA/Chitin/NCC composites. In addition, it is to evaluate the miscibility of the polymeric materials blended.

4.2.4.1 PVA/Chitin/NCC Composites

Figure 4.13 (a) illustrates that the neat PVA was smooth in surface and it showed no features attributed to any crystalline morphology. Therefore, it is reasonable to suggest that the semicrystallinity of PVA is likely to be submicroscopic in nature. It is interesting to note that NCC appeared as white dots, as revealed by the high-resolution micrographs (Figure 4.13 (b)). Individual NCC was observable under 100 nm scale and dispersed on PVA host matrix. However, these individual units tend to form larger agglomerates of NCC, as remarked by the arrows in Figure 4.13 (b). NCC possesses high tendency in agglomeration due to its inherent hydrophilic characteristic that promotes hydrogen bonding between individual NCC as discussed by Panaitescu et al. (2008), which is applicable in this case. By comparing Figure 4.13 (d) and Figure 4.13 (e), it was concluded that incorporation of 1.5 wt.% NCC into composite matrix resulted to more intense agglomeration of NCC which acted as the reinforcing filler. This led to inefficient stress transfer from polymer matrix to the reinforcing filler and thus resulted in poorer mechanical properties when compared with 1 wt.% NCC loading. Based on the mechanical and morphological analysis results, it is deduced that further tests are to be carried out on the composites with 1 wt.% NCC only. Therefore, this composition of NCC was used for further tests on the PVA/Chitin/NCC composites cross-linked by MA.

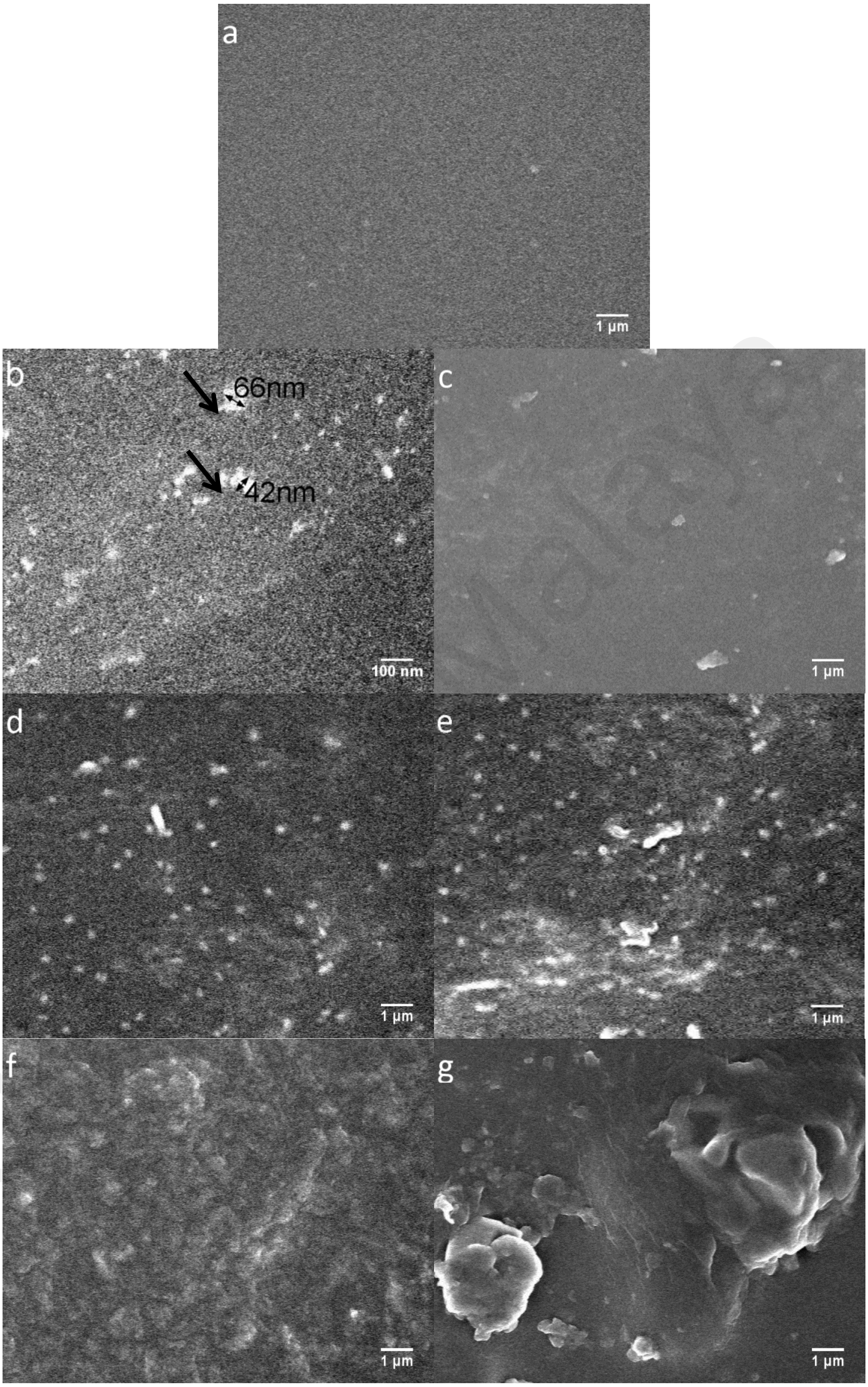

Figure 4.13: FESEM images of the (a) neat PVA, (b) PVA/NCC-1, (c) PVA/Chitin-10, (d) PVA/Chitin-10/NCC-1, (e) PVA/Chitin-10/NCC-1.5, (f) PVA/Chitin-20 and (g) PVA/Chitin-30. All of the images were captured at the same resolution-scale except image (b) which was captured up to nano-scale.

On the other hand, phase separation was observed for the PVA/Chitin binary blend in 80/20 and 70/30 mass ratio, as shown in 4.13 (f) and 4.13 (g) respectively. For PVA/Chitin-10 composite (Figure 4.13 (c)), chitin which appeared globular was evenly dispersed but embedded between PVA matrix, resulting the surface morphology to appear smooth. With increasing chitin content from 10 wt.% to 30 wt.%, it was observed that the surface morphology became rougher. This observation indicated that the segregation of the chitin from the PVA host matrix. FTIR analysis indeed revealed that intermolecular interactions existed between PVA and chitin in the form of hydrogen bonding. Moreover, the chitin was seen dispersed evenly throughout the PVA matrix regardless of chitin content incorporated. Thus, the as-synthesized PVA/Chitin composite films may experience partial miscibility. Nevertheless, improved mechanical properties of the composite film, in terms of Young's modulus and tensile strength were observed with increasing chitin content, as proven by the tensile test. It is reasonable to deduce that the reinforcement is attributed to the formation of the high strength network between chitin, which enables more efficient stress transfer (Mincea et al., 2012).

4.2.4.2 MA Cross-linked PVA Chitin/NCC Composites

Figure 4.14 (a) represented the PVA/NCC in the absence of MA and it appeared to be featureless and homogenous, characteristic to untreated PVA (Badr et al., 2010; Xia et al., 2016). For PVA/Chitin/NCC composites (Figure 4.14 (b)-4.14 (e)), the surface appeared to have some degree of phase separation between the PVA and chitin component at micrometer scale. Similar observation attributed to interaction between PVA and chitin was reported by other researchers (Y. M. Lee et al., 1996; Peesan et al., 2003). However, chitin which appeared as microdomains, were dispersed evenly throughout PVA and showed relatively good miscibility between the two materials. As discussed by Y. M. Lee et al. (1996), the heterogeneity of the dual components do not conclude that PVA and chitin are not partially miscible. This is due to the reasons that the sizes of microdomains were small and boundaries of the chitin microdomains were not distinctively separated to conclude that the dual components were immiscible. By comparing Figure 4.14 (b) and 4.14 (d), it was noted that the microdomains appeared to be less distinctive with increased MA, which served as the cross-linkers. This result is in general agreement with previous works which proved that cross-linkers led to reduced microphase separation (Merle et al., 2012; Riyajan et al., 2009). However, the increased content of chitin increased the apparent surface roughness of the PVA/Chitin-30/NCC/MA-30, as indicated by Figure 4.14 (e).

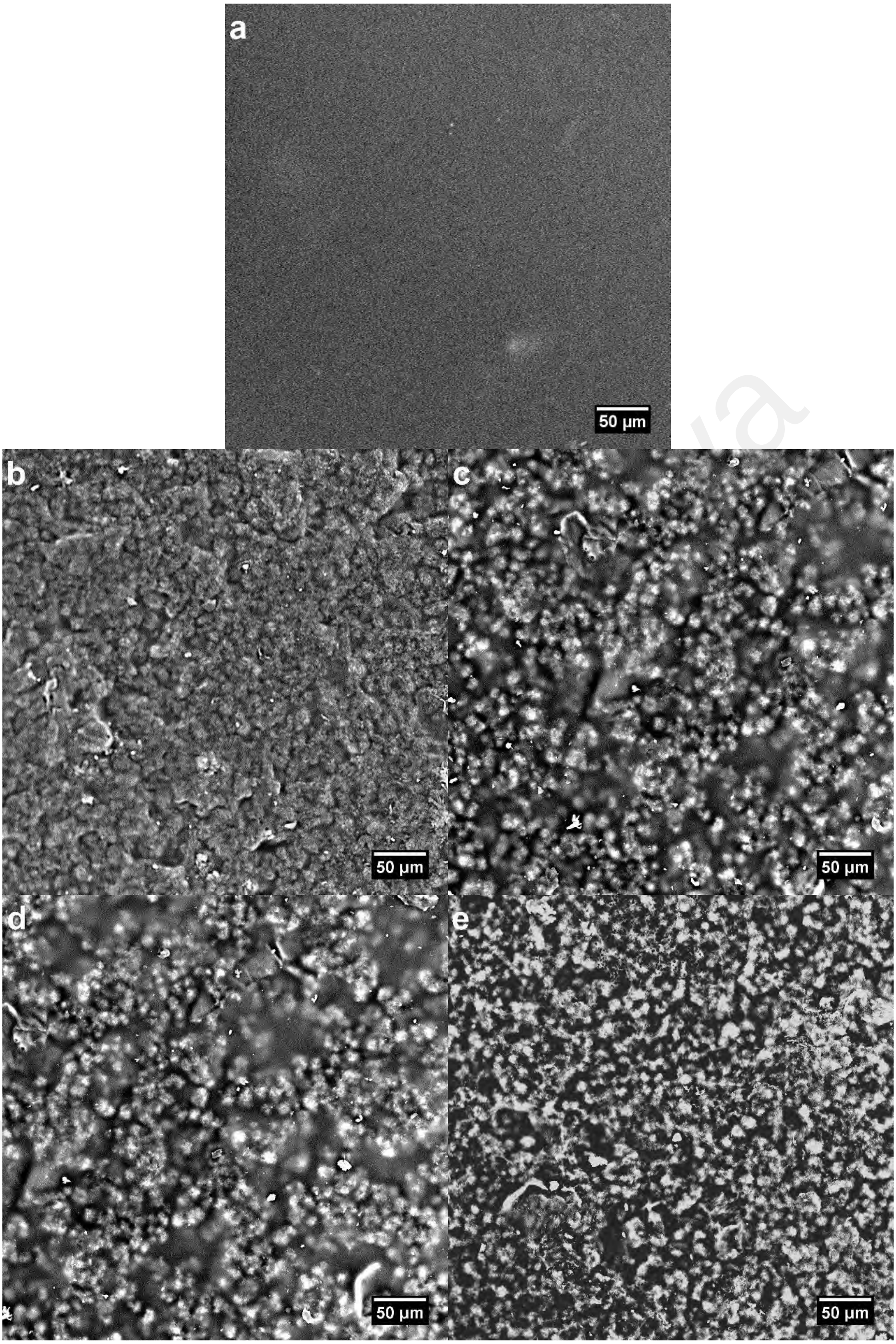

Figure 4.14: SEM micrographs of the (a) PVA/NCC, (b) PVA/Chitin-10/NCC, (c) PVA/Chitin-10/NCC/MA-30, (d) PVA/Chitin-10/NCC/MA-50, (e) PVA/Chitin-30/NCC/MA-30.

4.2.5 DSC Analysis

Through differential scanning calorimetry (DSC), the thermal transitions of the PVA/Chitin/NCC composites were investigated. The thermal transitions discussed were the glass transition temperature (T_g) and melting temperature (T_m). In addition, the thermal transitions of PVA/Chitin/NCC composites upon the incorporation of MA were investigated.

4.2.5.1 PVA/Chitin/NCC Composites

Figure 4.15 shows the heating thermograms for neat PVA, PVA/α-chitin blends at 90/10, 80/20 and 70/30 mass ratios and the selected binary blend films reinforced with 1 wt.% NCC, respectively.

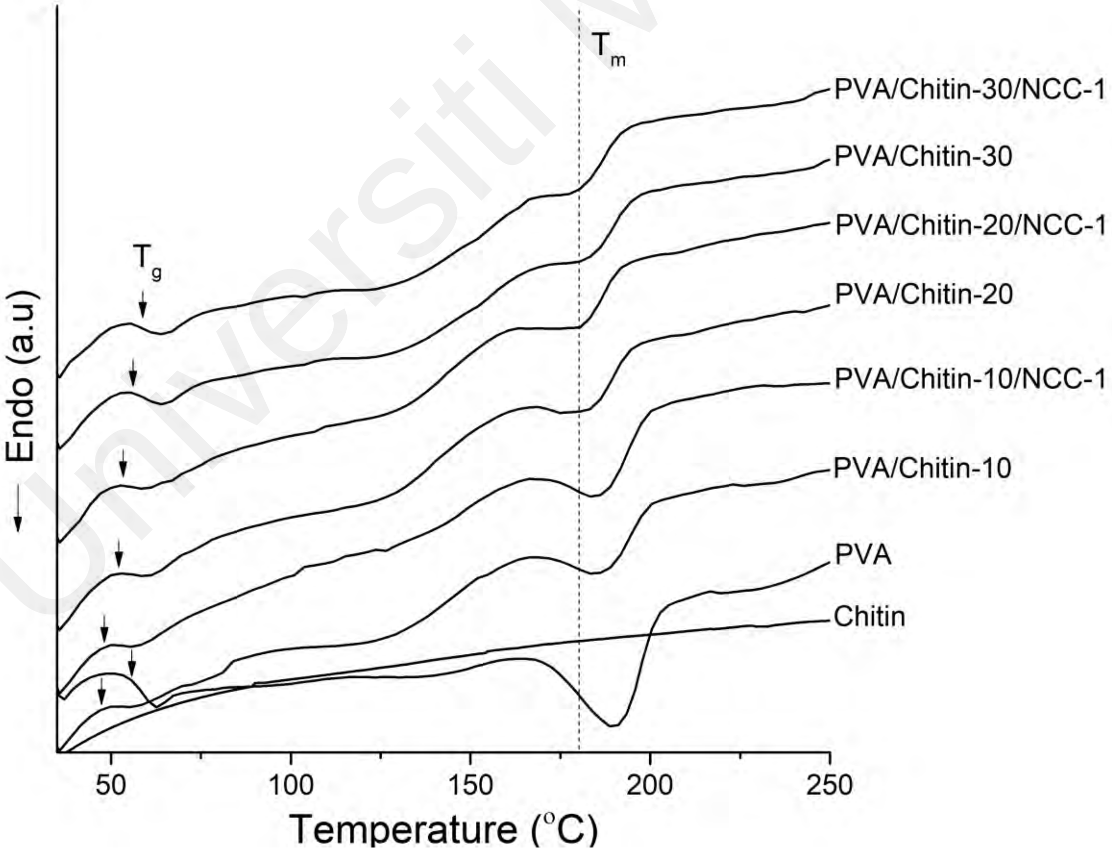

Figure 4.15: DSC thermograms of neat PVA, PVA/Chitin and PVA/Chitin/NCC-1 composites.

The result of neat chitin thermogram was not reported in Table 4.1 as its glass transition temperature (T_g) and melting temperature (T_m) were not distinguishable from DSC thermogram, in accordance to the work of Peesan et al. (2003). This phenomenon is due to the nature of chitin with rigid-rod molecular backbones arrangement, resulting in its high susceptible to degradation before melting. From the heating thermograms, the glass transition and melting phenomena of PVA, PVA/Chitin and the selected PVA/Chitin/NCC composites were determined, as summarized in Table 4.1.

Table 4.1: DSC result summaries for neat PVA, PVA/Chitin and PVA/Chitin/NCC composites reinforced with 1 wt.% NCC.

Samples	T_g (°C)	ΔH_f (J/g)	T_m (°C)	X_c (%)
PVA	55.09	14.87	191.21	9.24
PVA/Chitin-10	49.40	6.50	186.78	4.49
PVA/Chitin-10/NCC-1	50.06	8.21	186.07	5.67
PVA/Chitin-20	52.64	5.77	183.40	3.98
PVA/Chitin-20/NCC-1	54.15	6.12	182.14	4.22
PVA/Chitin-30	55.61	2.77	181.72	2.46
PVA/Chitin-30/NCC-1	58.04	3.04	180.39	2.69

Miscibility between the two constituents at various mass compositions was investigated using DSC by observing the T_g values of the neat PVA and PVA-based composites. As seen in Figure 4.15, only single T_g peak was present in the respective thermograms for each blend composition. The resulting T_g value was shifted to the right to higher temperatures with increasing α-chitin content. This indicates improved adhesion between the dual components in the amorphous phase at the molecular level (Peesan et al., 2003). In addition, T_m depression of PVA occurred as the α-chitin content increased from 0 wt.% to 30 wt.%, which was from 186.78°C to 181.72°C. This phenomena also supported partial miscibility between PVA and chitin, where PVA chains adhered with the chitin surface were likely to restrict the ordered association of PVA molecules, reducing crystal growth of PVA, in agreement to the chitin/PVA blends prepared by Kubota et al. (1998). Furthermore, the degrees of crystallinity of PVA (X_c) in the composites were estimated from the heat of fusion, ΔH_f using Equation 3.3. This is regarded as an indication of the miscibility of each component. As expected, the degree of crystallinity of PVA decreased with increasing α-chitin content, as shown in Table 4.1. The decreased in PVA crystallinity suggested increasing miscibility between PVA and chitin. As reviewed by Guirguis (2012), the alteration in the crystalline structure may result from polymer-polymer interactions at the amorphous phase. Therefore, disorder in the crystals is created, reducing the enthalpy of the phase change (Guirguis, 2012).

The effects of the inclusion of NCC into the PVA matrix was also analyzed using DSC (Table 4.1). Noticeably, the T_g slightly increased with the addition of 1 wt.% NCC, when the PVA/Chitin mass ratio were 90/10, 80/20 and 70/30, respectively. These results suggested restricted segmental motion of the polymer chains due to decrease of free volume (E. Fortunati et al., 2013). Moreover, the composite systems had T_m shifted to lower temperature with the inclusion of NCC as filler. This is due to the hydrophilicity of the NCC, which increases the amount of bound water. Interestingly, water acts as a plasticizer which disrupts the interchain hydrogen bonds of polymer. Pereira et al. (2014) reported similar plasticizing effect in PVA films that were partially hydrolyzed with nanocrystalline cellulose isolated from banana pseudostems, which justifies the addition of NCC in the modification of melting temperature of the nanocomposite, in comparison to the neat PVA. Thus, this result suggests that incorporation of NCC filler led to enhancement of processability of the PVA composites (Pereira et al., 2014). Lastly, NCC reinforced PVA/Chitin composites garnered higher degree of crystallinity with the NCC introduced. For example, composite systems of

PVA/Chitin-10/NCC-1 (X_c = 5.67%) showed a higher degree of crystallinity by 16.28% with respect to binary system of PVA/Chitin-10 (X_c = 4.49%). This gives evidence that NCC acts as an effective heterogeneous nucleating agent which promotes the crystallization of the PVA matrix.

4.2.5.2 MA Cross-linked PVA/Chitin/NCC Composites

Figure 4.16 shows the DSC thermograms of PVA, chitin, the selected samples of PVA/Chitin and PVA/Chitin/NCC. DSC data results are summarized in Table 4.2. For neat PVA, the glass transition temperature (T_g) and melting temperature (T_m) were determined to be 57.03°C and 192.14°C, respectively. As expected, chitin homopolymer showed no significant transition at the heating range. It was widely reported that the T_g and T_m value for chitin could not be determined through DSC (Cho et al., 2001; Y. M. Lee et al., 1996; Peesan et al., 2003). This is due to the fact that the rigid nature of the chitin backbone chains which cause chitin being susceptible to degradation before melting (Peesan et al., 2003).

With reference to Table 4.2, PVA/Chitin/NCC composites showed improvement of T_g with respect to increasing chitin content, when MA content was constant at 30%. This is attributed to the presence of chitin which has reduced the free volume of the composites and restricted the segmental motion of the polymer chains (K. Qiu & Netravali, 2013). T_m of PVA/Chitin-30/NCC/MA-30 was recorded at 219.30°C, which was higher than the PVA/NCC/MA-30 with T_m at 207.20°C. Hence, it is deduced that chitin has promoted the growth of crystallites' size in PVA/Chitin/NCC composites. The degree of crystallinity (X_c) of PVA in composites have been calculated from the heat of fusion, ΔH_f using Equation 3.3.

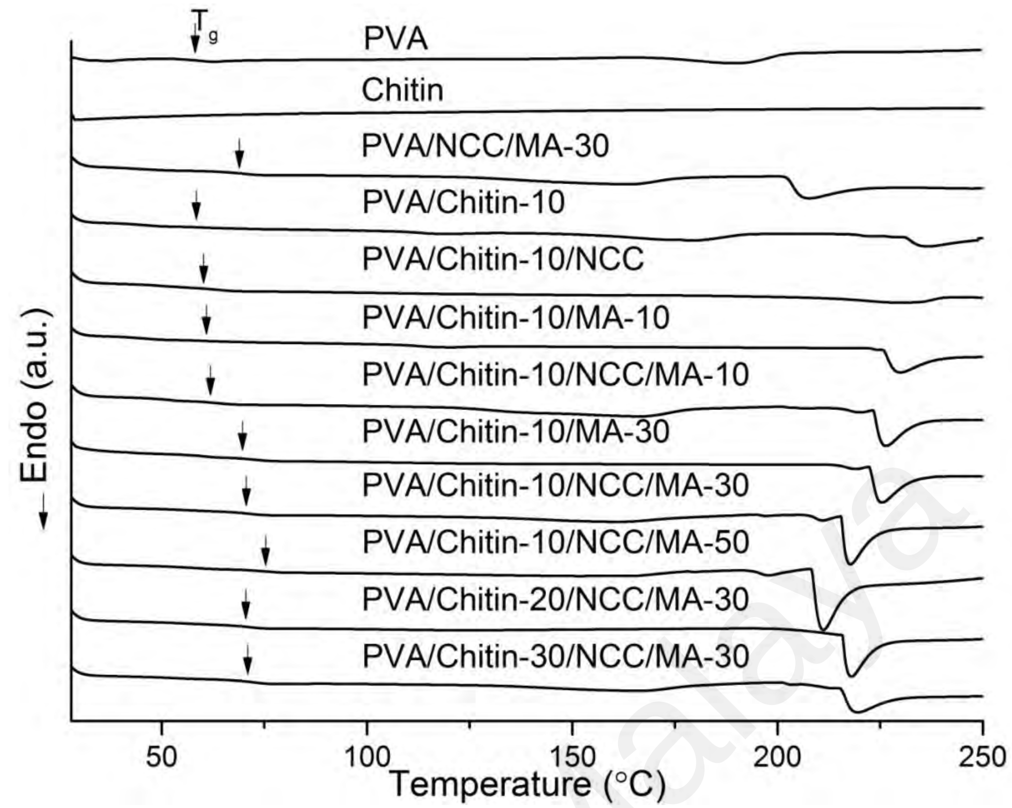

Figure 4.16: DSC thermograms of PVA, chitin, the selected samples of PVA/Chitin and MA cross-linked PVA/Chitin/NCC.

Table 4.2: DSC result summaries for the selected samples.

Samples	**T_g (°C)**	**ΔH_f (J/g)**	**T_m (°C)**	**X_c (%)**
PVA	57.03	15.13	192.14	10.44
PVA/NCC/MA-30	70.50	24.59	207.20	15.27
PVA/Chitin-10	59.80	10.30	236.00	7.11
PVA/Chitin-10/NCC	61.81	13.36	229.83	9.22
PVA/Chitin-10/MA-10	62.42	18.75	230.10	12.94
PVA/Chitin-10/NCC/MA-10	63.50	26.87	226.30	18.54
PVA/Chitin-10/MA-30	71.56	27.33	225.59	18.86
PVA/Chitin-10/NCC/MA-30	72.10	29.99	217.60	20.63
PVA/Chitin-10/NCC/MA-50	77.00	39.13	211.16	27.00
PVA/Chitin-20/NCC/MA-30	72.33	24.94	218.19	19.36
PVA/Chitin-30/NCC/MA-30	72.60	19.61	219.30	17.40

As shown in Table 4.2, chitin served as a nucleating agent when the content was at 10 wt.%. The degree of crystallinity increased from 15.27% to 20.63%, in comparison between PVA/NCC/MA-30 and PVA/Chitin-10/NCC/MA-30. In contrast, the mobility of PVA chains had been greatly disturbed at higher chitin content, retarding the development of PVA crystals (Cho et al., 2001). Hence, PVA/Chitin-30/NCC/MA-30 exhibited slightly lower crystallinity, determined to be 17.40%.

By comparing DSC thermograms of PVA/Chitin-10 and PVA/Chitin-10/NCC, it was noted that the introduction of NCC into the composite resulted to enhancement in T_g but reduction in T_m (Table 4.2). Since T_g is associated to polymer chains flexibility, the increase in T_g with the 1 wt.% NCC incorporated can be explained by the interactions between NCC and PVA/Chitin which has restricted the segmental motions of PVA chains (Peresin et al., 2014; Virtanen et al., 2014). As a consequence of the improved interactions, bigger crystalline domains could not be formed and hence T_m was reduced (B. Li et al., 2016; Peresin et al., 2014). However, NCC is a nucleating agent as suggested in other studies (Lu et al., 2008; Peresin et al., 2014; Virtanen et al., 2014). For instance, the X_c of PVA/Chitin-10/MA-30 was improved further in the presence of NCC, from 18.86% to 20.63%.

On the other hand, it was determined that the T_g of the PVA/Chitin-10/NCC composite was shifted the right to higher temperature with increasing MA content, from 61.81°C at 0% MA to 77.00°C at 50% MA (Table 4.2). The introduction of MA into PVA/Chitin/NCC had distorted the hydrogen bonding between the PVA chains, chitin and NCC. This may result in decrease stiffness of the polymer chains with the corresponding hydrogen bonding reduced or if MA had been serving as a plasticizer (Gohil et al., 2006). However, T_g had been improved instead due to the fact that MA had served as cross-linker which bonded polymer chains through ester linkage at the amorphous phase (Gohil et al., 2006; Peresin et al., 2014; Z. Xie et al., 2011). In terms of T_m in response to MA content, the incorporation of MA had caused hindrance to chain orientation, resulting in smaller crystallites formation (Maitra & Shukla, 2014; K. Qiu & Netravali, 2013). Thus, the melting temperature was the highest when MA was absent.

During the curing of a semi-crystalline polymer, such as PVA in this case, crystallization and cross-linking are affecting each other mutually (Ishida & Yoshie, 2008; Kang et al., 2002). Since the PVA/Chitin/NCC composites were cured at a temperature not exceeding the T_m of PVA, crystallization process was initiated before cross-linking (Oya et al., 2012). PVA/Chitin-10/NCC had higher X_c with increased content of MA of 0% to 50%, from 9.22% to 27.00%. This is due to the crystallization process had proceeded to completion at earlier stage of curing, before cross-linking was initiated and completed at higher temperature. Therefore, the influence of cross-linking was minimal towards crystallization reaction in the PVA/Chitin/NCC composites. Similar phenomenon had been reported by Ishida and Yoshie (2008) as well as Oya et al. (2012). The studies concluded that polymers network cross-linked with crystalline phase pre-existed would result in relatively stiff and hard materials while those material obtained through cross-linking, followed by crystallization would have softer properties. Hence, the former remark correlated with the results of this current study.

4.2.6 Swelling Tests

Swelling test was employed to investigate the swelling capability of the PVA-based composite with or without MA incorporated. Swelling test served as a technique to deduce the nature of polymer network. This is because generally the swelling behavior of composite film is mainly influenced by the nature of polymer network such as the contents of hydrophilic groups, relaxation of amorphous region, degree of crystallinity and the degree of cross-linking between polymer chains. Other contributing factors include diffusion coefficient, pH and temperature of solvents (Abd El-Mohdy & Mostafa, 2013; Z. Xie et al., 2011). However, the other contributing factors were constant in the present investigation. Hence, the variance in swelling behaviors observed for the respective PVA/Chitin/NCC composites and MA cross-linked PVA/Chitin/NCC composites were mainly attributed to the differences on the nature of polymer network.

4.2.6.1 PVA/Chitin/NCC Composites

The equilibrium percentage degrees of swelling for all the PVA/Chitin composites, with or without 1 wt.% NCC were summarized in Figure 4.17. Comparatively among the samples studied, the equilibrium percentage degree of swelling of neat PVA was the second lowest, at 376.25 ± 21.35%. With increasing α-chitin content alone, the degree of swelling of PVA/Chitin blend was found to increase from 467.79 ± 27.15% to 627.99 ± 30.90%, when chitin content increased from 10 wt.% to 30 wt.%. Addition of 30 wt.% chitin drastically improved swelling capability of neat PVA by 66.91%. This phenomenon agrees well with previous study that postulates the tight adsorption of the water molecule to the α-chitin structure prepared by the calcium-methanol solvent system (Tamura et al., 2006). In addition, this increasing trend of swelling due to chitin is in general agreement with results obtained for β-chitin/poly(vinyl alcohol) blend films (Peesan et al., 2003). The increased swelling capability of blend films with chitin loading are due to the increased amorphous of the PVA matrix, as depicted by DSC analysis.

As for 1 wt.% loading of NCC as filler, the swelling capability showed further decrease. By comparing the equilibrium swelling percentage of PVA/Chitin-30 and PVA/Chitin-30/NCC, it was determined that swelling capability of PVA/Chitin-30 decreased by 6.41% with the addition of 1 wt.% NCC, which was from 627.99 ± 30.90% to 587.73 ± 23.54%. The NCC bristle with polar groups forms intermolecular interactions with PVA-based matrix through hydrogen bonding. Herein, attachment of water molecules to NCC is decreased and this leads to less water build-up within films which appear as films swelling (Rao et al., 2007).

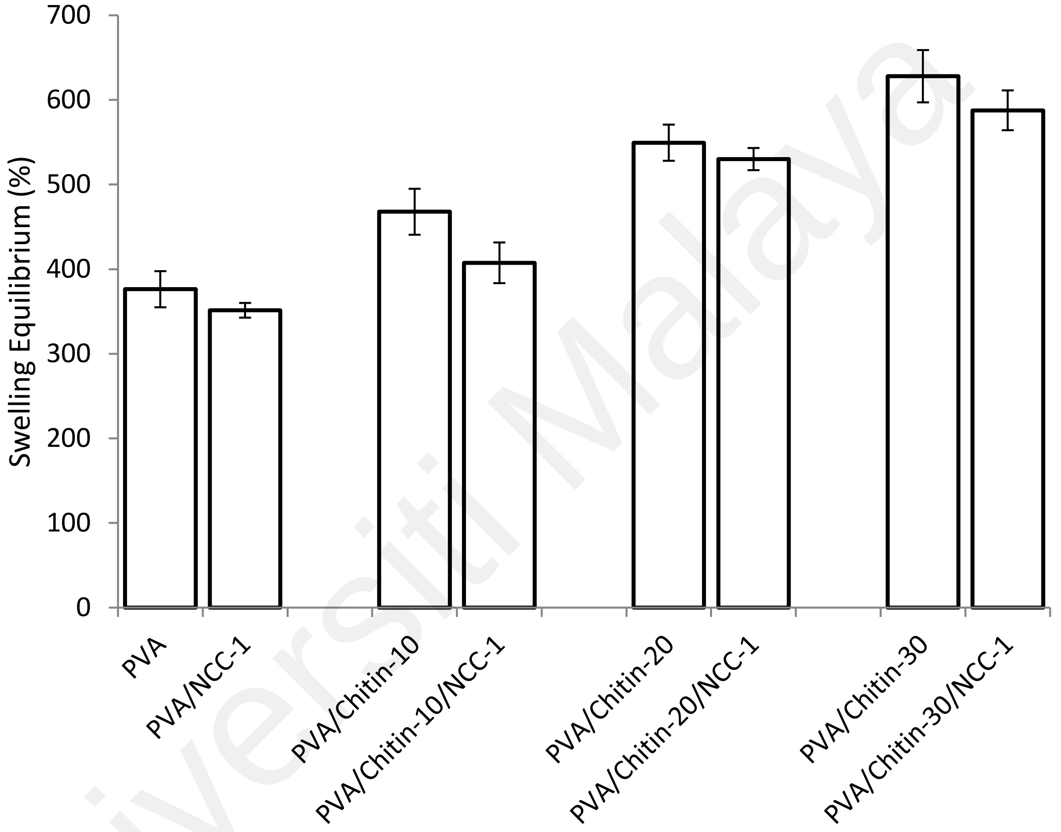

Figure 4.17: Equilibrium percentage degree of swelling for samples with 0 wt.% and 1 wt.% NCC under condition at 25°C.

4.2.6.2 MA Cross-linked PVA/Chitin/NCC Composites

In the absence of MA, the swelling equilibrium percentage of PVA/Chitin/NCC composite was found to be enhanced from 353.60 ± 16.52% to 503.07 ± 9.68%, when chitin content was varied from 10 wt.% to 30 wt.% (Figure 4.18). This result is in accordance with the previous finding which suggests that the tight adsorption of the water molecule is associated to the α-chitin structure prepared by the saturated calcium-methanol solvent system (Tamura et al., 2006). Moreover, this increasing trend of swelling attributed to chitin is in accordance with the results determined for β-chitin/poly(vinyl alcohol) blend films (Peesan et al., 2003).

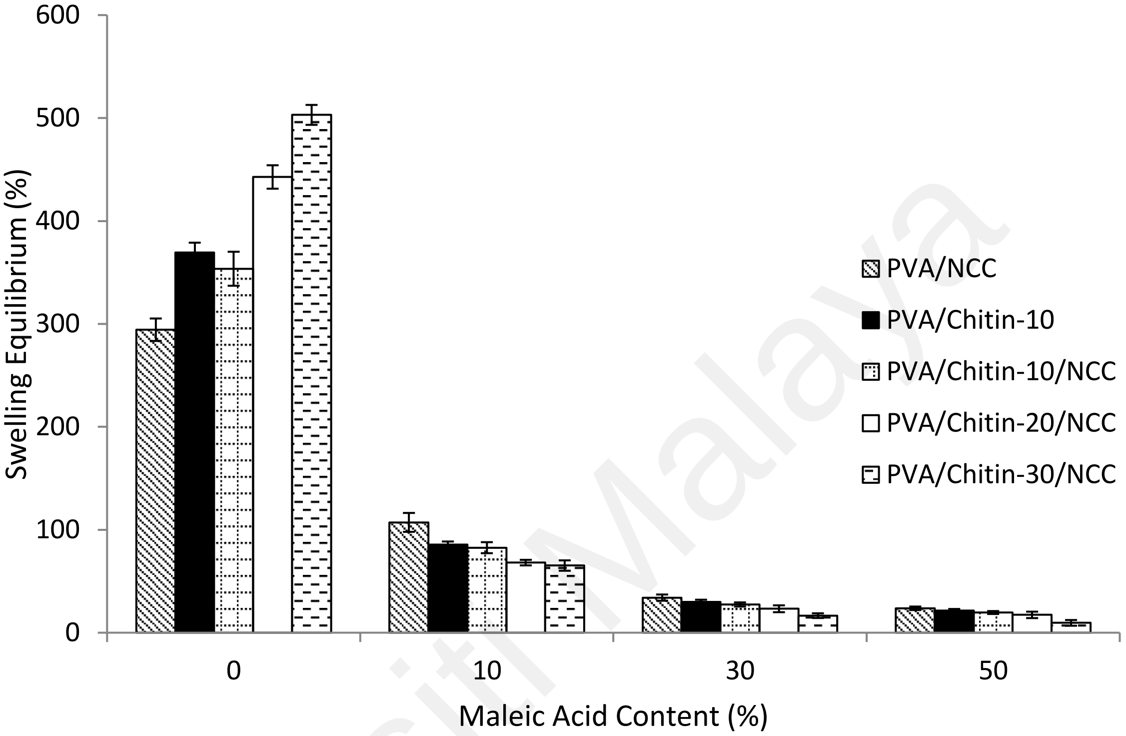

Figure 4.18: Swelling equilibrium percentage of sample composites after water immersion for 24 h under condition at 25°C.

Contrarily, the degree of swelling increased corresponding to the increased PVA content in the MA cross-linked composite. For instance, it was determined that the swelling equilibrium percentage of PVA/NCC was 107.18 ± 9.17%, which swelled 64.31% higher over PVA/Chitin-30/NCC with reported value of 65.23 ± 5.05% when MA content for both are constant at 10%. Similar findings were also reported by Parida et al. (2011) and Costa-Júnior et al. (2009), respectively. This is because PVA contains abundant of hydrophilic free hydroxyl (-OH) groups which interacts with water molecules (H_2O) through hydrogen bonds. As a result, more water molecules could diffuse into the PVA-based composite film when the content of PVA in the composite is higher. Hence, composite films constituent of higher composition of PVA and lower chitin content tend to swell with higher degree due to the increased bound water through hydrogen bonding (Rao et al., 2007; Zaikov & Jiménez, 2005).

By comparing the swelling capabilities of PVA/Chitin-10 and PVA/Chitin-10/NCC under varied MA, it was concluded that the swelling capability of the composite decreased slightly with the loading of 1 wt.% NCC (Figure 4.18). For instance, the equilibrium swelling percentage of PVA/Chitin-10 was decreased by 3.33% upon addition of 1 wt.% NCC, from 85.46 ± 3.15% to 82.61 ± 5.36%. This is due to the involvement of free hydroxyl groups of PVA in the formation of new intermolecular interactions with NCC instead with water (Rao et al., 2007). Therefore, this leads to lesser water build-up within the composite which appears as swelling.

Upon addition of MA into the PVA/Chitin/NCC composites, the swelling were greatly suppressed with increasing MA content. From Figure 4.18, it was noted that PVA/Chitin-10/NCC composite with 0% MA showed higher swelling, up to 353.60 ± 16.52%. However, the swelling was reduced to 19.61 ± 2.41% in the presence of 50% MA. This result shows that the percentage of swelling of the composite had decreased by 94.45%. This was due to the cross-linking of the polymer chains through esterification. The ester linkages formed through the carboxyl groups (-COOH) of MA had consumed much of the free hydroxyl groups in the composites. Moreover, it was postulated that the composite exhibited lower tendency for hydrogen bonding with water as well as having a more compact network structure via cross-linking reactions (Parida et al., 2011; Z. Xie et al., 2011). The compact network structure is correlated to lower chain mobility, chain motion and less free volume. Due to the reduced free volume, less water could diffuse into the composites. Consequently, cross-linked PVA/Chitin/NCC composites showed decrease in swelling (B. Han et al., 2003).

4.2.7 Water Solubility Test

Water solubility test is imperative for adsorption application to determine the workability of the PVA/Chitin/NCC composite in aqueous medium. This is because the composite will have to be remained in aqueous medium during adsorption operation.

4.2.7.1 PVA/Chitin/NCC Composites

Figure 4.19 shows a decrease in water solubility percentage with increasing loading of chitin. PVA exhibited the highest solubility in distilled water, amounted to 90.45 ± 1.95% upon immersion time of 1 h. This finding is in accordance with reported value of 90.80% in a similar past study done by Sriupayo et al. (2005). This is due to the water solubility behavior of PVA that varies based on its degree of hydrolysis and polymerization. PVA solubility has its maximum at 88% of hydrolysis, while higher solubility is garnered for lower degree of polymerization (Alexy et al., 2003). Therefore, the PVA composites of the present investigation portrayed high water solubility. This is attributed to the inherent characteristic of partially hydrolyzed PVA used which constituent degree of hydrolysis at 87% to 89%. Partially hydrolyzed grades of PVA exhibit greater water affinity to water at room temperature over those of the fully hydrolyzed grades of PVA due to the fact that the presence of 11% to 13% acetate groups have weaken hydrogen bonding between PVA polymer chains (Gohil & Ray, 2009). On the other hand, addition of 30 wt.% chitin to PVA drastically reduced the solubility of neat PVA for up to 39.87%, which was from 90.45 ± 1.95% to 54.38 ± 1.87%. This is because the chitin interacts with PVA through hydrogen bonding. Therefore, increasing chitin loading improves water resistance of the composites from dissolution which are similar with the findings of Sriupayo et al. (2005).

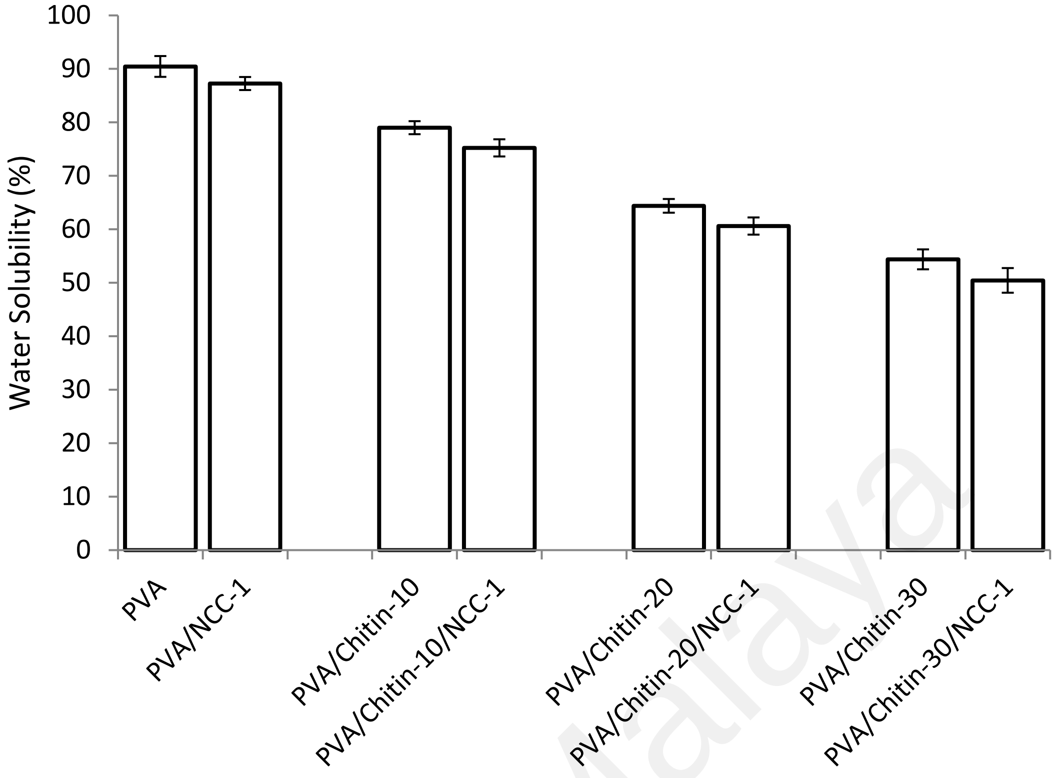

Figure 4.19: Water solubility for the samples upon immersion in water for 1 h under condition at 25°C.

In addition, the presence of 1 wt.% NCC in PVA helped in further improving stability of the composites in distilled water. By comparing the solubility percentage of PVA/Chitin-30 and PVA/Chitin-30/NCC, it was figured out that solubility of PVA/Chitin-30 further decreased from 54.38 ± 1.87% to 50.44 ± 2.31%, due to the 1 wt.% NCC incorporated. This is attributed to the loading of cellulose in the form of nanocrystals are insoluble in nature which result in lower affinity and reactivity to water. The water uptake of composites made of hydrophilic polymer matrices have been found reduced through the incorporation of cellulose nanocrystals in the soy protein isolate films (Y. Wang et al., 2006), carrageenan films (S nchez-Garc a et al., 2010) and glycerin plasticized carboxymethyl cellulose (Choi & Simonsen, 2006). The findings of improved water resistance with chitin or NCC loading may contribute in enhancing the stability and workability of PVA in aqueous media for applications where chemical alterations are minimally required.

4.2.7.2 MA cross-linked PVA/Chitin/NCC Composites

Figure 4.20 illustrates on the water solubilities of a series of PVA/Chitin/NCC composites as a function of varied content of MA, which served as the cross-linker. For PVA/Chitin/NCC composites with 0% MA incorporated, the composites did not hold dimensional stabilities even in water at room temperature. This highlighted the importance of incorporating additional cross-linker for the PVA-based composites to gain practical functionalities in aqueous media. Irrespective of the MA content dosed, PVA/Chitin/NCC composites garnered reduced water solubility with the increased chitin content of 0 wt.% to 30 wt.%. For example, 30% MA cross-linked PVA/NCC with water solubility of 15.43 ± 1.30% gained decreased water solubility by 68.30% with 30% chitin incorporated. Hence, 30% MA cross-linked PVA/Chitin-30/NCC achieved water solubility of 4.89 ± 1.03%. As evidenced by Sriupayo et al. (2005), the decreased in the solubility of PVA/Chitin composites in comparison to neat PVA was attributed to the strong hydrogen bonding between PVA molecules and the α-chitin.

Similarly, the presence of 1 wt.% NCC also contributed to the slight improvement in water solubility of the MA cross-linked PVA/Chitin/NCC composites. It was determined that the 30% MA cross-linked PVA/Chitin-30 with water solubility recorded as 10.97 ± 1.52% was higher by 33.29% in solubility than the 30% MA cross-linked PVA/Chitin-30/NCC which exhibited water solubility of 8.23 ± 1.18%. This is ascribed to the increased intermolecular interactions between PVA and NCC which resulted to the improved water solubility (Rao et al., 2007).

Furthermore, the water solubilities of PVA/Chitin/NCC composites decreased significantly with the increasing dosage of 0% to 50% MA. By considering the PVA/Chitin-10/NCC composite only, it was revealed that the water solubility decreased from 69.78 ± 0.50% to 5.64 ± 1.27%, in correspondent to the MA which varied from

0% to 50%. The enhancement of water solubility was amounted to 91.92%. This is because the solubilities of PVA-based composites in water also depend upon the crosslink density, apart from the degree of hydrolysis. Similar significant reductions in water solubilities of PVA-based composites with respect to increased contents of dicarboxylic acid were observed by other researchers (Gohil et al., 2006; Gohil & Ray, 2009; K. Qiu & Netravali, 2013). Addition of dicarboxylic acid such as MA resulted to interchain cross-linking which subsequently decreased the number density of free hydroxyl groups. As a result, this reduced the extensive solvation of the polymer matrices by diffusing water and contributed to the decreased water solubilities (Gohil & Ray, 2009; B. Han et al., 2003).

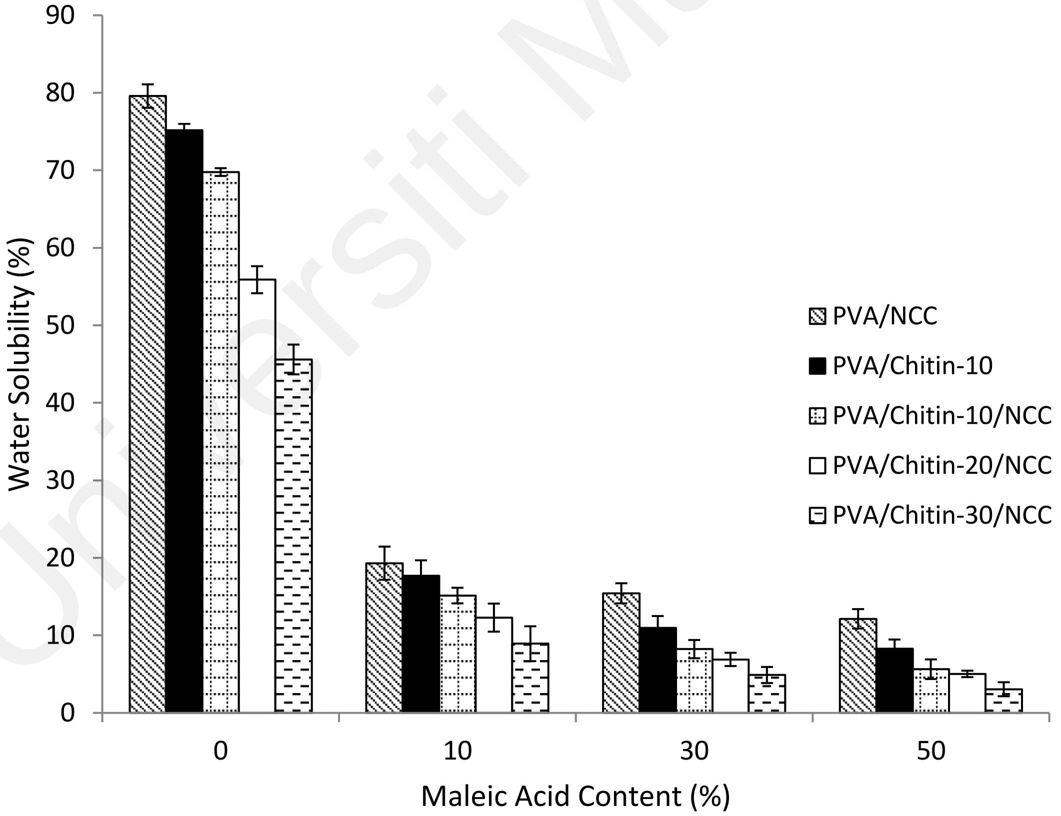

Figure 4.20: Water solubility of a series of PVA/NCC and PVA/Chitin/NCC composites with the varied dosage of 0% to 50% MA.

4.2.8 Gel Content

Sol-gel analyses of the PVA-based composites with or without MA incorporated were carried out in cold (25°C) and hot water (80°C), respectively. To be noted, polymeric gel could be categorized into physical gel or chemical gel. The physical gel constitutes of network with randomized junction points that are formed through the weaker physical bonding, which will segregate when exposed to hot water. Physical bonding is attributed to hydrogen bonding, presences of crystallites, Van der Waals interactions and other weak interactions. As for chemical gel, it is more stabilized since the chemical bonding such as covalent bonding impart the gel with structural integrity even in the hot water (Gohil et al., 2006; Riyajan et al., 2009).

4.2.8.1 PVA/Chitin/NCC Composites

As summarized in Figure 4.21, the gel content determined for PVA/Chitin and PVA/Chitin reinforced by 1 wt.% NCC increased with the increasing content of chitin which ranged from 0 wt.% to 30 wt.%. As observed, the gel content determined at 25°C for PVA/NCC-1 and PVA/Chitin-30/NCC-1 were 13.24 ± 0.41% and 51.18 ± 1.33%, respectively. The improvement of gel content with the 30 wt.% chitin introduced was by 2.86 times. It was postulated that there were improved intermolecular interactions between PVA and chitin with increased content of chitin. As denoted by FTIR analysis in section 4.1.2.2, the intermolecular interactions between PVA and chitin involved hydrogen bonding, which was a form of physical bonding. Hence, higher gel contents were obtained when samples were immersed in 25°C water. This is due to the reason that the gel content retained at 25°C water composed of both physical gels and chemical gels while gel content remained in 80°C water were chemical gels (Gohil et al., 2006; Riyajan et al., 2009).

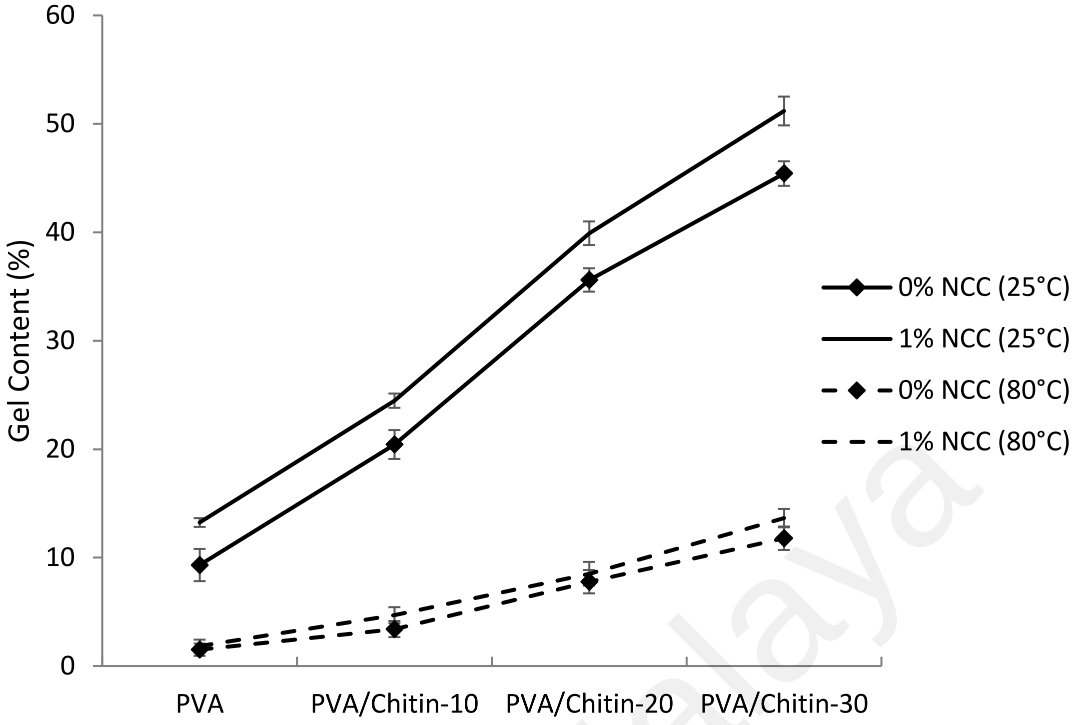

Figure 4.21: Gel content of neat PVA, PVA/Chitin and PVA/Chitin/NCC composites reinforced with 1 wt.% NCC determined through immersion in cold water (25°C) and hot water (80°C) for 24 h.

Additionally, the reinforcement of the PVA-based composites by the 1 wt.% NCC resulted to slight improvement in water stability of the composites both in 25°C and 80°C distilled water. At 25°C, gel content recorded for PVA/Chitin-30 and PVA/Chitin-30/NCC were 45.41 ± 1.13% and 51.18 ± 1.33%, respectively. With the addition of 1 wt.% NCC, the gel content increased by 12.71%. This is because NCC in the form of nanocrystals are insoluble in nature. The hydrogen bonding between PVA and NCC which helped in the increased durability against water. Indeed, physical bonding initiated from hydrogen bonding and presence of crystallites would serve to impart some structural stability. However, it is insufficient to maintain the structural stability of PVA-based composites which have large number of free hydroxyl groups that lead to solvation by water (Gohil et al., 2006; Peresin et al., 2014).

4.2.8.2 MA Cross-linked PVA/Chitin/NCC Composites

Figure 4.22 depicts that PVA-based composites which were heat treated at 140°C for 90 min in the absence of MA portrayed low resistance to water. Moreover, MA-treated PVA/Chitin/NCC composites with higher fraction of PVA were found to have lower gel fraction. At constant 10% MA, PVA/NCC and PVA/Chitin-30/NCC consisted of chemical gel content (in 80°C hot water) amounting to 59.87 ± 1.73% and 79.27 ± 2.06%, respectively. With higher PVA content, the amount of hydrophilic -OH groups of the MA-treated PVA/Chitin/NCC composite is more abundant. The increase in the hydrophilic groups results in the increase of polar nature of the composite. Hence, the solubility of the composite with higher PVA content in water is increased and therefore the gel content is lowered (Gohil et al., 2006).

As shown in Figure 4.22, the presence of 1 wt.% NCC in the PVA-based composites helped in slightly improving stability of the composites in distilled water. At constant 10% MA, chemical gel content (80°C) recorded for PVA/Chitin-10 and PVA/Chitin-10/NCC were 63.23 ± 1.01% and 65.52 ± 1.36%, respectively. With the addition of 1% NCC, the chemical gel content increased by 3.62%. This is attributed to the loading of cellulose in the form of nanocrystals are insoluble in nature which results in lower affinity and reactivity to water. Indeed, physical bonding initiated from hydrogen bonding and presence of crystallites would contribute to some structural stability. However, it is insufficient to maintain its structural integrity (Gohil et al., 2006; Peresin et al., 2014). This is due to the fact that PVA/Chitin/NCC composites comprised of large number of hydroxyl groups which result in extensive solvation. Water diffuses through the physically bonded PVA/Chitin/NCC composites and subsequently, hydrolytic cleavage of hydrogen bonds in polymer chains occurs (Kenawy et al., 2014). Hence, a chemical cross-linker such as MA has to be included into the PVA/Chitin/NCC composites for improved structural integrity.

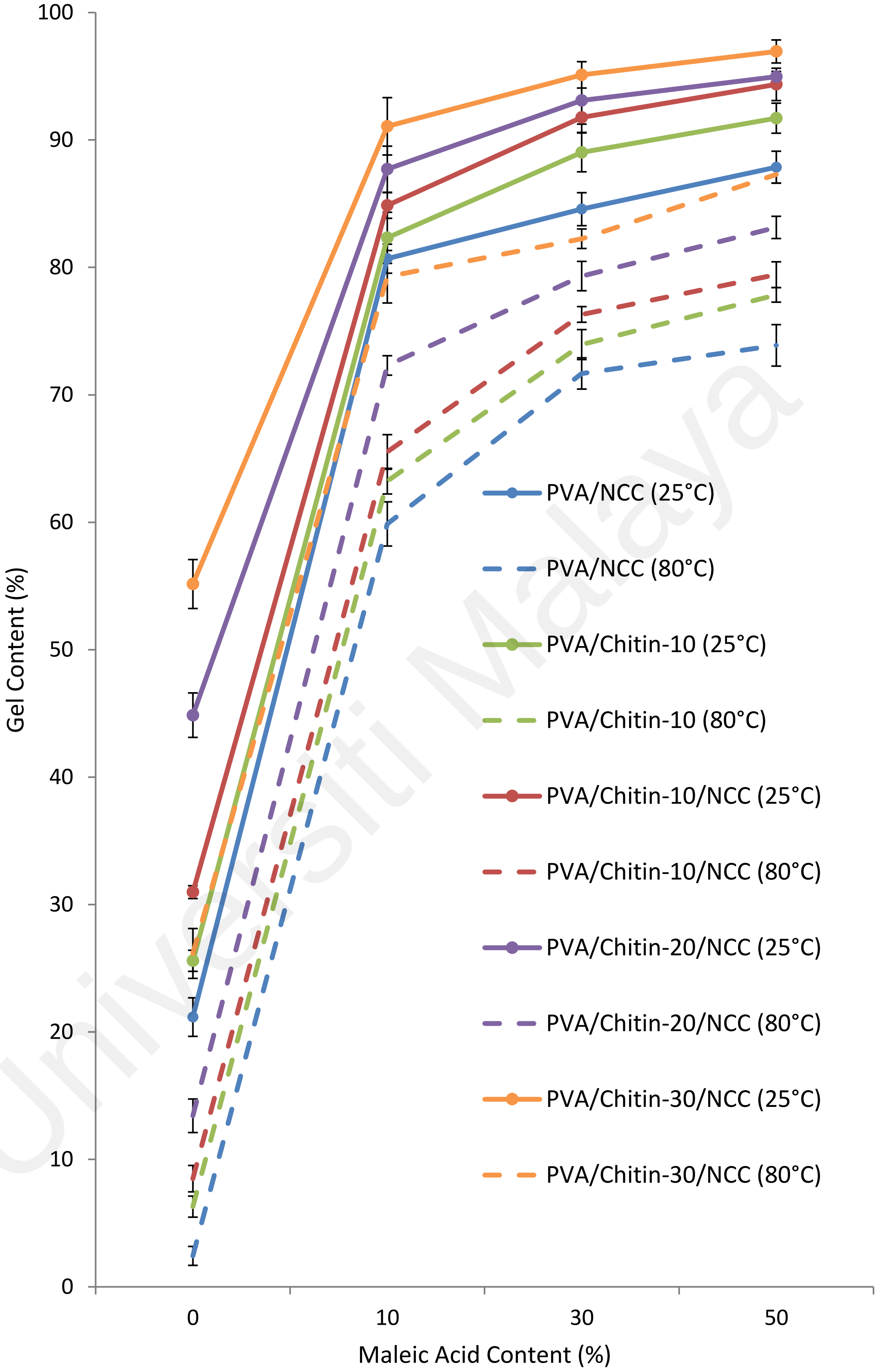

Figure 4.22: Gel content of composite samples determined through immersion in cold water (25°C) and hot water (80°C) for 24 h.

In the presence of MA, gel content of the PVA/Chitin/NCC composites were remarkably improved which also implied the enhanced water durability of the composites. Gel content determined through cold water immersion consisted of both physical gel and chemical gel. Hence, gel contents determined through hot water immersion were relatively lower as the physical gels disintegrated at higher temperature. As reported by Peresin et al. (2014), permanent stability is observed only in the case where the composite is chemically cross-linked. Figure 4.22 shows that PVA/Chitin/NCC composites with MA introduced contained high gel content even when immersed in hot water. This implies successful cross-linking of polymeric chains with MA through esterification (Gohil et al., 2006; K. Qiu & Netravali, 2013). The esterification process in this present study can be regarded as irreversible due to the prompt removal of water produced during curing process, in contrast to the reversible esterification reaction which occurs at aqueous state (Meng et al., 2000). Furthermore, there is an increment of chemical gel content (in hot water) corresponding to increased content of MA from 0% to 50%. PVA/Chitin-10/NCC with 0% MA with 8.49 ± 1.04% gel content, improved by 8.35 times to consisted of 79.43 ± 1.01% chemical gel when 50% MA was utilized. This is due to the higher amount of MA which provides higher level of -COOH functional groups for a denser cross-linking (Birck et al., 2014; Gohil et al., 2006).

4.2.9 Contact Angle Measurement

The water contact angle formed by the intersection of the liquid-solid interface and the liquid-vapor interface could be envisaged to indicate surface hydrophilicity of the composite film. Surface hydrophilicity is desired as it contributes to greater tendency in attachment of hydrophilic groups onto the PVA-based composites. In other words, higher surface hydrophilicity indicates greater wettability of material to water. It is envisaged that the surface hydrophilicity of PVA-based composites would contribute to the efficacy of the composite for dye adsorption application.

4.2.9.1 PVA/Chitin/NCC Composites

Figure 4.23 summarizes the static water contact angle for the varied PVA/Chitin composites, with or without 1 wt.% NCC incorporated. Neat PVA portrayed a water contact angle of 69.57 ± 0.92°, which gave evidence that the PVA utilized was a hydrophilic material. PVA is inherently a hydrophilic polymer which is attributed to the hydrogen bonding that occurs on the surface between free OH groups and the water molecules. When considering NCC as an independent factor, it was observed that the water contact angle increased by 23.80% with the decrease content of PVA, changing from 69.57 ± 0.92° to 86.13 ± 0.35° when the chitin content was varied from 0 wt.% to 30 wt.%. This behavior corresponded to the more hydrophobic characteristics of the chitin when compared with the PVA which substantially reduced the proportion of hydrogen bonding of surface functional groups of polymers with water molecules. Chitin is more hydrophobic in nature since chitin consists of both -OH and more hydrophobic (-NHC=OCH$_3$) acetyl amine groups (Bahrami et al., 2003; Gohil et al., 2006; R. A. Lusiana et al., 2013).

For the PVA/Chitin/NCC composites with chitin varying from 0 wt.% to 30 wt.%, the water contact angle of the PVA/Chitin/NCC composites further increased in the presence of 1 wt.% NCC. By comparing PVA/Chitin-10 and PVA/Chitin-10/NCC, it was evident that incorporation of 1 wt.% NCC led to increased hydrophobicity of the material, which was from 76.73 ± 0.90° to 79.63 ± 0.81°. A plausible explanation for this result is that improved intermolecular interactions between polymer matrix and NCC resulted to the disfavor of the hydrogen bonding sites for water molecules (Kord et al., 2016). Similarly, Kord et al. (2016) reported the increase in contact angle of

PVA/nanofibrillated cellulose composite, which was from 73° to 85°, when the NCC content was increased from 0 wt.% to 5 wt.%. In addition, increased hydrophobicity of PVA-based composite with the introduction of NCC had been reported in the work of Noshirvani et al. (2017).

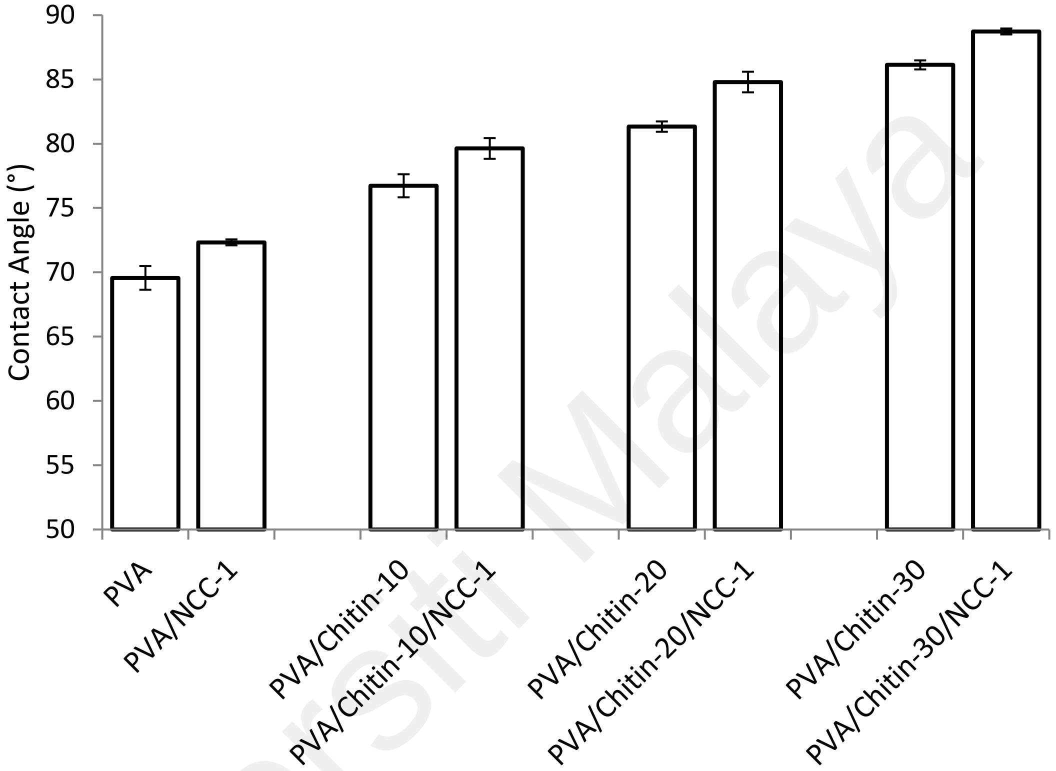

Figure 4.23: Static water contact angle static for PVA and the varied PVA/Chitin composites, with or without 1 wt.% NCC incorporated.

4.2.9.2 MA Cross-linked PVA/Chitin/NCC Composites

The results of the investigation are tabulated in Figure 4.24. PVA/NCC with 0% MA showed the highest hydrophilic value among all the samples, with a contact angle of 71.50 ± 1.21°. Furthermore, it was shown that PVA/Chitin-30/NCC with 0% MA exhibited contact angle of 89.10 ± 0.14°, an increment of 24.62% over the PVA/NCC with 0% MA sample. It is known that PVA is a highly hydrophilic material due to its abundance of free hydroxyl (-OH) groups. On the other hand, chitin consists of both -OH and more hydrophobic (-NHC=OCH$_3$) acetyl amine groups (Bahrami et al., 2003;

Gohil et al., 2006; R. A. Lusiana et al., 2013). Hence, contact angle of PVA/Chitin/NCC composites with higher PVA content is smaller, signifies greater wettability when MA is an independent factor.

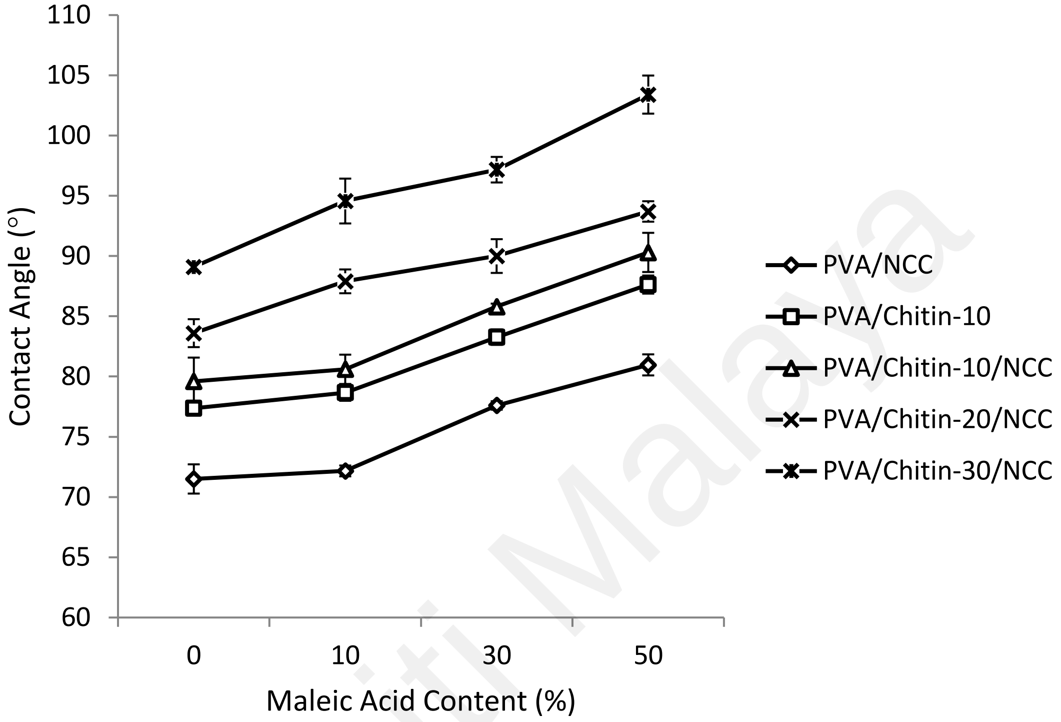

Figure 4.24: Static water contact angle of MA-treated sample composites.

By comparing the contact angles determined for PVA/Chitin-10 and PVA/Chitin-10/NCC as a function of MA, it was derived that the inclusion of 1 wt.% NCC in the PVA/Chitin/NCC composite also slightly increased the contact angle of the composite (Figure 4.24). For example, it was determined that the water contact angle of PVA/Chitin-10/NCC was 80.60 ± 1.24° which increased by 2.45% over the PVA/Chitin-10 with reported value of 78.67 ± 0.68° when MA content for both are constant at 10%. This indication of reduced wettability is associated to the reduced number of free hydroxyl groups in the composite to be bonded with water molecules. This is due to the involvement of the hydroxyl groups in intermolecular interactions of PVA-based matrix with NCC (Popescu, 2017).

With the introduction of MA, the contact angle increased which corresponding to increased surface hydrophobicity. It was determined that the contact angle of PVA/Chitin-10/NCC increased from 79.60 ± 1.97° to 90.30 ± 1.63° when the MA content varied from 0% to 50% while the chitin content was fixed at 10 wt.%. The increment difference was amounted to 13.44%. It was suggested that the MA incorporated led to the consumption of the hydrophilic -OH groups in composites for ester linkage formation during cross-linking reaction (Bolto et al., 2009; Z. Xie et al., 2011). With the reduction of -OH groups, their mobility from the bulk towards surface of films decreased accordingly (Bahrami et al., 2003). Therefore, the surface hydrophilicity of composite was reduced which in turn reduced its swelling and solubility (Bolto et al., 2009). Hence, the hydrophilicity of PVA/Chitin/NCC composites could be regulated by varying the PVA/Chitin ratio and the amount of MA.

4.3 Adsorption Studies

MA cross-linked PVA/Chitin/NCC composites were investigated for the roles as dye adsorbents through adsorption studies of MB dyes onto the composites. The FTIR spectra of the selected MA cross-linked PVA/Chitin/NCC adsorbent, before and after MB adsorption were compared to determine the chemical alteration on the adsorbent. Points of zero charge (pH_{pzc}) of the adsorbents were investigated through pH drift method to provide an insight on the acidic or basic nature of the surface active sites for dye adsorption. Adsorption studies were carried out to delineate the effect of composite composition, solution pH, adsorbent dosage and initial dye concentration on the equilibrium adsorption capacity of composites studied. From the batch adsorption studies, experimental results for the adsorption isotherms, kinetics and the thermodynamics of adsorption process onto the selected composites were determined. Reusability studies of the selected composites were included to determine the potential application of the composites to be reuse as effective adsorbents for five times. The last section provided the comparison of adsorption capacity between the best MA cross-linked PVA/Chitin/NCC composite and other reported polymeric adsorbents.

4.3.1 FTIR Spectroscopic Analysis of MA Cross-linked PVA/Chitin/NCC Adsorbent, Before and After MB Adsorption

MA cross-linked PVA/Chitin/NCC composites were investigated for the roles as the adsorbents. The FTIR spectra of a selected MA cross-linked PVA/Chitin/NCC adsorbent, before and after MB adsorption are compared to identify the chemical alteration on the adsorbent, as shown in Figure 4.25. C-H stretching bands which centered around 2920 cm^{-1} had become more intense upon MB adsorption. The intensification of the peaks after MB adsorption indicated that more C-H bonds had been incorporated and bonded to the PVA-based adsorbent (Agarwal et al., 2016). In addition, the presence of intense peak at 1599 cm^{-1} was assigned to heterocyclic C=N and C=C vibrations, characteristics to MB (Agarwal et al., 2016; Ovchinnikov et al., 2016). Furthermore, the strong absorption band observed at 1331 cm^{-1} after MB adsorption was attributed to the C-N vibrations for N-CH_3 groups of MB which further proved that MB was presence on the adsorbent (Ovchinnikov et al., 2016).

The interactions between the functional groups of MA cross-linked PVA/Chitin/NCC and MB led to the displacement of absorption bands to higher wavenumber and change in intensity of absorption bands. Similar spectral changes were reported in literature (Baheri et al., 2016; Zayed et al., 2016). One of the indications of interactions of MB and MA cross-linked PVA/Chitin/NCC through hydrogen bonding were the shifting of both asymmetric and symmetric C-O stretching vibration bands of PVA. Shifting of asymmetric C-O stretching of PVA was observed from 1074 cm^{-1} to 1084 cm^{-1} and for symmetric C-O stretching of PVA, it was from 1026 cm^{-1} to 1039 cm^{-1}. The shifting of the two peaks was indicated by arrows in the illustration shown in Figure 4.25.

Moreover, the intensification of hydrogen bonded O-H stretching band at the 3500 cm-1-3000 cm-1 region upon MB adsorption further justified that the adsorption of MB onto the adsorbent studied involved hydrogen bonding. On the other hand, the significant reduction in intensities of both C=O band (1711cm-1) and C=C band (1660 cm-1) upon adsorption of MB clarified the involvement of conjugated ester group in bonding MB onto the MA cross-linked PVA/Chitin/NCC adsorbent. All these observations indicated the involvement of other interactions between MB and adsorbent which may include electrostatic interaction, surface complexing and Van der Waals interactions. Moreover, Figure 4.26 illustrates the digital images of the selected PVA/Chitin-10/NCC/MA-30 adsorbent sample, before and after MB adsorption which also shows the attachment of MB on the adsorbent's surface.

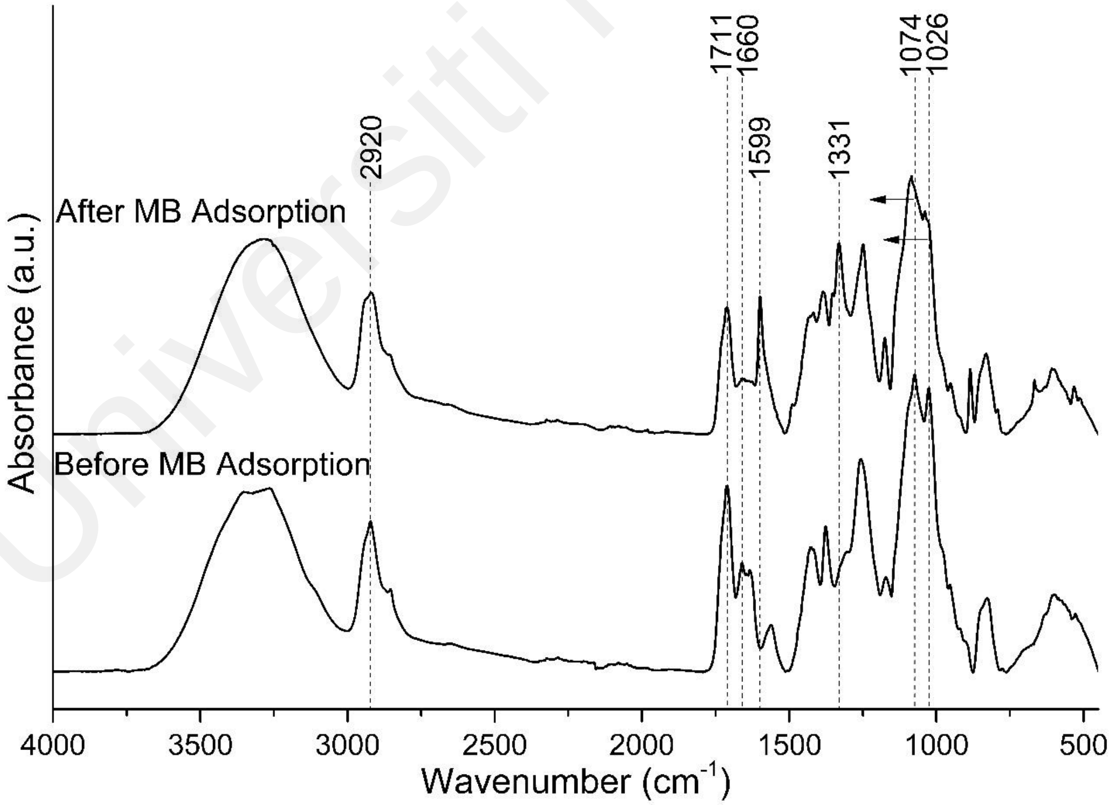

Figure 4.25: FTIR spectra of the selected PVA/Chitin-10/NCC/MA-30 adsorbent sample, before and after MB adsorption.

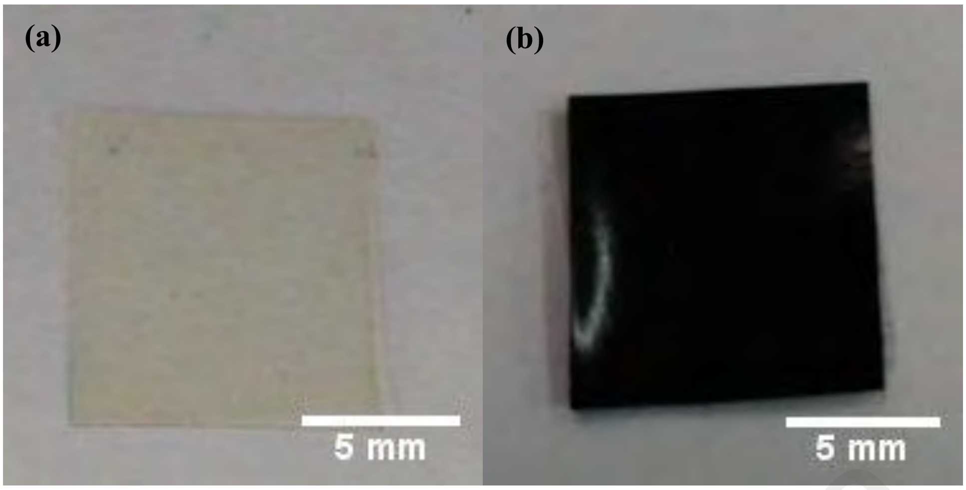

Figure 4.26: Digital images of the selected PVA/Chitin-10/NCC/MA-30 adsorbent sample, (a) before and (b) after MB adsorption.

4.3.2 Point of Zero Charge (pH_{pzc}) by pH Drift Method

Studies on the point of zero charge (pH_{pzc}) of adsorbents serve to give an insight on the types of surface active site and the adsorption ability of the adsorbents' surface. pH drift method was utilized in determining the point of zero charge for the selected sample adsorbents. Through this method, the basic or acidic nature of the composite adsorbents could be identified (Hussin et al., 2015).

4.3.2.1 MA Cross-linked PVA/Chitin/NCC Composite Adsorbents

The graph of pH_{final} against $pH_{initial}$ was plotted, as shown in Figure 4.27. The intersections of the curves with the straight diagonal line are regarded as the end points of the pH_{pzc} (Pirbazari et al., 2015). The pH_{pzc} indicates the condition whereby the surface charge density on a material is zero. pH_{pzc} determined for the respective composites were tabulated in Table 4.3.

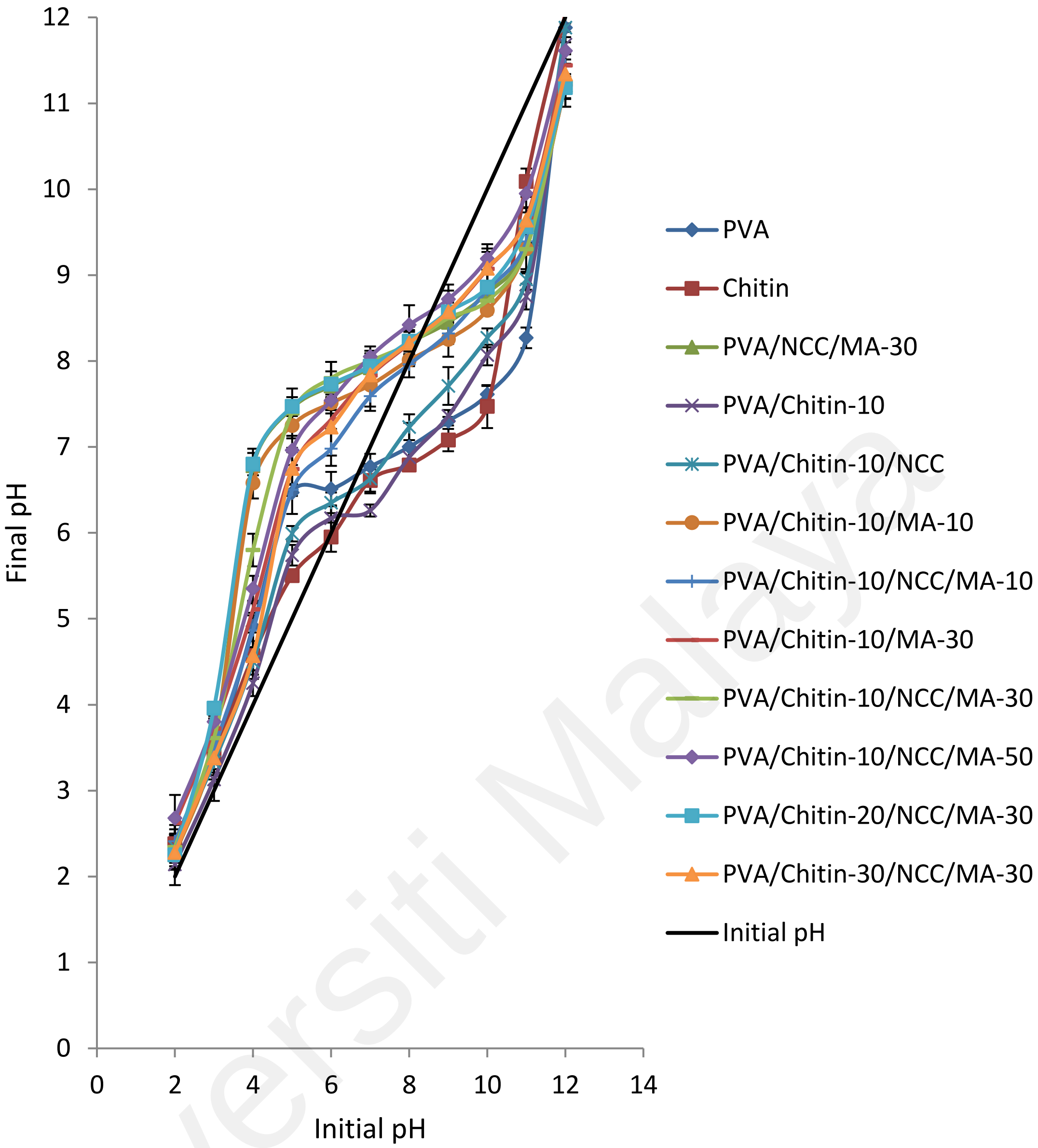

Figure 4.27: Determination of point of zero charge (pH_{pzc}) for the selected composite samples.

As summarized in Table 4.3, the pH_{pzc} of neat PVA was recorded to be 6.80, which was equivalent to the pH of distilled water used. This implies that PVA used is neutral since PVA is a non-ionic polymer which has abundance of hydroxyl groups that renders it soluble in water (El Feky et al., 2010). However, chitin was slightly acidic in nature, with pH_{pzc} determined as 6.00. This finding is in agreement with the studies found in literature. From literature, it is determined that free amino group of chitin tend to be deprotonated as it has low acid dissociation constant (pKa) value of 5.5-6.3 (Casey & Wilson, 2015; Zargar et al., 2015).

Table 4.3: Point of zero charge (pH_{pzc}) for the selected composite samples.

Sample	pH_{pzc}
PVA	6.80
Chitin	6.00
PVA/NCC/MA-30	8.40
PVA/Chitin-10	6.20
PVA/Chitin-10/NCC	6.25
PVA/Chitin-10/MA-10	8.00
PVA/Chitin-10/NCC/MA-10	8.05
PVA/Chitin-10/MA-30	8.30
PVA/Chitin-10/NCC/MA-30	8.35
PVA/Chitin-10/NCC/MA-50	8.55
PVA/Chitin-20/NCC/MA-30	8.30
PVA/Chitin-30/NCC/MA-30	8.20

Moreover, PVA/Chitin/NCC composites exhibited reduction in pH_{pzc} upon the incorporation of chitin. By comparing the results of PVA and PVA/Chitin-10/NCC, it was determined that pH_{pzc} was reduced by pH 0.55 when chitin varied from 0% to 10%, which was from pH 6.80 to pH 6.25. This is because chitin with free amino groups (pH_{pzc} = 6.0) which tended to be protonated at low pH was introduced into the neutral PVA-based matrix which reduced the overall surface charge of the composites.

On the other hand, the incorporation of NCC contributed to slight increase on the adsorbents' surface charge. For example, the increase of pH_{pzc} was amounted to pH 0.05 when comparison was made between PVA/Chitin-10 and PVA/Chitin-10/NCC. The insignificant contribution of NCC towards pH_{pzc} was related to the very small decrease amount of ionizable amino functional groups in chitin when NCC was incorporated (Wiśniewska et al., 2015).

When the MA content was varied from 0% to 50% and the chitin content was fixed at 10 wt.%, it was interesting to note that the pH_{pzc} of PVA/Chitin-10/NCC/MA-50 which was 8.55 increased by 36.8% over the PVA/Chitin-10/NCC that showed pH_{pzc} at 6.25. Introduction of MA results to the formation of unsaturated diesters which is susceptible to be attacked by a base to give yield to carbanion, as illustrated in Figure 4.28. Therefore, the pH_{pzc} of the PVA/Chitin-10/NCC/MA-50 composite increased significantly due to the increase in the amount of the surface unsaturated diesters groups which were responsible to the formation of carbanions of the composite.

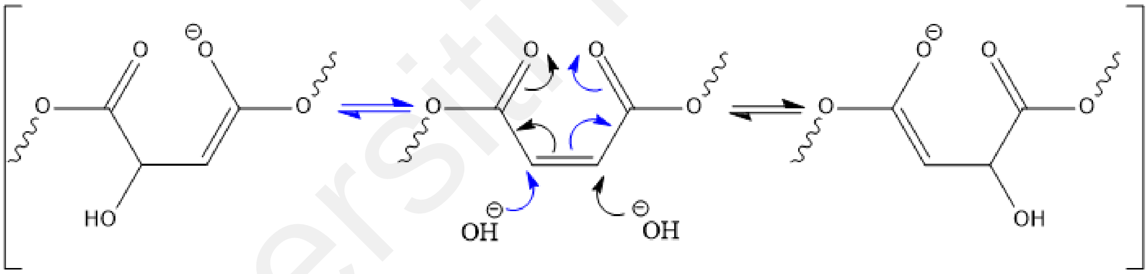

Figure 4.28: Formation of carboanion when the unsaturated diesters are attacked by a base.

As verified by the pH drift method, MA cross-linked PVA/Chitin/NCC composites investigated showed reported pH_{pzc} in the range of 8.05-8.55. Generally, cationic dye as adsorbate is favored at $pH > pH_{pzc}$, due to presence of negatively-charged functional groups on the adsorbent's surface. Contrarily, the surface becomes positively charged when solution $pH < pH_{pzc}$, favoring adsorption of anionic adsorbate (Kushwaha et al., 2014; Pirbazari et al., 2015). Hence, adsorption of MB which is cationic is considered as more effective at $pH > 8.55$ in this study. Therefore, solution of pH 9 was chosen for batch adsorption studies.

4.3.3 Effect of Composite Composition on MB Adsorption

Figure 4.29 shows the effect of various PVA/Chitin/NCC compositions on the adsorption of MB dyes when dependent factors of adsorption such as initial dyes concentration, adsorbent dosage, dye solution's pH, contact time and temperature were constant. The mean values of triplicate studies obtained were shown in Table 4.4.

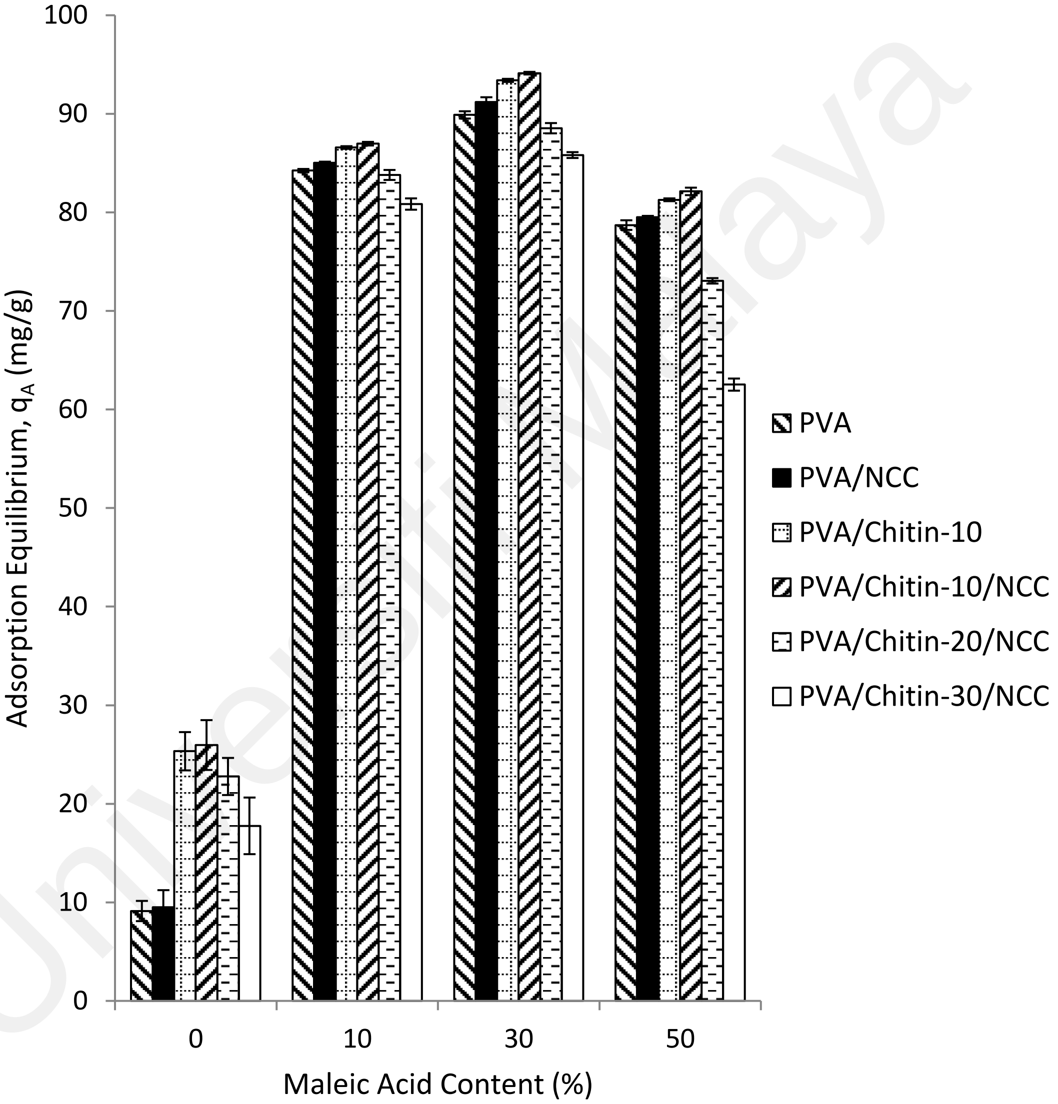

Figure 4.29: Effect of various PVA/Chitin/NCC compositions on adsorption of MB dyes (Initial MB concentration = 50 mg/L, pH = 9, adsorbent dosage = 0.5 g/L and contact time = 30 h at 25°C).

Table 4.4: Adsorption equilibrium and removal percentage summaries of various PVA/Chitin/NCC composites on adsorption of MB dyes.

Sample	Adsorption Equilibrium, $q_{A\ (exp.)}$ (mg/g)	Removal Percentage (%)
PVA	9.12 ± 1.03	9.68 ± 1.39
PVA/NCC	9.52 ± 1.72	10.10 ± 1.86
PVA/Chitin-10	25.33 ± 1.94	26.83 ± 2.21
PVA/Chitin-10/NCC	25.96 ± 2.53	27.56 ± 2.81
PVA/Chitin-20/NCC	22.77 ± 1.88	24.18 ± 2.02
PVA/Chitin-30/NCC	17.76 ± 2.87	18.85 ± 3.13
PVA/MA-10	84.24 ± 0.17	86.65 ± 0.40
PVA/NCC/MA-10	85.02 ± 0.12	87.20 ± 0.25
PVA/Chitin-10/MA-10	86.58 ± 0.14	88.20 ± 0.31
PVA/Chitin-10/NCC/MA-10	86.97 ± 0.18	88.11 ± 0.44
PVA/Chitin-20/NCC/MA-10	83.80 ± 0.50	85.06 ± 0.80
PVA/Chitin-30/NCC/MA-10	80.85 ± 0.58	83.04 ± 0.56
PVA/MA-30	89.89 ± 0.37	93.05 ± 0.42
PVA/NCC/MA-30	91.21 ± 0.47	93.92 ± 0.52
PVA/Chitin-10/MA-30	93.39 ± 0.16	94.71 ± 0.23
PVA/Chitin-10/NCC/MA-30	94.13 ± 0.13	96.12 ± 0.19
PVA/Chitin-20/NCC/MA-30	88.54 ± 0.52	90.28 ± 0.83
PVA/Chitin-30/NCC/MA-30	85.82 ± 0.30	87.84 ± 0.69
PVA/MA-50	78.71 ± 0.49	80.96 ± 0.54
PVA/NCC/MA-50	79.52 ± 0.13	81.44 ± 0.20
PVA/Chitin-10/MA-50	81.28 ± 0.14	82.25 ± 0.21
PVA/Chitin-10/NCC/MA-50	82.13 ± 0.38	83.81 ± 0.48
PVA/Chitin-20/NCC/MA-50	73.05 ± 0.28	73.99 ± 0.33
PVA/Chitin-30/NCC/MA-50	62.53 ± 0.62	63.95 ± 0.65

In the absence of MA, the composites portrayed low resistance in aqueous medium which implied that the composites were not feasible to act as the adsorbent. Hence, the adsorption results of the composites with 0% MA incorporated were poor, with removal percentage recorded to be below 30%. The adsorption equilibrium of MB was the highest at the PVA/Chitin-10/NCC composition, regardless of MA content incorporated, ranging from 10% to 50% (refer to Figure 4.29 and Table 4.4). This observation was due to the reason that MA cross-linked PVA/Chitin-10/NCC composites exhibited more abundant adsorption sites when compared to PVA/NCC, PVA/Chitin-20/NCC and PVA/Chitin-30/NCC composite, independent of MA. Adsorption equilibrium of PVA/NCC/MA-30 and PVA/Chitin-10/NCC/MA-30 were 91.21 ± 0.47 mg/g and 94.13 ± 0.13 mg/g, respectively. By comparing the two composite adsorbents, it was shown that PVA/Chitin-10/NCC/MA-30 adsorbed an additional of 3.20% MB over the PVA/NCC/MA-30. This was related to the slight reduced point of zero charges (pH_{pzc}) when chitin was incorporated into the PVA-based matrix. In other words, the electrostatic interactions in between PVA/Chitin-10/NCC/MA-30 and MB were stronger at pH 9. As aforementioned, the points of zero charges (pH_{pzc}) of composite adsorbents were verified by the pH drift method (Figure 4.27 and Table 4.3) (Dhananasekaran et al., 2016; Hosny & Khalaf-Alaa, 2013). Moreover, the additional amino groups of chitin that consisted of non-bonding electrons also served as the adsorption sites.

Nonetheless, the PVA/NCC composites exhibited relatively higher adsorption capacities towards MB than PVA/Chitin-20/NCC and PVA/Chitin-30/NCC when MA content was an independent factor. This is due to hydrogen bonding, Van der Waals interactions and diffusion which are also known as detrimental factors for the adsorption process (Dhananasekaran et al., 2016; S. Umoren et al., 2013). PVA and chitin were previously reported as adsorbents for MB (Agarwal et al., 2016; Dhananasekaran et al., 2016; S. Umoren et al., 2013). Despite this, it was determined previously that chitin consisted of less active adsorption sites for MB in comparison to PVA. This was deduced by the fact that increasing chitin content from 10 wt.% to 30 wt.% resulted in less adsorption, when MA concentration was constant. By comparing the adsorption equilibrium of PVA/Chitin-10/NCC/MA-30 and PVA/Chitin-30/NCC/MA-30, it was determined that adsorption capability of PVA/Chitin-30/NCC/MA-30 decreased by 8.82 % when the chitin content was varied from 10 wt.% to 30 wt.% and MA content was remained at 30%.

By comparing the MA cross-linked PVA/Chitin-10 and PVA/Chitin-10/NCC samples, it was determined that the incorporation of NCC resulted to slight improvement to the adsorption capability of the composite (refer to Figure 4.29 and Table 4.4). As determined, PVA/Chitin-10/MA-50 composite recorded adsorption equilibrium of 81.28 ± 0.14 mg/g was lower than PVA/Chitin-10/NCC/MA-50 composite, which has adsorption equilibrium of 82.13 ± 0.38 mg/g. The increment is associated to content of NCC which consists of free polar groups which serve as additional active adsorption sites. The presence of polar groups such as -OH groups enables the adsorption of MB onto composite adsorbents through hydrogen bonding and Van der Waals forces.

On the other hand, it was observed that neat PVA utilized was partially hydrolyzed which portrayed low resistance in water. This was attributed to its abundance of adsorption sites such as hydroxyl groups which reacted with the water due to hydrogen bonding, resulting to its dissolution in water (Hassan et al., 2002; Kenawy et al., 2014). Furthermore, PVA has been reported to be a water-soluble polymer whose water solubility depends on its degree of hydrolysis, molecular weight and the tendency of PVA in forming hydrogen bond in water (Hassan et al., 2002). Therefore, introduction of MA as the cross-linker of the PVA-based composites was imperative to tune the adsorption capabilities and resistance of the composites in the aqueous solution. As shown in Table 4.4 and Figure 4.29 respectively, incorporation of 30% MA to the PVA-based composites was the optimum content to improve the adsorption capabilities of the composites. For example, PVA/MA-10 composite recorded adsorption equilibrium of 84.24 ± 0.17 mg/g was lower than PVA/MA-30 composite, which has adsorption equilibrium of 89.89 ± 0.37 mg/g. However, PVA/MA-30 which showed values at 89.89 ± 0.37 mg/g, which was higher than PVA/MA-50 with adsorption equilibrium of 78.71 ± 0.49 mg/g. At 10% of MA, cross-linking of the PVA-based polymeric networks was less effective in stabilizing the overall integrity of the composite in comparison to the sample with 30% MA. Hence, the composite with 10% MA had dissolved in aqueous solution to a greater extent and resulted to the loss of adsorption sites for binding MB dye. Contrarily, at high content of 50% MA, the decrease in MB adsorption was associated to the decrease amount of free -OH groups which had been used in cross-linking. This limitation for adsorptions of dyes with increased cross-linking had been reported by previous studies (Wan Ngah et al., 2011; Zendehdel et al., 2010). Hence, it was shown that PVA/Chitin-10/NCC/MA-30 would be the best composition for removal of MB. From these results, only eight compositions of varied MA cross-linked PVA/Chitin/NCC adsorbents, with and without NCC included which showed high adsorption equilibriums were selected for further testing to evaluate the effects of other dependent factors on adsorption.

4.3.4 Effect of Solution pH

Figure 4.30 depicts the effect of solution pH on the adsorption of MB by the selected PVA-based composites when other variables are controlled. From the results, it was observed that solution pH showed a significant influence on the adsorption process. As MB is a positively-charged species in aqueous state, the degree of MB adsorption onto the adsorbent's surface is also determined by the surface charge of the adsorbent, which in turn is affected by the solution pH. As determined, adsorption of MB onto the selected adsorbents followed the same trends, with PVA/Chitin-10/NCC/MA-30 showing the highest adsorption capability for the whole pH range studied. It was revealed that the adsorption was the lowest at pH 2. The minimum adsorption equilibriums for the sample composites observed at pH 2 were in the range of 3.17 ± 0.16 mg/g to 17.50 ± 0.79 mg/g. This was attributed to the presence of extremely high H^+ concentration at low solution pH which competed effectively with the positively-charged dyes for the adsorption sites. This observation was also reported by other researchers (Osasona et al., 2013; Pirbazari et al., 2015).

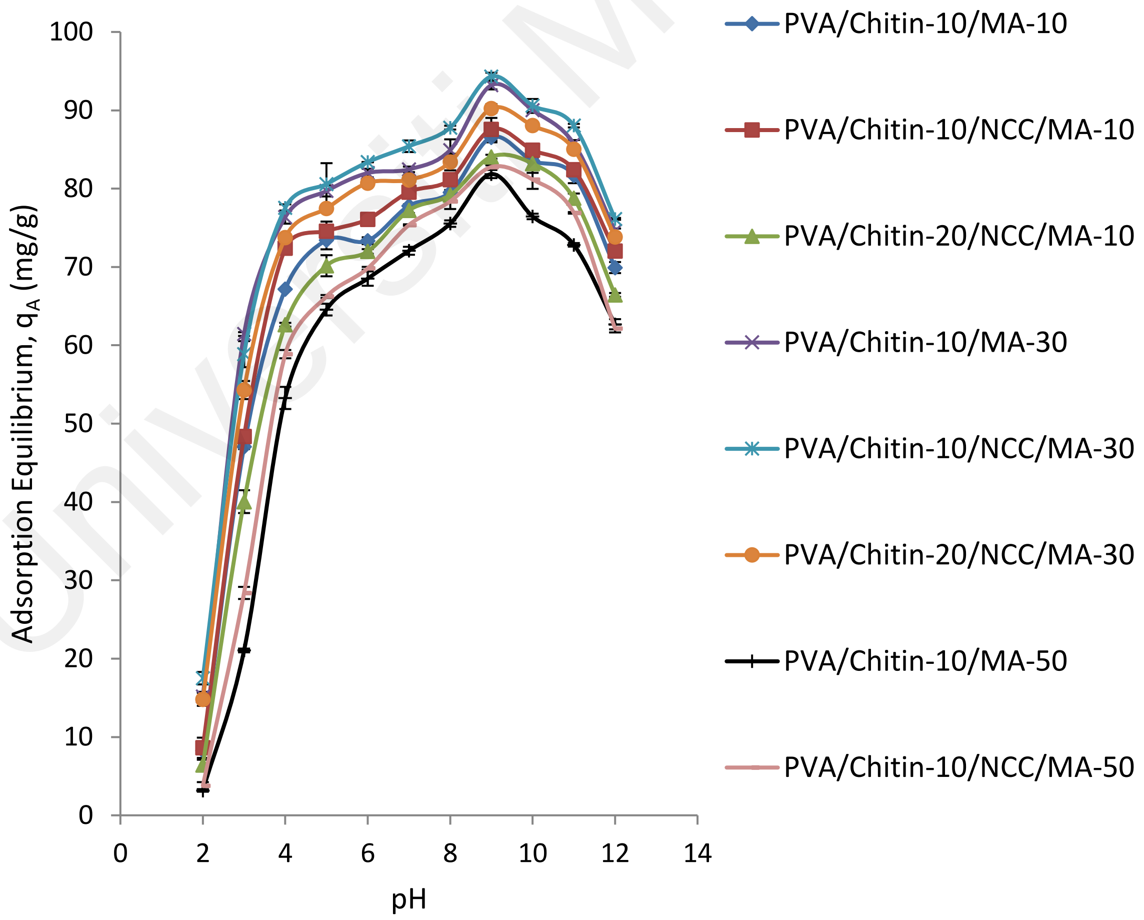

Figure 4.30: Effect of solution pH on MB adsorption of the selected composite samples (Initial MB concentration = 50 mg/L, adsorbent dosage = 0.5 g/L and contact time = 30 h at 25°C).

Using the pH drift method (Gatabi et al., 2016; Y. Yang et al., 2004), the pH_{pzc} of the adsorbents were determined to be in the range of 8.05-8.55 (Figure 4.27). At the solution pH range of 3 to 8, the adsorption capabilities of the composites were increasing despite of the solutions pH were below the pH_{pzc} of the composite adsorbents tested. This is because the adsorption of MB onto the PVA-based composites is not only governed by electrostatic attractions between the cationic dyes and anions formed from of unsaturated maleic diesters but may involve other adsorption mechanisms. The anions are formed when the unsaturated diesters are attacked by a base, as disclosed previously in Figure 4.28. With reference to the FTIR results and considering functional groups available in the composite adsorbents and MB previously, other possible adsorption mechanisms are involved. These include hydrogen bonding, electrostatic interaction, polar-π interaction, complexation through dative bonds and Van der Waals interactions, as summarized in Figure 4.31.

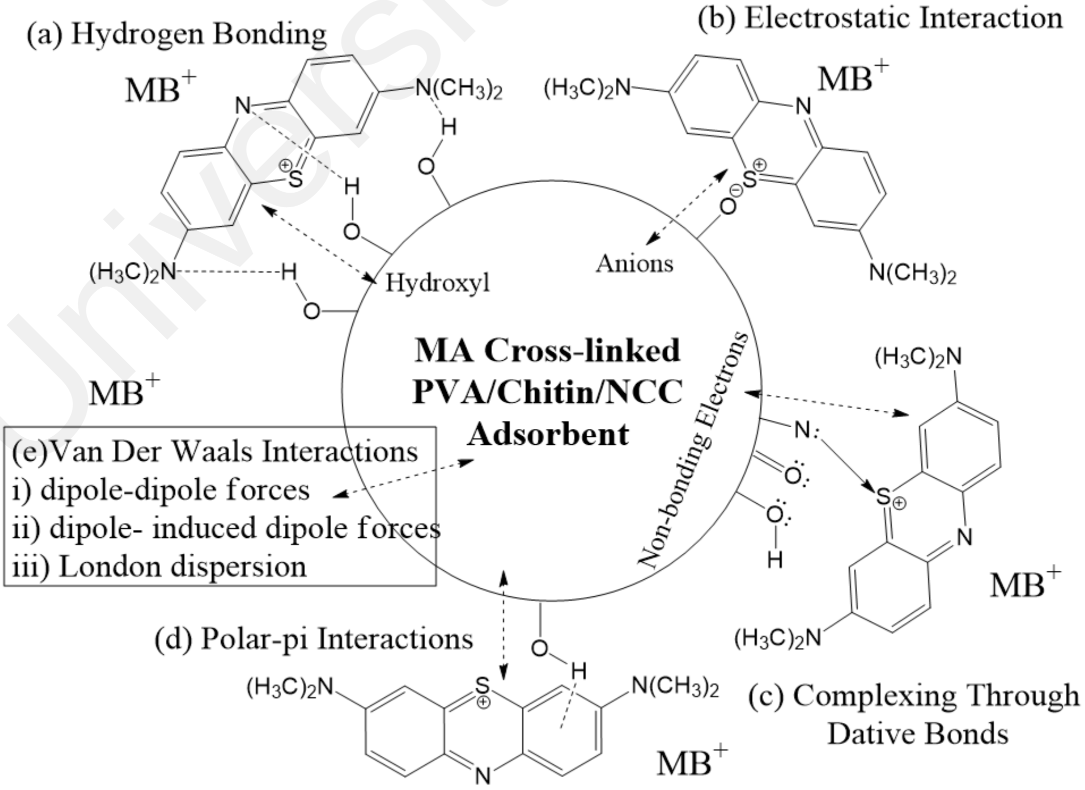

Figure 4.31: Possible adsorption mechanisms for MB adsorption onto the MA cross-linked PVA/chitin/NCC composite adsorbent.

For the selected sample composites studied, maximum adsorptions were all achieved at pH 9. This phenomenon could be explained on the basis of point of zero charge (pH_{pzc}) for the adsorbents. Previous works had proven that generally cationic dye adsorption is preferred when solution $pH > pH_{pzc}$ while anionic dye adsorption is favored at $pH < pH_{pzc}$. This is due to the adsorbent's surface which is negatively-charged only when solution $pH > pH_{pzc}$ (Kushwaha et al., 2014; Pirbazari et al., 2015). Hence, the cationic MB dyes achieved better uptake at pH 9 due to the enhanced electrostatic force of attraction between the oppositely-charged adsorbent's surface and dyes. Moreover, at higher solution pH level of pH 10-12, adsorption equilibriums of adsorbents decreased. This is because higher amount of hydroxyl ions (OH^-) was available at high solution pH, which attracted the adsorbed dye to escape from adsorbents' surface, neutralizing cationic dyes (J. Y. Luo et al., 2015). From this result, it was deduced that pH 9 was indeed suitable as the working pH for MB adsorption and kinetic studies.

4.3.5 Effect of Adsorbent Dosage

For a given initial concentration of dye solution, adsorbent dosage is a pivotal determining factor in the evaluation of adsorption efficiency. Figure 4.32 illustrates the effect of adsorbent dosage on the adsorption equilibrium and removal percentage of MB onto composite adsorbents samples when initial MB dye concentration are fixed at 50 mg/L. For all composite adsorbents samples, it was noted that the adsorbent equilibriums decreased with increasing adsorbent dosage. Such trends were observed due to the reason that there were more adsorption sites remained vacant at higher adsorbent dosage (S. Umoren et al., 2013; X. Yang et al., 2016).

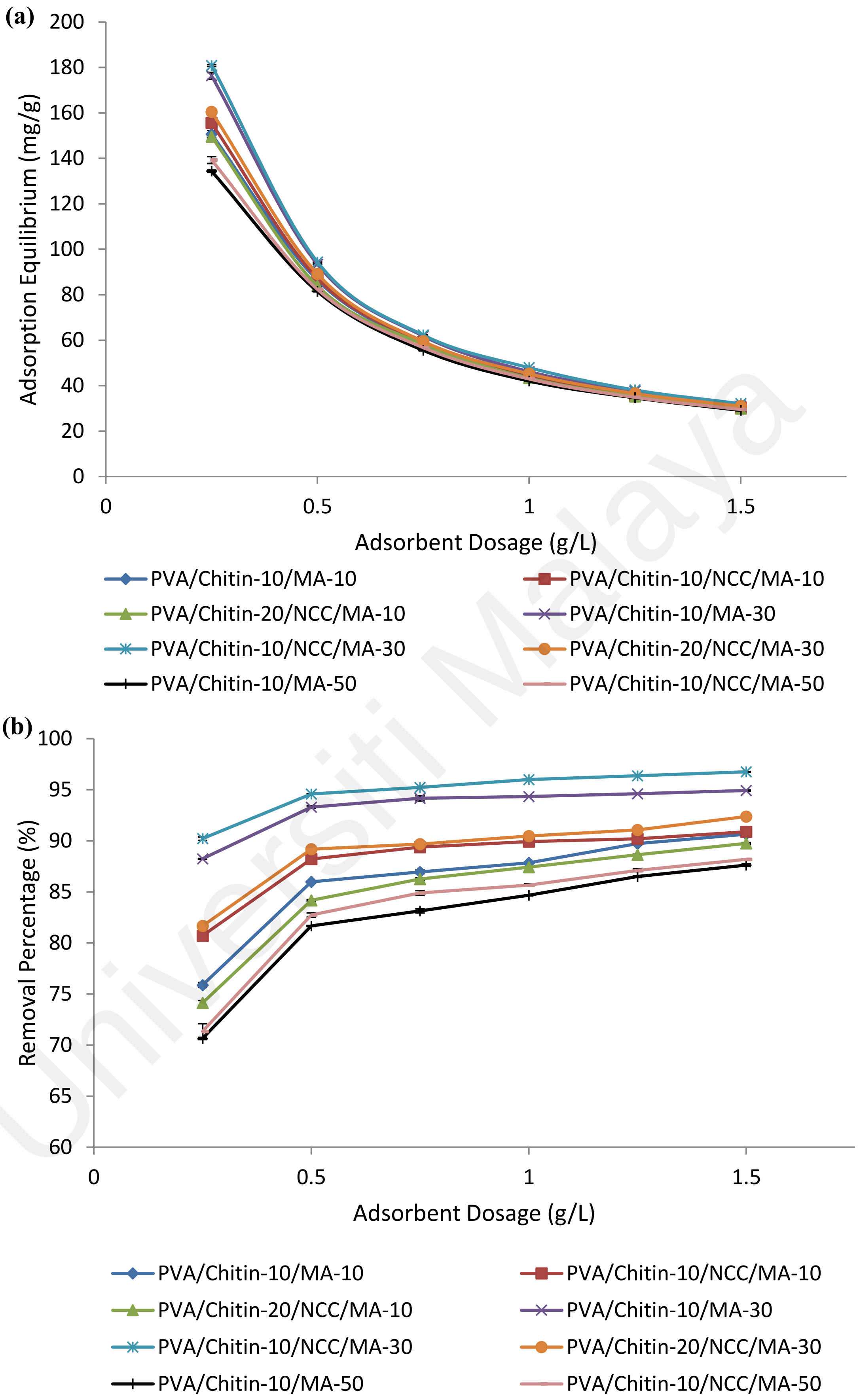

Figure 4.32: Effect of adsorbent dosage on the (a) adsorption equilibrium and (b) removal percentage of MB dyes onto the selected composite adsorbents (Initial MB concentration = 50 mg/L, pH = 9 and contact time = 30 h at 25°C).

On the other hand, removal percentages of MB increased with increasing adsorbent dosage. This phenomenon is attributed to the increased surface area provided by higher adsorbent dosage, which signifies greater amount of active sites available for adsorption (M Abd El-Latif et al., 2010; X. Yang et al., 2016). From the results, adsorbent dosage of 0.5g/L was deduced as the desired dosage in these experimental settings. This is because 0.5 g/L of adsorbent led to comparable removal percentages from those of higher dosage, in the 0.75-1.5 g/L range.

4.3.6 Effect of Initial Dyes Concentration

It was clear to note that the adsorption equilibriums of the selected composite adsorbents were increased in response to increased initial concentration of MB dyes (Figure 4.33). As illustrated, the quantity of MB adsorbed at equilibrium increased from about 70 mg/g to 160 mg/g when initial MB concentration varied from 40 mg/L to 90 mg/L. For instance, PVA/Chitin-10/NCC/MA-30 contributed to the highest adsorption equilibriums, with records of 79.34 ± 0.91 mg/g at 40 mg/L and 163.04 ± 0.25 mg/g at 90 mg/L, respectively. This enhancement of adsorption capacity is due to the higher mass transfer driving force associated to increased initial dyes concentration (Baheri et al., 2016; Rashidzadeh & Olad, 2013).

However, the dyes removal percentage decreased in response to the increase in initial dyes concentration. This is because the adsorption sites of the adsorbent would be excessively saturated when high concentration of MB dyes is used (Baheri et al., 2016; Rashidzadeh & Olad, 2013; S. Umoren et al., 2013). Similarly, PVA/Chitin-10/NCC/MA-30 showed the best removal percentage among samples tested. Even at 90 mg/L MB concentration, PVA/Chitin-10/NCC/MA-30 had the removal percentage at 92.18%.

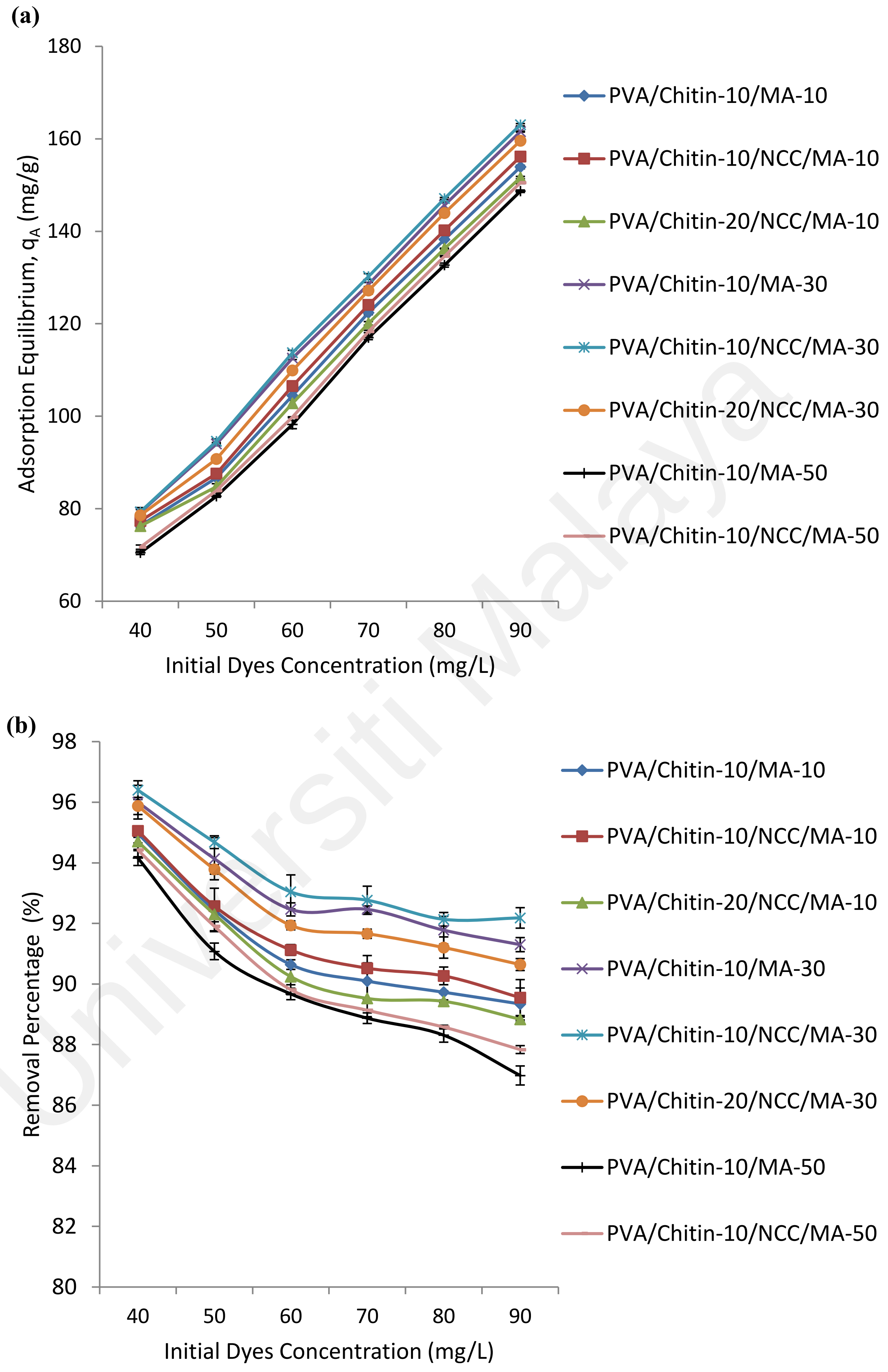

Figure 4.33: Effect of initial dyes concentration on the (a) adsorption equilibrium and (b) removal percentage of MB dyes onto the selected composite adsorbents (Adsorbent dosage = 0.5 g/L, pH = 9 and contact time = 30 h at 25°C).

Moreover, the removal percentage utilizing 50 mg/L of MB was comparable to those of 40 mg/L MB. Besides, the adsorption equilibriums and removal percentages of the respective adsorbents were indistinguishable at 40 mg/L. Therefore, 50 mg/L of initial MB concentration was selected for all adsorption studies since higher adsorption equilibrium was obtained at this concentration.

4.3.7 Adsorption Isotherms

Langmuir isotherm model is the well-known adsorption isotherm model for monolayer adsorption. The model is expressed as Equation 3.9. q_A values of dyes were calculated using Equation 3.8, as described earlier. For the selected composite adsorbents, the experimental data C_A/q_A were plotted against C_A (Figure 4.34 (a)). K_L and q_M were derived from the intercept and slope value of the plot, respectively. Correlation coefficients (R^2) were also investigated.

Further analyses of Langmuir equations were carried out and dimensionless equilibrium parameters (R_L) were determined. R_L were used as indicators of adsorptions' feasibility of the experiments, as expressed in Equation 2.9. The value of R_L indicates the adsorption nature of the dye with the adsorbent. For R_L value which is more than 1, the adsorption process is unfavorable. If R_L value is equal to 1, the adsorption is linear. For the R_L value lies in between 0 and 1, it indicates that the adsorption favorable. R_L equals to 0 indicates irreversible adsorption process (Dhananasekaran et al., 2016; M. Kumar et al., 2009). In brief, the adsorption data which were derived from the Langmuir equation were listed in Table 4.5. R_L values for the adsorption of MB onto all of the composite adsorbents evaluated were within the 0 to 1 range, which indicated that the adsorption processes were favorable. The experimental data were further interpreted using the linearized Freundlich adsorption isotherm.

For heterogeneous adsorbents, it is best modeled to the Freundlich adsorption isotherm equation (Dhananasekaran et al., 2016; Liang et al., 2014). This is because Freundlich isotherm predicts the adsorption of a heterogeneous system whereby it is not of monolayer formation. In linearized form, it is expressed as Equation 3.10.

K_F is the Freundlich isotherm constant related to adsorption capacity $[(mg/g)\cdot(L/mg)^{1/n}]$ and 1/n is the unit less Freundlich adsorption intensity parameter. The adsorption process is most favorable when $0.1 < 1/n \leq 0.5$. For $0.5 < 1/n \leq 1$, the process is easy to adsorb and if $1/n > 1$, it is highly unfavorable and difficult (Dhananasekaran et al., 2016). Moreover, the value of 1/n gives indication on adsorbent's surface heterogeneity whereby value closer to zero signifies greater heterogeneity (Nassar et al., 2017).

In the present investigation, K_F and n were derived from the intercept and the slope value of the plots as shown in Figure 4.34 (b), respectively. Correlation coefficient (R^2) and the Freundlich parameters were tabulated (Table 4.5). 1/n were determined to be in the 0.5496-0.6001 values, which implied the easy uptake of MB dyes on the PVA-based adsorbents which were heterogeneous on surface. K_F values of adsorbent samples were determined to be 34.31-54.46 $(mg/g)\cdot(L/mg)^{1/n}$. The magnitude of K_F values indicated that the adsorbent PVA/Chitin-10/NCC/MA-30 showed the highest adsorption affinity toward MB dyes among the adsorbent samples investigated.

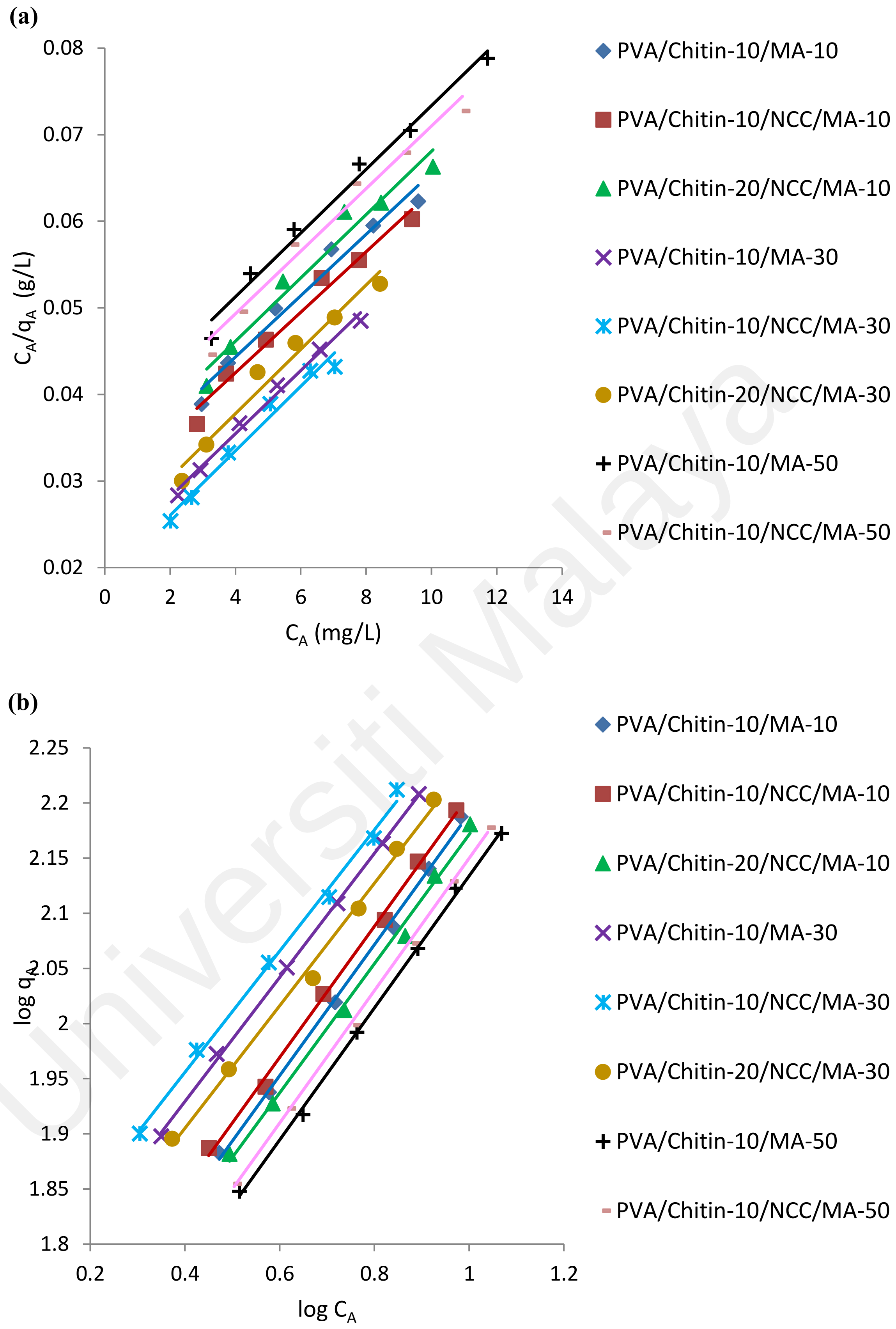

Figure 4.34: (a) Langmuir isotherm; (b) Freundlich isotherm for adsorption of MB onto the selected composite adsorbents.

Table 4.5: Parameters determined for Langmuir isotherm and Freundlich isotherm for MB adsorption onto the selected composite adsorbents.

Sample	Langmuir Isotherm				Freundlich Isotherm			
	K_L (L/mg)	q_M (mg/g)	R^2	R_L	K_F (mg/g)·(L/mg)$^{1/n}$	q_M (mg/g)	1/n	R^2
PVA/Chitin-10/MA-10	0.1174	282.5	0.9712	0.0865 - 0.1755	39.50	403.0	0.5937	0.9973
PVA/Chitin-10/NCC/MA-10	0.1223	286.5	0.9778	0.0833 - 0.1697	41.00	419.2	0.5943	0.9971
PVA/Chitin-20/NCC/MA-10	0.1161	273.2	0.9648	0.0874 - 0.1772	38.54	380.8	0.5856	0.9952
PVA/Chitin-10/MA-30	0.1749	274.0	0.9903	0.0597 - 0.1251	50.60	456.8	0.5625	0.9993
PVA/Chitin-10/NCC/MA-30	0.2009	268.1	0.9782	0.0524 - 0.1107	54.46	467.5	0.5496	0.9959
PVA/Chitin-20/NCC/MA-30	0.1714	259.1	0.9716	0.0609 - 0.1273	48.20	423.1	0.5553	0.9956
PVA/Chitin-10/MA-50	0.1007	271.7	0.9857	0.0994 - 0.1990	34.31	356.6	0.5984	0.9986
PVA/Chitin-10/NCC/MA-50	0.1036	277.0	0.9774	0.0969 - 0.1945	35.46	371.0	0.6001	0.9987

Calculated R^2 values of Freundlich isotherms were all closer to unity, ranging from 0.9952 and 0.9993. By comparing the R^2 of Langmuir isotherms and Freundlich isotherms, it was deduced that the present adsorption processes were best fitted to Freundlich isotherm. Since Langmuir isotherm is associated to monolayer coverage and uniform activity distribution on the adsorbent surface, the less fitting is an expected result. This is because adsorption of MB dye is more vibrant, with tendency of forming multiple layers of adsorption. Moreover, variations of sorption activity are common with surface coverage. Therefore, it can be concluded that the Freundlich isotherm model is suited more to the experimental data than the Langmuir isotherm fitted because of the higher correlation factor.

Hence, the Freundlich maximum adsorption capacities (q_M) were further resolved with constant initial dyes concentration of 50 mg/L. This estimation of maximum adsorption capacity by Freundlich constant had been reported by other researchers (Hamdaoui & Naffrechoux, 2007; Nassar & Abdallah, 2016). The q_M was recorded to be 467.5 mg/g by the PVA/Chitin-10/NCC/MA-30 sample.

4.3.8 Adsorption Kinetics

Adsorption kinetics is important to give information on the efficiency of the adsorption. The pseudo-first order kinetic and the pseudo-second order kinetic were used to study the adsorption kinetics of MB onto the selected sample composites. The linearized pseudo-first order kinetic and linearized pseudo-second order kinetic model equations are represented as Equation 3.11 and Equation 3.12, respectively. Graphs and parameters derived from the kinetic studies for the selected sample composites are separately shown in Figure 4.35 and Table 4.6. k_1 (1/min) and k_2 [g/(mg·min)] are the rate constants of the pseudo-first order kinetic model and pseudo-second order kinetic model, respectively.

Upon correlating the experimental data against both kinetic models, all of the correlation coefficients (R^2) determined from pseudo-second order kinetic model were higher than that of the pseudo-first order kinetic model. It was determined that all the R^2 values obtained from the pseudo-second order model were closer to unity (R^2= 0.9924-0.9987), implying that the adsorption of the composites studied were well fitted to the model. Moreover, the calculated adsorption equilibrium uptake ($q_{A\ (cal.)}$) for the respective samples as deduced from pseudo-second order kinetics were close to the experimental adsorption equilibrium uptake ($q_{A\ (exp.)}$). These results indicated that the adsorptions were of pseudo-second order in nature. Similar kinetics nature were observed in the adsorption of MB onto unmodified PVA (S. Umoren et al., 2013), PVA/poly (acrylic acid)/clay (Kamal, 2014), PVA/graphene oxide (X. Yang et al., 2016). This conformation to pseudo-second order kinetics gave assumption that the adsorption depends on the adsorbate as well as the adsorbent, involving both chemisorption and physisorption processes (Baraka, 2012; Saad et al., 2015).

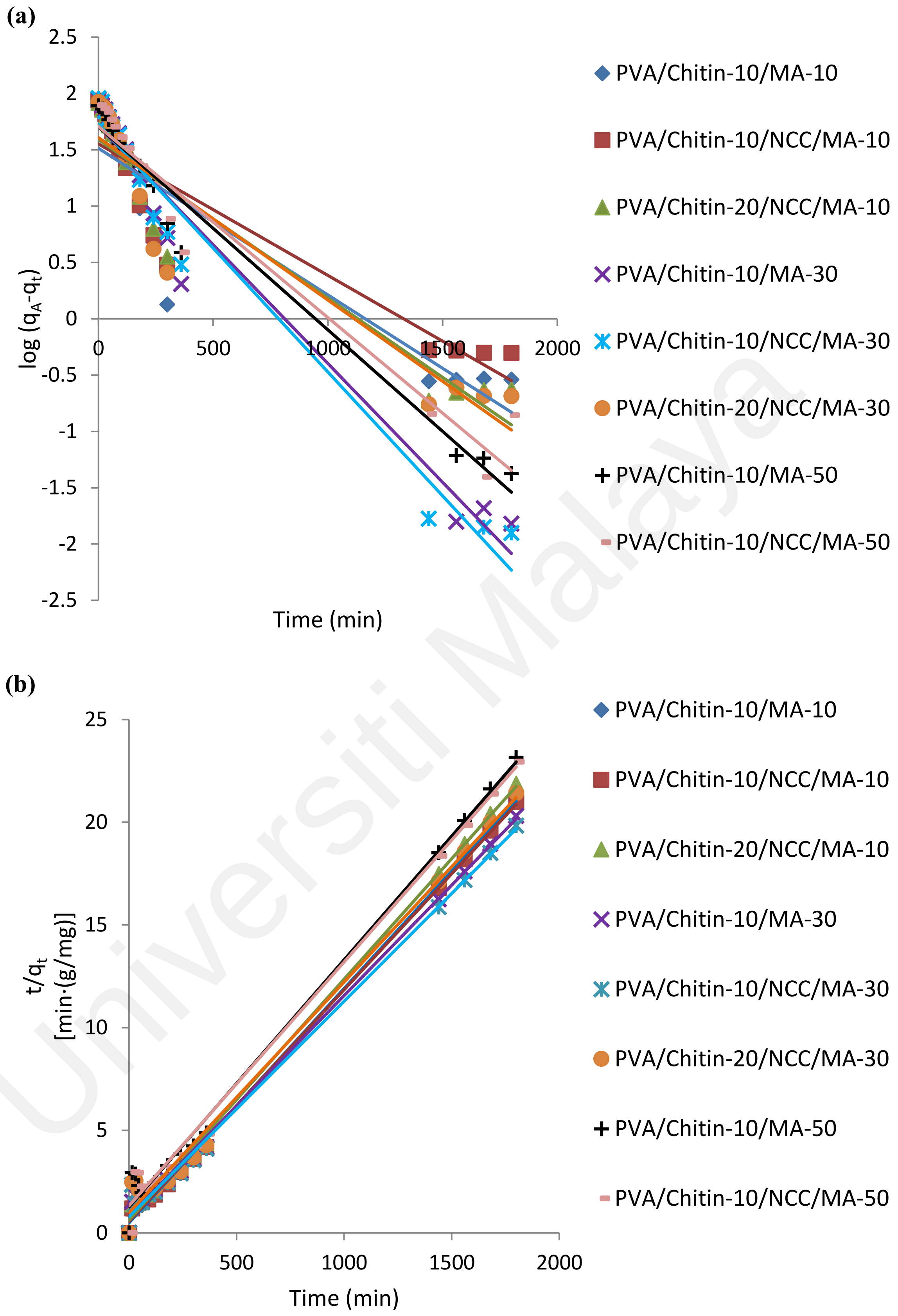

Figure 4.35: Linearized plots of (a) pseudo-first order kinetic and (b) pseudo-second order kinetic for adsorption of MB onto the selected sample composites.

Table 4.6: Parameters determined by linearized plots of pseudo-first order kinetic and pseudo-second order kinetic for MB adsorption onto the selected sample composites.

Sample	**$q_{A\ (exp.)}$ (mg/g)**	**Pseudo-first order**			**Pseudo-second order**		
		k_1 (1/min)	**$q_{A\ (cal.)}$ (mg/g)**	**R^2**	**k_2 [g/(mg·min)]**	**$q_{A\ (cal.)}$ (mg/g)**	**R^2**
PVA/Chitin-10/MA-10	86.58	2.994×10^{-3}	32.58	0.8494	2.641×10^{-4}	87.72	0.9987
PVA/Chitin-10/NCC/MA-10	86.97	2.764×10^{-3}	35.66	0.8623	2.307×10^{-4}	88.50	0.9982
PVA/Chitin-20/NCC/MA-10	83.80	3.224×10^{-3}	38.97	0.9192	2.194×10^{-4}	85.47	0.9983
PVA/Chitin-10/MA-30	93.39	4.836×10^{-3}	51.43	0.9636	1.449×10^{-4}	92.59	0.9970
PVA/Chitin-10/NCC/MA-30	94.13	5.067×10^{-3}	53.30	0.9707	1.400×10^{-4}	95.24	0.9955
PVA/Chitin-20/NCC/MA-30	88.54	3.224×10^{-3}	40.59	0.8933	1.275×10^{-4}	89.29	0.9924
PVA/Chitin-10/MA-50	81.28	4.145×10^{-3}	50.56	0.9741	1.146×10^{-4}	83.33	0.9930
PVA/Chitin-10/NCC/MA-50	82.13	3.915×10^{-3}	50.91	0.9513	1.072×10^{-4}	84.03	0.9927

4.3.9 Adsorption Thermodynamic

In this study, the thermodynamic behaviors for the adsorption of the selected adsorbents were investigated using the thermodynamic equations depicted earlier in Section 3.4.3.7. As for ΔG°, the values were calculated based on Equation 3.14. From Equation 3.16, the values of ΔH° and ΔS° were determined respectively from the slope and intercept of the plot of log K_c versus 1/Temperature. Dimensionless K_c constants were obtained at three different solution temperatures of 25°C, 35°C and 45°C.

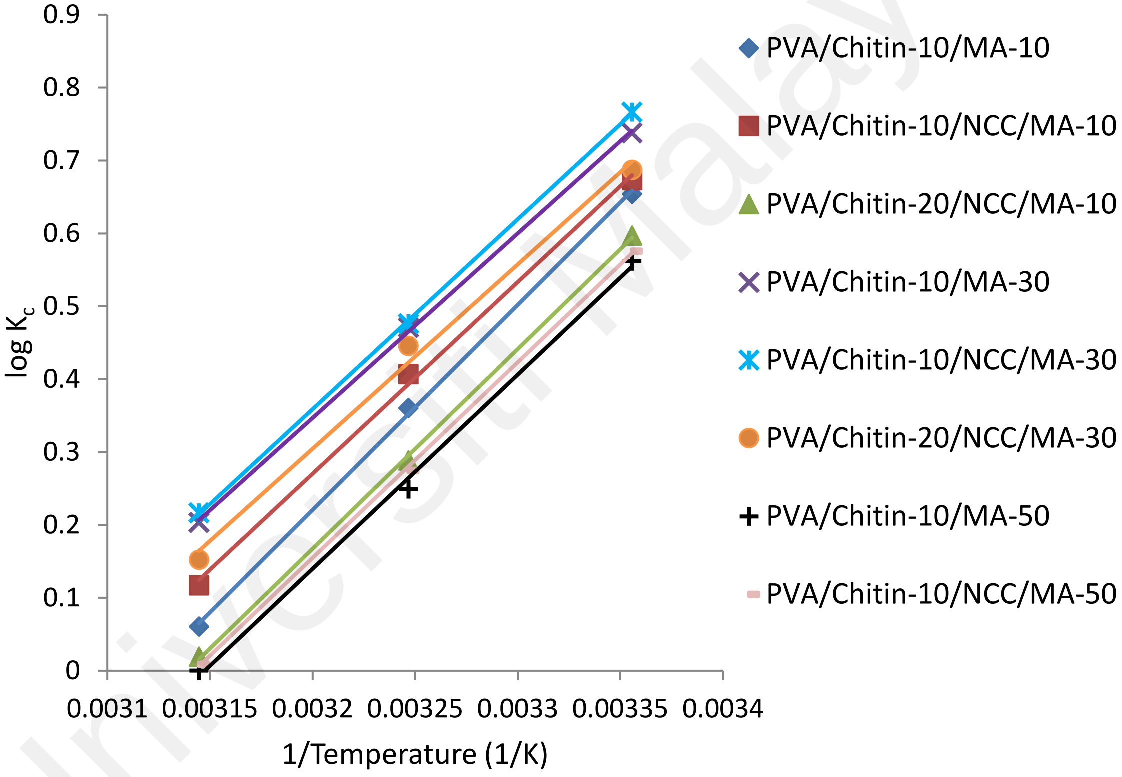

Figure 4.36: Plot of log K_c versus 1/Temperature for MB adsorption onto the selected composite adsorbents.

As observed in Figure 4.36, the slopes of the linear lines were negative with increasing temperature of 298 K to 318 K. This implied that the adsorption processes were exothermic in nature. The calculated values of ΔH°, ΔS° and ΔG° for the adsorption of MB onto the selected PVA-based adsorbents were summarized in Table 4.7.

Table 4.7: Thermodynamic parameters for MB adsorption onto the selected composite adsorbents.

Samples	Enthalpy change of Reaction ΔH° (kJ/mol)	Entropy change of Reaction ΔS° (J/mol·K)	Gibbs Free Energy Change ΔG° (kJ/mol)			Correlation Coefficient R^2
			298 K	308 K	318 K	
PVA/Chitin-10/ MA-10	-53.85	-168.1	-3.734	-2.126	-0.369	0.9994
PVA/Chitin-10/ NCC/MA-10	-50.37	-156.0	-3.841	-2.401	-0.715	0.9981
PVA/Chitin-20/ NCC/MA-10	-52.46	-164.7	-3.408	-1.701	-0.118	0.9996
PVA/Chitin-10/ MA-30	-48.48	-148.5	-4.212	-2.779	-1.239	0.9996
PVA/Chitin-10/ NCC/MA-30	-49.89	-152.8	-4.374	-2.809	-1.320	0.9998
PVA/Chitin-20/ NCC/MA-30	-48.43	-149.1	-3.921	-2.630	-0.929	0.9944
PVA/Chitin-10/ MA-50	-51.00	-160.5	-3.206	-1.469	-0.002	0.9978
PVA/Chitin-10/ NCC/MA-50	-51.39	-161.5	-3.283	-1.620	-0.056	0.9997

As shown in Table 4.7, the negative values of ΔH° determined further confirmed that the adsorption reactions occurred on the adsorbate-adsorbent systems were exothermic in nature. These findings were consistent with the results obtained whereby the adsorption performance decreased with increasing solution temperature. This phenomenon was characteristic of an exothermic reaction. This might be due to the successive desorption of MB adsorbate due to the deterioration of weak Van der Waals forces between the adsorbate and adsorbent. Similar findings on the exothermic nature of MB dyes adsorption onto adsorbents were reported by other researchers (Baheri et al., 2016; Kamal, 2014; Ma et al., 2012; Paşka et al., 2014; S. Umoren et al., 2013). These results are advantageous from the standpoints of economy since MB removal could be feasible at room temperature, without the addition cost of power regeneration as required by endothermic reactions (Paşka et al., 2014).

According to literature, if the ΔH° value of adsorbent is at the 40-400 kJ/mol range, the process is chemisorption which includes strong electrostatic chemical bonding between cationic dyes and adsorbent surface. On the other hand, when the ΔH° value is less than 40 kJ/mol, it reveals that the adsorption is physisorption (Ma et al., 2012; Öztürk & Malkoc, 2014; Raj, 2002; Taleb et al., 2009). In this study, all of the ΔH° values were found to be more than 40 kJ/mol. This suggested the occurrence of chemisorption on the adsorbents studied.

However, the adsorption performance decreased with the rise in temperature in the present study. This reversible adsorption behavior indicated that physisorption was presence. Hence, these results concluded that the adsorption of MB onto the PVA-based adsorbents comprised of both physisorption and chemisorption mechanisms. This revelation was in good agreement with what had been discussed in other research works. From literature, it was reported that both physical and chemical bonding could simultaneously occur on the adsorbent. The nature of adsorption proposed was that multilayers of physically bonded adsorbate being adsorbed on top of an underlying chemisorped adsorbate layer (El-Araby et al., 2017; Hema & Arivoli, 2008; Saad et al., 2015; Taleb et al., 2009).

Adsorption of MB cationic dyes onto the selected MA cross-linked PVA/Chitin/NCC composites displayed negative ΔS° values. This negative entropy change corresponded to decreased degree of freedom of the adsorbed MB species at the solid-solution interface during the adsorption process (Baheri et al., 2016; Baraka, 2012; Taleb et al., 2009; S. Umoren et al., 2013). Moreover, it indicated the ease of reusability of the adsorbent (Baraka, 2012). Negative values of ΔS° values were also determined for the sorption of MB dyes onto PVA (S. Umoren et al., 2013), 4A-zeolite/PVA (Baheri et al., 2016) and SAPO-34-zeolite/PVA (Ghahremani et al., 2015). The negative values of ΔH° and ΔS° obtained suggested that the adsorption of MB onto the MA cross-linked PVA/Chitin/NCC composites studied will be spontaneous even at lower temperatures (El-Araby et al., 2017).

Referring to Table 4.7, it was deduced that the adsorption of MB onto the MA cross-linked PVA/Chitin/NCC composites studied displayed negative values of G°. This data obtained implied that adsorption processes were spontaneous and thermodynamically feasible at the temperature range (298 K-318 K) studied. Such spontaneity of adsorptions of MB were also observed on Sericin/β-cyclodextrin/PVA composite (Zhao et al., 2015) and PVA/Glutaraldehyde/β-cyclodextrin (Ghemati & Aliouche, 2014). In addition, the increase of ΔG° in respond to increased temperature demonstrated that the adsorption is more feasible at lower temperature (Baheri et al., 2016; Ghahremani et al., 2015; S. Umoren et al., 2013). For instance, the increment of ΔG° of PVA/Chitin-10/ MA-10, which was from -3.734 kJ/mol at 298 K to -0.369 kJ/mol at 318 K, indicating a decrease in dye adsorption with increased temperature. From this thermodynamic study, it was determined that the MB adsorption onto PVA/Chitin-10/NCC/MA-30 was the most spontaneous and feasible, as indicated by the highest negativity of ΔG° determined at 298 K-318 K. Contrarily, the least feasibility of adsorption was reflected by PVA/Chitin-10/ MA-50, with the highest ΔG° recorded at 298 K-318 K.

Overall, it could be denoted that the thermodynamic behaviors of adsorption process show variation depend on the types of the adsorbent being used. This is because adsorbent and adsorbate exhibit distinctive physical and chemical characteristics which influence the adsorption process.

4.3.10 Reusability Studies

Desorption studies were performed to investigate the nature of adsorption and reusability of the adsorbent (Nesic et al., 2014; Rashidzadeh & Olad, 2013). In this work, desorption was enabled with the use of 1M HCl and adsorption-desorption cycles were repeated for five times. Adsorption percentage and desorption percentage of adsorbents were determined based on the Equation 3.7 and Equation 3.17, respectively. Referring to Figure 4.37 (a), all of the PVA adsorbents with varied compositions displayed decrease in adsorption percentage after repeated adsorption cycles. The losses of adsorption percentage were most significant for composite samples constituent of 10% MA. For example, PVA/Chitin-10/NCC/MA-10 sample which had adsorption percentage of 87.23 ± 0.12% at first adsorption cycle, decreased by 28.68% to adsorption percentage of 62.21 ± 0.34% at the fifth adsorption cycle. This decreased adsorption performance was associated to water solubility of the samples with only 10% MA, as supported by the increased desorption percentage of those composite adsorbents after repeated desorption cycles (Figure 4.37 (b)).

As for composite adsorbents with 30% MA and 50% MA, the removal percentages were decreased by small percentages at each adsorption-desorption cycle. Considering the PVA/Chitin-10/NCC/MA-30 with adsorption percentage of 95.41 ± 0.55% at the first adsorption cycle, adsorption percentage of 83.67 ± 1.08% was retained at the fifth adsorption cycle. The difference in adsorption percentage of PVA/Chitin-10/NCC/MA-30 between first and fifth cycle was amounted to 12.30%. By comparing the loss of adsorption percentage between the first and fifth cycle of PVA/Chitin-10/NCC/MA-10 and PVA/Chitin-10/NCC/MA-30, the latter composite with 30% MA was superior over the composite with 10% MA incorporated by 33.17%.

Since inorganic acid like HCl instead of neutral water was an efficient desorbing agent, this indicated that the desorption was comprised of ion exchange (Nesic et al., 2014). Hence, the adsorption percentage was decreased at each interval due to the reduced availability of adsorption sites. By summing up desorption percentages of the PVA/Chitin-20/NCC/MA-30, it was determined that the accumulated loss of adsorption sites was as much as 56.85%. However, it was found out that the adsorption percentage of the PVA/Chitin-20/NCC/MA-30 was recorded at 77.80 ± 0.50% during the fifth adsorption cycle. This is due to the fact that the adsorption process is not solely dependent on the availability of adsorption sites for monolayer coverage. Therefore, the adsorption percentages are remaining high even with the loss of adsorption sites. On the other hand, incomplete desorption is associated to the formation of strongly adsorbed complexes between functional groups of the adsorbent and MB (Rashidzadeh & Olad, 2013). Among samples, PVA/Chitin-10/NCC/MA-30 exhibited highest MB dyes removal percentage of 95.41 ± 0.55% at the first adsorption run. A removal percentage of 83.67 ± 1.08% was retained at the fifth adsorption cycle, which implied its high reusability potential.

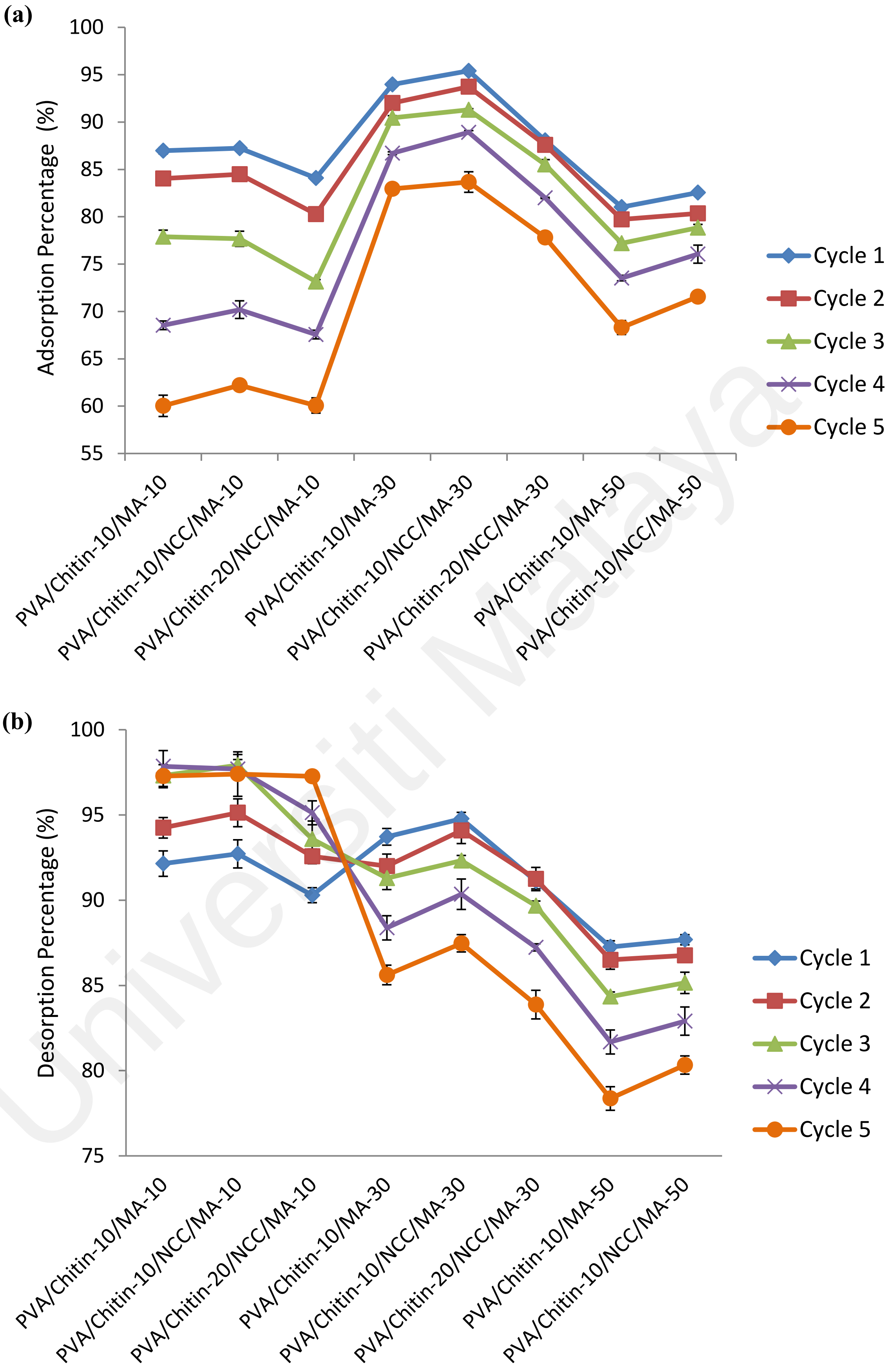

Figure 4.37: (a) Adsorption percentage and (b) desorption percentage of MB with the selected composite adsorbents for five consecutive cycles.

4.3.11 Comparison of Adsorbent Efficiency with Other Adsorbent

Table 4.8 showed comparisons between maximum adsorption capacities (q_M) for the adsorption of MB on PVA/Chitin-10/NCC/MA-30 adsorbent and a few reported polymeric adsorbents. It was evident that the prepared PVA/Chitin-10/NCC/MA-30 adsorbent had relatively higher adsorption capacity compared to most of the adsorbents tabulated. However, accurate comparison of adsorption capacity is challenging as different researchers utilize different adsorbent dosage, initial dye concentration and pH range for the experiments. Besides, it is well known that adsorption capacity increases significantly with increasing adsorbent dosage, initial adsorbate concentration and pH of the working solution (Baheri et al., 2016; Rashidzadeh & Olad, 2013).

The adsorption capacity of PVA/Chitin-10/NCC/MA-30 composite prepared in this study was comparable to the poly(vinyl alcohol)/graphene oxide composite prepared by X. Yang et al. (2016). PVA/Chitin-10/NCC/MA-30 composite prepared is advantageous over the poly(vinyl alcohol)/graphene oxide in terms of energy saving during production. This is because graphene oxide used is synthesized from expandable graphite. Production of expandable graphite could be a concern since it involves high energy sintering and acidic vapor could be released along the production process (Gulnura et al., 2018; Sridhar et al., 2010). Nevertheless, this comparison led to a conclusion that the as-prepared adsorbent is a promising alternative adsorbent for the removal of MB from aqueous solution.

Table 4.8: Comparison of adsorption capacities with other adsorbents for the removal of MB dye.

Adsorbent Name	Name of dyes	Adsorbent Dosage (g/L)	Initial Dyes Concentration (mg/L)	Solution pH	Maximum adsorption capacity, q_M (mg/g)	References
Poly(vinyl alcohol)	MB	4	25	4	13.80	(S. Umoren et al., 2013)
Poly(vinyl alcohol)	MB	-	30	6	23.30	(Agarwal et al., 2016)
α-chitin	MB	1	10	6	6.90	(Dhananasekaran et al., 2016)
Poly(vinyl alcohol)/chitosan	MB	20	20	9	~30.00	(Casey & Wilson, 2015)
PVA/GA/β-cyclodexrin	MB	-	25	11	27.25	(Ghemati & Aliouche, 2014)
Poly(vinyl alcohol)/poly(acrylic acid	MB	2.5	50	6	34.20	(Kamal, 2014)
Poly(vinyl alcohol)/poly(acrylic acid /clay	MB	2.5	50	6	28.80	(Kamal, 2014)
Poly(vinyl alcohol)/4A-zeolite	MB	1	10	8.5	41.08	(Baheri et al., 2016)
Poly(vinyl alcohol)/polyaniline/clinoptilolite	MB	1	10	-	44.44	(Rashidzadeh & Olad, 2013)

‘Table 4.8, continued’

Adsorbent Name	Name of dyes	Adsorbent Dosage (g/L)	Initial Dyes Concentration (mg/L)	Solution pH	Maximum adsorption capacity, q_M (mg/g)	References
Poly(vinyl alcohol)/attapulgite	MB	5	40	5	169.50	(L. Yang et al., 2011)
Poly(vinyl alcohol)/graphene oxide	MB	0.5	50	6	476.20	(X. Yang et al., 2016)
PVA/Chitin-10/NCC/MA-30	MB	0.5	50	9	467.50	This current study

4.4 Summary

In the first part of chapter, it was determined NCC obtained from chemical treatment of OPEFB fibers with ammonium persulfate was of nano-sized, with 90% of the particles (D90) was smaller than 83.00 nm. Besides, FTIR technique was used to investigate the differences of chemical structures between PVA/Chitin/NCC composites and MA cross-linked PVA/Chitin/NCC composites. It was evidenced from the increase in tensile strength that the NCC filler serves as an effective reinforcing filler at 1wt.% of NCC due to the efficient stress transfer from the matrix to the filler. In addition, the mechanical properties of PVA/NCC, PVA/Chitin and PVA/Chitin/NCC samples as a function of MA content were also discussed.

Through differential scanning calorimetry (DSC), the thermal transitions of the PVA/Chitin/NCC composites and PVA/Chitin/NCC composites upon the incorporation of MA were investigated, respectively. The thermal transitions discussed were the glass transition temperature (T_g) and melting temperature (T_m). Besides, other physicochemical characterizations which include swelling tests, water solubility tests, gel contents and water contact angle measurements were carried out on the composites studied. All these studies helped to provide insight over the processability and stability of the PVA/Chitin/NCC composites in aqueous medium, with and without MA incorporated.

The PVA/chitin/NCC composites obtained were used for MB dyes adsorption. Furthermore, only eight compositions of varied MA cross-linked PVA/Chitin/NCC composites, with and without NCC included which showed high adsorption equilibriums were selected for further testing to evaluate the effects of other dependent factors on adsorption. The effects of other dependent factors discussed include solution pH, adsorbent dosage and initial dyes concentration. It is figured out that PVA/Chitin-10/NCC/MA-30 was the best composite composition for the removal of MB, after experimental parameters were optimized. Adsorption isotherm studies revealed the better fitting of data to Freundlich isotherm in comparison to Langmuir isotherm, with the calculated maximum adsorption capacity amounted to 467.5 mg/g. The adsorption kinetics were determined to be of pseudo-second order. From thermodynamic studies, it was evaluated that the adsorption processes were spontaneous, exothermic and less-ordered reactions. The PVA/Chitin-10/NCC/MA-30 adsorbent exhibited high adsorption reusability since the adsorption percentage achieved was 83.67 ± 1.08%, even at the fifth adsorption-desorption cycle. Lastly, it was determined that the prepared PVA/Chitin-10/NCC/MA-30 adsorbent had relatively higher adsorption capacity compared to most of the adsorbents tabulated.

CHAPTER 5: CONCLUSIONS AND RECOMMENDATIONS

5.1 Conclusions

As highlighted in Chapter 1.2, there are objectives in this thesis. These studies are aimed at utilizing novel PVA-based composites for potential application in the removal of cationic dyes through adsorption.

In the quest of fulfilling the main purpose of the current thesis, the NCC-reinforced PVA/Chitin (PVA/Chitin/NCC) composites were first prepared and characterized. It was confirmed that the PVA/Chitin/NCC composites were successfully prepared. This is indicated by the FTIR spectra of PVA/Chitin/NCC which showed the respective characteristics bands of PVA, α-chitin and NCC. With addition of 1 wt.% NCC, a maximum improvement of 57.64% and 50.66% in tensile strength and Young's Modulus were achieved, respectively. Based on the mechanical and morphological analysis results, it was deduced that 1 wt.% NCC acted as the effective reinforcing filler when the NCC loading was varied at 0 wt.% to 1.5 wt.%. Incorporation of 1.5 wt.% NCC into composite matrix resulted in more intense agglomeration of NCC. This led to inefficient stress transfer from polymer matrix to the reinforcing filler and thus resulted in poorer mechanical properties when compared with 1 wt.% NCC loading. Therefore, 1 wt.% of NCC was used for further tests on the PVA/Chitin/NCC composites.

Furthermore, it was identified that the chitin exhibited intermolecular interaction with PVA matrix through hydrogen bonding as indicated through FTIR. However, the composites showed low structural integrity at aqueous medium in the absence of cross-linker. Hence, it was deduced that modification of PVA-based composites through cross-linking reaction was imperative to improve the workability of composites in aqueous medium. Corresponding to the second objective in this study, it was determined that PVA-based composites consist of α-chitin and OPEFB fiber-sourced NCC were successfully modified by MA to exhibit improved physicochemical properties while retaining film-forming capabilities. FTIR results confirmed that the PVA-based composites had been successfully cross-linked by MA through esterification reaction. As deduced by DSC results, the influence of cross-linking was minimal towards crystallization reaction in the PVA/Chitin composites. Maximum tensile strength, elongation at break and Young's Modulus of the respective PVA/Chitin/NCC composites were achieved at different content of MA, depending on the PVA/Chitin mass ratio. Upon cross-linking, PVA/Chitin/NCC composites garnered improved water resistance but lowered swelling capabilities with increasing content of chitin and MA. This was due to increased gel content as determined in this study. In addition, it was determined that increased content of MA resulted to enhancement in surface hydrophobicity of the composite. In brief, this chemically cross-linked PVA/Chitin/NCC formulated with sustainable resources showed tunable physicochemical properties rendering it applicable for film or membrane fabrication which is stable in contact with aqueous media. These PVA-based composites had been explored in terms of its applicability for dyestuff dye effluent treatment by investigating the adsorptive capabilities of composites towards a model cationic dye, namely methylene blue (MB). At the experimental settings, it was deduced that incorporation of 30% MA to the PVA/Chitin/NCC composites was the optimum content to improve the adsorption capabilities of the composites towards the MB dye.

It was remarked that the adsorption capacities of MB using the PVA/Chitin/NCC composites with MA incorporated were dependent on the other external adsorption parameters such as solution pH, adsorbent dosage and initial dyes concentration. The selected MA cross-linked PVA/Chitin/NCC composites achieved good uptake of the cationic MB at pH 9 were due to the enhanced electrostatic force of attraction between the oppositely-charged adsorbents' surface and dyes. From the results, adsorbent dosage of 0.5g/L and 50 mg/L of initial MB concentration was deduced to be optimum parameters for adsorption in these experimental settings. Last but not least, the adsorption processes were best fitted to Freundlich isotherm model and the processes were of pseudo-second order kinetic. From thermodynamic study, parameters such as ΔG°, ΔH° and ΔS° were determined. Based on the thermodynamic parameters obtained, it was concluded that the MB adsorption onto the MA cross-linked PVA-based composites were spontaneous, exothermic and less-ordered reactions. It was revealed that the adsorption of MB onto the adsorbents comprised of both physisorption and chemisorption mechanisms.

As a conclusion, the best adsorption performance could be achieved by PVA/Chitin-10/NCC/MA-30 when the external adsorption parameters were optimized. Reusability study showed that the removal efficiency of PVA/Chitin-10/NCC/MA-30 was retained at 83.67 ± 1.08% even at the fifth adsorption cycle. Comparisons of adsorption capacities with other adsorbents also showed that PVA/Chitin-10/NCC/MA-30 composites could be used as an alternative adsorbent for the removal of MB dyes from aqueous solution. Utilization of this eco-friendly adsorbent for treatment of dye effluent would serve as a proactive measure for achieving environmental sustainability.

5.2 Recommendations

For future study, it would be interesting to further evaluate the adsorption performance of the PVA-based adsorbents prepared in this study for removing wastewater effluents such as heavy metal ions, pharmaceutical by-products and other types of dyes emanating from different industrial process. This will serve to evaluate the suitability of the adsorbent to be used on removing other types of water contaminants other than the model dye studied in this work. Furthermore, competitive sorption among the adsorbates onto the adsorption sites could be explored by introducing two or more adsorbates into the adsorption system. These studies will serve to provide insight concerning adsorption capabilities of the adsorbent which may be interfered by other components present in the effluents.

In addition, upon completion of batch equilibrium experiments which indicate the adsorption capacity of the adsorbent towards the dyes, continuous flow mode of adsorption study has to be carried out (Chowdhury, 2013). Through the continuous flow mode of adsorption study, influent enters and elutes from a column packed with adsorbent in a continuous manner. Hence, complete equilibrium is not established in between the solutes present in the solution and the amount adsorbed during the short contact time. Equilibrium has to be continuously re-established when fresh influent enters. However, this type of dynamic equilibrium of sorption has been reported to be effective on large scale wastewater treatment and cyclic adsorption-desorption. From experiments, breakthrough curve is attainable from continuous flow mode of adsorption study which further assists in evaluating operation life span and reusability of column bed (Chowdhury, 2013; Russo et al., 2017). From critical review of Russo et al. (2017), the authors suggest that the ideal way to design an adsorption column is indeed to start from a detailed laboratory-scale batch adsorption studies and interpret the data with a rigorous model. Upon investigating the crucial aspects of the adsorption system, the behavior of an adsorption column could be more predictable, and this is beneficial for the scale-up of the adsorption system.

Other than this, it is interesting to explore ways to surface treat the adsorbent to increase its surface area. Improvement on the adsorption capability of adsorbent would be expected as adsorption is dependent on surface coverage. The number of adsorption sites available on adsorbates is directly proportional to surface area of the adsorbent. Considering the importance of surface treatment, many polymer surface modification techniques have been reported in literatures over the years. Surface modification techniques could be categorized into three main types which are physicochemical, mechanical, and biological methods (Michael et al., 2017). Current works have applied the physicochemical techniques to improve the interactions between the polymers and dyes, resulting in increased adsorption capacities of adsorbent studied. Other physicochemical techniques could be further explored include chemical vapour deposition, electromagnetic radiations, plasma treatments, chemical conjugation and chemical grafting (Ávila-Orta et al., 2013; Michael et al., 2017). Moreover, it is desired that future works to be extended on the mechanical methods to improve the surface roughness and friction by altering the surface topography. Mechanical methods to be further studied include roughening techniques and micromanipulation. Under micromanipulation, the polymer surface is to be carved at a microlevel or nanolevel with a special highly précised manipulating probes coupled with scanning tunneling microscope or atomic force microscope (Michael et al., 2017).

References

Abd El-Kader, F. H., Gaafer, S. A., & Abd El-Kader, M. F. (2014). Characterization and optical studies of 90/10 (wt/wt%) PVA/beta-chitin blend irradiated with gamma-rays. *Spectrochimica Acta, Part A: Molecular and Biomolecular Spectroscopy, 131*, 564-570.

Abd El-Mohdy, H., & Mostafa, T. B. (2013). Synthesis of polyvinyl alcohol/maleic acid hydrogels by electron beam irradiation for dye uptake. *Journal of Macromolecular Science, Part A, 50*(1), 6-17.

Abdeen, Z. (2011). Swelling and reswelling characteristics of cross-linked poly (vinyl alcohol)/chitosan hydrogel film. *Journal of Dispersion Science and Technology, 32*(9), 1337-1344.

Agarwal, S., Sadegh, H., Monajjemi, M., Hamdy, A. S., Ali, G. A., Memar, A. O., et al. (2016). Efficient removal of toxic bromothymol blue and methylene blue from wastewater by polyvinyl alcohol. *Journal of Molecular Liquids, 218*, 191-197.

Aitomäki, Y., & Oksman, K. (2014). Reinforcing efficiency of nanocellulose in polymers. *Reactive and Functional Polymers, 85*, 151-156.

Akkaya, G., Uzun, İ., & Güzel, F. (2007). Kinetics of the adsorption of reactive dyes by chitin. *Dyes and Pigments, 73*(2), 168-177.

Alaba, P. A., Oladoja, N. A., Sani, Y. M., Ayodele, O. B., Mohammed, I. Y., Olupinla, S. F., et al. (2018). Insight into wastewater decontamination using polymeric adsorbents. *Journal of Environmental Chemical Engineering, 6*(2), 1651-1672.

Alavudeen, A., Venkateshwaran, N., & Jappes, J. W. (2006). *A textbook of engineering materials and metallurgy*: Firewall Media.

Alexy, P., Bakoš, D., Cr , G., Kram , Z., Hoffmann, J., Julino , M., et al. (2003). Poly(vinyl alcohol)–collagen hydrolysate thermoplastic blends: II. Water penetration and biodegradability of melt extruded films. *Polymer Testing, 22*(7), 811-818.

Ali Ashjarana, & Hajilarib, M. (2013). Adsorption anionic dye on bacterial and plant cellulose: thermodynamic and kinetic study. *Research Journal of Pharmaceutical, Biological and Chemical Sciences, 4*(3), 985-994.

Ávila-Orta, C. A., González-Morones, P., Espinoza-González, C. J., Martínez-Colunga, J. G., Neira-Velázquez, M. G., Sáenz-Galindo, A., et al. (2013). Toward greener chemistry methods for preparation of hybrid polymer materials based on carbon nanotubes. *Syntheses and applications of carbon nanotubes and their composites*, 1-20.

Azizi, S., Ahmad, M. B., Hussein, M. Z., Ibrahim, N. A., & Namvar, F. (2014). Preparation and properties of poly(vinyl alcohol)/chitosan blend bionanocomposites reinforced with cellulose nanocrystals/ZnO-Ag multifunctional nanosized filler. *International Journal of Nanomedicine, 9*, 1909-1917.

Badr, S., Sheha, E., Bayomi, R., & El-Shaarawy, M. (2010). Structural and electrical properties of pure and H2SO4 doped (PVA) 0.7 (NaI) 0.3 solid polymer electrolyte. *Ionics, 16*(3), 269-275.

Baheri, B., Ghahremani, R., Peydayesh, M., Shahverdi, M., & Mohammadi, T. (2016). Dye removal using 4A-zeolite/polyvinyl alcohol mixed matrix membrane adsorbents: preparation, characterization, adsorption, kinetics, and thermodynamics. *Research on Chemical Intermediates, 42*(6), 5309-5328.

Bahrami, S. B., Kordestani, S. S., Mirzadeh, H., & Mansoori, P. (2003). Poly (vinyl alcohol)-chitosan blends: preparation, mechanical and physical properties. *Iranian Polymer Journal, 12*, 139-146.

Baraka, A. (2012). Adsorptive removal of tartrazine and methylene blue from wastewater using melamine-formaldehyde-tartaric acid resin (and a discussion about pseudo second order model). *Desalination and Water Treatment, 44*(1-3), 128-141.

Bayramoğlu, G., Bektaş, S., & Arıca, M. Y. (2003). Biosorption of heavy metal ions on immobilized white-rot fungus *Trametes versicolor*. *Journal of Hazardous Materials, 101*(3), 285-300.

Bhatnagar, A., & Sillanpää, M. (2009). Applications of chitin-and chitosan-derivatives for the detoxification of water and wastewater—a short review. *Advances in Colloid and Interface Science, 152*(1), 26-38.

Birck, C., Degoutin, S., Tabary, N., Miri, V., & Bacquet, M. (2014). New crosslinked cast films based on poly (vinyl alcohol): Preparation and physico-chemical properties. *eXPRESS Polymer Letters, 8*(12), 941-952.

Bledzki, A., Reihmane, S., & Gassan, J. (1996). Properties and modification methods for vegetable fibers for natural fiber composites. *Journal of Applied Polymer Science, 59*(8), 1329-1336.

Bolto, B., Tran, T., Hoang, M., & Xie, Z. (2009). Crosslinked poly(vinyl alcohol) membranes. *Progress in Polymer Science, 34*(9), 969-981.

Brinchi, L., Cotana, F., Fortunati, E., & Kenny, J. (2013). Production of nanocrystalline cellulose from lignocellulosic biomass: technology and applications. *Carbohydrate Polymers, 94*(1), 154-169.

Carmen, Z., & Daniela, S. (2012). Textile organic dyes–characteristics, polluting effects and separation/elimination procedures from industrial effluents–a critical overview. In T. Puzyn, & A. Mostrag-Szlichtyng (Eds.), *Organic pollutants ten years after the stockholm convention-environmental and analytical update* (pp. 55-81). Croatia: InTech.

Casey, L. S., & Wilson, L. D. (2015). Investigation of chitosan-PVA composite films and their adsorption properties. *Journal of Geoscience and Environment Protection, 3*(2), 78-84.

Castro-Guerrero, C. F., & Gray, D. G. (2014). Chiral nematic phase formation by aqueous suspensions of cellulose nanocrystals prepared by oxidation with ammonium persulfate. *Cellulose, 21*(4), 2567-2577.

Castro, C., Vesterinen, A., Zuluaga, R., Caro, G., Filpponen, I., Rojas, O. J., et al. (2014). In situ production of nanocomposites of poly (vinyl alcohol) and cellulose nanofibrils from Gluconacetobacter bacteria: effect of chemical crosslinking. *Cellulose, 21*(3), 1745-1756.

Chandumpai, A., Singhpibulporn, N., Faroongsarng, D., & Sornprasit, P. (2004). Preparation and physico-chemical characterization of chitin and chitosan from the pens of the squid species, *Loligo lessoniana* and *Loligo formosana*. *Carbohydrate Polymers, 58*(4), 467-474.

Cho, Y.-W., Nam, C.-W., Jang, J., & Ko, S.-W. (2001). Preparation and characterization of chitin/poly (vinyl alcohol) blends using aqueous acetic acid solution as a cosolvent. *Journal of Macromolecular Science, Part B, 40*(1), 93-104.

Choi, Y., & Simonsen, J. (2006). Cellulose nanocrystal-filled carboxymethyl cellulose nanocomposites. *Journal of Nanoscience and Nanotechnology, 6*(3), 633-639.

Chowdhury, Z. Z. (2013). *Preparation, characterization and adsorption studies of heavy metals onto activated adsorbent materials derived from agricultural residues.* (Doctor of Philosophy), University of Malaya.

Costa-Júnior, E. S., Barbosa-Stancioli, E. F., Mansur, A. A., Vasconcelos, W. L., & Mansur, H. S. (2009). Preparation and characterization of chitosan/poly (vinyl alcohol) chemically crosslinked blends for biomedical applications. *Carbohydrate Polymers, 76*(3), 472-481.

Dasari, A., Yu, Z.-Z., & Mai, Y.-W. (2005). Effect of blending sequence on microstructure of ternary nanocomposites. *Polymer, 46*(16), 5986-5991.

Dave, R., & Madamwar, D. (2006). Esterification in organic solvents by lipase immobilized in polymer of PVA–alginate–boric acid. *Process Biochemistry, 41*(4), 951-955.

DeMerlis, C., & Schoneker, D. (2003). Review of the oral toxicity of polyvinyl alcohol (PVA). *Food and Chemical Toxicology, 41*(3), 319-326.

Deng, Q., Li, J., Yang, J., & Li, D. (2014). Optical and flexible α-chitin nanofibers reinforced poly (vinyl alcohol)(PVA) composite film: Fabrication and property. *Composites Part A Applied Science and Manufacturing, 67*, 55-60.

Dhananasekaran, S., Palanivel, R., & Pappu, S. (2016). Adsorption of Methylene Blue, Bromophenol Blue, and Coomassie Brilliant Blue by α-chitin nanoparticles. *Journal of Advanced Research, 7*(1), 113-124.

Dobias, B., Qiu, X., & von Rybinski, W. (1999). Adsorption at the Solid-Liquid Interface. In B. Dobias, X. Qiu, & W. von Rybinski (Eds.), *Solid - Liquid Dispersions* (Vol. 81, pp. 332-333): Taylor & Francis.

Dolphen, R., Sakkayawong, N., Thiravetyan, P., & Nakbanpote, W. (2007). Adsorption of Reactive Red 141 from wastewater onto modified chitin. *Journal of Hazardous Materials, 145*(1), 250-255.

Dorigato, A., & Pegoretti, A. (2012). Biodegradable single-polymer composites from polyvinyl alcohol. *Colloid and Polymer Science, 290*(4), 359-370.

E. Bachmann, W., & C. Deno, N. (1951). *The Nitrosation of Hexamethylenetetramine and Related Compounds1* (Vol. 73).

El-Araby, H. A., Ibrahim, A. M. M. A., Mangood, A. H., & Adel, A.-H. (2017). Sesame husk as adsorbent for Copper (II) ions removal from aqueous solution. *Journal of Geoscience and Environment Protection, 5*(7), 109.

El-Latif, M. A., El-Kady, M., Ibrahim, M., & Ossman, M. (2010). Alginate/polyvinyl alcohol—kaolin composite for removal of methylene blue from aqueous solution in a batch stirred tank reactor. *Journal of American Science, 6*(5), 280-292.

El-Latif, M. A., Ibrahim, A. M., & El-Kady, M. (2010). Adsorption equilibrium, kinetics and thermodynamics of methylene blue from aqueous solutions using biopolymer oak sawdust composite. *Journal of American Science, 6*(6), 267-283.

El Feky, A., Shalaby, M., El-Shamy, O., & Selim, S. (2010). Adsorption of some surfactants onto polyvinyl alcohol as hydrophobic polymer surface. *Journal of Dispersion Science and Technology, 31*(8), 1091-1099.

Fan, Y., Saito, T., & Isogai, A. (2007). Chitin nanocrystals prepared by TEMPO-mediated oxidation of α-chitin. *Biomacromolecules, 9*(1), 192-198.

Filipkowska, U., & Rodziewicz, J. (2009). Effectiveness of dye RB5 adsorption onto chitin and chitosan under static and dynamic conditions. *Progress on Chemistry and Application of Chitin and its Deritatives, 14*, 33-40.

Filson, P. B., Dawson-Andoh, B. E., & Schwegler-Berry, D. (2009). Enzymatic-mediated production of cellulose nanocrystals from recycled pulp. *Green Chemistry, 11*(11), 1808-1814.

Fortunati, E., Luzi, F., Puglia, D., Terenzi, A., Vercellino, M., Visai, L., et al. (2013). Ternary PVA nanocomposites containing cellulose nanocrystals from different sources and silver particles: part II. *Carbohydrate Polymers, 97*(2), 837-848.

Fortunati, E., Puglia, D., Luzi, F., Santulli, C., Kenny, J. M., & Torre, L. (2013). Binary PVA bio-nanocomposites containing cellulose nanocrystals extracted from different natural sources: Part I. *Carbohydrate Polymers, 97*(2), 825-836.

Gaaz, T. S., Sulong, A. B., Akhtar, M. N., Kadhum, A. A. H., Mohamad, A. B., & Al-Amiery, A. A. (2015). Properties and applications of polyvinyl alcohol, halloysite nanotubes and their nanocomposites. *Molecules, 20*(12), 22833-22847.

Gao, C.-D., Ren, J.-L., Wang, S.-Y., Sun, R.-C., & Zhao, L.-H. (2014). Preparation of polyvinyl alcohol/xylan blending films with 1, 2, 3, 4-butane tetracarboxylic acid as a new plasticizer. *Journal of Nanomaterials, 2014*, 8.

Gatabi, M. P., Moghaddam, H. M., & Ghorbani, M. (2016). Point of zero charge of maghemite decorated multiwalled carbon nanotubes fabricated by chemical precipitation method. *Journal of Molecular Liquids, 216*, 117-125.

Gea, S., Zulfahmi, Z., Yunus, D., Andriayani, A., & Hutapea, Y. A. (2018). The Isolation of Nanofibre Cellulose from Oil Palm Empty Fruit Bunch Via Steam Explosion and Hydrolysis with HCl 10%. *Journal of Physics: Conference Series, 979*(1), 012063.

Ghahremani, R., Baheri, B., Peydayesh, M., Asarehpour, S., & Mohammadi, T. (2015). Novel crosslinked and zeolite-filled polyvinyl alcohol membrane adsorbents for dye removal. *Research on Chemical Intermediates, 41*(12), 9845-9862.

Ghemati, D., & Aliouche, D. (2014). Dye adsorption behavior of polyvinyl alcohol/glutaraldehyde/β-cyclodextrin polymer membranes. *Journal of Applied Spectroscopy, 81*(2), 257-263.

Gohil, J., Bhattacharya, A., & Ray, P. (2006). Studies on the crosslinking of poly (vinyl alcohol). *Journal of Polymer Research, 13*(2), 161-169.

Gohil, J., & Ray, P. (2009). Studies on oxalic acid as a crosslinker of polyvinyl alcohol. *Polymers & Polymer Composites, 17*(7), 403.

Golka, K., Kopps, S., & Myslak, Z. W. (2004). Carcinogenicity of azo colorants: influence of solubility and bioavailability. *Toxicology Letters, 151*(1), 203-210.

González‐campos, J. B., Prokhorov, E., Luna‐Bárcenas, G., Galván, A. M., Sanchez, I. C., Nuño Donlucas, S. M., et al. (2009). Relaxations in chitin: evidence for a glass transition. *Journal of Polymer Science Part B: Polymer Physics, 47*(9), 932-943.

Gonzalez, J. S., Ludueña, L. N., Ponce, A., & Alvarez, V. A. (2014). Poly (vinyl alcohol)/cellulose nanowhiskers nanocomposite hydrogels for potential wound dressings. *Materials Science and Engineering: C, 34*, 54-61.

Grande, R., & Carvalho, A. J. (2011). Compatible ternary blends of chitosan/poly (vinyl alcohol)/poly (lactic acid) produced by oil-in-water emulsion processing. *Biomacromolecules, 12*(4), 907-914.

Guirguis, O. W. (2012). Thermal and structural studies of poly (vinyl alcohol) and hydroxypropyl cellulose blends. *Natural Science, 04*(01), 57-67.

Gulnura, N., Kenes, K., Yerdos, O., Zulkhair, M., & Di Capua, R. (2018). *Preparation of Expanded Graphite Using a Thermal Method.* Paper presented at the IOP Conference Series: Materials Science and Engineering.

Gupta, A. P., & Arora, G. (2011). Preparation and characterization of guar-gum/polyvinylalcohol blend films. *Journal of Materials Science and Engineering. B, 1*(1B), 28.

Gupta, S. S., & Bhattacharyya, K. G. (2011). Kinetics of adsorption of metal ions on inorganic materials: a review. *Advances in Colloid and Interface Science, 162*(1), 39-58.

Hallensleben, M. L., Fuss, R., & Mummy, F. (2000). *Polyvinyl compounds, others*: Wiley‐VCH Verlag GmbH & Co. KGaA.

Halsey, G. D. (1952). The role of surface heterogeneity in adsorption. *Advances in Catalysis, 4*, 259-269.

Hamdaoui, O., & Naffrechoux, E. (2007). Modeling of adsorption isotherms of phenol and chlorophenols onto granular activated carbon: Part I. Two-parameter models and equations allowing determination of thermodynamic parameters. *Journal of Hazardous Materials, 147*(1), 381-394.

Han, B., Li, J., Chen, C., Xu, C., & Wickramasinghe, S. (2003). Effects of degree of formaldehyde acetal treatment and maleic acid crosslinking on solubility and diffusivity of water in PVA membranes. *Chemical Engineering Research and Design, 81*(10), 1385-1392.

Han, J., Lei, T., & Wu, Q. (2013). Facile preparation of mouldable polyvinyl alcohol-borax hydrogels reinforced by well-dispersed cellulose nanoparticles: physical, viscoelastic and mechanical properties. *Cellulose, 20*(6), 2947-2958.

Hasan, M. B. (2008). *Adsorption of reactive azo dyes on chitosan/oil palm ash composite adsorbent: batch and continuous studies.* (Master), Universiti Sains Malaysia

Hashemian, S. (2014). A comparative study of cellulose agricultural wastes (almond shell, pistachio shell, walnut shell, tea waste and orange peel) for adsorption of violet B dye from aqueous solutions. *Oriental Journal of Chemistry, 30*(4), 2091-2098.

Hassan, C. M., Trakampan, P., & Peppas, N. A. (2002). Water solubility characteristics of poly (vinyl alcohol) and gels prepared by freezing/thawing processes *Water Soluble Polymers* (pp. 31-40): Springer.

Hema, M., & Arivoli, S. (2008). Adsorption kinetics and thermodynamics of malachite green dye unto acid activated low cost carbon. *Journal of Applied Sciences and Environmental Management, 12*(1).

Hennink, W. E., & van Nostrum, C. F. (2002). Novel crosslinking methods to design hydrogels. *Advanced Drug Delivery Reviews, 54*(1), 13-36.

Ho, Y.-S. (2006). Review of second-order models for adsorption systems. *Journal of Hazardous Materials, 136*(3), 681-689.

Ho, Y., Ng, J., & McKay, G. (2000). Kinetics of pollutant sorption by biosorbents. *Separation and Purification Methods, 29*(2), 189-232.

Hosny, W. M., & Khalaf-Alaa, P. A. (2013). Potentiometric study and biological activity of some metal ion complexes of polyvinyl alcohol (PVA). *International Journal of Electrochemical Science, 8*, 1520-1533.

Huang, R., & Rhim, J. (1993). Modification of poly (vinyl alcohol) using maleic acid and its application to the separation of acetic acid ‐ water mixtures by the pervaporation technique. *Polymer International, 30*(1), 129-135.

Hunger, K. (2007). *Industrial Dyes: Chemistry, Properties, Applications*: Wiley.

Hussin, Z. M., Talib, N., Hussin, N. M., Hanafiah, M. A., & Khalir, W. K. (2015). Methylene blue adsorption onto NaOH modified durian leaf powder: isotherm and kinetic studies. *American Journal of Environmental Engineering, 5*(3A), 38-43.

Hyder, M. N. (2008). *Preparation, characterization and performance of poly(vinyl alcohol) based membranes for pervaporation dehydration of alcohols.* (Doctor of Philosophy Thesis on the Internet), University of Waterloo, Ontario, Canada. Retrieved from https://uwspace.uwaterloo.ca/bitstream/handle/10012/4014/Hyder_Ph.D_2008.pdf?sequence=1&isAllowed=y

Ishida, K., & Yoshie, N. (2008). Two-way conversion between hard and soft properties of semicrystalline cross-linked polymer. *Macromolecules, 41*(13), 4753-4757.

Jayakumar, R., Chennazhi, K. P., Srinivasan, S., Nair, S. V., Furuike, T., & Tamura, H. (2011). Chitin scaffolds in tissue engineering. *International Journal of Molecular Sciences, 12*(3), 1876-1887.

Jia, X., Chen, Y., Shi, C., Ye, Y., Abid, M., Jabbar, S., et al. (2014). Rheological properties of an amorphous cellulose suspension. *Food Hydrocolloids, 39*, 27-33.

Jiang, L., Yang, T., Peng, L., & Dan, Y. (2015). Acrylamide modified poly (vinyl alcohol): crystalline and enhanced water solubility. *RSC Advances, 5*(105), 86598-86605.

Junkasem, J., Rujiravanit, R., & Supaphol, P. (2006). Fabrication of α-chitin whisker-reinforced poly (vinyl alcohol) nanocomposite nanofibres by electrospinning. *Nanotechnology, 17*(17), 4519.

Kalia, S., Dufresne, A., Cherian, B. M., Kaith, B., Avérous, L., Njuguna, J., et al. (2011). Cellulose-based bio-and nanocomposites: a review. *International Journal of Polymer Science, 2011*.

Kamal, H. (2014). Removal of Methylene Blue from aqueous solutions using composite hydrogel prepared by gamma irradiation. *Journal of American Science, 10*(4), 125-133.

Kang, H., Lin, Q., Armentrout, R. S., & Long, T. E. (2002). Synthesis and characterization of telechelic poly(ethylene terephthalate) sodiosulfonate ionomers. *Macromolecules, 35*(23), 8738-8744.

Kargarzadeh, H., Ahmad, I., Thomas, S., & Dufresne, A. (2017). *Handbook of Nanocellulose and Cellulose Nanocomposites, 2 Volume Set*: John Wiley & Sons.

Kaya, M., Baran, T., Mentes, A., Asaroglu, M., Sezen, G., & Tozak, K. O. (2014). Extraction and characterization of α-chitin and chitosan from six different aquatic invertebrates. *Food Biophysics, 9*(2), 145-157.

Kenawy, E.-R., Kamoun, E. A., Eldin, M. S. M., & El-Meligy, M. A. (2014). Physically crosslinked poly (vinyl alcohol)-hydroxyethyl starch blend hydrogel membranes: Synthesis and characterization for biomedical applications. *Arabian Journal of Chemistry, 7*(3), 372-380.

Khor, E. (2014). *Chitin: Fulfilling a Biomaterials Promise* (2 ed.). Victoria, Canada: Elsevier Science.

Kietzke, T., Neher, D., Landfester, K., Montenegro, R., Güntner, R., & Scherf, U. (2003). Novel approaches to polymer blends based on polymer nanoparticles. *Nature Materials, 2*(6), 408-412.

Kim, S. S., Kim, S. H., & Lee, Y. M. (1996). Preparation, characterization and properties of β‐chitin and N‐acetylated β‐chitin. *Journal of Polymer Science Part B: Polymer Physics, 34*(14), 2367-2374.

Kim, S. S., Kim, S. J., Moon, Y. D., & Lee, Y. M. (1994). Thermal characteristics of chitin and hydroxypropyl chitin. *Polymer, 35*(15), 3212-3216.

Kojima, Y., Usuki, A., Kawasumi, M., Okada, A., Fukushima, Y., Kurauchi, T., et al. (1993). Mechanical properties of nylon 6-clay hybrid. *Journal of Materials Research, 8*(5), 1185-1189.

Kord, B., Malekian, B., Yousefi, H., & Najafi, A. (2016). Preparation and characterization of nanofibrillated Cellulose/Poly (vinyl alcohol) composite films. *Maderas. Ciencia y tecnología, 18*(4), 743-752.

Ku, H., Wang, H., Pattarachaiyakoop, N., & Trada, M. (2011). A review on the tensile properties of natural fiber reinforced polymer composites. *Composites Part B: Engineering, 42*(4), 856-873.

Kubota, N., Go Konaka, & Eguchi, Y. (1998). Characterization of blend films of chitin regenerated from porous chitosan with poly (vinyl alcohol) *Sent Gakkaishi*, 212-218.

Kumar, M., Tripathi, B. P., & Shahi, V. K. (2009). Crosslinked chitosan/polyvinyl alcohol blend beads for removal and recovery of Cd (II) from wastewater. *Journal of Hazardous Materials, 172*(2), 1041-1048.

Kumar, M. N. R. (2000). A review of chitin and chitosan applications. *Reactive and Functional Polymers, 46*(1), 1-27.

Kushwaha, A. K., Gupta, N., & Chattopadhyaya, M. (2014). Removal of cationic methylene blue and malachite green dyes from aqueous solution by waste materials of Daucus carota. *Journal of Saudi Chemical Society, 18*(3), 200-207.

Labuschagne, P. W., Germishuizen, W. A., Verryn, S. M., & Moolman, F. S. (2008). Improved oxygen barrier performance of poly (vinyl alcohol) films through hydrogen bond complex with poly (methyl vinyl ether-co-maleic acid). *European Polymer Journal, 44*(7), 2146-2152.

Lagergren, S. (1898). About the theory of so-called adsorption of soluble substances. *Kungliga Svenska Vetenskapsakademiens Handlingar, 24*(4), 1-39.

Langmuir, I. (1918). The adsorption of gases on plane surfaces of glass, mica and platinum. *Journal of the American Chemical society, 40*(9), 1361-1403.

Lani, N. S., Ngadi, N., Johari, A., & Jusoh, M. (2014). Isolation, characterization, and application of nanocellulose from oil palm empty fruit bunch fiber as nanocomposites. *Journal of Nanomaterials, 2014*, 1-9.

Largitte, L., & Pasquier, R. (2016). A review of the kinetics adsorption models and their application to the adsorption of lead by an activated carbon. *Chemical Engineering Research and Design, 109*, 495-504.

Lee, S.-Y., Mohan, D. J., Kang, I.-A., Doh, G.-H., Lee, S., & Han, S. O. (2009). Nanocellulose reinforced PVA composite films: effects of acid treatment and filler loading. *Fibers and Polymers, 10*(1), 77-82.

Lee, Y. M., Kimt, S. H., & Kimt, S. J. (1996). Preparation and characteristics of β-chitin and poly (vinyl alcohol) blend. *Polymer, 37*(26), 5897-5905.

Leng, T. (2016). *Cellulose Nanocrystals: Particle Size Distribution and Dispersion in Polymer Composites.* Université d'Ottawa/University of Ottawa.

Lesbani, A., Turnip, E. V., Mohadi, R., & Hidayati, N. (2015). Study adsorption desorption of Manganese (II) using impregnated chitin-cellulose as adsorbent. *International Journal of Science and Engineering, 8*(2), 104-108.

Leung, A. C., Hrapovic, S., Lam, E., Liu, Y., Male, K. B., Mahmoud, K. A., et al. (2011). Characteristics and properties of carboxylated cellulose nanocrystals prepared from a novel one-step procedure. *Small, 7*(3), 302-305.

Li, B., Cao, J., Cao, X., Guo, B., & Lu, H. (2016). Preparation and characterization of chemically crosslinked polyvinyl alcohol/carboxylated nanocrystalline cellulose nanocomposite hydrogel films with high mechanical strength. *Journal of Macromolecular Science, Part B, 55*(5), 518-531.

Li, F., Wu, X., Ma, S., Xu, Z., Liu, W., & Liu, F. (2009). Adsorption and desorption mechanisms of Methylene blue removal with iron-oxide coated porous ceramic filter. *Journal of Water Resource and Protection, 1*(1), 35.

Li, J., Revol, J. F., & Marchessault, R. (1997). Effect of degree of deacetylation of chitin on the properties of chitin crystallites. *Journal of Applied Polymer Science, 65*(2), 373-380.

Li, W., Wu, Q., Zhao, X., Huang, Z., Cao, J., Li, J., et al. (2014). Enhanced thermal and mechanical properties of PVA composites formed with filamentous nanocellulose fibrils. *Carbohydrate Polymers, 113*, 403-410.

Liang, R., Hu, A., Hatat-Fraile, M., & Zhou, N. (2014). Fundamentals on adsorption, membrane filtration, and advanced oxidation processes for water treatment. In A. Hu, & A. Apblett (Eds.), *Nanotechnology for Water Treatment and Purification* (pp. 1-45). Cham: Springer International Publishing.

Lim, J.-L., & Okada, M. (2005). Regeneration of granular activated carbon using ultrasound. *Ultrasonics Sonochemistry, 12*(4), 277-282.

Lin, Y., Cai, W., He, H., Wang, X., & Wang, G. (2012). Three-dimensional hierarchically structured PAN@ γ–AlOOH fiber films based on a fiber templated hydrothermal route and their recyclable strong Cr (VI)-removal performance. *RSC Advances, 2*(5), 1769-1773.

Loeppky, R. N., Outram, J. R., Tomasik, W., & Faulconer, J. M. (1983). Rapid nitrosamine formation from a tertiary amine: The nitrosation of 2-(N,N-Dimethylaminomethyl)pyrrole. *Tetrahedron Letters, 24*(40), 4271-4274.

Lu, J., Wang, T., & Drzal, L. T. (2008). Preparation and properties of microfibrillated cellulose polyvinyl alcohol composite materials. *Composites Part A: Applied Science and Manufacturing, 39*(5), 738-746.

Luo, J. Y., Lin, Y. R., Liang, B. W., Li, Y. D., Mo, X. W., & Zeng, Q. G. (2015). Controllable dye adsorption behavior on amorphous tungsten oxide nanosheet surfaces. *RSC Advances, 5*(122), 100898-100904.

Luo, X., Wang, X., Bao, S., Liu, X., Zhang, W., & Fang, T. (2016). Adsorption of phosphate in water using one-step synthesized zirconium-loaded reduced graphene oxide. *Scientific Reports, 6*, 39108.

Luo, X., & Zhang, L. (2009). High effective adsorption of organic dyes on magnetic cellulose beads entrapping activated carbon. *Journal of Hazardous Materials, 171*(1-3), 340-347.

Lusiana, R., & Isdadiyanto, S. (2016). Urea permeability of citric acid crosslinked chitosan-poly (vinyl alcohol) blend membranes. *International Journal of Chemical Engineering and Applications, 7*(3), 186.

Lusiana, R. A., Siswanta, D., Mudasir, M., & Hayashita, T. (2013). The influence of PVA. Cl. Citric acid/chitosan membrane hydrophicility on the transport of creatinine and urea. *Indonesian Journal of Chemistry, 13*(3), 262-270.

Ma, J., Jia, Y., Jing, Y., Yao, Y., & Sun, J. (2012). Kinetics and thermodynamics of methylene blue adsorption by cobalt-hectorite composite. *Dyes and Pigments, 93*(1), 1441-1446.

Maitra, J., & Shukla, V. K. (2014). Cross-linking in hydrogels-a review. *American Journal of Polymer Science, 4*(2), 25-31.

Malhotra, S. K., Goda, K., & Sreekala, M. S. (2012). Advances in Polymer Composites: Macro- and Microcomposites – State of the Art, New Challenges, and Opportunities *Part One Introduction to Polymer Composites* (pp. 3-15): Wiley-VCH Verlag GmbH & Co. KGaA.

Marin, E., Rojas, J., & Ciro, Y. (2014). A review of polyvinyl alcohol derivatives: Promising materials for pharmaceutical and biomedical applications. *African Journal of Pharmacy and Pharmacology, 8*(24), 674-684.

Marzec, A. (2014). *The effect of dyes, pigments and ionic liquids on the properties of elastomer composites.* Université Claude Bernard-Lyon I.

McKay, G., Ho, Y., & Ng, J. (1999). Biosorption of copper from waste waters: a review. *Separation and Purification Methods, 28*(1), 87-125.

Meng, P., Chen, C., Yu, L., Li, J., & Jiang, W. (2000). Crosslinking of pva pervaporation membrane by maleic acid. *Tsinghua Science and Technology, 5*(2), 172-175.

Merle, G., Hosseiny, S. S., Wessling, M., & Nijmeijer, K. (2012). New cross-linked PVA based polymer electrolyte membranes for alkaline fuel cells. *Journal of Membrane Science, 409–410*, 191-199.

Mia, R., Selim, M., Shamim, A., Chowdhury, M., & Sultana, S. (2019). Review on various types of pollution problem in textile dyeing & printing industries of Bangladesh and recommandation for mitigation. *Journal of Textile Engineering & Fashion Technology, 5*(4), 220-226.

Michael, F. M., Khalid, M., Walvekar, R., Siddiqui, H., & Balaji, A. B. (2017). Surface modification techniques of biodegradable and biocompatible polymers.

Mincea, M., Negrulescu, A., & Ostafe, V. (2012). Preparation, modification, and applications of chitin nanowhiskers: A review. *Reviews On Advanced Materials Science, 30*(3), 225-242.

Mishra, S., Bajpai, R., Katare, R., & Bajpai, A. (2007). Radiation induced crosslinking effect on semi-interpenetrating polymer networks of poly (vinyl alcohol). *eXPRESS Polymer Letters, 1*(7), 407-415.

Mittal, V. (2015). *Surface modification of nanoparticle and natural fiber fillers*. Weinheim: Wiley.

Mohammad Mahdi Dadfar, S., Kavoosi, G., & Mohammad Ali Dadfar, S. (2014). Investigation of mechanical properties, antibacterial features, and water vapor permeability of polyvinyl alcohol thin films reinforced by glutaraldehyde and multiwalled carbon nanotube. *Polymer Composites, 35*(9), 1736-1743.

Mohy Eldin, M. S., Aly, K. M., Khan, Z. A., Meky, A. E., Saleh, T. S., & Elbogamy, A. S. (2016). Development of novel acid–base ions exchanger for basic dye removal: phosphoric acid doped pyrazole-g-polyglycidyl methacrylate. *Desalination and Water Treatment, 57*(50), 24047-24055.

Mondal, S. (2017). Review on Nanocellulose Polymer Nanocomposites. *Polymer-Plastics Technology and Engineering*, 1-15.

Muhd Julkapli, N., Akil, H. M., & Ahmad, Z. (2011). Preparation, properties and applications of chitosan-based biocomposites/blend materials: a review. *Composite Interfaces, 18*(6), 449-507.

Nakamura, S., Gillham, J., & Tovolsky, A. (1970). Torsional Braid analysis of cellulose. *Reports on Progress in Polymer Physics in Japan, 13*, 89-90.

Nassar, M. Y., & Abdallah, S. (2016). Facile controllable hydrothermal route for a porous CoMn2O4 nanostructure: synthesis, characterization, and textile dye removal from aqueous media. *RSC Advances, 6*(87), 84050-84067.

Nassar, M. Y., Mohamed, T. Y., Ahmed, I. S., & Samir, I. (2017). MgO nanostructure via a sol-gel combustion synthesis method using different fuels: an efficient nano-adsorbent for the removal of some anionic textile dyes. *Journal of Molecular Liquids, 225*, 730-740.

Nesic, A. R., Velickovic, S. J., & Antonovic, D. G. (2014). Novel composite films based on amidated pectin for cationic dye adsorption. *Colloids and Surfaces B: Biointerfaces, 116*, 620-626.

Ng, H.-M., Sin, L. T., Bee, S.-T., Tee, T.-T., & Rahmat, A. (2017). Review of nanocellulose polymer composite characteristics and challenges. *Polymer-Plastics Technology and Engineering, 56*(7), 687-731.

Ngah, W. W., Kamari, A., & Koay, Y. (2004). Equilibrium and kinetics studies of adsorption of copper (II) on chitosan and chitosan/PVA beads. *International Journal of Biological Macromolecules, 34*(3), 155-161.

Ngah, W. W., Teong, L., & Hanafiah, M. (2011). Adsorption of dyes and heavy metal ions by chitosan composites: A review. *Carbohydrate Polymers, 83*(4), 1446-1456.

Nigrawal, A., Prajapati, S. C., & Chand, N. (2012). Mechanical and thermal properties of nano-cellulose obtained from sisal fiber reinforced polyvinyl alcohol (PVA) bio-composites. *Journal of Scientometric Research, 50*(1), 41.

Nishio, Y., & Manley, R. J. (1988). Cellulose-poly (vinyl alcohol) blends prepared from solutions in N, N-dimethylacetamide-lithium chloride. *Macromolecules, 21*(5), 1270-1277.

Nkhwa, S., Lauriaga, K. F., Kemal, E., & Deb, S. (2014). Poly(vinyl alcohol): Physical Approaches to Designing Biomaterials for Biomedical Applications. *Conference Papers in Science, 2014*, 7.

Noshirvani, N., Hong, W., Ghanbarzadeh, B., Fasihi, H., & Montazami, R. (2017). Study of cellulose nanocrystal doped starch-polyvinyl alcohol bionanocomposite films. *International Journal of Biological Macromolecules*.

Ooi, Z. X., Ismail, H., Bakar, A. A., & Aziz, N. A. A. (2012). Properties of the crosslinked plasticized biodegradable poly (vinyl alcohol)/rambutan skin waste flour blends. *Journal of Applied Polymer Science, 125*(2), 1127-1135.

Osasona, I., Faboya, O. L., & Oso, A. O. (2013). Kinetic, equilibrium and thermodynamic studies of the adsorption of methylene blue from synthetic wastewater using cow hooves. *British Journal of Applied Science & Technology, 3*(4), 1006-1021.

Ovchinnikov, O. V., Evtukhova, A. V., Kondratenko, T. S., Smirnov, M. S., Khokhlov, V. Y., & Erina, O. V. (2016). Manifestation of intermolecular interactions in FTIR spectra of methylene blue molecules. *Vibrational Spectroscopy, 86*, 181-189.

Oya, N., Saitoh, S., Furuhashi, Y., & Yoshie, N. (2012). Mechanical property tuning of semicrystalline network polymers by controlling rates of crystallization and crosslinking. *Journal of Polymer Science Part A: Polymer Chemistry, 50*(10), 1926-1932.

Öztürk, A., & Malkoc, E. (2014). Adsorptive potential of cationic Basic Yellow 2 (BY2) dye onto natural untreated clay (NUC) from aqueous phase: mass transfer analysis, kinetic and equilibrium profile. *Applied Surface Science, 299*, 105-115.

Panaitescu, D. M., Vuluga, D. M., Paven, H., Iorga, M. D., Ghiurea, M., Matasaru, I., et al. (2008). Properties of polymer composites with cellulose microfibrils. *Molecular Crystals and Liquid Crystals, 484*(1), 86-98.

Papancea, A., & Patachia, S. (2015). Characterization of dyes loaded polyvinyl alcohol (PVA) based hydrogels through CIELAB method. *Environmental Engineering & Management Journal, 14*(2), 361-371.

Parida, U. K., Nayak, A. K., Binhani, B. K., & Nayak, P. (2011). Synthesis and characterization of chitosan-polyvinyl alcohol blended with cloisite 30B for controlled release of the anticancer drug curcumin. *Journal of Biomaterials and Nanobiotechnology, 2*(04), 414.

Park, J.-C., Ito, T., Kim, K.-O., & Kim, K.-W. (2010). Electrospun poly (vinyl alcohol) nanofibers: effects of degree of hydrolysis and enhanced water stability. *Polymer Journal, 42*(3), 273-276.

Park, J. S., Park, J. W., & Ruckenstein, E. (2001). Thermal and dynamic mechanical analysis of PVA/MC blend hydrogels. *Polymer, 42*(9), 4271-4280.

Paşka, O. M., Păcurariu, C., & Muntean, S. G. (2014). Kinetic and thermodynamic studies on methylene blue biosorption using corn-husk. *RSC Advances, 4*(107), 62621-62630.

Patel, A., & Vavia, P. (2010). Evaluation of synthesized cross linked polyvinyl alcohol as potential disintegrant. *Journal of Pharmacy & Pharmaceutical Sciences, 13*(2), 114-127.

Pavaloiu, R.-D., Stoica-Guzun, A., Stroescu, M., Jinga, S. I., & Dobre, T. (2014). Composite films of poly(vinyl alcohol)–chitosan–bacterial cellulose for drug controlled release. *International Journal of Biological Macromolecules, 68*, 117-124.

Peesan, M., Rujiravanit, R., & Supaphol, P. (2003). Characterisation of beta-chitin/poly (vinyl alcohol) blend films. *Polymer Testing, 22*(4), 381-387.

Pereira, A. L., do Nascimento, D. M., Souza Filho Mde, S., Morais, J. P., Vasconcelos, N. F., Feitosa, J. P., et al. (2014). Improvement of polyvinyl alcohol properties by adding nanocrystalline cellulose isolated from banana pseudostems. *Carbohydrate Polymers, 112*, 165-172.

Peresin, M. S., Vesterinen, A. H., Habibi, Y., Johansson, L. S., Pawlak, J. J., Nevzorov, A. A., et al. (2014). Crosslinked PVA nanofibers reinforced with cellulose nanocrystals: water interactions and thermomechanical properties. *Journal of Applied Polymer Science, 131*(11), 40334-40346.

Pirbazari, A., Pargami, N., Ashja, N., & Emami, M. (2015). Surfactant-coated tea waste: Preparation, characterization and its application for methylene blue adsorption from aqueous solution. *Journal of Environmental & Analytical Toxicology, 5*(5), 1.

Plazinski, W., Rudzinski, W., & Plazinska, A. (2009). Theoretical models of sorption kinetics including a surface reaction mechanism: a review. *Advances in Colloid and Interface Science, 152*(1-2), 2-13.

Popescu, M.-C. (2017). Structure and sorption properties of CNC reinforced PVA films. *International Journal of Biological Macromolecules, 101*, 783-790.

Pour, Z. S., & Ghaemy, M. (2015). Removal of dyes and heavy metal ions from water by magnetic hydrogel beads based on poly (vinyl alcohol)/carboxymethyl starch-g-poly (vinyl imidazole). *RSC Advances, 5*(79), 64106-64118.

Prado, A. G. S., Torres, J. D., Faria, E. A., & Dias, S. l. C. L. (2004). Comparative adsorption studies of indigo carmine dye on chitin and chitosan. *Journal of Colloid and Interface Science, 277*(1), 43-47.

Program, N. T. (1990). Executive summary of safety and toxicity information for methylene blue trihydrate 7220-79-3. *US Department of Health and Human Services*.

Qiu, H., Lv, L., Pan, B.-c., Zhang, Q.-j., Zhang, W.-m., & Zhang, Q.-x. (2009). Critical review in adsorption kinetic models. *Journal of Zhejiang University-Science A, 10*(5), 716-724.

Qiu, K., & Netravali, A. N. (2013). Halloysite nanotube reinforced biodegradable nanocomposites using noncrosslinked and malonic acid crosslinked polyvinyl alcohol. *Polymer Composites, 34*(5), 799-809.

Raj, G. (2002). Introduction to Surface and Interface Chemistry *Surface Chemistry* (4 ed., pp. 164). Meerut, India: Krishna Prakashan.

Rao, K., Subha, M., Sairam, M., Mallikarjuna, N., & Aminabhavi, T. (2007). Blend membranes of chitosan and poly (vinyl alcohol) in pervaporation dehydration of isopropanol and tetrahydrofuran. *Journal of Applied Polymer Science, 103*(3), 1918-1926.

Rashidzadeh, A., & Olad, A. (2013). Novel polyaniline/poly (vinyl alcohol)/clinoptilolite nanocomposite: dye removal, kinetic, and isotherm studies. *Desalination and Water Treatment, 51*(37-39), 7057-7066.

Rault, J., Gref, R., Ping, Z., Nguyen, Q., & Neel, J. (1995). Glass transition temperature regulation effect in a poly (vinyl alcohol)—water system. *Polymer, 36*(8), 1655-1661.

Reddy, N., & Yang, Y. (2010). Citric acid cross-linking of starch films. *Food Chemistry, 118*(3), 702-711.

Riyajan, S.-A., Chaiponban, S., Chusri, S., & Voravuthikunchai, S. P. (2012). Mechanical properties and cure test of a natural rubber/poly (vinyl alcohol) blend. *Rubber Chemistry and Technology, 85*(1), 147-156.

Riyajan, S.-A., Chaiponban, S., & Tanbumrung, K. (2009). Investigation of the preparation and physical properties of a novel semi-interpenetrating polymer network based on epoxised NR and PVA using maleic acid as the crosslinking agent. *Chemical Engineering Journal, 153*(1–3), 199-205.

Rogojanu, A., Rusu, E., Olaru, N., Dobromir, M., & Dorohoi, D. (2011). Development and characterization of poly (vinyl alcohol) matrix for drug release. *Digest Journal of Nanomaterials & Biostructures, 6*(2), 809-818.

Roohani, M., Habibi, Y., Belgacem, N. M., Ebrahim, G., Karimi, A. N., & Dufresne, A. (2008). Cellulose whiskers reinforced polyvinyl alcohol copolymers nanocomposites. *European Polymer Journal, 44*(8), 2489-2498.

Rubentheren, V., Ward, T. A., Chee, C. Y., & Nair, P. (2015). Physical and chemical reinforcement of chitosan film using nanocrystalline cellulose and tannic acid. *Cellulose, 22*(4), 2529-2541.

Rubentheren, V., Ward, T. A., Chee, C. Y., Nair, P., Salami, E., & Fearday, C. (2016). Effects of heat treatment on chitosan nanocomposite film reinforced with nanocrystalline cellulose and tannic acid. *Carbohydrate Polymers, 140*, 202-208.

Russo, V., Trifuoggi, M., Di Serio, M., & Tesser, R. (2017). Fluid ‐ solid adsorption in batch and continuous processing: A review and insights into modeling. *Chemical Engineering & Technology, 40*(5), 799-820.

Saad, N., Al-Mawla, M., Moubarak, E., Al-Ghoul, M., & El-Rassy, H. (2015). Surface-functionalized silica aerogels and alcogels for methylene blue adsorption. *RSC Advances, 5*(8), 6111-6122.

Safa, Y., & Bhatti, H. N. (2011). Adsorptive removal of direct dyes by low cost rice husk: Effect of treatments and modifications. *African Journal of Biotechnology, 10*(16), 3128-3142.

Saheb, D. N., & Jog, J. (1999). Natural fiber polymer composites: a review. *Advances in Polymer Technology, 18*(4), 351-363.

Sain, M., & Panthapulakkal, S. (2006). Bioprocess preparation of wheat straw fibers and their characterization. *Industrial Crops and Products, 23*(1), 1-8.

Sánchez-García, M. D., Hilliou, L., & Lagarón, J. M. (2010). Morphology and water barrier properties of nanobiocomposites of κ/ι-hybrid carrageenan and cellulose nanowhiskers. *Journal of Agricultural and Food Chemistry, 58*(24), 12847-12857.

Sehaqui, H., Allais, M., Zhou, Q., & Berglund, L. A. (2011). Wood cellulose biocomposites with fibrous structures at micro-and nanoscale. *Composites Science and Technology, 71*(3), 382-387.

Shi, J., Shi, S. Q., Barnes, H. M., & Pittman, J., Charles U. (2011). A chemical process for preparing cellulosic fibers hierarchically from kenaf bast fibers. *BioResources, 6*(1), 879-890.

Shu, J., Cheng, S., Xia, H., Zhang, L., Peng, J., Li, C., et al. (2017). Copper loaded on activated carbon as an efficient adsorbent for removal of methylene blue. *RSC Advances, 7*(24), 14395-14405.

Silva, F. C., Lima, L. C. B., Bezerra, R. D. S., Osajima, J. A., & Silva Filho, E. C. (2015). Use of Cellulosic Materials as Dye Adsorbents — A Prospective Study. In D. M. Poletto (Ed.), *Cellulose - Fundamental Aspects and Current Trends* (pp. 115-132): InTech.

Silvério, H. A., Flauzino Neto, W. P., & Pasquini, D. (2013). Effect of incorporating cellulose nanocrystals from corncob on the tensile, thermal and barrier properties of poly(vinyl alcohol) nanocomposites. *Journal of Nanomaterials, 2013*, 1-9.

Sridhar, V., Jeon, J.-H., & Oh, I.-K. (2010). Synthesis of graphene nano-sheets using eco-friendly chemicals and microwave radiation. *Carbon, 48*(10), 2953-2957.

Sriupayo, J., Supaphol, P., Blackwell, J., & Rujiravanit, R. (2005). Preparation and characterization of α-chitin whisker-reinforced poly (vinyl alcohol) nanocomposite films with or without heat treatment. *Polymer, 46*(15), 5637-5644.

Sultanova, N., Kasarova, S., & Nikolov, I. (2009). Dispersion properties of optical polymers. *Acta Physica Polonica A, 116*, 585-587

Taleb, M. F. A., El-Mohdy, H. A., & El-Rehim, H. A. (2009). Radiation preparation of PVA/CMC copolymers and their application in removal of dyes. *Journal of Hazardous Materials, 168*(1), 68-75.

Tamura, H., Nagahama, H., & Tokura, S. (2006). Preparation of chitin hydrogel under mild conditions. *Cellulose, 13*(4), 357-364.

Tang, L., & Weder, C. (2010). Cellulose whisker/epoxy resin nanocomposites. *ACS Applied Materials & Interfaces, 2*(4), 1073-1080.

Thomas, S., Joseph, K., Malhotra, S. K., Goda, K., & Sreekala, M. S. (2013). *Polymer composites, nanocomposites*: Wiley.

Tokura, S., Nishimura, S. I., Sakairi, N., & Nishi, N. (1996). *Biological activities of biodegradable polysaccharide.* Paper presented at the Macromolecular symposia.

Tolstov, A., Matyushov, V., & Klimchuk, D. (2012). Controlled structure-dependent synthesis of polymer/nanosilver composites for highly efficient antibacterial coatings *Technological Innovations in Sensing and Detection of Chemical, Biological, Radiological, Nuclear Threats and Ecological Terrorism*. Netherlands: Springer Netherlands.

Tubbs, R. K. (1965). Melting point and heat of fusion of poly (vinyl alcohol). *Journal of Polymer Science Part A: Polymer Chemistry, 3*(12), 4181-4189.

Umoren, S., Etim, U., & Israel, A. (2013). Adsorption of methylene blue from industrial effluent using poly (vinyl alcohol). *Journal of Materials and Environmental Science, 4*(1), 75-86.

Umoren, S. A., Etim, U. J., & Israel, A. U. (2013). Adsorption of methylene blue from industrial effluent using poly (vinyl alcohol). *Journal of Materials and Environmental Science, 4*(1), 75-86.

Virtanen, S., Vartianen, J., Setälä, H., Tammelin, T., & Vuoti, S. (2014). Modified nanofibrillated cellulose–polyvinyl alcohol films with improved mechanical performance. *RSC Advances, 4*(22), 11343-11350.

Wan Ngah, W. S., Teong, L. C., & Hanafiah, M. A. K. M. (2011). Adsorption of dyes and heavy metal ions by chitosan composites: A review. *Carbohydrate Polymers, 83*(4), 1446-1456.

Wang, C., Zheng, Y., Qiao, K., Xie, Y., & Zhou, X. (2015). An environmentally friendly preparation and characterization of waterborne polyurethane hydrogels by polyvinyl alcohol physical cross-linking to improve water absorption. *RSC Advances, 5*(90), 73882-73891.

Wang, Y., Cao, X., & Zhang, L. (2006). Effects of cellulose whiskers on properties of soy protein thermoplastics. *Macromolecular Bioscience, 6*(7), 524-531.

Wilder, E. A., Guo, S., Lin-Gibson, S., Fasolka, M. J., & Stafford, C. M. (2006). Measuring the modulus of soft polymer networks via a buckling-based metrology. *Macromolecules, 39*(12), 4138-4143.

Wiśniewska, M. (2012). Temperature effects on the adsorption of polyvinyl alcohol on silica. *Open Chemistry, 10*(4), 1236-1244.

Wiśniewska, M., Ostolska, I., Szewczuk-Karpisz, K., Chibowski, S., Terpiłowski, K., Gun'ko, V. M., et al. (2015). Investigation of the polyvinyl alcohol stabilization mechanism and adsorption properties on the surface of ternary mixed nanooxide AST 50 (Al2O3–SiO2–TiO2). *Journal of Nanoparticle Research, 17*(1), 12.

Xia, L. L., Li, C. L., & Wang, Y. (2016). In-situ crosslinked PVA/organosilica hybrid membranes for pervaporation separations. *Journal of Membrane Science, 498*, 263-275.

Xie, K., Hou, A., & Chen, Y. (2008). *The mathematical model of dye diffusion and adsorption on modified cellulose with triazine derivatives containing cationic and anionic groups.* Paper presented at the Journal of Physics: Conference Series.

Xie, Z., Hoang, M., Duong, T., Ng, D., Dao, B., & Gray, S. (2011). Sol–gel derived poly (vinyl alcohol)/maleic acid/silica hybrid membrane for desalination by pervaporation. *Journal of Membrane Science, 383*(1), 96-103.

Xu, X.-J., Huang, S.-M., & Zhang, L.-H. (2009). Biodegradability, antibacterial properties, and ultraviolet protection of polyvinyl alcohol-natural polyphenol blends. *Polymer Composites, 30*(11), 1611-1617.

Yagub, M. T., Sen, T. K., Afroze, S., & Ang, H. M. (2014). Dye and its removal from aqueous solution by adsorption: A review. *Advances in Colloid and Interface Science, 209*, 172-184.

Yahagi, T., Degawa, M., Seino, Y., Matsushima, T., Nagao, M., Sugimura, T., et al. (1975). Mutagenicity of carcinogenic azo dyes and their derivatives. *Cancer Letters, 1*, 91-96.

Yang, H., Yan, R., Chen, H., Lee, D. H., & Zheng, C. (2007). Characteristics of hemicellulose, cellulose and lignin pyrolysis. *Fuel, 86*(12–13), 1781-1788.

Yang, L., Li, Y., Hu, H., Jin, X., Ye, Z., Ma, Y., et al. (2011). Preparation of novel spherical PVA/ATP composites with macroreticular structure and their adsorption behavior for methylene blue and lead in aqueous solution. *Chemical Engineering Journal, 173*(2), 446-455.

Yang, X., Li, Y., Du, Q., Wang, X., Hu, S., Chen, L., et al. (2016). Adsorption of Methylene Blue from Aqueous Solutions by Polyvinyl Alcohol/Graphene Oxide Composites. *Journal of Nanoscience and Nanotechnology, 16*(2), 1775-1782.

Yang, Y., Chun, Y., Sheng, G., & Huang, M. (2004). pH-dependence of pesticide adsorption by wheat-residue-derived black carbon. *Langmuir, 20*(16), 6736-6741.

Yaseen, D., & Scholz, M. (2019). Textile dye wastewater characteristics and constituents of synthetic effluents: a critical review. *International Journal of Environmental Science and Technology, 16*(2), 1193-1226.

Yoon, S. D., Chough, S. H., & Park, H. R. (2006). Effects of additives with different functional groups on the physical properties of starch/PVA blend film. *Journal of Applied Polymer Science, 100*(5), 3733-3740.

Younes, I., & Rinaudo, M. (2015). Chitin and chitosan preparation from marine sources. Structure, properties and applications. *Marine Drugs, 13*(3), 1133-1174.

Yu, C., & Li, B. (2008). Preparation and characterization of carboxymethyl polyvinyl alcohol–graphite nanosheet composites. *Polymer Composites, 29*(9), 998-1005.

Zaharia, C., Suteu, D., Muresan, A., Muresan, R., & Popescu, A. (2009). Textile wastewater treatment by homogenous oxidation with hydrogen peroxide. *Environmental Engineering and Management Journal, 8*(6), 1359-1369.

Zaikov, G. E., & Jiménez, A. (2005). *Polymer Analysis, Degradation, and Stabilization*: Nova Science Publishers.

Zargar, V., Asghari, M., & Dashti, A. (2015). A review on chitin and chitosan polymers: structure, chemistry, solubility, derivatives, and applications. *ChemBioEng Reviews, 2*(3), 204-226.

Zayed, M. F., Eisa, W. H., & Anis, B. (2016). Removal of methylene blue using Phoenix dactylifera/PVA composite; an eco-friendly adsorbent. *Desalination and Water Treatment, 57*(40), 18861-18867.

Zendehdel, M., Barati, A., Alikhani, H., & Hekmat, A. (2010). Removal of methylene blue dye from wastewater by adsorption onto semi-inpenetrating polymer network hydrogels composed of acrylamide and acrylic acid copolymer and polyvinyl alcohol. *Journal of Environmental Health Science & Engineering, 7*(5), 431-436.

Zhang, Y., Zhu, P. C., & Edgren, D. (2010). Crosslinking reaction of poly (vinyl alcohol) with glyoxal. *Journal of Polymer Research, 17*(5), 725-730.

Zhao, R., Wang, Y., Li, X., Sun, B., Jiang, Z., & Wang, C. (2015). Water-insoluble sericin/β-cyclodextrin/PVA composite electrospun nanofibers as effective adsorbents towards methylene blue. *Colloids and Surfaces B: Biointerfaces, 136*, 375-382.

Zhou, C., Wu, Q., Lei, T., & Negulescu, I. I. (2014). Adsorption kinetic and equilibrium studies for methylene blue dye by partially hydrolyzed polyacrylamide/cellulose nanocrystal nanocomposite hydrogels. *Chemical Engineering Journal, 251*, 17-24.

Zhu, G., Wang, F., Xu, K., Gao, Q., & Liu, Y. (2013). Study on properties of poly (vinyl alcohol)/polyacrylonitrile blend film. *Polímeros, 23*(2), 146-151.

List of Publications

C. F. Mok, Y. C. Ching, F. Muhamad, N. A. Abu Osman & Ramesh Singh (2017). Poly(vinyl alcohol)-α-chitin bionanocomposites reinforced by oil palm empty fruit bunch fibers-derived nanocellulose. - Published by International Journal of Polymer Analysis and Characterizations (ISI indexed).

C. F. Mok, Y. C. Ching, F. Muhamad & N. A. Abu Osman (2020). Adsorption of Dyes using Poly(vinyl alcohol) (PVA) and PVA-based Polymer Composite Adsorbents: A review. - Published by Journal of Polymers and the Environment (ISI indexed).

C. F. Mok, Y. C. Ching, F. Muhamad & N. A. Abu Osman (2020). Maleic acid cross-linked poly(vinyl alcohol)/chitin composites reinforced with oil palm empty fruit bunch (OPEFB) fibers-derived nanocellulose. - Published by Journal of Applied Polymer Science (ISI indexed).

C. F. Mok, Y. C. Ching, F. Muhamad & N. A. Abu Osman (2020). Reusable and eco-friendly adsorbents for removal of cationic dye: Maleic acid cross-linked poly(vinyl alcohol)/chitin/nanocellulose composites. - Under review by Journal of Polymer Research (ISI indexed).